School of Pharmacy

Development of a Pharmacodynamic Model of Murine Malaria

Peter Luke Gibbons

This thesis is presented for the Degree of

Doctor of Philosophy

of

Curtin University

February 2015

Declaration

To the best of my knowledge and belief this thesis contains no material previously published by any other person except where due acknowledgment has been made.

This thesis contains no material which has been accepted for the award of any other degree or diploma in any university.

Peter L. Gibbons

February 2015

Contents

Declaration....2

Contents....3

Abstract....11

Acknowledgements....12

Publications....14

Communications....15

Abbreviations....16

CHAPTER ONE....19

1. Literature review....19

1.1 Introduction....19

1.2 Malaria....21

1.2.1 Discovering malaria....21

1.2.2 Geographical distribution....22

1.2.3 Malaria species....23

1.2.4 Life cycle of the malaria parasite....25

1.2.5 Clinical features of malaria....29

1.2.6 Malaria immunity....30

1.2.7 Diagnosis....32

1.2.8 Enumeration of malaria parasites....35

1.2.9 Parasite clearance....37

1.2.10 Mathematical models of malaria transmission....40

1.2.11 Mathematical models of within host asexual dynamics....43

1.2.12 The importance of mathematical models of malaria....45

1.3 The fight against malaria 45

1.3.1 Antimalarial strategies 48

1.3.2 Antimalarial treatment strategies 50

1.3.3 A brief history of antimalarial chemotherapy 51

1.3.4 Classification of antimalarial chemotherapeutic agents 53

1.3.5 Optimisation of antimalarial chemotherapy 56

1.4 Resistance 57

1.4.1 A brief history of chemotherapy resistance 58

1.4.2 Determinants of antimalarial resistance 61

1.4.3 Combating antimalarial drug resistance 62

1.5 Malaria models 63

1.5.1 *In vitro* models of malaria 64

1.5.2 Animal models of malaria 65

1.5.3 Non-human primate models of malaria 66

1.5.4 *In vivo* models for drug screening 68

1.5.5 Murine models of malaria 69

1.5.6 The value of murine malaria models 71

1.5.7 *P. berghei* murine malaria 71

1.5.8 *P. berghei* antimalarial chemotherapeutic tests 75

1.5.9 Humanised models of murine malaria 78

1.6 Aims of this thesis 80

CHAPTER TWO 83

2. Materials and Methods 83

2.1 Materials 83

2.1.1 Chemicals and Materials 83

2.1.2 Parasites 84
2.1.3 Mice 84
2.1.4 Animal welfare....85
2.1.5 Euthanasia 86
2.1.6 Animal holding....86
2.2 Methods 87
2.2.1 Initial *P. berghei* malaria infection....87
2.2.2 Passage of the *P. berghei* malaria infection 88
2.2.3 Cryopreservation of *P. berghei* malaria 89
2.2.4 Preparation and staining of blood films 89
2.2.5 Parasite enumeration and staging....90
2.2.6 Formulation of dihydroartemisinin 91
2.2.7 Dihydroartemisinin treatment methodology 92
2.2.8 Modelling and statistical analysis 93
CHAPTER THREE....94
3. Establishing a murine malaria infection model....94
3.1 Introduction 94
3.1.1 Development of antimalarial treatment regimens 94
3.1.2 Antimalarial pharmacodynamics....95
3.1.3 Animal models of malaria 96
3.1.4 *P. berghei* malaria 97
3.1.5 *P. berghei* chemotherapy screening tests 99
3.1.6 *P. berghei* as a pharmacodynamic malaria model....100
3.1.7 Artemisinin 101
3.1.8 Artemisinin-based antimalarial monotherapies....104
3.1.9 Dihydroartemisinin....105

3.1.10 Aims 106
3.2 Methods 108
3.2.1 Mice 108
3.2.2 *P. berghei* infection 108
3.2.3 Hosts and dihydroartemisinin ranging studies 108
3.2.4 Parasite enumeration and staging 110
3.2.5 Parasite inoculation studies 110
3.2.6 Erythrocyte population and blood studies 111
3.2.7 Formulation of dihydroartemisinin 112
3.2.8 Dihydroartemisinin treatment 112
3.2.9 Dihydroartemisinin pharmacokinetics 113
3.2.9.1 Drug administration and blood sampling 113
3.2.9.2 Pharmacokinetic analysis 114
3.3 Results 116
3.3.1 *P. berghei* malaria model in Swiss mice 116
3.3.2 Parasite inoculation study 116
3.3.3 Erythrocyte population studies 117
3.3.4 Pathophysiological studies 122
3.3.5 Haemoglobin concentration 122
3.3.6 Platelet concentration 123
3.3.7 Liver and spleen weight 124
3.3.8 White blood cell population changes 125
3.3.9 Dihydroartemisinin single dose treatment 127
3.3.10 Dihydroartemisinin treatment staging 127
3.3.11 Dihydroartemisinin pharmacokinetics 128
3.4 Discussion 130

CHAPTER FOUR....135

4. Establishing a mathematical model of murine *P. berghei* infection and single dose monotherapy with dihydroartemisinin....135

4.1 Introduction....135

4.1.1 Mathematical models – limitations and pitfalls....136

4.1.2 Data modelling methodology....139

4.1.3 Mathematical models of infection....140

4.1.4 Mathematical models of malaria infection....141

4.1.5 Compartmental modelling....143

4.1.6 Aims....145

4.2 Methods....147

4.2.1 Relationship between time and parasite burden....147

4.2.2 Conceptual model of *P. berghei* infection....149

4.2.3 Mathematical model of *P. berghei* infection in SAAM II....151

4.2.4 Validation of mathematical model of *P. berghei* infection....152

4.3 Results....155

4.3.1 Relationship between time and parasite bioburden....155

4.3.2 Constructing a compartmental model of *P. berghei* infection....155

4.3.3 Effective parasite multiplication factor (EPMF)....158

4.3.4 *P. berghei* pharmacodynamic model....163

4.3.5 Dihydroartemisinin administration and the *P. berghei* model....165

4.3.6 Dihydroartemisinin treatment on parasite stages....171

4.4 Discussion....172

4.4.1 Protocol for the development of a murine model of infection and drug treatment....175

CHAPTER FIVE....178

5. Using a mathematical model of murine *P. berghei* and single dose monotherapy to predict multiple dose outcomes. 178

5.1 Introduction 178

5.1.1 Removing monotherapies from the clinical setting 179

5.1.2 The importance of antimalarial monotherapies 179

5.1.3 New approaches for optimum dose selection 180

5.1.4 Aims 182

5.2 Methods 184

5.2.1 Incorporating multiple dose treatment into the compartmental model 184

5.2.2 Predicting outcomes of multiple dose dihydroartemisinin monotherapy 186

5.2.3 Determining the optimum dose interval for dihydroartemisinin 187

5.2.4 Criteria for comparing treatment regimens 188

5.2.5 Internal validation of the multiple dose model of dihydroartemisinin treatment 188

5.2.6 External validation of the multiple dose model of dihydroartemisinin treatment 189

5.3 Results 191

5.3.1 Determining the optimum dose interval for dihydroartemisinin 191

5.3.2 Predicting multiple dose dihydroartemisinin treatment outcomes 194

5.3.3 Dihydroartemisinin *in vivo* multiple dose treatment 197

5.4 Discussion 200

CHAPTER SIX 206

6. Using a mathematical model of murine *P. berghei* single dose monotherapy to predict multiple dose combination outcomes. 206

6.1 Introduction 206

6.1.1 History of chloroquine use 207
6.1.2 Artemisinin based combinations 208
6.1.3 Chloroquine and artemisinin based combinations 209
6.1.4 Chloroquine studies in murine models 210
6.1.5 Aims 211
6.2 Methods 213
6.2.1 Selection of a dihydroartemisinin combination partner 213
6.2.2 Chloroquine pharmacodynamic data 213
6.2.3 Chloroquine pharmacodynamic model construction 216
6.2.4 Dihydroartemisinin and chloroquine treatment model 218
6.3 Results 220
6.3.1 Chloroquine single dose treatment modelling 220
6.3.2 Chloroquine single dose model 221
6.3.3 Chloroquine multiple dose modelling 223
6.3.4 Determination of the optimum dose interval for chloroquine 225
6.3.5 Dihydroartemisinin and chloroquine combination modelling 228
6.3.6 Optimum dose interval for a dihydroartemisinin and chloroquine combination 230
6.3.7 Parasite elimination functions for single, multiple and combination regimens 231
6.3.8 Staging of parasites following treatment with chloroquine 234
6.3.9 Effects of parasitaemia at the time of drug treatment 235
6.4 Discussion 236
6.4.1 Treatment parasite density and efficacy studies 236
6.4.2 Modelling chloroquine treatment 238
6.4.3 Modelling dihydroartemisinin and chloroquine combination treatment 239
7. Conclusion 242

References.....245

APPENDIX 1 – Development of a pharmacodynamic model of murine malaria and treatment with dihydroartemisinin 286

APPENDIX 2 – Reagents and Buffers 295

Abstract

The rational design of antimalarial therapies has historically been compromised by a paucity of pharmacodynamic data. Many antimalarials have been deployed at suboptimal doses contributing to the spread and development of resistance. Borrowing from antimicrobial experience, focus is now turning to methods to optimise dosing and combination therapy. The findings of the studies presented in this thesis demonstrate a modified *P. berghei* murine malaria model for collecting detailed *in vivo* pharmacodynamic data and a novel *in silico* mathematical model which enables optimisation of doses and combination therapy. These models provide an important contribution to preclinical knowledge, and the potential to assist in the development of methods to optimise clinical treatment.

Acknowledgements

First and foremost I would like to thank Professor Kevin Batty for his mentorship, continual support, endurance and patience during the course of my post graduate studies. You have been an excellent mentor and have helped to instilled in me a love of science and appreciation of the scientific method, all the while patiently supporting some of my crackbrain ideas. You have always been honest and pushed me to think about what I am trying to communicate and accomplish. I appreciate the time and space you have given me to explore. Thanks to Dr Andrew Crowe, for your support, help and supervision in getting my thesis completed. I love how passionately you express yourself when discussing science. You have been a great example to me of a self driven researcher in the modern university environment.

My thanks to Ken Ilett, Tim Davis and Hugh Barrett for your help and direction, especially in the early years of my work. Thank you Hugh for your advice and assistance in putting together the SAAM II model of malaria.

Thanks to Brioni Moore, Madhu Page-Sharp, Verity Archer, Jillian Stoney, and the staff and students at Curtin University School of Pharmacy, Biomedical Sciences and UWA School of Pharmacology. You have all been great friends, colleagues and help to me over the course of my candidature.

Big thank you to Megan McManus, whose love, patience and support have helped me over the past year complete this thesis. It has not been the best of

times, but it's over now and you won't have to hear me explain how proud I am of these experiments anymore. I promise.

Finally, I would like to thank my family. I have and always will count myself very blessed to have such a loving, caring and supportive group of people to share my life. Special thanks to Grandma McKernan. Despite your concerns I wouldn't finish before you died Grandma, I happily prove you wrong. I'm your Grandson and I love you, love you, love you. Your support has been greatly appreciated, even when I didn't show it. As has yours mum. Your constant nagging and offers to help have been appreciated and you've helped me get to this point. There are no other two people I would dedicate this thesis to, especially as you are the only two who will get a copy, and probably read some of it, other than Kevin, Andrew and my examiners.

I have thoroughly enjoyed completing my thesis. I wouldn't do it again, but I will publish again.

Publications

Gibbons PL, Batty KT, Barrett PHR, Davis TME, Ilett KF. 2007. Development of a pharmacodynamic model of murine malaria and antimalarial treatment with dihydroartemisinin. International Journal for Parasitology 37(14):1561-1576

Batty KT, Gibbons PL, Davis TME, Ilett KF. 2008. Short Report: Pharmacokinetics of Dihydroartemisinin in a Murine Malaria Model. American Journal of Tropical Medicine and Hygiene., 78(4):641–642

Kashyap P, Batty KT, Moore BR, Gibbons PL, Bulitta JB, Kirkpatricka, CM. 2013. Mechanism-Based Model of Parasite Growth and Dihydroartemisinin Pharmacodynamics in Murine Malaria. Antimicrobial Agents and Chemotherapy 57:508-516.

Communications

Gibbons PL, Barrett PHR, Ilett KF, Davis TME, Batty KT. Optimisation of dihydroartemisinin antimalarial monotherapy using a pharmacodynamic model of murine malaria. Poster: Curtin Health Science Research Symposium*, September 2007 (Perth, WA).*

Batty KT, Moore BR, Andrzejewski C, Jago JD, Law A, Stoney J, Gibbons PL, Ilett KF. Murine malaria treatment model for antimalarial combinations. Poster: ***Annual Meeting of the American Society of Tropical Medicine and Hygiene (ASTMH)****, November 2007 (Philadelphia, USA).*

Gibbons PL, Stoney JR, Barrett PHR, Ilett KF, Davis TME, Batty KT. Optimisation of therapeutic regimens using pharmacodynamic modelling of in vivo murine malaria infection. Poster: ***XVI International Congress for Tropical Medicine and Malaria (ICTM),*** *September 2005 (Marseilles, France).*

Moore BR, Jago JD, Batty KT. Pharmacodynamic study of dihydroartemisinin in the asplenic murine malaria model. Poster: ***XVI International Congress for Tropical Medicine and Malaria (ICTM)****, September 2005 (Marseilles, France).*

Jago JD, Moore BR, Andrzejewski C, Gibbons PL, Ilett KF, Batty KT. Pharmacodynamic study of piperaquine and dihydroartemisinin in a murine malaria model. Poster: ***XVI International Congress for Tropical Medicine and Malaria (ICTM),*** *September 2005 (Marseilles, France).*

Abbreviations

ACT	artemisinin combination therapy
ARC	Animal Resource Centre
ARTS	artesunate
BC	Before Christ
CQ	chloroquine
DDT	dichlorodiphenyltrichloroethane
DHA	dihydroartemisinin
DMSO	dimethyl sulfoxide
EDTA	ethylenediaminetetraacetic acid (anticoagulant)
ED_{50}	effective dose 50%
ED_{90}	effective dose 90%
FOV	field of view
GDP	gross domestic product
GMEP	Global Malaria Eradication Program
HCl	hydrochloric acid
HRP2	histidine-rich protein 2
IC_{50}	concentration of drug required to inhibit growth by 50%
i.m.	intramuscular
i.p.	intraperitoneal
i.v.	intravenous
L	liter(s)
LD_{50}	lethal dose 50%

LOD	limit of detection
MIC	mean inhibitory concentration
min	minute(s)
mg/kg	milligrams per kilograms
mm	millimeter(s)
NaCl	sodium chloride
NaOH	sodium hydroxide
P. berghei	*Plasmodium berghei*
P. chabaudi	*Plasmodium chabaudi*
PCR	polymerase chain reaction
PCT	parasite clearance time
PD	pharmacodynamic
P. falciparum	*Plasmodium falciparum*
PfEMP1	*Plasmodium falciparum* erythrocyte membrane protein 1
PK	pharmacokinetic
P. knowlesi	*Plasmodium knowlesi*
P. malariae	*Plasmodium malariae*
P. ovalae	*Plasmodium ovalae*
PQ	piperaquine
PRBC	parasitised red blood cells
QHS	artemisinin
qPCR	quantitative real-time polymerase chain reaction
RBC	red blood cells

SERCA	sarco/endoplasmic reticulum Ca^{2+}-ATPase
s.c.	subcutaneous
S.D.	standard deviation
SPF	specific pathogen free
WBC	white blood cells
WHO	World Health Organization

CHAPTER ONE

1. Literature review

1.1 Introduction

Malaria is one of the most severe public health problems world wide and is likely to have killed more humans than any other disease [280]. It is a leading cause of death in many developing countries. Of the ten leading causes of death in the developing world, malaria is the only one with a real prospect for eradication [228]. The World Heath Organization's World Malaria Report 2013 [434] estimated that 3.4 billion people in 104 countries live in areas at risk of malaria transmission. In 2012 this report estimated 627,000 deaths from 216 million clinical episodes. Ninety percent of the deaths were in the African region, 6% in the South-East Asian Region and 3% in the Eastern Mediterranean Region. Seventy seven percent of global deaths in 2012 were children [434]. Children and groups with low or little immunity, such as pregnant women, travellers, migrants or sufferers of autoimmune deficiency syndrome are most at risk of death or serious health consequences [132, 240].

Malaria is a curable disease. It is not an inevitable burden. Disease eradication is not a simple proposition at a global level. Global eradication requires a multifaceted, sustained strategy with funding and significant infrastructure as well as organisational support. Global malaria eradication is an achievable goal [55, 125, 149]. However, despite technological and increased understanding of

the disease, malaria is returning to areas where it had previously been eradicated, and population growth is increasing the number of human hosts in endemic areas [154, 296]. Eradication is a long term goal with elimination feasible in the short term [149].

Malaria inflicts a serious social and economic toll in endemic areas. Costs to individuals and small communities include purchase of drugs, preventative measures, travel to clinics, lost days of work and absence from school [331]. This often occurs in populations that are least able to cope with these additional costs of living. Costs to governments include health facilities, purchase of drugs and medical supplies, public health intervention programs and lost productivity due to lost days of work. Analysis of the Gross Domestic Product (GDP) of countries before and after malaria eradication demonstrates measurable benefits to GDP in all cases including Greece, Italy, Spain, Portugal, Jamaica and Western Europe [134]. Direct costs due to malaria including illness, treatment and death have been estimated at US $12 billion per year. Lost economic growth and development far exceed this, representing a serious socioeconomic burden resulting in a multitude of indirect generational opportunity costs. In 2008 the Gates Foundation with Roll Back Malaria published combined estimates for global malaria control and eradication of $6 billion US annually, falling to US $1.5 billion over three decades [238].

1.2 Malaria

1.2.1 Discovering malaria

The term malaria derives from the Italian mal'aria or "bad air" and records of malaria-like symptoms appear in records dating back to 2700 BC in Chinese medical writings [57] and Hippocrates in the 4th century BC noted the principal symptoms [51]. A number of Roman writers linked malaria to swamps. Despite many observations, the source of the disease or malaise was thought to be bad air or water up until the late 1800s. As well as symptoms, treatments were also observed and recorded.

In 1880, Alphonse Laveran, a French army surgeon in Constantine, Algeria discovered parasites in the blood of patients suffering from malaria [51, 56]. Six years later Camillo Golgi, an Italian neurophysiologist, established that there were at least two forms of the disease with differing fever periodicity. He also observed the fever coincided with the release of merozoites into the blood stream [57, 78, 342].

In 1897 Ronald Ross, a British officer in the Indian Medical Service demonstrated that malaria parasites could be transmitted from infected patients to mosquitoes [323]. This solved malaria transmission. In 1899 transmission of human malaria parasites was demonstrated by an Italian group led by Giovanni Grassi [98]. Mosquitoes were fed on malarial patients in Rome and the mosquitoes sent to London to feed on healthy volunteers, who developed malaria. The complete sporogenic cycle of *Plasmodium falciparum*, *P. vivax* and

P. malariae was demonstrated [57, 78, 342]. After thousands of years of suffering to malaria, humanity was now armed with the basic understanding of the disease and its vector, to enable the beginning of the war between *Plasmodium* and humans that is still in the balance today. There is still a great deal that needs to be elucidated and accomplished before malaria can be considered to be globally controlled, let alone eradicated.

1.2.2 Geographical distribution

Understanding the geographical distribution of malaria is important when implementing any global strategies to control the disease. Knowledge of disease distribution, as well as population distributions, urbanisation maps, climate maps and altitude maps have been used to identify populations at risk from malaria. Studies by Guerra *et al* in 2006 identified over 3 billion of the planet's population as being at risk from malaria [155-157]. Seventy five percent of those at risk are from 10 countries. Globally these top ten malaria endemic countries in order of highest population at risk are India, China, Indonesia, Bangladesh, Pakistan, Nigeria, Vietnam, Thailand, the Democratic Peoples Republic of the Congo and the Philippines [157]. The World Health Organization (WHO) estimates that more than 90% of the over 0.6 million deaths attributed to malaria annually occur in Africa [434].

Malaria transmission occurs predominantly in sub tropical regions in sub-Saharan Africa, Central and South America, the Middle East, the Indian Subcontinent, South-East Asia and Oceania (Figure 1.1 [137]). In malaria

endemic areas there is large variation in the intensity of transmission and risk of infection. Areas higher than 1500m and areas with less than 1000mm annual rainfall typically have less malaria [434]. Urban areas are also usually lower risk, although uncontrolled population growth can increase urban transmission [205]. There is growing concern over the possible influence of climate change on infectious disease distribution [282]. Malaria is the disease of greatest public concern and seems most likely to be sensitive to climatic change. Malaria is often seasonal around weather and research in India has demonstrated a link between extreme climatic events and malaria epidemics [49]. Recent studies indicate that malaria epidemic risk increases five-fold the year after an El Nino weather event [49].

1.2.3 Malaria species

There are over 550 species in the order of Haemosporidia, of which the genus *Plasmodium* constitutes almost half of these species [336]. Species are entirely parasitic with part of the lifecycle spent in a vertebrate host, and part in an invertebrate host, which is generally a mosquito. Vertebrate hosts include mammals, birds and reptiles. Five *Plasmodium* species have been identified that can infect humans, *Plasmodium falciparum* (*P. falciparum*), *P. vivax*, *P. ovalae*, *P. malariae* and *P. knowlesi* [21, 96, 192, 293]. A comparison of the characteristics of the five malaria species that infect humans is shown in Table 1.1

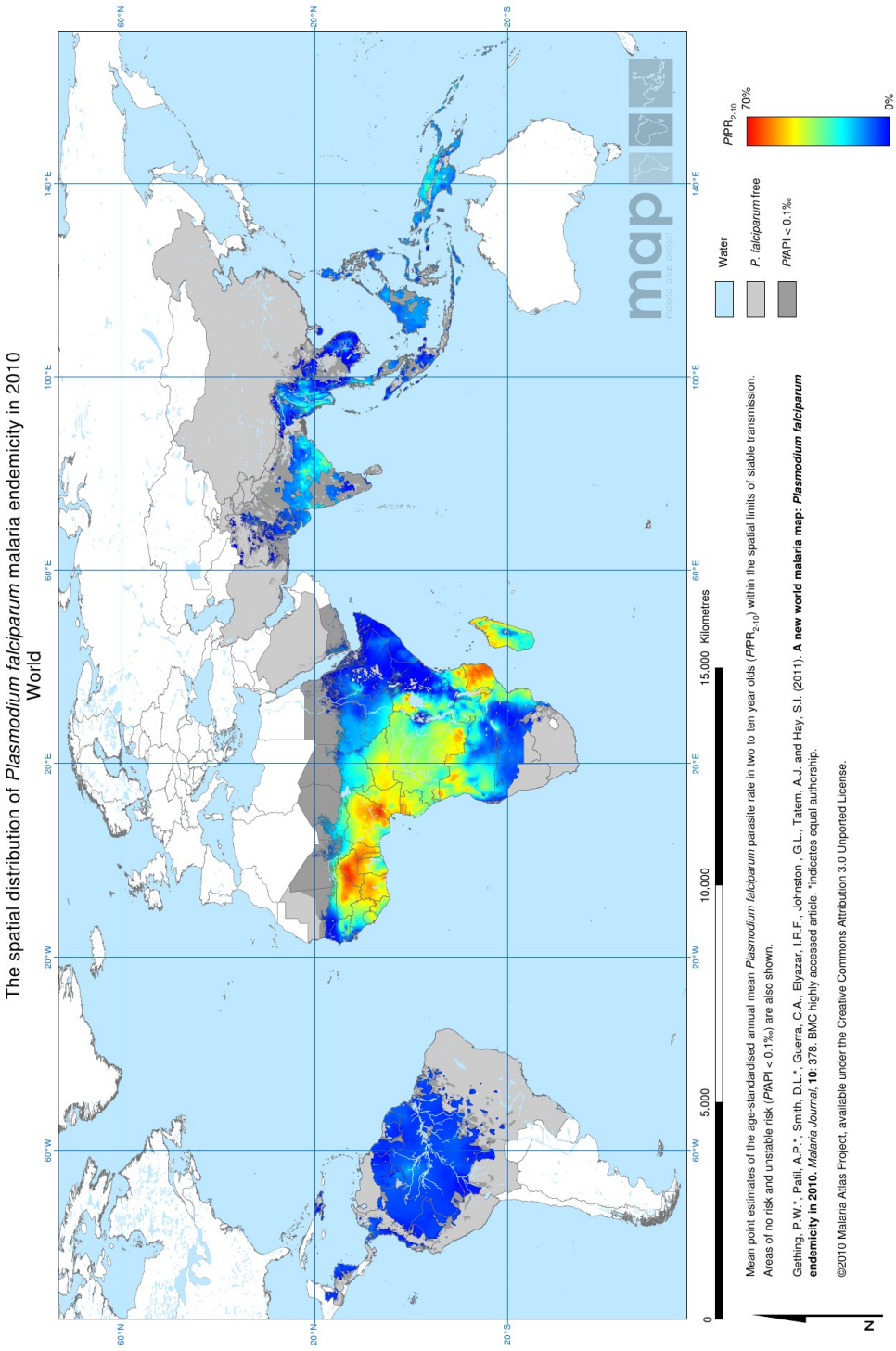

Figure 1.1 – 2010 global distribution of *P. falciparum* malaria as published by the Malaria Atlas Project [137].

.

Table 1.1 – Characteristics of human malaria species (adapted from [111, 136, 193, 243, 319, 351, 388, 436])

	P. falciparum	*P. malariae*	*P. ovalae*	*P. vivax*	*P. knowlesi*
Distribution (% of cases per region)	80-90% Africa 40-50% SE Asia 4-30% S Asia, S America	2-3% Africa Sporadic Asia, S America	8% parts of Africa Sporadic Asia	70-90% Asia, S America 50-60% SE Asia 1-10% Africa	Reported in SE Asia up to 70%
Erythrocytic Life Cycle (hrs)	48	72	48	48	24
Merozoites per erythrocyte Schizont	8-24	6-12	6-14	12-24	10-16
Exoerythrocytic Cycle (days)	6	13	9	8	9
Merozoites per tissue Schizont	40000	2000	15000	>10000	?
Erythrocytic preference	All	Mature erythrocytes	Reticulocytes	Reticulocytes	?
Complications	Cerebral	renal	-	-	-
Fever Pattern	Tertian, sub tertian	Quartan	Tertian	Tertian	Quotidian
Severe Malaria	Up to 24%	rare	rare	Up to 22%	6-10%
Anaemia	++++	++	+	++	?
Drug resistance	Yes	No	No	Yes	No

1.2.4 Life cycle of the malaria parasite

The life cycle of the malaria parasite consists of two distinct species phases. Sporogony is the phase occurring in the female *Anopheles* mosquito while schizogony is the exoerythrocytic and erythrocytic stages occurring in human hosts [348]. After feeding on a malaria infected host, *Anopheles* mosquito have gametocytes introduced into the stomach. Fertilisation of the female gametocytes occurs in the stomach. The zygote develops into a mobile ookinete within 24 h and moves to the stomach wall where it develops into an oocyst. Oocyst mature over one to two weeks and rupture to release up to 10,000 sporozoites which migrate to the mosquito salivary glands [304].

Humans may be infected with malaria while being fed on by carrier *Anopheles* mosquitoes. The process of withdrawing blood introduces mosquito saliva into the host's bloodstream, including malaria sporozoites if the mosquito is infected. Sporozoites are taken up by hepatocytes where they develop over a week. Upon maturation, the hepatic schizonts rupture releasing more than 10,000 merozoites into the host's bloodstream. In *P. vivax* and *P. ovalae* infections some sporozoites become dormant, as hypnozoites, which can remain in the hepatocytes for months or years until they cause a relapsed malaria infection [294, 296]. Merozoites quickly invade healthy erythrocytes beginning the erythrocytic life cycle.

The erythrocytic life cycle ranges from 24-72 h depending on the species of parasite (Table 1.1) with the *P. falciparum* cycle taking approximately 48 h. In *P. falciparum* infections, merozoites develop over a 24 h period into early trophozoites (rings) then into mature trophozoites by 26-38 h and then schizonts (Figure 1.2). As the trophozoites develop, the vacuole which gives them a characteristic ring profile expands and haemozoin accumulates in the vacuole as the parasite digests the erythrocyte's haemoglobin. Infected erythrocytes finally rupture releasing 8-24 merozoites that go on to infect healthy erythrocytes and continue the infection. The destruction of erythrocytes causes anaemia and also releases pyrogenic material which is responsible for the symptoms of fever [294, 296].

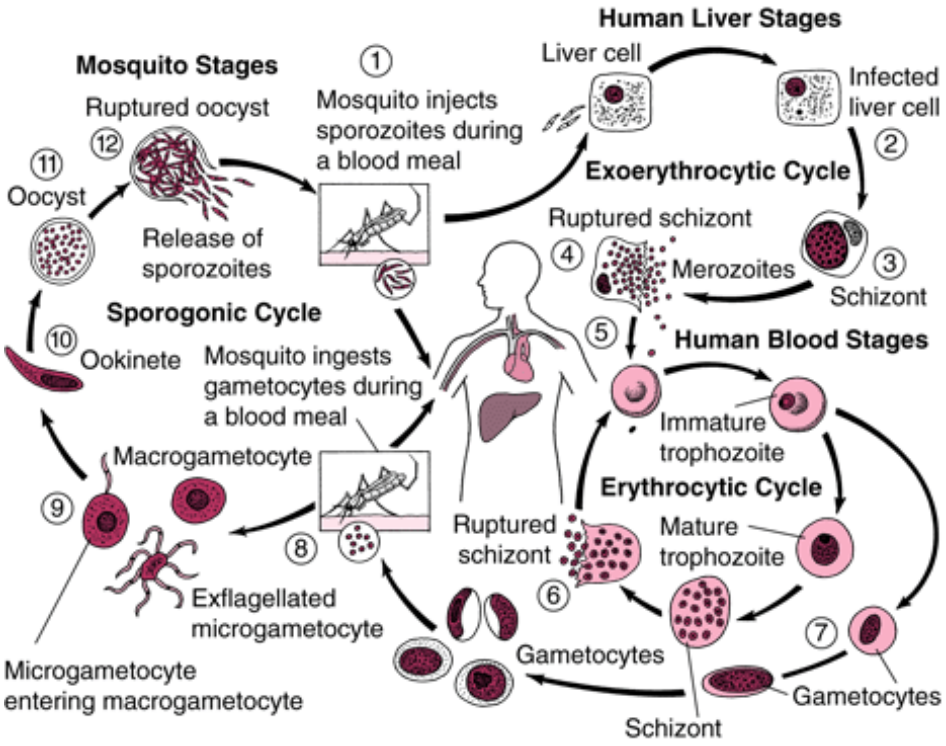

Figure 1.2 – Diagram of *P. falciparum* malaria life cycle [304].

A small number of merozoites will develop as gametocytes which infect feeding *Anopheles* mosquitoes. In *P. falciparum* infections, as opposed to other strains, mature trophozoite and schizont stage infected erythrocytes do not remain in the peripheral circulation but instead sequester in the microvasculature of organs by inserting adhesion molecules into the erythrocyte's cell membrane. Sequestered parasites adhering to brain microvasculature result in cerebral malaria. There are a number of morphological differences between the human malaria species as shown in Figure 1.3 [248].

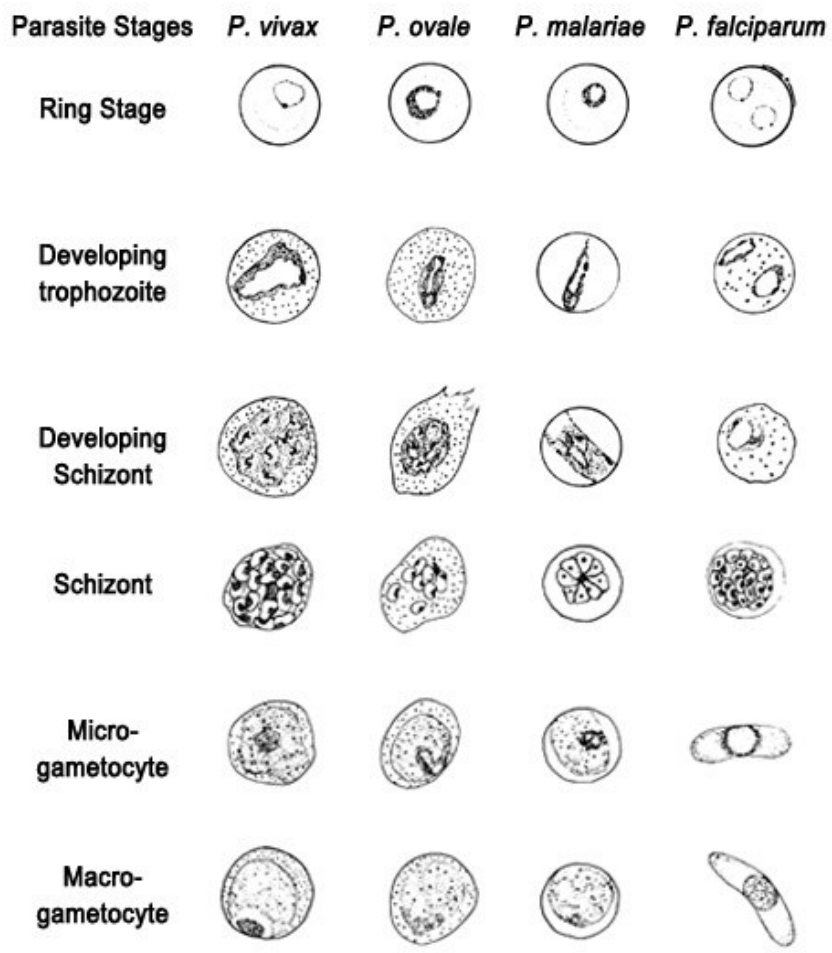

Figure 1.3 – Morphological Differences between Human *Plasmodium* Species [248].

P. falciparum is characterised by rings and the absence of older stages which sequester. The rings tend to be smaller but more numerous than in other species. Erythrocytes infected by more than one merozoite are more common and the gametocytes of *P. falciparum* are distinctively crescent shaped [248]. *P. vivax* is characterised by enlarged infected erythrocytes and "Schuffner' dots" which have the appearance of granules. *P. ovale* is similar to *P. vivax* with enlarged infected erythrocytes and "Schuffner' dots" however it forms elongated erythrocytes and has fewer merozoites. *P. malariae* displays band form

trophozoites which stretch across erythrocytes and merozoites often appear in a rosette pattern with a clump of pigment in the centre [248]. The morphology of *P. knowlesi* is similar to that of *P. falciparum* in the early stages, however late trophozoite, schizonts and gametocytes appear indistinguishable from *P. malariae* [220].

1.2.5 Clinical features of malaria

P. falciparum is the most widespread and severe form of malaria responsible for most malarial mortality. *P. vivax* is almost as widespread as *P. falciparum* (Figure 1.1) but rarely results in death to the host [75]. The signs and symptoms of uncomplicated malaria are relatively similar between the different forms except for variations in fever periodicity [129]. The classic symptom of malaria is intermittent high fever, caused by rupture of red blood cells during merozoite release. This fever has a typical 48 h periodicity in relatively synchronous *vivax* infections, while fever becomes more continuous in other malaria infections. Fever is preceded by a range of non-specific symptoms including malaise, fatigue, headache, myalgia, anorexia, dyspepsia, nausea, vomiting and diarrhoea [129].

Anaemia (erythrocyte count $<3x10^6$ per μL), thrombocytopaenia (platelets $<150x10^9$ per L), splenomegaly and hepatomegaly are also commonly seen especially in *P. falciparum* and *P. vivax* infections [130]. Renal impairment is common though typically mild. The most serious complication of falciparum infection is cerebral malaria caused by sequestration of late stage trophozoite

and schizont infected erythrocytes in cerebral microvasculature. Symptoms of cerebral malaria include seizures and coma, prior to which patients become delirious and psychotic [130].

1.2.6 Malaria immunity

Malaria is a disease that mainly affects immune naïve individuals, particularly children under 5 years of age [240] and pregnant women [132]. In regions of high transmission intensity, the immunity to uncomplicated malaria develops slowly and chronic infection seems to be necessary for maintaining a protective immunity [59]. Low immunogenicity and high heterogeneity of malaria antigens allowing parasites to evade humoral immunity may be the explanation for this slow immune protection [266]. Alternatively, parasites could induce immune dysregulation inhibiting the development of protective cellular immunity [122]. Antibody responses against specific antigens are short-lived and dependent on the presence of circulating parasites [58, 77, 95], suggesting that memory formation and longevity of either B and T cell responses or both are perturbed.

Immunity to severe malaria develops after a number of infections, indicating the existence of antigenic homogeneity in parasites causing severe disease [159]. As well as this acquired or adaptive immunity gained through repeated exposure to infection, innate immunity plays an important role in endemic areas.

Innate immunity involves scavenging cells such as dendritic cells, natural killer (NK) cells, natural killer T cells and $\gamma\delta$T cells. Dendritic cells are important for the

activation of immune responses and link innate and adaptive immunity. They reside in almost all tissues and screen their environment by pinocytosis and phagocytosis of protein and cellular debris. When they encounter foreign antigens, dendritic cells are activated and leave the tissue via the lymph or blood and migrate to the draining lymph node and the spleen. During migration, dendritic cells mature and interact with T cells secreting cytokines, which are important for activation of other leucocytes, such as NK cells, monocytes/macrophages, and B cells [28]. For a more in depth review of innate immunity see “Early interactions between blood-stage *Plasmodium* parasites and the immune system” [398].

P. falciparum differs from other human malaria species as it can achieve much higher parasitaemia and the mature forms of the erythrocytic stages sequester in micro vasculature. Sequestration ensures that at least a proportion of the infected erythrocytes mature without passage through the spleen where they can be removed by cordal macrophages due to reduced deformability and opsonisation [19, 85, 86]. Sequestration of infected erythrocytes is mediated by *P. falciparum* erythrocyte membrane protein (PfEMP1), which is inserted into the membrane of infected cells approximately 18 h after invasion and is encoded by 59 *var* genes, providing the antigenic variation to evade the host humoral immune response [210]. PfEMP1 mediates not only adhesion of endothelial cells in microvasculature, but also red blood cells and leucocytes.

1.2.7 Diagnosis

Early and accurate diagnosis of malaria is essential for effective disease management and malaria surveillance [434]. Misdiagnosis can result in significant morbidity and mortality as well as inappropriate drug use, which can lead to resistance. The WHO recommends prompt malaria diagnosis by either microscopy or malaria rapid diagnostic test in all patients with suspected malaria before treatment is administered [434].

The long time standard for definitive diagnosis in nearly all settings is direct microscopic examination of intracellular parasites on Giemsa stained blood films, and microscopy is still considered the “gold standard” by some experts [259, 333]. Microscopy allows differentiation between species, quantification of parasite density and elucidation of parasite stages including distinguishing asexual forms from gametocytes. The method is simple and requires little expensive equipment [45, 174, 437]. However, the technique is time consuming and microscopists need to be trained to ensure reliability [45], especially at low parasitaemia [411].

There are several alternative diagnostic tests available besides direct light microscopy (Table 1.2). Various rapid diagnostic tests exist which do not quantify parasitaemia but can identify species or differentiate between species. These antigen detection or dipstick tests require no electricity or special equipment, are fast, require little training and can be stored at ambient temperatures. These tests can however remain positive after parasite clearance

[259]. Molecular tests identifying parasite genetic material through polymerase-chain reaction techniques are also available. These methods effectively distinguish between parasite species and identify resistance and mixed infections. They are however costly, require electricity, special equipment and require a high degree of operator training. Fluorescent microscopy provides faster results than light microscopy techniques however have poor sensitivity at low parasite densities. Electricity and specialised equipment and consumables are also required for fluorescent diagnosis. It should be noted that a requirement for reliable electricity, which is assumed in first world settings, is often lacking in areas where malaria diagnosis is of greatest importance, such as many areas in Africa.

The diagnostic performance of microscopic methods has been shown to be equivalent in clinical settings in both sensitivity and specificity to other diagnostic methods, although this may be over estimated. Ochola *et al.* [275] found that HRP2-based techniques are better than standard microscopy for monitoring *P. falciparum* infections in clinical cases in endemic areas, and that microscopy is still important for the diagnosis of mixed infections and parasite quantification. The role of microscopy as the gold standard for malaria diagnosis has been questioned due to false negative results at lows levels of infection, due to the limit of detection and errors in species identification in mixed infections [94, 275].

Table 1.2 – Techniques currently available for detecting malaria parasites in the human host – table adapted from Bloland 2001 [45, 198, 259, 275, 308, 345, 353, 365, 439].

Method	Sensitivity/Specificity	Limit of Detection (parasites/ul)	Cost*	Advantages	Disadvantages
Rapid diagnostic test based on pLDH: (OptiMal - Flow Inc)	sens: spec:	100	1.00	• Differentiates *P.falciparum* from non-falciparum infections. • Speed and ease of use; minimal training requirements to achieve reliable result. • Reportedly does not remain positive after clearance of parasites. • No electricity, no special equipment needed; could be used in community outreach programmes.	• Cannot differentiate between non-falciparum species. • Will not quantify parsitaemia (+/- only).
Rapid diagnostic stick test based on PfHRP-II: (*Para*Sight-F – Becton – Dickinson; Malaria PfTest – ICT Diagnostics)	sens: 84% –97% spec: 81%–100% lower values probably due to low parasite densities	100	0.80 to 1.00	• Speed and ease of use; minimal training requirements to achieve reliable results. • No electricity, no special equipment needed; could be used at health post/ community outreach. • Card format easier to use for individual tests; dipstick test easier to use for batched testing.	• Will not diagnose non-falciparum malaria although subsequent generation tests will be able to do this. • Will not quantify parasitaemia (+/- only). • Can remain positive after clearance of parasites.
Light microscopy	Optimal conditions: sens: >90% spec: 100% Typical field conditions: sens: 25%–100% spec: 56%–100%	5-20 (thick film) 50-200 (thin film)	0.03 to 0.08**	• Species-specific diagnosis. • Quantification of parasitaemia aids treatment follow-up.	• Requires relatively high degree of training and supervision for reliable results. • Sensitivity and specificity dependent on training and supervision. • Special equipment and supplies needed. • Electricity desirable. • Time-consuming.
Fluorescent microscopy: • Acridine orange [AO] stained thick blood smears); • Quantitative Buffy Coat (QBC™) – (Becton-Dickinson)	AO: 42%–93% sens/ 52–93% spec QBC: 89% sens/ >95% spec	100 100	0.03 (AO) to 1.70 (QBC)	• Results attainable more quickly than normal microscopy.	• Special equipment and supplies needed. • Sensitivity of AO poor with low parasite densities. • Electricity required. • Unreliable species diagnosis; non-specific staining of debris and non-parasitic cells. • QBC will not quantify parasitaemia. • Acridine orange is a hazardous material.
Clinical, especially based on formal algorithm such as Integrated Management of Childhood Illnesses (IMCI) or similar algorithm	Variable depending on level of clinical competency, training, and malaria risk (endemicity): with IMCI: low risk: sens: 87% spec: 8% high risk: sens: 100% spec: 0%		Variable depending on situation.	• Speed and ease of use. • No electricity, no special equipment needed beyond normal clinical equipment (thermometer, stethoscope, otoscope, timer).	• Can result in high degree of misdiagnosis and over-treatment for malaria. • Requires close supervision and retraining to maximize reliability.

Table modified from Stennies, 1999, CDC unpublished document.
* Approximate or projected cost given in US dollars per test performed and reflects only cost of expendable materials unless otherwise noted.
** Cost includes salaries of microscopists and expendable supplies; does not include cost of training, supervision, or equipment.

Another common diagnostic technique is clinical or presumptive diagnosis. Reliable diagnosis cannot be made on the basis of symptoms because of their non specific nature; however clinical diagnosis is common in many portions of the malaria-endemic world. In these areas resources and trained staff are so scarce that clinical diagnosis is the only practical option. This method is fast, simple and low cost, consisting of diagnosis being largely made on the basis of

fever symptoms. This approach can identify most patients who do need antimalarial treatment but is also likely to lead to considerable over diagnosis and over treatment [45].

1.2.8 Enumeration of malaria parasites

Since 1910, when Ross and Thomson proposed a method for enumeration of parasite density [326], it has been accepted that parasite density is highly correlated to the severity of the disease, and an important aspect of diagnosis and disease treatment. Clinical practice has since developed and conventional thick and thin films stained with Giemsa, Wright's or Field's stain are the long time standards for diagnosis and enumeration [411].

Blood for films can be acquired clinically by pricking a finger or earlobe or by venepuncture collected in an anticoagulant tube. Blood from a finger or earlobe is ideal as the density of trophozoites and schizonts is greater in blood from a capillary rich area. Additionally, blood collected via venipuncture should be used quickly after being drawn to minimise alteration of the morphology of white blood cells and parasites [259]. Thin films are prepared by spreading approximately 1μL of whole blood along a microscope slide to produce a uniform monolayer of blood cells [140]. The films are then fixed with methanol prior to staining. Thick films are prepared by spreading approximately 3μL of whole blood in a circular pattern to produce a uniform layer of blood approximately 10mm in diameter. The films are stained unfixed, which causes lysis of red blood cells [140, 259]. Thick films provide a much greater degree of sensitivity than thin films for

detection of low levels of parasitaemia. Thin films provide a greater specificity than thick films and allow simpler morphological identification. The thin film is often preferred for routine estimation of parasitaemia as organisms are easier to see and count. Examination of sequential films enables response to therapy to be easily monitored.

The sensitivity that can be achieved by an experienced microscopist using thick films is approximately 50 parasites per μL of blood, assuming 5×10^6 red blood cells per μL. This is equivalent to 0.001% infection. The routinely achievable sensitivity is closer to 0.01% or 500 parasites per μL [254]. Compared with thick films, thin films are only one tenth as sensitive [411].

The most important aspect of reporting malaria enumeration is the estimation of the level of parasitaemia present on a blood film. Several methods have been described using either thin or thick films [431]. Using thick films the parasites present in 1μL can be estimated using white blood cells (WBC) and assuming 8000WBC/μL. The microscopist counts the number of parasites until 200 WBC have been observed, then multiplies the number of parasites by 40 to estimate parasites/μL. This type of estimation can be improved if an accurate WBC count is known. Using thin films the number of parasitised RBC observed in 10,000 RBC is approximated by determining an approximate number of RBC per field of view. If a field of view contains approximately 250 RBC, 40 fields of view would need to have infected RBC counted. The number of parasitised cells is then

expressed as a percentage. From a percentage the number of parasites present in 1μL of blood can be estimated by assuming that 1μL of blood contains 5×10^6 RBC. The accuracy of this method can be increased if the number of RBC/μl is known accurately.

It should be noted that parasite enumeration in endemic areas tends to be expressed as parasites/μL, while in non endemic areas, where parasitaemia is usually low, percentage of infected erythrocytes is used [259]. Counting parasites in a limited number of fields (for example 10, rather than 40) is used when higher parasitaemia are observed in endemic areas. The methods outlined here for parasite enumeration are acceptable for the clinical management of malaria. However for accurate parasite enumeration thin films should be used to determine the percentage parasitaemia [151].

1.2.9 Parasite clearance

Malaria parasites are cleared from the bloodstream by the reticuloendothelial system, and principally the spleen, where damaged or dead parasites are removed, and previously parasitised red blood cells are returned to the circulation [85]. Asplenic patients demonstrate a reduced capacity to remove parasites despite intense antimalarial therapy and even when parasites are determined to be non viable. This has led to the theory that splenic pitting may be the principal mechanism for removal of circulating parasites following antimalarial therapy [86, 219]. Other tissues, particularly the liver, are also believed to play a role in parasite clearance, although this has not been fully

elucidated. The deposition of haemozoin in macrophages and Kupffer cells during malaria infection indicates that the liver could take on some of the storage and extraction functions of the spleen [413]. This is also backed by the ability of the liver to remove bacteria, viruses and other organisms from the circulation [19].

Parasite clearance can be divided into several stages. The three basic phases are lag, clearance and patency (or “tail”). During the lag phase parasitaemia can continue to increase after treatment administration as the drugs are absorbed, distributed and act to destroy parasites. A lag phase is not seen in all cases [128]. The second phase is clearance, where the spleen and possibly the liver act to remove parasitised RBC or parasites from circulation. There is some suggestion that the rate of clearance is dependent on the drug treatment [104, 128, 196, 232, 233, 428]. Late in a successful clearance phase parasitaemia will drop below the limit of detection (patency). At these very low levels accurate data of parasitaemia is difficult to obtain. It is thought that at these low levels the immune system is able to clear the remaining infection more effectively.

Parasite clearance time (PCT) is the time from commencement of treatment to the first of at least two negative smears. The PCT is reliant on the frequency of smears, so the time to reach 50% of the original parasitaemia (PCT_{50}) is often used as a measure of drug efficacy [425]. PCT is important as a potential indicator of treatment failure and parasite resistance to drug treatment. This is particularly critical for artemisinin based compounds where prolonged parasite

clearance is the only currently identified indicator of resistance [128]. Sowunmi *et al* [361] proposed that *P. falciparum* clearance exceeding two days is associated with risk of treatment failure and resistance, and could be used as a criterion to change therapy in children.

Several studies have investigated modelling of parasite clearance to provide a parasite clearance estimator (PCE). Modelling allows standardisation of parasite clearance estimates from parasite density time profiles and facilitates improved epidemiological investigations of resistance. This is accomplished by identification and exclusion of the lag (if it exists) and patency phases and calculation of the slope of the clearance phase. Parasite clearance follows a first order process and so the clearance rate is constant [105]. If parasitaemia at time t is given by $P_t = P_0^{(-kt)}$ where P_0 is the initial parasitaemia, then the reduction in the parasite population in a unit time is $1 - e^{-k}$. The clearance rate constant is equal to the minus slope of the $\log_e$ parasitaemia-time profile. Several models have been proposed to identify the clearance phase and elucidate the PCE including log-linear, log-quadratic and log-cubic [104, 128]. Log-linear PCE models clinical data with little or no lag phase and little or no tail. Log-quadratic models a lag phase with little tail while a log-cubic models both lag and tail (Figure 1.4). In a comparison of quinine and ACT treatment data by Flegg *et al* [128] using the modelling described here, quinine data showed a greater lag phase and an extended lag phase compared with ACT data.

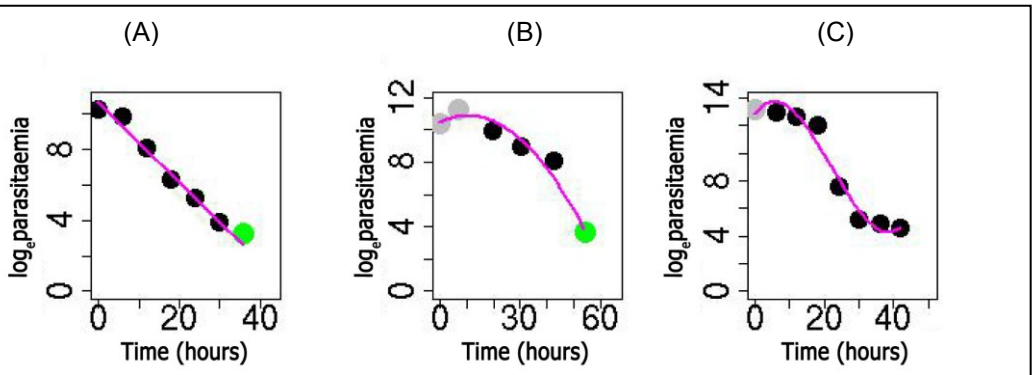

Figure 1.4 – Typical (A) linear, (B) quadratic and (C) cubic shaped log parasitaemia time profiles in falciparum malaria [128]. Polynomial fits are shown in pink, black points represent data and green points represent censored values.

There are a number of examples of more advanced modelling of parasitaemia-time data in humans [318, 334]. These are referred to as within-host models of individual infection or asexual blood stage models as distinct from epidemiological models of population infection and transmission.

1.2.10 Mathematical models of malaria transmission

Mathematical models of malaria transmission began with Ronald Ross, soon after his demonstration of transmission by mosquitoes. Ross himself explained [245]

"To say that a disease depends upon certain factors is not to say much, until we can also form an estimate as to how largely each factor influences the whole result. And the mathematical method of treatment is really nothing but the application of careful reasoning to the problems at issue…from such reasoning alone we derive the very important practical conclusion that in order to

counteract malaria anywhere we need not banish Anopheles there entirely – we need only to reduce their number below a certain figure."

With the discovery of malaria parasites and the role of the mosquito vector, the fight against malaria was to begin in earnest, initially with modelling epidemiology. Ross believed that understanding malaria epidemiology would provide the answer to fighting the disease. In Ross' epidemiological compartmental model of infectious disease, transmission of infectious agents in the host population is the basic process that requires description. Ross' model (Table 1.3) showed that reduction of mosquito numbers below a "transmission threshold" was sufficient to counter malaria [324]. In the 1950s George Macdonald similarly concluded that "*The aim of mathematical epidemiology is to integrate circumstantial data into one coherent whole*" [236]. One of Macdonald's most important contributions to malaria theory was his emphasis on defining and measuring parameters, such as the basic reproductive number and stability index, that were operationally relevant for eradication [84].

Macdonald integrated biological information of latency in the mosquito due to parasite development and identified the survival of adult female mosquitoes as the weakest element in the malaria cycle. Macdonald suggested that increasing the daily mortality of the vector from 5% to about 45% would be enough to solve the malaria problem, and this formed the basis for a DDT-focussed WHO coordinated campaign [236]. The campaign was hugely successful in full eradication of malaria from some 35-40 countries, however failed ultimately in

tropical areas with stable malaria [245]. The failure was due to an incomplete understanding of malaria, its biology and epidemiology, rather than a failure of the models and their concept. Macdonald's original modelling did not include population dynamics, seasonal *Anopheles* population dynamics and elements of the malaria cycle that were at that time undiscovered [245]. Shortcomings of these models were used to improve understanding and improve epidemiological modelling, as demonstrated by Anderson and May by including latency in humans (Table 1.3). Since then, epidemiological modelling has progressed to include vector characteristics, human immunity, parasite diversity, insecticide resistance dynamics, drug resistance dynamics, environmental and seasonal changes and spatial heterogeneity [26, 113, 117, 158, 206, 245].

McKenzie made a number of astute comments in his article *Why Model Malaria?* in 2000 [245]. "*The utility of a malaria model depends not so much on how well a mathematical job has been accomplished as on how well a particular biological question has been translated, how thoroughly each assumption and its consequences have been tested, how carefully the range of relevance has been bounded, how closely descriptions and predictions fit data and the broader purpose, and how much its development has suggested explanations and deepened biological understanding." "Models are made to fit past and predict future data because these achievements improve hypotheses." "A model is useful if it sharpens questions, points to what is missing in our data or in our conceptual grasp, and contributes to a larger process that will render it obsolete; a model that cannot be shown to be wrong is typically of little use*."

Table 1.3 – Basic malaria models where S_h, I_h, E_h and S_m, I_m, E_m are epidemiological compartments representing susceptible, infected and exposed human and mosquito populations. Table adapted from Mandal *et al* 2011 [239].

Models	Reproductive Number	Parameters
Ross Model $\frac{dI_h}{dt} = a\,b\,m\,I_m\,(1 - I_h) - r\,I_h$ $\frac{dI_m}{dt} = a\,c\,I_h\,(1 - I_m) - \mu_2\,I_m$	$\frac{m a^2 b c}{r \mu_2}$	a : Man biting rate [0.01-0.5 day^{-1}] b : Proportion of bites that produce infection in human [0.2-0.5]
Macdonald Model $\frac{dI_h}{dt} = a\,b\,m\,I_m(1 - I_h) - r\,I_h$ $\frac{dE_m}{dt} = a\,c\,I_h(1 - E_m - I_m) - a\,c\,I_h(t-\tau_m)\,[1 - E_m(t-\tau_m) - I_m(t-\tau_m)]\,e^{-\mu_2\tau_m} - \mu_2 E_m$ $\frac{dI_m}{dt} = a\,c\,I_h(t-\tau_m)\,[1 - E_m(t-\tau_m) - I_m(t-\tau_m)]\,e^{-\mu_2\tau_m} - \mu_2 I_m$	$\frac{m a^2 b c}{r \mu_2} e^{-\mu_2 \tau_m}$	c : Proportion of bites by which one susceptible mosquito becomes infected [0.5] m : Ratio of number of female mosquitoes to that of humans [0.5-40] r : Average recovery rate of human [0.005-0.05 day^{-1}] μ_1: Per capita rate of human mortality [0.017 year^{-1}] μ_2: Per capita rate of mosquito mortality [0.05-0.5 day^{-1}] τ_m: Latent period of mosquito [5-15 days] τ_h: Latent period of human [10-100 day]
Anderson and May Model $\frac{dE_h(t)}{dt} = a\,b\,m\,I_m(t)(1 - E_h(t) - I_h(t)) - a\,b\,m\,I_m(t-\tau_h)\,[1 - E_h(t-\tau_h) - I_h(t-\tau_h)]\,e^{-(r+\mu_1)\tau_h} - r\,E_h(t) - \mu_1 E_h(t)$ $\frac{dI_h(t)}{dt} = a\,b\,m\,I_m(t-\tau_h)\,[1 - E_h(t-\tau_h) - I_h(t-\tau_h)]\,e^{-(r+\mu_1)\tau_h} - r\,I_h(t) - \mu_1 I_h(t)$ $\frac{dE_m(t)}{dt} = a\,c\,I_h(t)\,[1 - E_m(t) - I_m(t)] - a\,c\,I_h(t-\tau_m)[1 - E_m(t-\tau_m) - I_m(t-\tau_m)]e^{-\mu_2\tau_m} - \mu_2 E_m(t)$ $\frac{dI_m(t)}{dt} = a\,c\,I_h(t-\tau_m)[1 - E_m(t-\tau_m) - I_m(t-\tau_m)]e^{-\mu_2\tau_m} - \mu_2 I_m(t)$	$\frac{m a^2 b c}{r \mu_2} e^{-\mu_2 \tau_m} e^{-\mu_1 \tau_h}$	

1.2.11 Mathematical models of within host asexual dynamics

Several groups have developed mathematical models of *P. falciparum* asexual parasitaemia or within host parasite dynamics [17, 175, 256]. This is a complex process involving the estimation of a large number of biological variables as described by Molineaux *et al* [256], including:

- total parasite density
- basic parasite multiplication
- density of parasite variants
- probability that a parasitised RBC switches gene variant
- variables describing the probability of a variant escaping innate immune responses

This simplified list outlines the daunting task facing modelling of within host *P. falciparum* dynamics, particularly when considering there are 50 parasite variants per clone. There is also a paucity of untreated *P. falciparum* infection data in humans which serves as the basis for this modelling, due to ethical considerations in acquiring data. The data used in these studies is an untreated subset of 35 of 334 patients infected with either *P. falciparum* or *P. vivax* to treat neurosyphilis from the early 20th century [52, 53, 118, 121, 187, 188].

Models of within host parasite dynamics have been studied to improve epidemiological modelling [191] and to assist in planning and evaluation of intervention trials and control programs [175-178, 256]. Since mathematical models of malaria are contingent on a detailed understanding of the parasite lifecycle, they have improved understanding of infection biology as modellers strive to provide ever more biologically realistic models. This includes understanding of merozoite and gametocyte dynamics [112] resulting synchronicity [395], immune interactions [395] and infection transmission [191].

1.2.12 The importance of mathematical models of malaria

In 2010 the WHO published a progress and impact series report on "Mathematical Modeling to Support Malaria Control and Elimination" [84] for Roll Back Malaria. This report outlines the requirement for global malaria control and eradication to be based on conceptual and mathematical models that allow knowledge to be extrapolated and synthesised in a rational way, providing critical quantitative insights. The reliance on mathematical models is due to the diversity in the range of conditions, biological, environmental and socio-economic that effect malaria. Responses cannot be based solely on evidence acquired through randomised trials in a number of settings [84]. The report also highlights that many questions cannot be answered by field trials as they may be too expensive or unethical.

History is a testament that there are no simple solutions to global control and eradication of malaria. It has taught the lesson that mathematical modelling of biology and epidemiology are crucial to the fight against malaria [84].

1.3 The fight against malaria

Malaria eradication efforts in the Roman Campagna prior to 1889 were based on broad ideas of cleansing the water, air and land without really understanding the source of the malaria sickness [358]. Control programs tended to be successful in developed countries that already had the infrastructure and organisations in place to run large scale health programs.

The first successfully recorded malaria control program was executed from 1905-1910 during the construction of the Panama Canal. Cases dropped from 21,000 of 26,000 workers on the project in 1906 to 5,600 of over 50,000 employees in 1912 through a program of insect and malaria control [78].

A major malaria epidemic during World War I affecting British, French and German armies provided the impetus for research into improved malaria treatment options. This spurred efforts to produce synthetic antimalarials. This era saw synthetic antimalarials provide a cheap, safe and very effective treatment for the malaria infected [78].

In 1939 Paul Müller in Switzerland discovered the insecticidal properties of Dichloro-diphenyl-trichloroethane (DDT). DDT was used for malaria control at the end of World War II after proving to be effective against malaria carrying mosquitoes. Following on from successful war time efforts to control Malaria in troop populations around troop training areas and military bases, the US began the National Malaria Eradication Program in 1947. From 15,000 cases of malaria annually in 1947, malaria was considered eradicated from the US by 1951 [78].

With the success of control programs and availability of DDT and synthetic antimalarials the WHO submitted a proposal for the eradication of malaria worldwide at the 1955 World Health Assembly [279]. Eradication efforts were based around house spraying, drug treatment and surveillance but excluded most of sub-Saharan Africa. Macdonald collected data to test Ross' model for

malaria eradication and helped to explain that insecticides such as DDT worked because they greatly reduced the number of mosquitoes that survived sporogony and could transmit malaria [256]. The program was successful in nations with temperate climates and seasonal malaria transmission, but had negligible traction in countries such as Indonesia, Afghanistan and Nicaragua. The emergence of drug resistance, widespread resistance to insecticides, wars, population movements, sustained funding issues and lack of community participation meant the ultimate failure and abandonment of the program in 1978 [78].

An easily overlooked consequence of the Global Malaria Eradication Program was the attrition to professional staff and research malariologists, which occurred due to the routine workload imposed during the program, war, economic crisis, inadequate funding and a lack of newly trained malaria professionals who would not be required in a world in which malaria was eradicated [265]. In the mid 1970s, WHO launched the Special Program for Research and Training in Tropical Diseases (TDR) in an effort to re-establish the role of research in malaria control which was lacking due to professional attrition, yet critically required to address problems with the Global Malaria Eradication Program [265]. Despite important successes by the TDR, there has existed a rift between malaria control programs and research bodies in which research projects have had little operational bearing on control programs, which themselves have lacked capacity to carry out and guide research [265].

In the early 21st century a concerted effort by endemic countries, donors and global malaria partners has seen a resurgence of interest in combating malaria and a strengthening in malaria control [435]. The gains achieved in this time have no parallel since the Global Malaria Eradication Program [93, 277]. Cohen *et al* [93] have linked 91% of the 75 malaria resurgences since 1930 to weakening of control programmes. There is need to develop practical solutions to the financial and operational threats to sustaining successful malaria control.

1.3.1 Antimalarial strategies

The goal of antimalarial strategies, or malaria control, is to reduce the incidence of infections and deaths due to malarial parasites. Control can be simply divided into preventative actions, which generally target reducing disease transmission, or when this fails, treatment, which requires effective diagnostic tools and therapies. Antimalarial strategies are most effective when multiple strategies are employed simultaneously and include both preventative and treatment strategies. The ultimate end of control programs is to reduce disease transmission to the point where it is no longer a public health problem. Malaria control strategies include vector control, transmission control, prophylaxis, vaccination and treatment.

Malaria chemotherapy can be broadly divided into vaccination, prophylaxis and treatment. Despite substantial effort towards vaccine development for *P. falciparum*, few candidates have shown significant efficacy in clinical trials [65]. Many problems exist in development of an effective vaccine, however the most

telling is the parasite's sophisticated ability to avoid detection by the host immune system. *Plasmodium* express a large number of antigens, have high antigenic variation and antigen allelic polymorphism (or sequence diversity) [33]. Studies have also suggested that *Plasmodium* may immunomodulate by reducing dendritic cell function [142, 252, 253], but also by invading and replicating in dendritic cells [441, 442]. A lack of understanding of parasite host interactions is also a factor in effective vaccines not having been developed.

Malarial chemoprophylaxis generally refers to the use of antimalarial drugs to prevent infection. Mass chemoprophylaxis has been attempted to varying degrees of success and can range from blanket mass administration, as in chloroquine laced salt, to more specific target groups being children and/or pregnant women. An important concern with these types of mass drug administration campaigns is development of resistance. However, prophylactic administration of chloroquine to children in Ghana and Madagascar did not result in the emergence of resistance [307]. This was despite weekly administration to over 1 million children of chloroquine over a 12 year period in Madagascar [161]. Resistance to pyrimethamine after mass prophylaxis in children is well documented [25, 80]. There are also suggestions that chloroquinized salt may have been a major factor in the development of chloroquine resistant *P. falciparum* [284].

1.3.2 Antimalarial treatment strategies

Early diagnosis and prompt treatment is one of the key technical components of any effective malaria control program [5]. The effectiveness of this intervention is reliant upon antimalarial drugs which should be effective and safe, as well as available and affordable to the population at risk. The rational use of antimalarial drugs shortens the duration of illness and reduces chances of severe illness and death. It also reduces the chances and speed of the development of parasite resistance to antimalarial drugs.

In its 2001 Antimalarial Drug Combination Therapy Report of a WHO Technical Consultation [46] the purpose in establishing a national antimalarial treatment policy is outlined to "*enable the population at risk of malaria infection to have access to safe, good quality, effective, affordable and acceptable antimalarial drugs, in order to:*

- *ensure a rapid and long lasting clinical cure for individual malaria patients*
- *prevent progression of uncomplicated malaria to severe disease and death*
- *shorten clinical episodes of malaria and reduce the occurrence of malaria-associated anaemia in populations residing in areas of high malaria transmission*
- *reduce consequences of placental malaria infection and maternal malaria-associated anaemia through chemoprophylaxis or preventive intermittent treatment during pregnancy*

- *delay the development and spread of resistance to antimalarial drugs."*

The report goes on to outline the need to balance two key principles; prompt treatment and ensuring that drugs have a maximum useful therapeutic life. The discovery of the antimalarial properties of chloroquine combined with its safety and low cost spurred malaria eradication efforts in the 1950s. Chloroquine development and distribution was one of the most significant public health interventions of the 20th century [414]. The emergence of resistance diminished its efficacy and led to the demise of these initial eradication efforts, largely due to treatment failure, which in turn led to a resurgence of the disease [416].

1.3.3 A brief history of antimalarial chemotherapy

In 1820, Pierre Joseph Pelletier and Jean Bienaime Caventou announced the isolation of an alkaloid from the Cinchona bark with curative properties, which they named quinine [64]. Quinine quickly became routine for treatment of malaria and remained frontline treatment for malaria in many countries until the early 21st century.

During the First World War Germany was unable to obtain quinine, and as a result many of its soldiers suffered from malaria in southern Europe. To prevent this occurring again, German chemists began working on synthetic alternatives. By the 1930s mepacrine, a simplified version of quinine, was being produced in Germany [357]. Similarly, during the Second World War American troops did not have access to either quinine or mepacrine and set about producing mepacrine

and also developed chloroquine, which proved to protect troops very effectively [321, 373].

Several drug discoveries produced during war efforts were used as prototypes for developing new antimalarials. Proguanil was developed by the British from efforts during the Second World War and led to the development of pyrimethamine. These two compounds began to be used in combination during the 1970s as Fansidar®. Similarly, the Americans developed mefloquine and much later atovaquone from discoveries during the Second World War [321].

Post Second World War, armed with DDT and chloroquine, the WHO began its program to eradicate malaria, which was planned similarly to the successful smallpox eradication program. However, it proved impossible to drain all marshes in tropical regions, *Anopheles* developed resistance to DDT and chloroquine showed decreasing efficacy. Malarial resistance to chloroquine was emerging and during the 1970s chloroquine resistance spread.

The US and Chinese during this time were both searching for new alternatives to chloroquine with different mechanisms of action to avoid the existing parasite resistance mechanisms. The US developed mefloquine to replace chloroquine, while the Chinese isolated artemisinin. At the end of the 1970s Western malariologists Nicholas White and David Warrell became aware of the claims about artemisinin as an antimalarial treatment in China, and in 1981 obtained a

sample of artemisinin to test the Chinese claims. It was confirmed that artemisinin was indeed an effective antimalarial [64].

With all other widely used antimalarials showing diminishing clinical effectiveness, spreading multidrug parasite resistance, and the failure of tropical malaria control programs, artemisinin presented itself as the only saviour. However, use of artemisinin was delayed as it was costly to produce, poorly water soluble making delivery to patients difficult, there were fears of parasite resistance developing to this new drug and it was required to undergo toxicological testing like other new pharmaceuticals in the Western world [64].

1.3.4 Classification of antimalarial chemotherapeutic agents

Antimalarial drugs are generally classified according to their chemical structure, or family, responsible for their antimalarial properties or the stage in the parasites life cycle they primarily display their antimalarial properties. Chemical classification of antimalarials is based on their chemical classes, functions, or a combination of these. Classes include endoperoxides, 4- and 8-aminoquinolines, sulfonamides, amino alcohols, antifolates, antibiotics and “others”. The antimalarial chemical classifications are represented in Figure 1.5 taken from Delves *et al* 2012 [109].

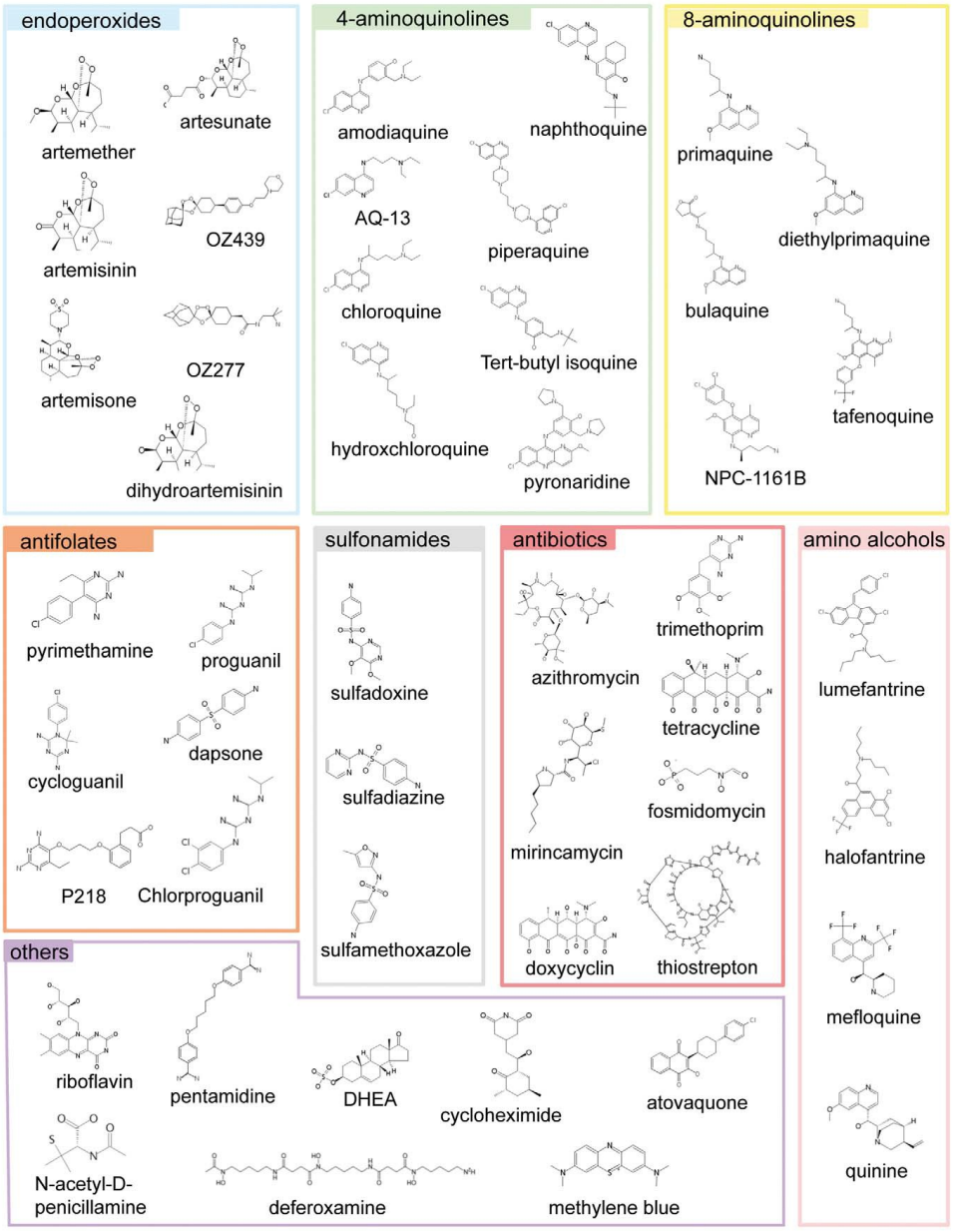

Figure 1.5 – The main classes of antimalarials. The chemical structures of all the main classes of antimalarials and other therapeutic and control molecules are assembled according to either the chemical classes they belong to (endoperoxides, 4- and 8-AQs, amino-alcohols) or their function (antifolate, antibiotics), or both (e.g., sulfonamides, a chemical class of antibiotic used in combined antimalarial therapies) [109].

Antimalarials can also be classified depending on which parasite stage they target as blood schizontocides, tissue schizontocides, gametocytocides,

hypnozoitocides and sporontocides. The stages and chemotherapies targeting these stages are outlined in Figure 1.6 taken from Delves *et al* 2012 [109].

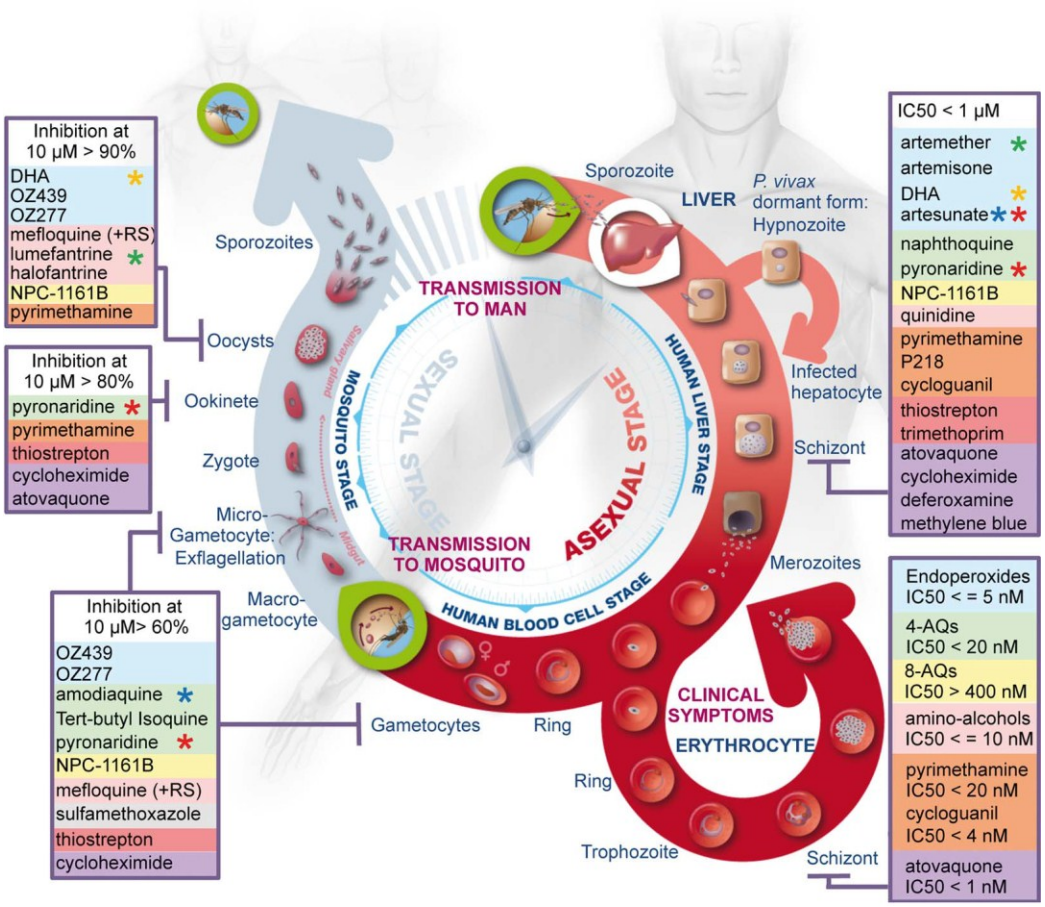

Figure 1.6 – Summary of the activity of the most widely used antimalarials throughout the life cycle of *Plasmodium*. The three main phases, i.e., liver stage, blood stage, and vector stage, of the life cycle of *Plasmodium* are shown. The two key entry points leading to transmission of the parasites from vector to host and from host to vector are indicated (green circles). Parasite forms specific to each stage are highlighted and drugs identified as inhibitors of development of these forms are listed in boxes and coloured as described in Figure 1.5. Stars highlight components of the main artemisinin combination therapies: green, coartem; red, pyramax; orange, eurartesim; blue, fixed dose artesunate+amodiaquine [109].

Blood schizontocides act on the asexual erythrocytic forms of *Plasmodium* species. The majority of common antimalarials fall into this category including

quinine, chloroquine, mefloquine, sulfadoxine, tetracyclines and artemisinin derivatives [27, 180, 208]. Tissue schizontocides target tissue schizonts or latent hypnozoites and include primaquine, pyrimethamine and proguanil. They are used as prophylactics or to prevent relapse of *P. vivax* or *P. ovalae* [27, 180, 208]. Gametocytocides kill sexual forms of *Plasmodium* and so prevent transmission to mosquitoes. Chloroquine and quinine have gametocytocidal activity against *P. vivax* and *P. malariae* but not against *P. falciparum*, for which primaquine is commonly used [27, 180, 208]. There is also some evidence that artemisinins have gametocytocidal activity against *P. falciparum [167, 306].* Sporontocides, including primaquine, pyrimethamine and proguanil prevent development of malaria in mosquitoes via inhibition of oocyst and sporozoites [27, 180, 208].

1.3.5 Optimisation of antimalarial chemotherapy

Many of the antimalarial drugs in current use were introduced at suboptimal doses [423]. Improved or optimised dosing should limit the emergence and spread of resistance and maximise cost benefit [382, 423]. However there is currently no clear or established method for assessing optimisation of antimalarial chemotherapy. White [423] suggests that investing in characterisation of drug pharmacokinetic and pharmacodynamic relationships will likely lead to improve antimalarial dose regimens. This would increase the chance of selecting optimum treatment regimens in the future and reduce suboptimal dosing.

1.4 Resistance

The control of malaria relies heavily on drug therapies. The Global Malaria Eradication Program failed due to a broad range of reasons, although chief among these was reliance on and development of resistance to chloroquine, and subsequently other chemotherapeutic agents. Chloroquine (CQ) was first introduced into the clinical setting in 1945, and its effectiveness drove the effort to eradicate malaria. However by the late 1950s CQ resistant *P. falciparum* was reported in South East Asia and South America. Within 50 years CQ resistant *P. falciparum* was almost ubiquitous [438]. *P. falciparum* strains also developed resistance to all commonly used antimalarials including mefloquine and sulfadoxine-pyrimethamine. In the past 50 years resistance to new antimalarials has developed within a short number of years after their introduction (Table 1.4).

Table 1.4 – Dates of Introduction and first reports of antimalarial drug resistance adapted from Wongsrichanalai *et a*l 2002 [43, 234, 290, 417, 438, 440].

Dates of introduction and first reports of antimalarial drug resistance			
Antimalarial Drug	**Introduced**	**First reported Resistance**	**Difference (years)**
Quinine	1632	1910	278
Chloroquine	1945	1957	12
Proguanil	1948	1949	1
Sulfadoxine-pyrimethamine	1967	1967	0
Mefloquine	1977	1982	5
Atovaquone	1996	1996	0
Artemisinins	1980	2008	28

Resistance is an operational rather than an absolute term, with large differences possible between *in vitro* and *in vivo* results although in general terms it is the "ability of a parasite to survive in the presence of concentrations of drug that normally destroy parasites of the same species or prevent their multiplication" [412]. For this reason the WHO developed an *in vivo* classification system of response to CQ in the 1970s (Table 1.5). This classification has subsequently been used for assessment of response to other drug treatments [32].

Table 1.5 – Classification of response to antimalarial drug treatment [32, 422].

Classification	Response	Criteria
S	Sensitive	Marked reduction in asexual parasitaemia to less than 25% of the admission parasite count within 48hrs of commencing drug treatment. Clearance of asexual parasitaemia with seven days and no recrudescence (radical cure).
RI	Low Grade Resistance	Marked reduction in asexual parasitaemia to less than 25% of the admission parasite count within 48hrs of commencing drug treatment. Clearance of asexual parasitaemia within seven days. Recrudescence within 28 days of commencing drug treatment.[a,b]
RII	High Grade Resistance	Marked reduction in asexual parasitaemia to less than 25% of the admission parasite count within 48hrs of commencing drug treatment. Parasitaemia is not cleared although parasites may be undetectable for a short period of time. Early recrudescence.[a]
RIII	High Grade Resistance	No significant reduction in asexual parasitaemia within 48hrs of commencing drug treatment. Parasitaemia is not cleared and may rise despite drug treatment.

[a] Recrudescence may be difficult to differentiate from reinfection. For RI and RII classifications to be considered valid, patients must remain in a non-endemic area where the risk of reinfection is low.
[b] The length of time for recrudescence may be substantially longer for drugs with exceptionally long elimination half-lives.

1.4.1 A brief history of chemotherapy resistance

P. falciparum drug resistance to quinine was first reported in 1910 [415, 419]. Treatment failure due to resistance was observed in the late 1940s [287]. A number of failures of the global malaria eradication program including funding,

administrative, organisational failings and insecticide resistance lead to a heavy dependence on drug treatment to maintain the program in many developing malarious regions. Subsequent over use and lack of controlled application of CQ coupled with the other failings of the eradication program led to the speedy development and spread of resistance. Treatment failure continued to be observed in the 1950s and 1960s to a variety of antimalarials [287]. By the 1970s chloroquine was no longer effective in the majority of South-East Asia and by 1978 the first cases of resistance in east Africa were reported. By the early 1980s 75% and 82% of infections in Kenya and Malawi respectively were found to be CQ resistant [47]. As resistance spread morbidity and mortality due to malaria increased [391, 452]. Alternative front line treatments were employed and CQ was replaced with combinations of sulfonamides and pyrimethamine [110]. This replacement of front line drugs was however very slow in some areas, contributing to the worsening spread and development of resistance. Between 1978 and 1988 resistance to CQ was reported in all tropical African countries and by 1989 resistance was widespread in sub-Saharan Africa [438]. Despite these reports, chloroquine remained the first line treatment of malaria until after 2000 in most of these countries [390]. Resistance to sulfadoxine-pyrimethamine was first observed on the Thai-Cambodian border in the mid 1960s [43]. By 1982 both pyrimethamine-sulphadoxine and chloroquine were ineffective against *P. falciparum* in Thailand [419]. A decade later quinine was only 50% effective and only 7 years after its introduction, mefloquine was less than 50% effective [419]. The emergence of mefloquine resistance may have

been influenced by the heavy use of quinine, which is functionally similar, prior to the introduction of mefloquine.

In 1971, Qinghao which was first documented as an antimalarial treatment in 340AD was rediscovered, purified and the chemical structure of the active constituent identified and officially named artemisinin [152]. Early clinical studies of artemisinin demonstrated rapid and high initial cure rates and high recrudescence [107, 171]. By the 1980s several semi-synthetic derivatives of artemisinin including dihydroartemisinin, artesunate, artemether and arteether had been developed as more potent treatment options. Due to increasing resistance and a lack of other suitable new antimalarials, artemisinin compounds began to be used clinically. The high frequency of recrudescence due to the short half-life of this family of compounds meant that artemisinins were soon paired with other existing antimalarials with longer half-lives. The artemisinin combination treatments (ACTs) allowed faster cure, less recrudescence, slowed the emergence of resistance and allowed compounds that were no longer effective monotherapies to continue to be used.

Until 2008, the artemisinin family of antimalarials remained the only group for which clinical resistance in *P. falciparum* had not been observed. In 2009 Dondorp *et al* [114] reported a marked reduction in *in vivo* sensitivity of *P. falciparum* cases to artesunate in western Cambodia and north-western Thailand. This spurred an already building international momentum for a resistance containment plan in Cambodia in an attempt to prevent the

emergence and spread of true artemisinin resistance, which could potentially stall current efforts to eradicate malaria, as CQ resistance had 50 years before.

1.4.2 Determinants of antimalarial resistance

The development and spread of resistance to CQ is evidence that determinants of both development and spread need to be understood to avoid the catastrophic consequences of similar resistance to artemisinin combination therapies. The determinants of resistance can be grouped into drug, human, parasite and vector.

Resistance to chemotherapy depends on certain drug factors. Resistance to drugs with short half-lives develops more slowly than drugs with long half-lives. Parasites are exposed to concentrations of short half-life drugs below the mean inhibitory concentration for shorter periods than for drugs with long elimination half-lives [415]. This is due to more frequent dosing and the shorter period after the last dose that parasites have exposure to less than mean inhibitory concerntrations. This is one of the major benefits of artemisinin compounds over longer half-life counterparts such as mefloquine, chloroquine and piperaquine. Drugs such as mefloquine may exert significant residual selection on new infections contracted after the treatment of the primary infection [438]. The maintenance of adequate drug concentrations for clearing the entire parasite population is important. Use of subtherapeutic doses in treatment, poor compliance and mass prophalactic drug administration risk killing susceptible parasites and selecting for those with greater fitness, leading to the emergence

and spread of resistance. Wide spread and intense use of drugs increases drug pressure and the probability of selection of resistant parasite populations.

Human factors such as immune status play an important role in resistance. Introduction of resistant malaria into non-immune populations increases the opportunity for emergence and spread of resistance. Immune populations are more able to clear low level parasite infections than the non-immune, so parasites with low or moderate resistance are more likely to be cleared in semi-immune populations.

Parasite factors also influence the emergence and spread of resistance. Increased risk of resistance emerging has been proposed in areas of both low and high levels of transmission [165, 257]. The fact that resistance developed earlier in areas of lower transmission, such as Thailand, and is still more prevalent in these areas seems to support the low transmission hypothesis. Other parasite determinants relating to genes and gene mutations are also important in the development and spread of resistance. Vector and environmental factors may effect the proliferation of resistant parasites over non-resistant strains.

1.4.3 Combating antimalarial drug resistance

The emergence and spread of drug resistant parasites is a major challenge in the fight against malaria. The efficacy of artemisinin based combination regimens must be maintained because no practical alternative exists.

Resistance and particularly multidrug resistance must be contained. Logically and out of necessity antimalarial combinations are required to limit spread and further emergence of antimalarial resistance. Unfortunately the use of effective combinations began too late to prevent or slow resistance and its spread.

Ensuring continued efficacy of existing agents requires surveillance, early and rapid detection of resistance, and containment of its spread [87, 115, 153, 270, 303, 346, 404]. This requires that resistance is detected while at a low level and low frequency, so well before it is an obvious clinical risk. The tools for this form of surveillance are molecular markers for resistance, *in vitro* susceptibility tests and therapeutic efficacy tests [251]. Each of these methods has distinct limitations and they struggle to detect the emergence of resistance early enough to allow effective containment [123, 251, 375, 404].

1.5 Malaria models

The study of human malaria involves an array of methods from epidemiology to population genetics to clinical studies in the field or hospital settings to analyses of post-mortem biopsies. There are however limitations involving collection, use and access to human data and samples. Access to post-mortem tissues can be obstructed by religious and cultural objection. There is often a lack of proper controls [454]. In depth longitudinal research requires invasive analysis to monitor disease and pathological progression and invasive biological sampling is often not possible. Models provide a necessary tool for researchers over which they can impose varying degrees of control to explore scientific

hypotheses. There are many types of malaria models aside from epidemiological and within host dynamic models which have already been discussed.

As with many biological systems and diseases, a significant proportion of human understanding of malaria has resulted from *in vitro* and *in vivo* models of the disease. These models allow study of specific aspects of the disease and facilitate varying degrees of control over variables be they biological, chemical, cultural, environmental and ethical that can confound purely clinical research. Clinical work and clinical research leading to improvement in patient care and effective treatment are the ultimate goals of any malaria research. There are however certain limitations to clinical research especially in the case of life threatening diseases. In humans infected with *P. falciparum*, it has been difficult to investigate the early kinetics of events leading to clinical manifestations, and the factors responsible for the onset of a variety of symptoms remain unclear. During the rare experimental inoculations performed in man, both the duration of the infection and the number of factors investigated were limited, due to the requirement for early treatment and other obvious ethical considerations [119, 244].

1.5.1 *In vitro* models of malaria

In vitro models of malaria have been used for some time predominantly in drug screening and parasite sensitivity studies using human [34, 35, 48, 71, 83, 271, 397] and animal malarias [173, 186, 312]. More complex *in vitro* models also

exist. Lertyot *et al* in 2005 [393] reported an *in vitro* blood brain barrier model utilising cultures of porcine brain capillary endothelial cells to study blood brain barrier disruption by *P. falciparum*. This *in vitro* system was used as a model of cerebral malaria to detect decreases in the endothelial barrier function and disruption of tight junction complexes.

The short coming of *in vitro* models is closely related to the advantages they provide. They enable a vast amount of experimental control however this comes at the expense of providing data that is relevant to the clinical setting. For this reason *in vitro* research is mostly useful for providing study of isolated mechanistic principles (such as in the case of Lertyot *et al* [393]) and elucidation of aspects of host-parasite biological involvement, which due to the simplification of the models may or may not be clinically relevant.

Animal models provide an important link between *in vitro* and clinical research and attempt to balance control and simplification of the clinical scenario while providing greater clinical understanding.

1.5.2 Animal models of malaria

Investigation of such a complex disease as malaria, which involves host and parasite biological systems and their interaction with each other and on chemotherapy agents is arguably best suited to research in an animal model in combination with limited human-based research [119] to confirm the translation of findings from preclinical to clinical. In this setting the time courses, doses,

parasite strains, environment, nutrition, and many other variables including host and parasite genetics can be controlled by the investigator. Animal models also allow indepth collection of data usually unable to be collected clinically due to it being overly invasive in humans. The data is more relevant to the clinical setting as it is being collected from a complete, or almost complete biological system with all its complex interactions. In many cases animal models are the only solution for researchers to test new hypotheses, which often can not be attempted in humans [215].

1.5.3 Non-human primate models of malaria

Early research into animal models of malaria focussed on infecting primates with human forms of malaria. There is a distinction between animal models of malaria, and animal models of human malaria, the later using human malaria such as *P. falciparum* in an animal model. Early models were animal models of human malaria. The traditional concept held at the time that susceptibility of an animal to human malaria depended upon it closeness to humans in evolutionary phylogeny. In 1893 Laveran made the first unsuccessful attempt to inoculate human malaria parasites into laboratory animals [190]. Arguably the first successful inoculation of parasites into animals is recorded by Mesnil and Rouband in 1917 with the successful infection of the black chimpanzee with *P. vivax* [190]. The infection in black chimpanzees lasted only 22 days, and some years later Mesnil and Roubaud dismissed their own initial claims of successful inoculation. While these early models were of limited clinical value, they paved the way for many more efforts to establish an animal model of malaria. From

1917 *P. falciparum* was used to inoculate bats, rhesus monkeys, *Macca irus* monkeys, black chimpanzees, pigs, guinea pigs, rats, mice, rabbits, dogs and golden hamsters [190].

There were several other reports of successful inoculations in black chimpanzees with *P. vivax* although these experiments required splenectomy of the animals in order for erythrocytic stages to be viable and parasitaemia to reach greater than one percent [190]. In 1966 Cadigan *et al* showed that the Thai gibbon, was susceptible to *P. falciparum* infection [67, 68, 146, 410]. The Thai gibbon was the closest animal model yet observed to human malaria, although the infection was not fatal, animals were splenectomised in order for parasitaemias to reach 8% and infected gibbons were not able to infect mosquito species with malaria. In the same year Young *et al* also successfully infected *Aotus* monkeys with *P. vivax* [449, 450]. The *Aotus* monkeys proved to be a very good model for human malaria, after several generations of infection monkeys were not required to be splenectomised and parasitaemias and symptoms were reported to be similar to the human disease. This discovery of *Aotus* monkeys as being more susceptible to human malaria than chimpanzees and gibbons also went against traditional concepts of human malaria susceptibility being associated with evolutionary links or similarities.

Despite the promise of non-human primate models of malaria as a research tool for human malaria there are some largedisadvantages. There is a high and growing degree of public concern and opposition on moral and ethical grounds

for utilising primate animal experimental models. Additionally chimpanzees and gibbons are large animals that are relatively scarce. *Aotus* monkeys are smaller, however they are difficult to rear under experimental conditions [133, 215].

It is worth noting that there has been expressions from the research community in recent years to supply additional funding to the non-human primate malaria models as they provide excellent human malaria models and have been underutilised [133, 215]. They lack some of the advantages of other animal models in that the genomes of the primate malarias have not been sequenced and this could provide valuable data for gene expression studies. There is also concern that without funding and encouraging of young researchers to utilise non-human primate models of malaria, these research models could be lost [215].

1.5.4 *In vivo* models for drug screening

The importance of *in vitro* systems for antimalarial drug screening has already been mentioned. This method is useful for identifying compounds with true plasmodicidal activity, however not compounds with plasmodistatic action such as proguanil, pyrimethamine and sulphonamides [381]. In W. Peters words “For screening of drugs against malaria one must eventually fall back on *in vivo* tests in laboratory models”. The evolution of *in vivo* models for drug screening can be divided into three periods. Between 1926-1935 tests for drug actions used *P. relictum* in canaries. During World War II a vast screening program developed based on the avian *P. gallinaceum* in domestic chicks. These models were

replaced shortly after the discovery of rodent *Plasmodium* species from 1948. The rodent malaria models soon became widely used and characterised for not only drug screening, but for studying many other aspects of malaria. Davey in 1963 summed up the difficultly of the choice between malaria models at that time, giving an indication of why the rodent malaria models are now so wide spread.

"*Monkeys are expensive and awkward to handle: they will also consume a lot of drug because of their size. Canaries are not easy to get in large numbers, they are relatively expensive, and they are delicate creatures. Mice are common, cheap, easily houses and handled. Chicks are also cheap and easy to handle, but they require extra heating. Finally, pigeons require much space, turkey poults are expensive, and ducks smell!*" [101]

1.5.5 Murine models of malaria

In 1948 Ignace Vincke reported *Plasmodium* species in African thicket rats [405]. It was subsequently discovered that these parasites, named *Plasmodium berghei*, were not only able to exist in their natural host, but also to infect laboratory rats, mice and hamsters [293]. Three other rodent-specific *Plasmodium* species were also isolated *P. vinckei, P. yoelli and P. chabaudi* [200, 211, 316]. Several other species of malaria parasites in rodents have been described although these have not been investigated in detail [201]. The rodent malaria species were found to be analogous to human malaria species in the most essential aspects of structure, physiology and the life cycle (Table 1.6) [74,

212]. The advantages of rodent-based models are that they are cheap, easy to develop and maintain, robust, and versatile relative to other animal models such as the non-human primate models [213]. Large scale invasive and interventional studies are possible in rodent models as opposed to simian and human models due largely to ethical and logistical considerations [379].

Table 1.6 – Characteristics of the four murine malaria parasites compared with human parasites [74, 201, 212, 293].

	Human Parasites	*P. berghei*	*P. vinckei*	*P. yoelli*	*P. chabaudi*
Merozoites per schizont	8-16	12-18	6-12	12-18	6-8
Reticulocyte preference	Yes/No	Yes	No	Yes	No
Synchronous blood infection	Yes/No	No	Yes	No	Yes
Sporozoites in glands days after infection	Temp dependent	13-14	10-13	9-11	11-13
Optimum Temp. for Mosquito transmission (°C)	>26	19-26	24-26	23-26	24-26
Duration of pre-erythrocytic cycle (h)	6-15 days	48-52	60-72	35-50	50-58
Duration of asexual blood stage (h)	48-72	22-24	24	18	24
Development time gametocytes (h)	48h – 12days	26-30	27	27	36

As with results from any model, those from murine models of malaria must be applied carefully to the clinical setting. Unsurprisingly there are important differences between human and rodent physiology. Extrapolation of findings from murine experiments are often controversial and concerns exist about the translational utility of animal models in pathogenesis, immunity, vaccine development and drug discovery [99, 427]. The goal of preclinical research is to

improve clinical understanding. This can only be accomplished with a good understanding of the strengths and weakness of a model, the basis of which is the similarities between the model and the clinical case.

1.5.6 The value of murine malaria models

Since their discovery, the murine models of malaria have been used extensively as screening tools for new antimalarial chemotherapy agents. They have also contributed to understanding of parasite morphology [11, 237, 349], genetics [72, 408, 409], protein function [249, 371, 372], immunity [216, 301, 368], vaccine development [116, 120, 172, 273, 300], drug development [260, 288, 322], resistance [204, 309, 321, 335], cerebral malaria [169, 195, 267, 315] and almost all other aspect of malaria researched. As well as the study of disease mechanisms, rodent models allow simple maintenance of the entire parasite life cycle in controlled and optimised laboratory conditions. Use of transgenic animals and parasites allows detailed study of host-parasite interactions [131, 144, 302, 314, 378, 455].

Developments in preclinical imaging technologies are providing researchers with greater opportunities to explore and characterise malaria pathology in animal models and explore the similarities with the human pathology.

1.5.7 *P. berghei* murine malaria

Plasmodium berghei is the most comprehensively studied and manipulated of the four murine malarias. *P. berghei* infects 37 animal species including African fruit bats and new born rabbits, however laboratory species of albino rats and

mice are by far the most commonly used hosts [293]. Early characterisation of *P. berghei* in laboratory rodents provided information on the similarities between *P. berghei* and human malaria species. These demonstrated similarities between the primate and *P. berghei* life cycles [447], ability to be passaged through anophelines [214], and similarities in sensitivities of drugs to *P. falciparum* and *P. berghei* [286]. Characteristics of *P. berghei* infections in laboratory rodents include a preference for reticulocytes, asynchronous infection and infection is generally lethal in laboratory models, although this is influenced by species and ages of hosts [453]. Cerebral effects may also be observed in certain rodent species, although the mechanisms for this are considerably different to those in human cerebral malaria. The morphology of asexual *P. berghei* is similar to that of *P. vivax* as can be seen in Figure 1.7 compared with Figure 1.3.

There are small differences between *P. berghei* parasites of different isolates and laboratory lines that influence the characteristics of infection. Variations are generally the result of variations in environmental factors, hosts and genetic differences between parasite isolates. These factors can influence the course and intensity of blood infections, gametocyte production, virulence and pathology [214].

P. berghei shows a pronounced preference for reticulocytes. There is little difference between isolates in terms of reticulocyte preference, however there are reports that the NK65 isolate has a greater preference for reticulocytes than

the ANKA isolate in Swiss mice [108]. The number of merozoites per erythrocytic schizont is greater in reticulocytes (~12-18 merozoites per RBC) than in more mature red blood cells (~6-12 merozoites) [212]. *P. berghei* schizonts preferentially sequester in the microvasculature of the spleen, lungs and adipose tissue. An exception to this is the ANKA isolate in BALB/c and C57BL/6 mouse strains which sequester in the brain [168].

Figure 1.7 – *P. berghei* erythrocytic stage morphology at time from RBC invasion [185].

There are a large number of factors which influence the virulence and pathology of *P. berghei* including age, diet, host genetics, parasite genetics and route and magnitude of the infection [13, 79, 124, 255, 299, 328, 329]. In most laboratory rodents *P. berghei* causes rapidly progressing infections leading to death within 1-3 weeks. This is not the case in older laboratory rats which are able to clear parasites without treatment [74]. The Leiden Malaria Research Group divided the course of the ANKA *P. berghei* isolate infection in Swiss mice into 3 stages.

- Stage 1 – during this early phase of infection parasite multiplication is on average 10-fold per 24 h (1 life cycle) up to a parasitaemia of ~1-3% [185].
- Stage 2 – above a parasitaemia of 3% due to the course of infection the pool of available healthy reticulocytes is reduced. As a result there is an increase in multiply infected reticulocytes which does not allow parasites to develop into mature schizonts. As a result the average parasite multiplication rate decreases below 10-fold in stage 2 [185].
- Stage 3 – the average parasite multiplication rate increases in stage 3 due to either a wave of production of reticulocytes in the host, or invasion of older red blood calls by parasites. The course of infection in stage 3 is much less predicable and is highly dependent on host and parasite factors [185].

Gametocyte production in *P. berghei* is influenced by environmental factors and genetic differences between isolates [184, 258]. Gametocyte infectivity to

mosquitoes generally decreases as infection progresses in laboratory rodents as numbers of oocysts decrease. This is influenced by some immune and non-immune-related blood factors [42, 63]. The infection rate of liver cells by sporozoites is highly dependent on the host species and innate immune responses [74, 199].

The age and gender of laboratory rats and mice is important to *P. berghei* models. Swiss rats and mice are less susceptible to *P. berghei* infection as their age increases, due to immune development so adolescent rats and mice are predominantly used [453]. There is also the potential that the oestrus cycle in female rats and mice may lead to variations in experimental results from 4 weeks of age depending upon strains and individual variation [429, 453].

1.5.8 *P. berghei* antimalarial chemotherapeutic tests

P. berghei antimalarial chemotherapeutic testing began in 1950 and was based on standard tests developed for surveying antimalarial drugs with *P. gallinaceum* as described by Curd *et al* and Tonkin and Hawking [100, 389]. With the discovery of murine malaria came the opportunity for drug testing in a mammalian model which was considered much more similar to the human disease than that in the avian model and was logistically easier. In this “Thurston Test” mice ranging from 15-20g were infected i.p. with 5-15 million parasites in 0.2ml [386]. Drugs were administered orally for four days commencing three to four h post inoculation and doses were normalised to mouse weight. Thin films were collected and examined on days five and seven and the percentage of

infected erythrocytes determined. The minimum effective dose was determined as the minimum drug dose to keep parasitaemia below one percent on the fifth day [387]. June Thurston's findings were [386]

"*P. berghei is half as sensitive to the action of quinine as P. gallinaceum. On the basis of the Quinine Equivalents, P. berghei is as sensitive as P. gallium to proguanil; it is less sensitive to pamaquin and slightly more sensitive to mepacrine and chloroqin; it is many times more sensitive than P. gallinaceum to sulphonamides. In its susceptibility to sulphadiazine, 4'-diaminodiphenyl sulphone and sulphanilamide, P. berghei resembles the malaria parasites of monkey and man more than it does the avian species. P-Aminobenzoic acid antagonised the activity of sulphadiazine. It is proposed to adopt the test against P. berghei in mice for routine screening experiments in this laboratory in place of the existing test against P. gallinaceum in chicks*."

The minimum effective dose determination used by Thurston was modified in subsequent years. In 1952 Rollo [320] reported chemotherapy responses in the form of a standard effective dose. It was the dose required to reduce parasitaemia to 50% that of controls [320]. This later became reported as the effective dose 50 (ED_{50}), and the effective dose to reduce parasitaemia to 90 percent that of controls, or ED_{90} [286].

The "Thurston Test" which was termed a "suppressive" or "prophylactic" test by Peters was modified and termed a therapeutic test. As the name would indicate

the therapeutic test differed from the suppressive Thurston test in that *P. berghei* infection in mice was left untreated to progress to 10% parasitaemia prior to chemotherapy, which was only 4 h post inoculation in the suppression test [286].

The “Rane test” was used to test the bulk of some 300,000 compounds for antimalarial action by the Walter Reed Army Institute for Research [293]. In this test mice were inoculated intraperitoneally with 10^6 *P. berghei* infected RBCs. Test drugs are then administered on day three after inoculation at a dose range of 80, 160, 320 and 640mg/kg subcutaneously [293]. The animals are observed daily for death or survival. Survival of twice that of controls is evidence of activity and survival past 60 days is considered cure. The maximum tolerated dose was described as the dose that produces no more than 1 in 5 toxic deaths. The maximum tolerated dose was compared with the minimum effective dose to give an indication of the therapeutic index. Promising compounds are then continued to the “4-day test” for a more accurate examination of their activity [293].

The suppressive and therapeutic tests were further developed into the “Peters 4-day test” which similarly comprises a 4-day suppressive test followed by a 4 day assessment of blood schizontocidal activity [289]. The 4-day suppressive test involves inoculating mice with $2x10^6$ *P. berghei* parasites on day zero. Groups of mice then receive a 30mg/kg dose once daily on days 0, 1, 2 and 3 via either s.c. or oral administration. Thin films are then collected on day 4 to preliminarily assess the activity of chemotherapy agents. The 4-day blood schizontocidal test is similar to the suppression test except mice are inoculated with 10^6 *P. berghei*

parasites on day zero and receive a dose on days 0, 1, 2 and 3 via a chosen administration route and dose as determined from the preliminary suppressive test. The ED_{50} and ED_{90} are then determined from semi log time-density plots from parasite data thin films prepared on day 4.

1.5.9 Humanised models of murine malaria

In attempts to bridge the gap between murine models and the clinical setting, development has gone into murine models containing human parasites. Humanised mouse models use immune compromised mouse strains such as scid (severe combined immunodeficiency), and NSG (NOD Scid gamma), sometimes in combination with pharmacological agents, to suppress the host immune responses [20, 344]. Human erythrocytes are then grafted into the animals, for example via a course of i.p. or retro-orbital injections, along with human serum to improve human erythrocyte survival [18]. This is continued until human erythrocytes constitute sixty percent of the host erythrocytes where upon they are inoculated with human parasitised RBC. As well as addressing the erythrocytic cycle, humanised models are in development to investigate gametocyte production, sequestration and liver infection. Liver investigation in humanised models is based on injections that kill murine hepatocytes followed by transplantation of human hepatocytes [18].

There are obvious potential benefits to humanised murine models of malaria in providing a relatively low cost (compared with clinical trials), high throughput *in vivo* model for human malaria [380]. However, they still require development,

characterisation and validation. These models also have certain disadvantages over more established and conventional murine malaria models such as cost and experimental complexity. Additionally *P. falciparum* is the only human parasite that has a humanised model, and this model is still incomplete [18]. Nevertheless humanised murine models have the potential to provide a useful tool for drug discovery and testing therapeutic efficacy, once validated [18].

No animal model, even those humanised, are prefect models of the human condition and disease. These models however do provide a useful insight into many aspects of disease and its treatment. Extrapolation from murine models to clinical practice should be explored with caution, and supported with clinical experimental evidence.

"A model is useful if it sharpens questions, points to what is missing in our data or in our conceptual grasp, and contributes to a larger process that will render it obsolete; a model that cannot be shown to be wrong is typically of little use." [245]

1.6 Aims of this thesis

The emergence and spread of clinical resistance to all antimalarial compounds, including the artemisinins more recently, highlights the need to improve and protect the use of existing chemotherapies. Antimalarial treatment strategies have been limited by the paucity of pharmacodynamic information for dosage regimen design.

Although murine malaria models have primarily been used for *in vivo* screening of new antimalarials, there is potential for broader applications. It is postulated in this thesis that a murine model could be used for pre-clinical stages of drug development, especially in dose-response studies, rational dose regimen design and evaluation of combination therapies. Sufficiently characterised, this *in vivo* malaria model could be used to provide detailed pharmacodynamic data for development of a mathematical *in silico* model of murine malaria. Such an *in vivo-in silico* model of murine malaria could provide an inexpensive, readily achievable and efficient malaria model to assist in optimisation of new and existing antimalarial therapies.

Whilst the overall aim of this thesis was to investigate and develop a *P. berghei* in *vivo-in silico* murine malaria model as a tool for the pharmacodynamic assessment of antimalarial drugs, the specific objectives included:

1. **To develop an *in vivo P. berghei* murine malaria model capable of producing detailed pharmacodynamic dose response data.**

   The *P. berghei* infection was characterised to develop an *in vivo P. berghei* model of malaria. The pharmacodynamic properties of dihydroartemisinin were investigated through a sub-therapeutic single dose study. It was hypothesised that this would provide detailed parasite pharmacodynamic graded dose response data (Chapter 3; Paper I).

2. **To develop an *in silico* mathematical model of *P. berghei* murine malaria and single dose dihydroartemisinin treatment.**

   The previous investigations detailed the characterisation of an *in vivo P. berghei* model of murine malaria and treatment with dihydroartemisinin. These data were used to develop a mathematical model of *P. berghei* infection and treatment. It was hypothesised that such a mathematical model could be used to simulate parasite dynamics of single dose treatment (Chapter 4; Paper I).

3. **To develop an *in silico* mathematical model of *P. berghei* murine malaria and multiple dose dihydroartemisinin treatment.**

   It was hypothesised that the *in vivo-in silico* model could be further developed to predict parasite dynamics after multiple dose treatment with dihydroartemisinin and to allow prediction of an optimised multiple dose treatment regimen (Chapter 5).

4. **To develop an *in silico* mathematical model of *P. berghei* murine malaria and combination treatment.**

   It was hypothesised that the *in vivo-in silico* model could be extended to other drugs (chloroquine) and that a combination dihydroartemisinin-chloroquine *in silico* model could be used to optimise and evaluate combination treatment (Chapter 6).

CHAPTER TWO

2. Materials and Methods

2.1 Materials

2.1.1 Chemicals and Materials

Artesunate (ARTS), dihydroartemisinin (DHA) and artemisinin (QHS) reference standards were gifts from Colonel Brian Schuster (Walter Reed Army Institute of Research, Washington DC, USA). DHA was obtained from Dafra Pharma NV (Turnhout, Belgium). All general chemicals were of analytical grade and were obtained from Sigma Aldrich (St Louis, MO, USA), BDH Laboratory Supplies (Poole, England) or Merck Pty. Limited, Kilsth, Victoria, Australia. De-ionized water was used for preparation of all buffers and aqueous solutions. Pentobarbitone injection was sourced as Nembutal®, 60mg/mL, Boehringer Ingelheim Pty Ltd, Artarmon, NSW and was diluted with saline to 12mg/mL.

Sterile disposable syringes and needles were obtained from Becton-Dickinson Medical Products (Singapore) or Terumo Medical Corporation (Elkton, MD, USA). Millex® 0.22μm disposable sterilizing filters were obtained from Millipore Corporation (Bedford, MA, USA). Sodium fluoride and sodium citrate blood collection tubes (Vacutainer®) were obtained from Becton-Dickinson Medical Products (Rutherford, NJ, USA).

2.1.2 Parasites

P. berghei ANKA parasites (Australian Army Malaria Institute, Milpo, QLD, Australia) were used for all experimental work. *P. berghei* ANKA was used as it is a well established model for testing antimalarial drug efficacy. It is characterised with a high mortality in rodents and is sensitive to all current antimalarial drugs [291].

2.1.3 Mice

An initial series of studies were undertaken to determine the age, weight and sex of animals to be used in further studies. A series of pilot studies were carried out which compared 6-8 week old male Swiss mice with 5-6 week old male Swiss mice and 5-6 week old female with male Swiss mice. 5 week old male Swiss mice were determined to be the most suitable experimental host as infection was stable and reliably reached 5% after 72 h following intra peritoneal infection. Additionally, male mice were selected because they are slightly larger than females of the same age and there can be physiological and biochemical complications with females due to hormone fluctuations [213].

Experimental work was performed using male out bred albino Swiss Arc:Arc(S) mice aged five weeks (Animal Resources Centre, Murdoch, Western Australia). Original breeding stock of Arc:Arc(S) mice was received from the Charles River Breeding Laboratories (Kingston, NY). The out bred Swiss model was selected as it provided an economical and robust model.

P. berghei malaria infection was maintained in inbred albino male BALB/c Arc mice aged 8 weeks (Animal Resources Centre, Murdoch, Western Australia). The strain is well established for passage of *P. berghei* infection as the animals are easy to handle, provide a stable infection for weekly passage and minimal immunological complications.

Male out bred albino Swiss Arc:Arc(S) mice aged five weeks (Animal Resources Centre, Murdoch, Western Australia) were used throughout the course of experimental work as sentinel mice. Sentinel mice were housed in separate cages on racks containing experimental mice cages. They received the same food, water and bedding as experimental mice. Sentinel mice were replaced every three months at which time their blood was harvested and sent for laboratory testing (Murine Virus Monitoring Service, Gilles Plains, South Australia) against a panel of known murine viral pathogens, including mouse hepatitis virus, mouse parvovirus and mouse pneumonia virus. Sentinel mice remained pathogen free for the duration of the research.

2.1.4 Animal welfare

All studies were conducted in accordance with the National Health and Medical Research Council (NHMRC) Australian Code of Practice for the Care and Use of Animals for Scientific Purposes (1990). The studies were approved by the Animal Ethics Committee of Curtin University of Technology.

2.1.5 Euthanasia

Animals were monitored and weighed daily during experiments. Animals were euthanized using a 20mg/mL i.p. pentobarbitone injection if animals were observed to be suffering. Additionally infected mice were euthanized if peripheral parasitaemia exceeded 40% and/or body weight decline by >10% in a 24 h period, both of which were found to be indicative of terminal deterioration in health of malaria-infected mice.

2.1.6 Animal holding

Mice were housed in the School of Pharmacy Animal Holding Facility (Curtin University of Technology, Bentley, Western Australia) at 22°C in a 12 h day/12 h night cycle with free access to sterilised commercial rodent food (Glen Forrest Stockfeeds, Perth, Western Australia) and sterilised water (pH 2.5). Non-porous, translucent plastic cages with stainless steel tops were used to house mice. Small and large cages were used with a maximum of 4 mice held in small cages and up to 12 in large cages. Drip dispenser plastic autoclavable drinking bottles with stainless steel tops and rubber o-rings were used to hold drinking water.

ALPHA-dri (Shepherd Specialty Papers; Able scientific, Perth, Western Australia) was selected as bedding material. This cellulose product produces lower levels of dust and does not contain chemical or compounds that may affect animal physiology like some wood chip bedding products [194].

Acidified drinking water was provided for mice to prevent bacterial contamination. The pH 2.5 water was prepared by adding 400μL of 32% w/v hydrochloric acid to 1 L Schott bottles of de-ionised water. Prior to provision to mice, water was autoclaved for 20 minutes at 121°C on a fluid cycle (School of Pharmacy, Curtin University, Perth, Western Australia).

All cage components, feed and bedding were autoclaved prior to use at 121°C for 15 minutes on a hard goods cycle (School of Pharmacy, Curtin University, Perth, Western Australia).

2.2 Methods

2.2.1 Initial *P. berghei* malaria infection

To establish the infection a suspension of cryopreserved *P. berghei* parasites was thawed and 200μL injected i.p. into two 8-week-old male Balb/c mice. Intra peritoneal injection was chosen as the route of administration because it was considered to be more versatile when considering formulation of different pharmaceuticals and reproducible when injecting large numbers of young mice than the i.v. route. Each day the mice were weighed and a blood sample obtained from the tail vein using a 26G needle and 100μL heparinised micro-haematocrit tube.

Approximately 7 days after infection mice were anaesthetised with 150μL of 12mg/mL pentobarbitone sodium (Nembutal® Injection, 60mg/mL, Boehringer Ingelheim Pty Ltd, Artarmon, NSW diluted with saline) and blood was removed

via cardiac puncture and placed into a sodium citrate blood collection tube (Vacutainer containing 0.5mL of 0.129M solution, Becton-Dickinson, NJ, USA). 100μL of blood was used to infect two healthy mice.

2.2.2 Passage of the *P. berghei* malaria infection

7 days after infection, at parasitaemia of approximately 20%, mice were anaesthetised with 150μL of 12mg/mL pentobarbitone sodium. All available blood was removed through cardiac puncture using a 26G1/4" needle from the ventricle after a midline incision to the sternum and cutting of the diaphragm. Blood was placed in a sodium citrate blood collection tube (Vacutainer containing 0.5mL of 0.129M solution, Becton-Dickinson, NJ, USA). 40μL of blood was diluted in 8mL Red Cell Diluent (1% of 40% formaldehyde in 109mM Trisodium Citrate, Appendix A2.4) and gently mixed. 10μL of this solution was then placed into an improved Neubauer counting chamber and the number of erythrocytes in 10 squares on the grid was counted. The number of erythrocytes per μL was determined using Equation 2.1.

Erythrocyte Count (per μL) =

(No. of cells counted in 10 squares)/Volume x Dilution Factor

Where Volume = 0.04 and dilution factor = 200

Equation 2.1

The volume of blood containing 10×10^7 infected erythrocytes was then removed from the citrate collection tube and diluted to 1mL using citrate-phosphate-dextrose solution (pH 6.9; Appendix A2.3). 100μL of this solution was then passaged by i.p. injection into healthy mice.

2.2.3 Cryopreservation of *P. berghei* malaria

Periodic samples of infected erythrocytes were cryopreserved to ensure access to viable *P. berghei* should the weekly infection maintained in BALB/c mice fail. Blood remaining in the citrate blood collection tube after passage was centrifuged at 3000g for 10 minutes to collect the erythrocytes. The supernatant was removed and the red cell pellet resuspended in saline (0.9M NaCl), and centrifuged at 3000g for 10 minutes. The red cells were washed twice in this way and then resuspended in 1mL 10% glycerol in Alsever's Solution (Appendix A2.5) then placed in a 1.5mL eppendorf tube and stored at -80°C.

2.2.4 Preparation and staining of blood films

Peripheral thin blood films were prepared using blood collected from the tail vein of mice. Single drops of heparinised blood from micro haematocrit tubes were placed at the base of clean glass slides (1.0-1.2mm thick 76×25mm rounded glass slides with frosted end; Rowe Scientific, WA, Australia). The edge of another slide held at 45 degree was drawn back into the blood drop and spread up the slide with a smooth, uninterrupted movement producing a section of blood smear with a uniform monolayer of cells. Slides were dried in air at 22°C prior to staining. The thin film was fixed in methanol for 1 min, stained in freshly prepared Giemsa stain solution for 20 min, rinsed with distilled water and dried in air. The Giemsa stain solution was prepared by diluting Giemsa stock 10% in Sorenson's phosphate buffer (pH 7.0; Appendix A2.9). Once dried, slides were cover slipped using DePex® mounting medium and 22×60mm glass cover slips.

2.2.5 Parasite enumeration and staging

The peripheral parasitaemia was determined as a percentage of the total erythrocytes by microscopic examination using 100 × magnification of thin films under oil immersion with ×10 eye pieces. One of the eye pieces contained a square 10×10 graticule to facilitate parasite enumeration by providing a set field of view with overlayed grid. Parasite densities <0.5%, 0.5-5% and >5% were determined by counting 100, 30 and 10 fields of view respectively which provided an acceptable error as indicated in Table 2.1. In general, one field of view contained approximately 200 erythrocytes.

The errors indicated in Table 2.1 represent the minimum variability without account for technical or observational errors. The confidence intervals were approximated using the formula $p \pm (z.SE(p))$ when $SE(p)$ is the standard error of p and z is 1.96 for 95% confidence intervals. $SE(p)$ was calculated as $[p(1-p)/n]^{1/2}$ where p is the percentage parasitaemia and n is the total number of cells counted.

Table 2.1 – rationale for number of field of views examined to accurately determine the percentage parasitaemia.

Parasitaemia (%)	0.02	0.1	1	4	10
No. FOV	100	100	30	30	10
No. Red Cells	20,000	20,000	6,000	6,000	1,000
No. Infected Cells	4	20	60	240	100
95% Confidence Interval	±0.02	±0.04	±0.25	±0.49	±1.86
Upper 95% CI	0.04	0.14	1.25	4.49	11.86
Lower 95% CI	0.0004	0.06	0.75	3.51	8.14

Some parasite films had the parasitised erythrocytes classified into the parasite life cycle stages. A morphological chart (Figure 2.1) was constructed and used to classify parasites as rings, early trophozoites, late trophozoites and schizonts).

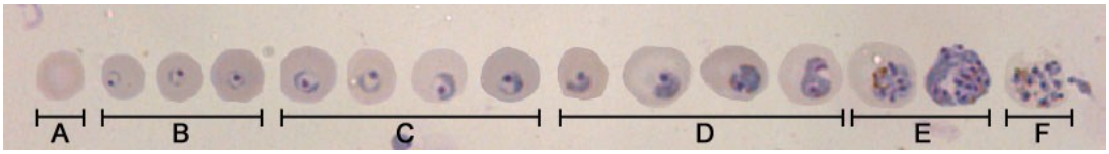

Figure 2.1 – *P. berghei* morphological chart (A) uninfected erythrocyte, (B) ring stages, (C) early trophozoites, (D) late trophozoites, (E) schizonts and (F) merozoites.

Ring stage parasites (B) were defined as having a defined nucleus with a crescent shaped edge to the vacuole. Early stage trophozoites (C) have a larger and partly filled vacuole while late stage trophozoites were defined as those with half to completely filled vacuoles (D). Schizonts were characterised by the presence of multiple nuclei, and no clear separation between nucleus and vacuole (E).

2.2.6 Formulation of dihydroartemisinin

In pilot studies 20% ethanol in propylene glycol was used as a vehicle for DHA in mice studies since it had been used in previous studies involving Wistar rats [40]. The solubility of DHA in ethanol however was not sufficient to allow injection of doses of DHA above ~75mg/kg without causing visible ethanol side effects to mice and compromising the experiments. With the intention of performing multiple dose studies requiring up to 5 doses of the vehicle, it was determined that ethanol was not a suitable vehicle in the mouse model. The LD_{50} for ethanol in Swiss mice is 8.1g/kg which equates to ~300µL per 30g

mouse [394]. It was determined in future studies the vehicle dose would be too close to the LD_{50}.

A series of basic solubility studies were conducted to determine a suitable vehicle for DHA formulation to be administered i.p.. The vehicle was required to reliably carry 50mg/mL of DHA, so that a single dose of 100mg/kg could be administered to mice in 100μL. Dimethyl sulfoxide (DMSO) was selected as it met the solubility requirements and also low toxicity of greater than 15g/kg in mice [183]. DMSO was mixed with polysorbate 80 (LD_{50} i.p. mice of 7600mg/kg) to further reduce the LD_{50} of the vehicle [327, 401]. For single 100μL i.p. doses the proportion of the LD_{50} of the two components of the vehicle was ~15% of the DMSO LD_{50} and ~18% of the polysorbate 80 LD_{50}.

The vehicle toxicology was tested. Four groups of four 5 week old male Swiss mice were injected with 100, 200, 300 or 400μL of 60% DMSO in polysorbate 80. No ill effects were observed in any mice. 400μL represents 60% of the DMSO LD_{50} and 72% of the polysorbate 80 LD_{50}.

2.2.7 Dihydroartemisinin treatment methodology

DHA was formulated in 60% v/v DMSO in Polysorbate 80, with a final injection volume of 100μL. The vehicle dose was less than 25% of the LD_{50} for both DMSO and Polysorbate 80 in mice.

Groups (generally n=8) of five week-old male Swiss mice received either single or multiple i.p. treatment starting 72 h after inoculation with 10^7 parasites, with either 0, 1, 3, 10, 30 or 100mg/kg DHA. Parasitaemia was monitored as described above until mice were euthanized according to pre-determined guidelines (2.1.5).

2.2.8 Modelling and statistical analysis

All modelling was performed using SAAM II Simulation, Analysis and Modelling Software for Kinetic Analysis (University of Washington Seattle, USA). All statistical analysis was performed using SAAM II, SigmaStat® 2004 (SPSS Inc., Chicago) and Microsoft Excel for Windows. Statistical Data was plotted using the statistical program SigmaPlot® 2004 (SPSS Inc., Chicago).

CHAPTER THREE

3. Establishing a murine malaria infection model

3.1 Introduction

Parts of the work in this Chapter have been published [39, 138]. Refer to APPENDIX 1 – Development of a pharmacodynamic model or murine malaria and treatment with dihydroartemisinin (pg 286).

3.1.1 Development of antimalarial treatment regimens

Antimalarial treatment regimens have traditionally been based on *in vitro* and clinical studies of drugs given alone or in combination, with particular focus on efficacy against *P. falciparum*. Although *in vitro* studies are valuable for screening antimalarial candidates and sensitivity testing [66, 160], they provide only limited pharmacodynamic information for dosage regimen design. Zaloumis *et al* [451] commented when assessing the utility of an antimalarial pharmacokinetic-pharmacodynamic (PK-PD) model for aiding clinical drug development that “the PD effect predicted from *in vitro* growth inhibition assays does not accord well with the PD effect of the antimalarial observed within the patient.”.

By comparison, well conducted clinical trials aim to assess parasite clearance and do not generate dose-response relationships that can be used in developing rational dosage strategies [222]. Novel pharmacodynamic models have been developed for a range of drugs [341], but there is a paucity of graded dose-

response data from clinical studies of *falciparum* malaria. Due to this dearth of PD information antimalarial treatment strategies have tended to rely on PK information with limited PD information provided by clinical data from curative therapy. Ideally detailed PD information in the form of graded dose-response data would input into treatment strategy design to produce an optimised strategy. This is the goal of establishing PK-PD relationships; to be able to design an optimal regimen which maximises the effect of the drug per unit dose or improves the convenience of treatment regimens [143]. Various PD models have been proposed, however the inability to examine subtherapeutic doses clinically limits the extent to which human PD information can be gathered [104, 105, 177, 347].

In vivo animal models can potentially provide relevant information that is otherwise very difficult to acquire clinically or *in vitro*. Any modelling approach should not be considered as a replacement to conducting clinical trials, but instead as a decision-making tool to improve the design of a clinical trial during drug development.

3.1.2 Antimalarial pharmacodynamics

Pharmacodynamics is the quantitative relationship between the observed drug concentration and the magnitude of the observed effect or the relationship between the drug and its receptors, its mechanism of action and therapeutic effect [360]. In disease chemotherapy, optimised PD is the goal and requires an understanding of the PK.

There are difficulties with PD evaluations in malaria. The most obvious difficulty is practical aspects of monitoring the PD effect in the clinical setting. The PD effect is typically the parasite bioburden, and parasitological recovery is conventionally assessed by parasite clearance from peripheral blood smears [425]. The relationship between parasitaemia and disease, particularly in *P. falciparum* infection, is arguably loose, as patients can present with coma, liver and renal dysfunction with low peripheral parasitaemia [126, 420]. There is also the complication of late stage sequestering of parasites in falciparum infections. This is less of a confounding issue for other forms of human and animal malaria where peripheral parasitaemia is a more accurate reflection of the disease state.

Immune status is also an important consideration in clinical PD. It has been understood since early reports by Yorke and Macfie [420] in 1924 that antimalarial treatment responses in semi-immune or immune patients is better than those in non-immune patients. For this reason in endemic areas age is an important factor in therapeutic response. Additionally immunity is temporarily disrupted in pregnancy and in certain infections.

3.1.3 Animal models of malaria

Isolation of wild non-human strains of malaria parasites have enabled the establishment of animal models for malaria which have a long established history in malaria research complementing *in vitro* and clinical research. They

are useful due to the limitations in scope and interpretation of *in vitro* studies as well as practical and ethical constraints in clinical studies. Animal models facilitate the examination of disease progression [332], host-parasite interactions such as immune responses [8, 88, 352, 448], organ studies [7, 10] and parasite disease mediation studies [332, 366, 369] which can ultimately lead to explanations of observations in humans. This is the goal of disease models, to better understand the disease in order to provide explanations for clinical observations, without putting humans at risk.

3.1.4 *P. berghei* malaria

Unlike *P. falciparum* in which sequestration of late stage parasites occurs, all *P. berghei* blood stages are visible in the peripheral circulation. Vinke and Lips (1948) described the morphology of *P. berghei* as follows:

"The ring stage is usually uninucleate and contains a large vacuole. Trophozoites are nonvacuolated, slightly amoeboid and contain fine granules of black pigment which are left behind at schizogony when from 6-20 merozoites with small nuclei are formed from each schizont. Parasitized erythrocytes hypertrophy but show no granulation. Polyparasitism is frequent, the cytoplasm of the parasites merging into confluent masses 10.6μ in diameter, which stain dark blue with Giemsa and which frequently contain no pigment. In heavy infections, erythroblasts are found in the circulation and are often invaded. Gametocytes are 7-8μ in diameter."

P. berghei is virulent in mice of all ages [57, 350] and displays more severe pathological changes and higher mortality rates than other rodent malarias. The 100% mortality of *P. berghei* infection in mice is normally due to severe anaemia, causing hypoxia and hypothermia [57] and death occurs from 5-20 days according to the number of inoculating parasites. The mortality rate is a major reason for *P. berghei* being the animal model of choice for chemotherapeutic studies [81, 82, 292].

The erythrocytic life cycle of *P. berghei* in vertebrate hosts is approximately 24 h and Mercado and Coatney [250] observed in 1951 that the number of merozoites produced per schizont varied during the course of the infection. Early in the infection the average number was 8 while on the third and seventh patent days it was 5.5 and 12.8 respectively. Fragility of erythrocytes, as determined by the number of extracellular parasites, increased towards the end of the infection.

Preferential invasion of reticulocytes by *P. berghei* merozoites was first noted in mice by Ramakrishnan and Prakash [313], while gametocytes developed exclusively in mature erythrocytes. The relationship between the number of parasites and reticulocytes has been suggested as an explanation as to why young animals become more heavily infected with *P. berghei* [179].

Vinke and van den Bulche [317] noted splenic enlargement and anaemia in infected mice in 1949. An increase in numbers of reticulocytes and erythroblasts as well as the presence of pigment in the liver, bone marrow and phagocytic

leucocytes in the circulation; and necrotic lesions in the liver have also been observed.

Passage of *P. berghei* parasites is usually achieved by diluting a small quantity of blood from an infected host with a suitable diluent and injecting infected erythrocytes into a new host either intra peritoneally (i.p.) or intravenously (i.v.) via a tail vein [57]. A standard inoculation dose of 10^7 parasitised erythrocytes in 100-200µL is commonly used in *in vivo* studies with *P. berghei* [57, 433]. Parasites have been shown to penetrate the mouse peritoneal wall into the blood stream within one minute of inoculation [44]. After inoculation an exponential increase in parasitaemia is observed, until a peripheral parasitaemia of 10-50% is achieved [350]. Rapid rises in parasitaemia and subsequent erythrocyte destruction can cause anaemia and host death within 5 days post inoculation [57, 350].

3.1.5 *P. berghei* chemotherapy screening tests

A number of standard *P. berghei in vivo* tests have developed since the 1950s when *P. berghei* models were first discovered, which are still in use today. These tests are commonly referred to the “Peters 4-day test” or simply the “4-day test” and the “Rane test” and originally developed as antimalarial screening tests. In the 4-day test drug treatment commences only hours after *P. berghei* infection and is repeated over 4 days after which parasite bioburden is compared with that in untreated mice via counting thin films. The 4-day test is

often referred to as a suppression test since treatment commences soon after infection.

The Rane test differs from the 4-day test in that drug treatment commences 72 h post inoculation with *P. berghei*. In this case the infection is established and so the test is more representative of treatment rather than infection suppression. After 72 h post infection, groups of animals are treated with different concentrations of the antimalarial candidate. An increase in animal survival past 7 days is considered the minimum effective response for an active compound. Compounds which increase animal survival past 30 days are considered curative [278].

3.1.6 *P. berghei* as a pharmacodynamic malaria model

The 4-day and Rane tests have tended to be employed as relatively simple screening tests that provide very useful, but limited pharmacodynamic information. This information tends to be either the level of suppression or cure of infection by a compound relative to control mice, or relative to an established antimalarial such as chloroquine.

There is the potential for a murine *P. berghei* model to be used to collect pharmacodynamic information on drug doses on the parasite population in the form of graded dose responses. This type of model could be based on the Rane test, with groups of mice infected and treatment starting 72 h later at an appropriate level of parasitaemia in an established infection. Much more regular

monitoring of parasitaemia through thin films than is seen in drug screening tests could provide detailed graded responses. The data from these *P. berghei* studies could potentially be scaled and used as input into clinical studies as a starting point to rational design of treatment regimens and multiple dose treatment timing. It also may provide a model to screen and assess effective combination therapies.

Despite the development of other research models of malaria including humanised mouse models [18] and efficacy testing in human volunteers [119, 244] there still exists a question about where detailed PD information can be reliably, cheaply and quickly obtained for antimalarial candidates in order to optimise treatment regimens [423]. Murine malaria is the only model that can realistically fill this gap. It would however, need to be part of a larger effort using for example, testing in a *P. falciparum* model in human volunteers and clinical studies.

3.1.7 Artemisinin

Early study of qinghaosu was carried out by the Qinghaosu Antimalaria Coordinating Research Group and results were published in English in 1979 [152]. This reported chemical, pharmacological and clinical results for studies using artemisinin. Pharmacologic studies reported 138.8mg/kg as the ED_{50} in mice against *P. berghei*, which were treated with 50mg/kg daily for 3 days. Monkeys infected with *P. cynomolgi* were treated with 200mg/kg daily for 3 days however 5 of 7 of the monkeys showed recrudescence. The LD_{50} in mice was

reported to be 5105mg/kg orally, 2800mg/kg i.m. and 1558mg/kg i.p.. 2099 human patients were effectively treated with Qinghaosu as either 2.5-3.2g tablets, 0.5-0.8g oil, 0.8-1.2g oil suspension or 1.2g water suspension, all given i.m. except for the tablets which were taken orally. The recrudescence rate was greater than 25%, and greater than 80% for the tablet treated group against *P. falciparum* infections [152]. The Qinghaosu Antimalaria Coordinating Research Group concluded that artemisinin could be given at a dose of 300mg daily for 3 days, and recommended the intramuscular route for optimum clinical efficacy [152].

A series of reports was subsequently published by the China Cooperative Research Group on qinghaosu and its derivatives as antimalarials in 1982 outlining pharmacokinetic and pharmacodynamic data of artemisinin and several semi-synthetic derivatives [1-4]. These findings were confirmed by Hien and White [171] a decade later and since that time the artemisinins have become front line treatment for malaria globally in the battle against malaria and drug resistant parasites.

Artemisinin monotherapy was registered in Vietnam during the 1990s as a first-line treatment. *In vitro* testing against *P. falciparum* led to clinical trials of various regimens which are shown in Table 3.1. Artemisinin monotherapy was required to continue for at least 5 days to reduce recrudescence, and a single dose of artemisinin and mefloquine was the most practical, effective, safe and inexpensive treatment for uncomplicated malaria [170].

Table 3.1 – Summary of clinical trials of artesunate monotherapy in the treatment of patients with *P. falciparum* malaria taken from Barrell and Fitton 1995 [31].

Country	No. of pts	Dosage regimen	Date of trial	Initial geometric mean parasite load (/mm^3 blood)	Follow-up period (d)	Mean parasite clearance time (h)	Mean time for reduction of fever (h)	Response rate [% (no.)][a]	RI (%) [other clinical failures]
Noncomparative study									
Thailand[40]	48	ART 300mg PO (100mg then 50mg q12h for 2d) then MEF 750mg 12h later	Jun-Nov 1991	17 741	28	37.8	38.1	90 (43)	10
Artesunate with mefloquine *vs* comparators									
Thailand[68]	50	ART 800mg PO (200mg q12h for 2d) then MEF 750mg	Jun-Aug 1993	22 919[b]	28	37.9	46.1	92 (46)	8
	57	MEF 750mg then 500mg 6h later	As above	17 045[b]	28	65.9***	52.1	74 (42)***	19 [RII/RIII – 7%]
Thailand[38]	39	ART 600mg PO (100mg then 50mg q12h for 5d) then MEF 750mg + 500mg	Jan-May 1991	28 825	28	37.5	37.5	100 (39)	
	40	ART 600mg PO (100mg then 50mg q12h for 5d)	As above	14 195	28	35.9	35.1	88 (35)	
	37	MEF 750mg + 500mg	As above	23 961	28	63.5***	69.7***	81 (30)	
Thailand[69]	12	ART 200mg PO SD then MEF 750 + 500mg at 6 and 12h	Reported in 1994	31 091	42	47.5	31.2	66 (8)	34
	8	MEF 750 + 500mg 6h later	As above	20 893	42	82.3**	44.7	75 (6)	25 [*P. vivax* in 1 pt]
Karen pts in Thailand[70]	27	ART 12 mg/kg PO (3 equal doses over 3d) then MEF 25 mg/kg	Jan-Dec 1993	327 748	28	9.6	36	70 (19)	
	28	Quinine dihydrochloride 20 mg/kg IV (3 doses q8h)[c] then MEF 25 mg/kg	As above	286 932		14.6***	82***	39 (11)	
Karen pts in Thailand[66]	124	ART 4 mg/kg PO SD then MEF 25 mg/kg	Jan 1992-Jun 1993	2 810	28	26.4[d]	48[e]	83 (103)	
	115	MEF 25 mg/kg	As above	3 549	28	36***[d]	79.2***[e]	78 (90)	
	108	ART 10 mg/kg PO (4 mg/kg then 2 mg/kg/day for 3d) + MEF 25 mg/kg	Oct 1992-Jun 1993	5 549	63	28.6[d]	36[e]	98 (100)[f]	
	129	MEF 25 mg/kg	As above	5 731	63	62.4***[d]	79.2***[e]	56 (64)[f]	
Karen pts in Thailand[101]	180	ART 12 mg/kg PO (4 mg/kg/d for 3d) + MEF 25 mg/kg	Jun 1993-May 1994	4 942	7-63	45.6	38.4		13.9[g]
	178	Artemether 12 mg/kg PO (4 mg/kg/d for 3d) + MEF 25 mg/kg	As above	5 323	7-63	45.6	38.4		12.3[g]
	182	MEF 25 mg/kg SD	As above	4 109	7-63	62.4	40.8		49.2[g]
Myanmar[K71]	24	ART 300mg IV (120mg then 60 mg/d for 3d) then MEF 1000mg	Feb 1989-Aug 1991	24 830	28	41.8	31.4		0 [2 deaths (8.3%)]
	50	Artemether 600mg IM (200mg then 100mg q12h for 2d) then MEF 1000mg	As above	33 290	28	27.3	42.4		0 [7 deaths (14%)]
	67	Quinine dihydrochloride 600mg IV q8h then quinine sulfate 600mg PO q8h for 10d, plus tetracycline 250mg PO q6h for 7d	As above	16 260	28	47.3	42.6		12.1 [23 deaths (34.3%)][h]

A major disadvantage of monotherapy with artemisinin and its family of antimalarials is the high recrudescence observed in clinical studies [106]. The short terminal half-life of artemisinins has been suggested as the reason for low monotherapeutic efficacy and as a result the artemisinins are best suited to use in artemisinin combination therapy (ACT) with longer half-life antimalarials with differing mechanisms of action [22, 242, 305]. ACTs are recommended for treatment of uncomplicated malaria throughout the world [430].

Artemisinin itself has not been used in ACTs because of its time dependent pharmacokinetics and low bioavailability. Artemisinin and artemether also have a marked ability for enzymatic auto induction when administered over several days [23, 145, 399].

It is believed that artemisinin resistance has emerged, which compromises the efficacy of the antimalarial combinations currently in use [207]. The impact of artemisinin resistance is therefore potentially large because hundreds of millions of doses of artemisinin combination treatments are dispensed every year [343]. Descriptions of artemisinin resistance do not always fulfil classical criteria for antimalarial resistance [14, 114, 298].

3.1.8 Artemisinin-based antimalarial monotherapies

A comment by Looareesuwan *et al* [235] on the purpose of their 1997 report on monotherapy studies into artemisinins raises some questions about the rational

design and implementation of antimalarial therapy regimens in the clinical setting.

"Although it is generally accepted that effective treatment with sodium artesunate monotherapy requires administration for 5-7 days, there is little evidence to support this."

Barradell and Fitton [31] succinctly reviewed artesunate monotherapy in 1995 (Table 3.1). Clinical trials with artesunate demonstrate that artemisinin monotherapy is highly effective for the treatment of acute malaria and that recrudescence with artemisinins is a significant problem, especially for short treatment regimens. Results from artesunate monotherapeutic studies indicate that treatment regimen duration, rather than total dose seems to be more important in reducing recrudescence [60]; treatment duration of 5 days or greater is required to achieve acceptable cure rates [62] and there is no benefit to 12 h dosing over 24 h dosing [61].

3.1.9 Dihydroartemisinin

Dihydroartemisinin (DHA) is a sesquiterpene lactone, a semi synthetic derivative and active metabolite of artemisinin. DHA has a very short plasma half-life in the order of 40-60 minutes [37]. Due to poor solubility and possible instability DHA has not been clinically utilised as much as other artemisinins [227]. This is despite the fact that DHA has been demonstrated to display greater *in vitro* and *in vivo* activity against *P. berghei* than either ART or QHS [186] with little

difference between their efficacy in clinical trials [171]. DHA has been combined with piperaquine as an efficacious combination treatment against *P. falciparum* [189, 359].

Dihydroartemisinin provides an interesting and clinically relevant antimalarial compound with which to examine the benefits of a pharmacodynamic model of murine malaria. The artemisinins will remain important in antimalarial therapy for many years to come and elucidation of their mechanisms of action and resistance, as well as optimising dosing regimens and combination antimalarials will be crucial in protecting this class from the emergence and spread of serious clinical resistance.

3.1.10 Aims

It is postulated that animal studies could be used as an appropriate intermediate stage of drug regimen development, between *in vitro* studies and clinical trials. A murine model was considered to be an established, convenient and cost-effective choice, whilst the use of an artemisinin-based drug has contemporary clinical relevance in pharmacodynamic model development.

The aims of the present series of studies were to develop an *in vivo* murine malaria model that could eventually be used to investigate both dose-response and regimen characteristics for antimalarial drugs, and ultimately to develop strategies for combination therapies. The initial aims were to:

(i) Establish and characterise a murine model of malaria

(ii) Validate a parasite enumeration procedure

(iii) Determine an infection regimen to allow examination of drug treatment

(iv) Formulate DHA for injection

(v) Determine approximate dose response range for DHA administration

(vi) Validate the murine model by investigating pharmacodynamics of graded single-dose treatment using DHA.

The hypotheses to be tested were:

(i) A reproducible and stable *P. berghei* infection model can be established to enable study of *P. berghei* infection and drug treatment.

(ii) A *P. berghei* infection model can be used to obtain detailed pharmacodynamic data on parasite population response to drug administration.

3.2 Methods

3.2.1 Mice

The studies were approved by the Animal Ethics Committee of Curtin University of Technology. All mice were obtained from the Animal Resources Centre (ARC), Murdoch, Western Australia. Male Swiss mice aged five-six weeks were used for experimental work. Male BALB/c mice aged 7-8 weeks were used to maintain the *P. berghei* infection.

3.2.2 *P. berghei* infection

Erythrocytic stages of *P. berghei* were maintained in 8-week-old male Balb/c mice and passaged weekly. The initial infection of ANKA *P. berghei* parasites was established from a suspension of cryopreserved *P. berghei* parasites (ANKA strain; originally obtained from the Australian Army Malaria Institute, Milpo, QLD, Australia) as described in 2.2.1. Blood harvested from infected BALB/c mice in citrate-phosphate-dextrose solution was administered by i.p. injection to infect the experimental mice.

3.2.3 Hosts and dihydroartemisinin ranging studies

A series of studies were undertaken to determine the age, weight and sex of animals to be used in further studies. A series of pilot studies were carried out which compared 6-8 week old male Swiss mice with 5-6 week old male Swiss mice and 5-6 week old female with male Swiss mice. All animals were infected with 10^7 parasitised erythrocytes i.p. and assigned into untreated control groups or into dose ranging groups to test the concentration of the lower therapeutic

limit of DHA. Doses of 0.1, 1, 10 and 25mg/kg DHA in 20% ethanol and 80% propylene glycol were administered approximately 72 h after infection and infection progression was monitored by once daily tail vein bleeds. The vehicle of 20% ethanol in propylene glycol was initially used as this was being used in parallel rat microsomal studies in the same laboratory. In further studies it was determined that ethanol in propylene glycol was an inappropriate vehicle for DHA in mice as increasing concentrations of DHA required vehicle concentrations approaching the LD_{50} of ethanol in mice.

It was determined that male Swiss mice at 5-6 weeks provided animals of a suitable weight (~30g) and size for handling and blood sampling for a PD model of malaria. Female Swiss mice were deemed too small and light (~20g) and there were some indications in the literature that female oestrus can create variations in results in chemotherapeutic research [429, 453]. Five week male Swiss mice provided the youngest feasible animal subjects possible. This age was selected to provide animals with immature immune systems for the PD model for as long as possible for potential use in multiple dose studies in which mice may survive for many weeks. The age would reduce the influence and possible complications due to the immune system in more mature mice as much as possible. Subsequently for all experimental studies recipient male Swiss mice aged five weeks received an i.p. inoculation of parasitised erythrocytes.

3.2.4 Parasite enumeration and staging

Parasitaemia was measured by microscopic quantitation from Giemsa-stained thin blood film smears made from tail vein bleeds as described in 2.2.5. A morphological chart (Figure 3.1) was constructed and used to classify parasites according to standard definitions of malaria morphological stages as rings, early and late trophozoites and schizonts [185].

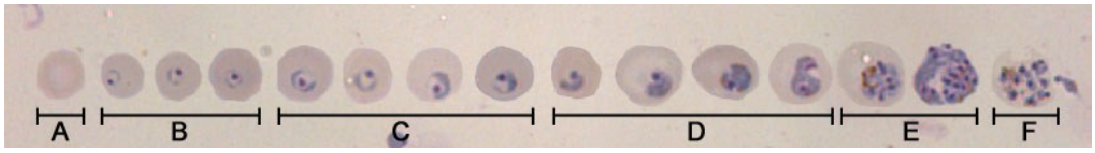

Figure 3.1 – *P. berghei* morphological classification chart showing uninfected RBC(A), ring stages(B), early trophozoites(C), late trophozoites(D), schzonts(E) and merozoites(F).

Ring stage parasites (B) were defined as having a defined nucleus with a crescent shaped edge to the vacuole. Early stage trophozoites (C) have a larger and partly filled vacuole while late stage trophozoites were defined as those with half to completely filled vacuoles (D). Schizonts were characterised by the presence of multiple nuclei, and no clear separation between nucleus and vacuole (E).

3.2.5 Parasite inoculation studies

Parasite inoculation studies were conducted to determine the most appropriate number of *P. berghei* infected RBCs to inoculate experimental mice with, in order to provide a stable reproducible model with an appropriate parasitaemia for drug studies. Four groups of three, five week old Swiss male mice were infected with either 10^5, 10^6 or 10^7 parasitised erythrocytes. The infection was

followed and thin blood films taken daily to monitor the development of the infection with different infecting inocula sizes. Subsequently for all experimental studies, recipient male Swiss mice aged five weeks received an i.p. inoculation of 10^7 parasitised erythrocytes.

3.2.6 Erythrocyte population and blood studies

Erythrocyte population and blood studies were conducted in order to characterise blood changes and other pathophysiological aspects of the *P. berghei* infection in the Swiss mouse model. Haematological changes are a common and obvious complication with malaria infections and include anaemia, white blood cell changes, thrombopathy and coagulopathies [246, 247, 362-364]. Erythrocyte population studies were conducted on five week old Swiss mice infected with 10^7 parasites. Eight mice were euthanized (pentobarbitone sodium 100mg/kg i.p.) every 24 h for 7 days after inoculation. Heparinised blood was harvested by cardiac puncture and red cell blood count (mean of triplicate measurements) was determined using a Cell-Dyn® 3500 automated Haematology Analyser (Diamond Diagnostics, Massachusetts, USA). Since mouse RBCs are smaller than human cells, the samples were run under the Veterinary mode using a Mouse parameter setting. As cell separation and counting occurs due to pre-calibrated mean corpuscular volume values, this ensured that red blood cells were counted as such, rather than being counted as large platelets in the human mode. Parasite density in the blood also was measured at each time point.

As well as erythrocyte and parasite density data, white blood cell population changes, haemoglobin concentration and platelet concentration data were collected over the course of infection using a Cell-Dyn® 3500 automated Haematology Analyser (Diamond Diagnostics, Massachusetts, USA). Spleen, liver and whole body weight measurements were also taken.

3.2.7 Formulation of dihydroartemisinin

Ethanol and ethanol in propylene glycol was used as a vehicle for DHA in mice studies as it had been used in previous studies, involving Wistar rats in our laboratory, which do not make up part of this Thesis [40]. The solubility of DHA in ethanol however was not sufficient to allow injection of doses of DHA above 50mg/kg or multiple doses within 24 h in Swiss mice without causing visible ethanol side effects and compromising the experiments. A series of solubility studies were conducted to obtain a suitable vehicle for DHA formulation to be administered i.p.

3.2.8 Dihydroartemisinin treatment

Dihydroartemisinin was formulated in 60% v/v DMSO in Polysorbate 80, with a final injection volume of 100μL. The vehicle dose was less than 25% of the LD_{50} for both DMSO and Polysorbate 80 in mice [327]. Initial safety studies were conducted using the drug vehicle at doses up to 400μL (for 30 g mice), with no observed adverse effects.

Five groups (n=8) of five week-old male Swiss mice received a single i.p. treatment 72 h after inoculation with 10^7 parasites, with either 0, 1, 3, 10, 30 or

100mg/kg DHA. Parasitaemia was monitored as described above until mice were euthanized according to pre-determined guidelines (parasitaemia >40% and/or body weight decline by >10% in a 24 hperiod, both of which were determined to be indicative of terminal deterioration in health of malaria-infected mice).

3.2.9 Dihydroartemisinin pharmacokinetics

3.2.9.1 Drug administration and blood sampling

Pharmacokinetic data for DHA in the *P. berghei* murine malaria model were collected. While PK investigations were not the focus of these studies, detailed PK data for the artemisinins in mice had not been previously reported. Studies have been reported in healthy and malaria-infected rats [224, 225, 311, 330, 444, 445] suggesting that the elimination half-life for DHA is approximately 15-25 minutes or two to three fold shorter than in humans [102].

Five week-old male Swiss mice were divided into healthy-uninfected (n = 66) or malaria-infected (n = 35) groups and the malaria-infected group received an i.p. injection of 10^7 uninfected RBC or 10^7 RBC as described previously (2.2.2). Approximately 72 h later post inoculation groups were administered 100mg/kg DHA. This occurred at a parasitaemia of approximately 5% in the malaria-infected group, which was confirmed by thin film examination. All mice received 100mg/kg sodium pentobarbitone 5-10 minutes prior to blood collection.

Blood was collected from the healthy group by cardiac puncture from groups of 3-6 mice at each time point of 2, 5, 7.5, 10, 15, 20, 25, 30, 40, 50, 60, 90 and 120 minutes after dosing (1mL fluoride/oxalate Vacutainer®; Becton-Dickinson, Franklin Lakes, NJ). Blood was collected from the malaria-infected group in a similar manner from groups of 3-5 mice at each time point of 2, 5, 10, 15, 30, 45, 60, 90 and 120 minutes. Blood was centrifuged at 3,000g for 7 minutes immediately after collection, and the plasma was separated and stored at -80°C until analysis.

3.2.9.2 Pharmacokinetic analysis

Stock solutions of 1mg/mL of DHA and the internal standard 1mg/mL artemisinin (QHS) in 45% acetonitrile in 0.1M Walpole's acetate buffer, pH 4.8 (A2.11) were prepared and stored in the dark at 4°C. Solutions were determined to be stable under these conditions for several weeks.

High performance liquid chromatography (HPLC) analysis was performed using a Waters 1525 binary pump, Waters 2487 Dual λ absorbance detectors with a 484 tunable absorbance detector. Separations were achieved using a LiChrospher® 100 RP_{18} (5μm) LiChroCART® 250-4 C_{18} column with a Waters Symmetry C_{18} (5μm, 3.9×20mm) guard column. The mobile phase was 45-50% acetonitrile in Walpole's acetate buffer, pH 4.8(A2.11) at a flow rate of 0.7mLs/min and post column derivatization with a solvent injection system at 60PSI using 1.2M KOH in 90% methanol at 0.4mL/min with a 69°C mixing block.

DHA in plasma was analysed using a validated HPLC assay [38] with modification of the extraction procedure. 200μL of plasma was mixed with internal standard (20μL of 5mg/L artemisinin in methanol), 100μL of 0.1M Walpole's acetate buffer, pH 4.8 (A2.11) and 900μL of 20% v/v ethyl acetate in butanol chloride. The mixture was gently agitated for 10-30 minutes at room temperature and the organic layer (typically 700-800μL) was aspirated and dried under nitrogen for 10 minutes. The residue pellet was reconstituted in 100-150μL of mobile phase (45-50% acetonitrile in Walpole's acetate buffer, pH 4.8(A2.11)), and the injection volume was 80μL and injected using a Waters 717 Plus autosampler. For each analytical batch a 5 or 8-point linear calibration curve was prepared using stock 1mg/mL DHA.

Analysis of pharmacokinetic data was performed by Professor Kevin Batty (School of Pharmacy, Curtin University). The mean plasma concentration for each sub-group in the healthy and malaria-infected groups was used to generate pharmacokinetic parameters. Noncompartmental PK analysis (Kinetica, version 4.2; Thermo Fisher Scientific, Inc., Waltham, MA) was used to estimate the area under the plasma concentration-time curve (AUC), terminal elimination half-life ($t_{½}$), apparent clearance (CL/F) and apparent volume of distribution (V/F).

3.3 Results

3.3.1 *P. berghei* malaria model in Swiss mice

The original *P. berghei* infection was established from cryopreserved stock on the 26 May 2001 in male Balb/c mice.

3.3.2 Parasite inoculation study

It was decided that a 5% parasitaemia would be used as a starting parasitaemia in later drug treatment studies. Drug studies were to be conducted in an established infection, and 5% parasitaemia represents a high enough parasitaemia to count blood films easily while the infection has not caused significant and irreversible physiological effects that may compromise experimental results. 5% also provides a starting infection in which the parasitaemia can drop over two orders of magnitude before the limit of detection is reached (2.2.5) (Figure 3.2).

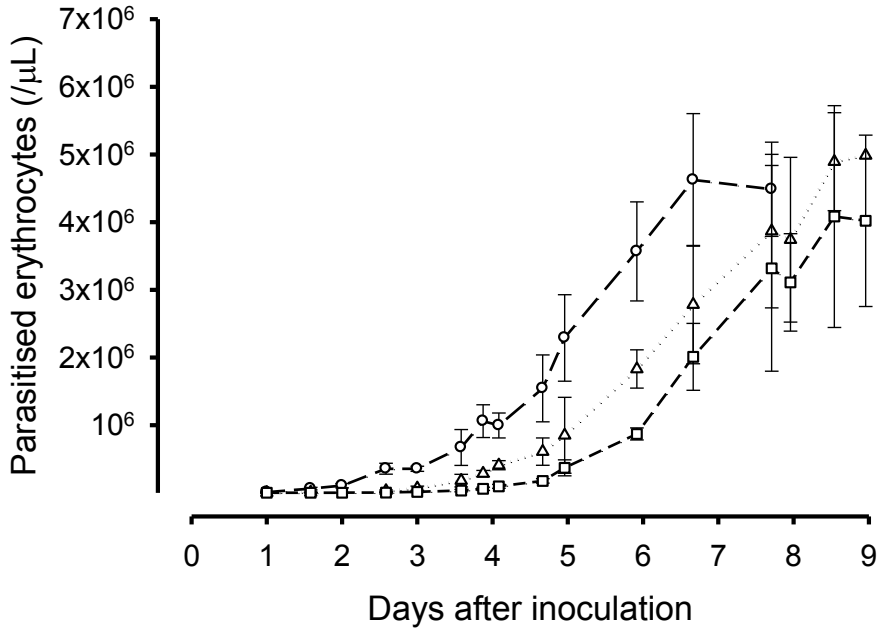

Figure 3.2 – *P. berghei* infection after inoculation with 10^5 (O), 10^6 (Δ) and 10^7 (□) parasitised erythrocytes.

3.3.3 Erythrocyte population studies

The percentage parasitaemia increased from 0.07±0.02% 24 h after infection with 1×10^7 infected erythrocytes up to 67±11% at 7 days after infection (Figure 3.3). Animals were euthanized at this point after a decrease in body weight of 10% over 24 h, which was used as an indicator that the infection was severe in order to minimise animal suffering (Figure 3.4).

Quantification of parasitaemia in a murine model is traditionally measured as a proportion, or percentage, of infected erythrocytes as in Figure 3.3. However, to characterise an infection model, it was considered necessary to convert the proportion of infected erythrocytes to the number of parasitised erythrocytes

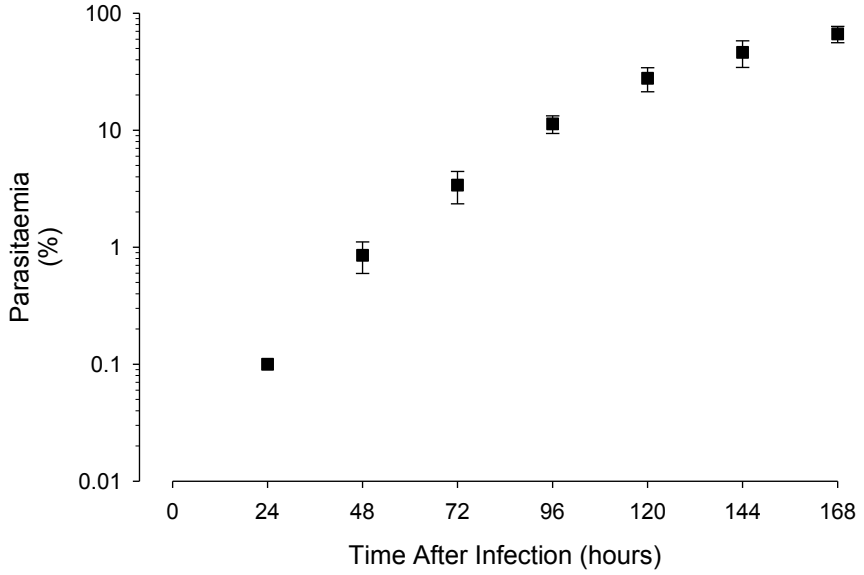

Figure 3.3 – Parasite density and SD measured in percentage of infected erythrocytes over the course of the *P. berghei* infection (n=8 for each data point).

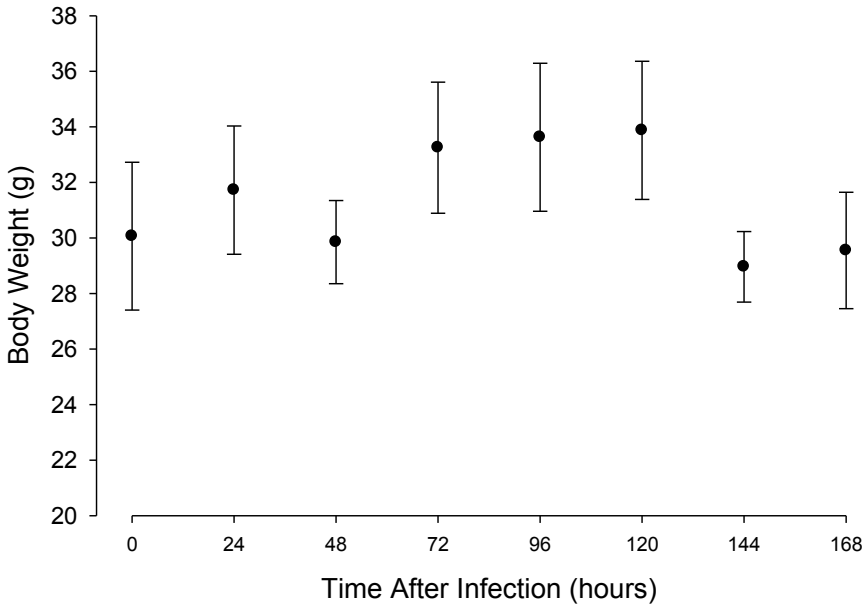

Figure 3.4 – Animal average body weight and SD during the *P. berghei* infection (n=8 for each data point)

per µL of whole blood. This is dependent on the erythrocyte count, which declines as malaria infection progresses (Figure 3.5), mainly due to clearance of parasitised erythrocytes by the spleen [230, 231]. There was no significant change in the erythrocyte population until after 72 h post infection, when the population decreased linearly until animals were euthanized (Figure 3.5).

Since the decline in erythrocyte count with increasing parasitaemia was considered an important variable to be incorporated into the murine model, the first step in model development was to define the relationship between the degree of parasitaemia and the erythrocyte count based on erythrocyte population studies.

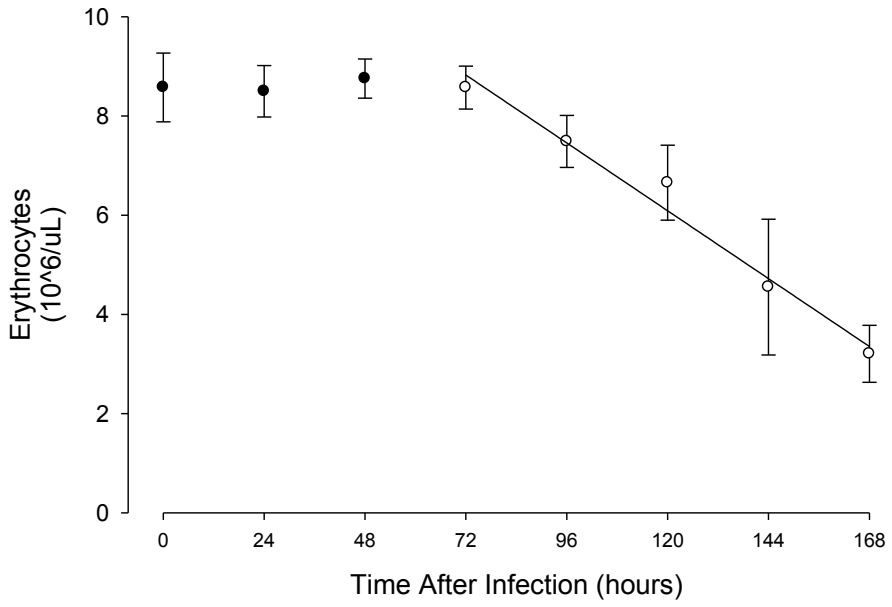

Figure 3.5 – Average and SD of the number of erythrocytes per µL over the course of a *P. berghei* infection after inoculation with 10^7 parasitised erythrocytes at T0 (n=8 for each data point). ◇ represent period from 72 h during which erythrocyte population decreases in a linear fashion.

These studies showed a significant inverse linear relationship between the parasitaemia and the number of erythrocytes (Figure 3.6; r^2 = 0.99; n = 64; P = 0.05). The mean erythrocyte count in healthy mice (n = 7) was 8.6 ± 0.7 × 10^6/µL. The relationship between erythrocyte count and parasite density was used to convert the percentage of parasitised erythrocytes determined by microscopy to parasitised erythrocytes/µL using Equation 3.1 below.

$$E_i(/\mu L) = [E_i(\%) \times 0.01] \times ([-0.085 \times E_i(\%)] + 8.6) \times 10^6$$

Equation 3.1

where: E_i is the number of infected erythrocytes and $E_i(\%)$ is the percentage of total erythrocytes in the thin blood film. The slope (-0.085) and intercept (8.6 × 10^6) values were derived from the erythrocyte count versus parasitaemia data shown in Figure 3.6.

The resulting relationship between the number of parasitised erythrocytes per µL as infection progresses is shown in Figure 3.7.

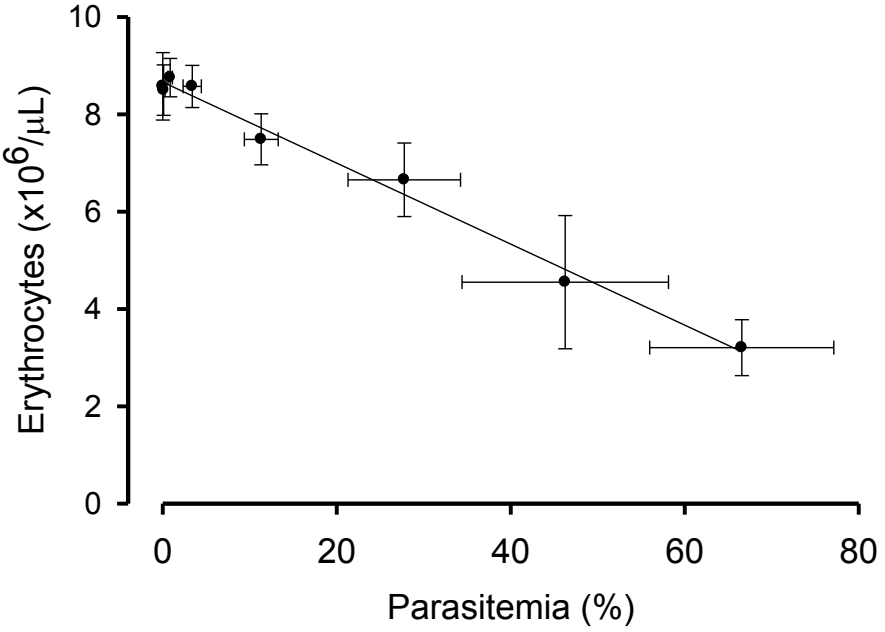

Figure 3.6 – Erythrocyte count (mean ± SD; n=8; triplicate analysis of each sample) verus parasitaemia in Swiss mice inoculated with *P. berghei.* There was a significant linear correlation between erythrocyte count and parasitaemia (P=0.05; r^2=0.99; n=64).

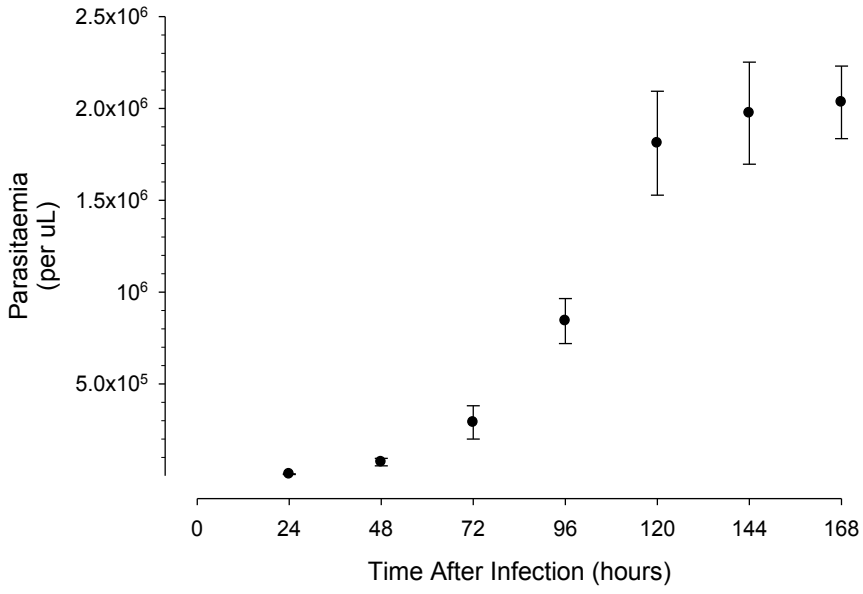

Figure 3.7 – Parasitaemia (mean ± SD; n=56) measured as the number of parasitised erythrocytes per μL of blood over the time course of infection.

3.3.4 Pathophysiological studies

During the erythrocyte studies other physiological parameters were measured in order to further understand infection. It was considered that this may be useful information in constructing a model of infection and disease progression in Swiss mice. White blood cell counts, liver weight, spleen weight, haemoglobin and platelet concentrations were determined from 8 sacrificed mice every 24 h during the course of infection for 168 h.

3.3.5 Haemoglobin concentration

During the course of *P. berghei* infection the whole blood haemoglobin concentration did not significantly change prior to 72 h post infection. From 96 hours post infection the haemoglobin concentration began to decrease to approximately 50% by 168 h post infection (Figure 3.8). As expected this corresponds to the fall in erythrocyte concentration which also decreases after 72 h to less than 50% control values as erythrocytes are removed and destroyed.

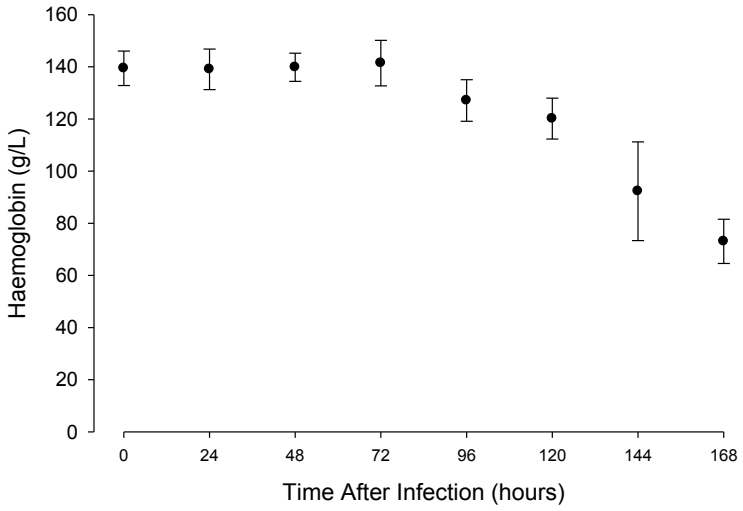

Figure 3.8 – Whole blood haemoglobin concentration (g/L; mean ± SD; n=8; ; triplicate analysis of each sample) as *P. berghei* infection progresses untreated.

3.3.6 Platelet concentration

During the course of the *P. berghei* infection platelet count decreased by up to 50% by day 6 post infection (Figure 3.9).

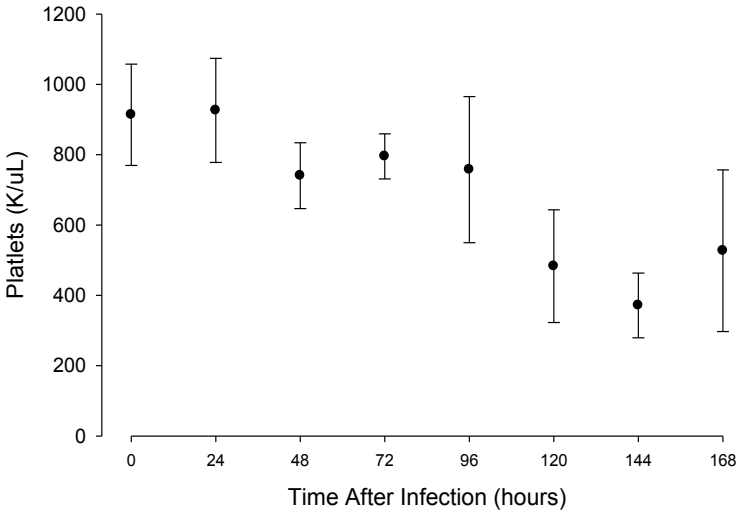

Figure 3.9 – Blood platelet concentration (K/μL; mean ± SD; n=8; ; triplicate analysis of each sample) as *P. berghei* infection progresses untreated.

3.3.7 Liver and spleen weight

During the course of the infection the liver weight as a percentage of the total body weight did not significantly change (Figure 3.10). Actual liver weights (i.e. not normalised using body weight) of infected mice therefore change over the course of the infection at a rate similar to whole body weight loss.

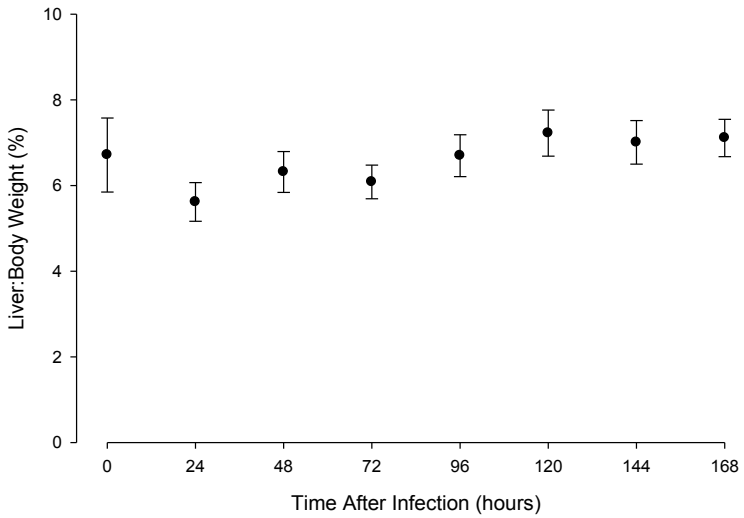

Figure 3.10 – Liver to body weight ratio expressed as a percentage over the course of untreated *P. berghei* infection (mean ± SD; n=8).

The spleen of infected animals underwent-significant weight increase relative to body weight from 72 h post infection (Figure 3.11A). Normalised spleen weights increased by 50% as the infection progressed. The spleens were visibly enlarged and had much darker and mottled colouring relative to healthy spleens (Figure 3.11B).

3.3.8 White blood cell population changes

During infection progression there was an almost exponential increase in total white blood cell counts (Figure 3.12). The white cell population changed during the course of the infection with an increase in the ratio of eosinophils to other white cells, and a decrease in neutrophils (Figure 3.13).

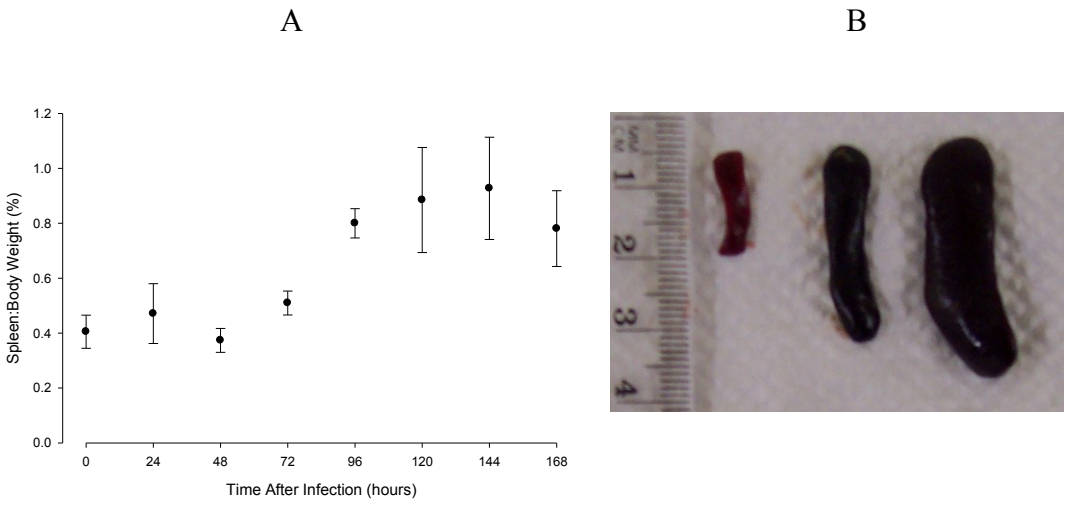

Figure 3.11 – (A) Spleen to body weight expressed as a percentage over the course of untreated *P. berghei* infection (mean ± SD; n=8). (B) Comparison of spleens from a healthy control (left) and *P. berghei* infected mice at 96 (centre) and 168 h (right) post infection alongside a ruler showing mm and cm increments.

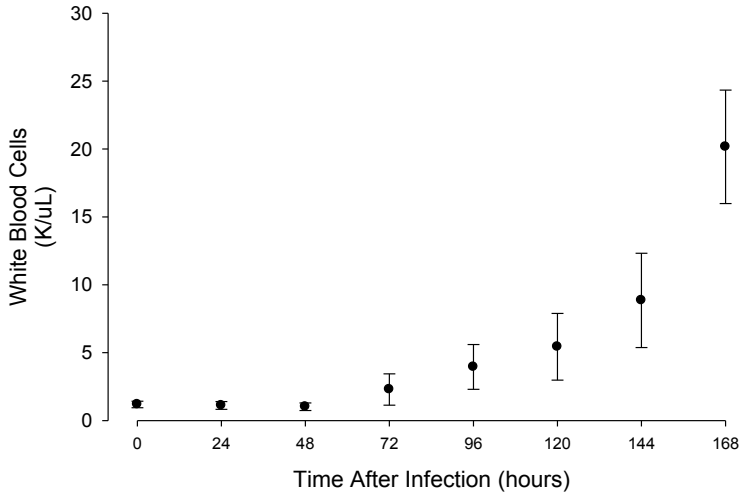

Figure 3.12 – Change in white blood cell counts over the course of *P. berghei* infection (mean ± SD; n=8).

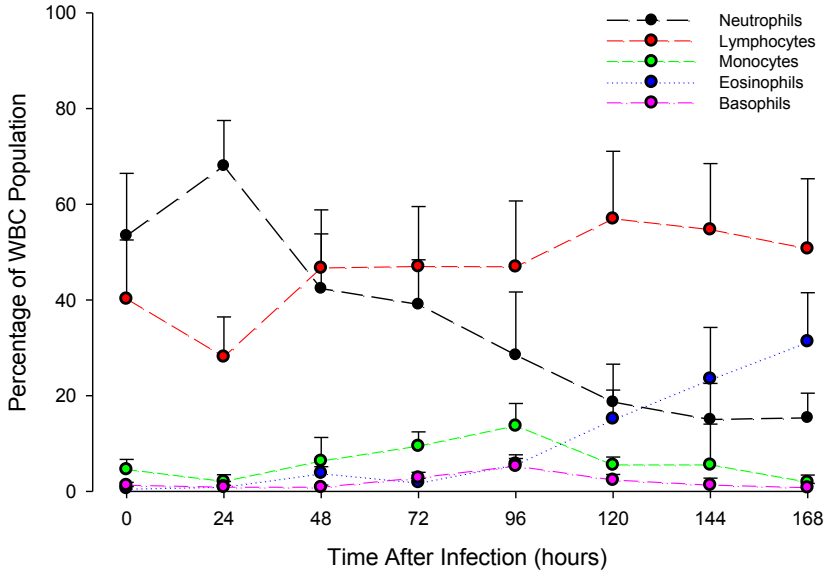

Figure 3.13 – Change in white blood cell population counts over the course of *P. berghei* infection (mean ± SD; n=8).

3.3.9 Dihydroartemisinin single dose treatment

P. berghei showed a graded dose response to DHA treatment (Figure 3.14). For 1, 3, 10, 30 and 100mg/kg doses nadir occurred approximately 18-24 h after administration and all doses were sub-therapeutic and leading to parasite recrudescence.

3.3.10 Dihydroartemisinin treatment staging

A series of blood films from a single mouse treated with 100mg/kg DHA at 72 h after inoculation were staged in order to examine changes in parasite population stages with DHA treatment and determine the usefulness of parasite staging data. Early stages (Rings) were least affected by DHA treatment while late stages (Schizonts) showed the greatest decrease (Figure 3.15).

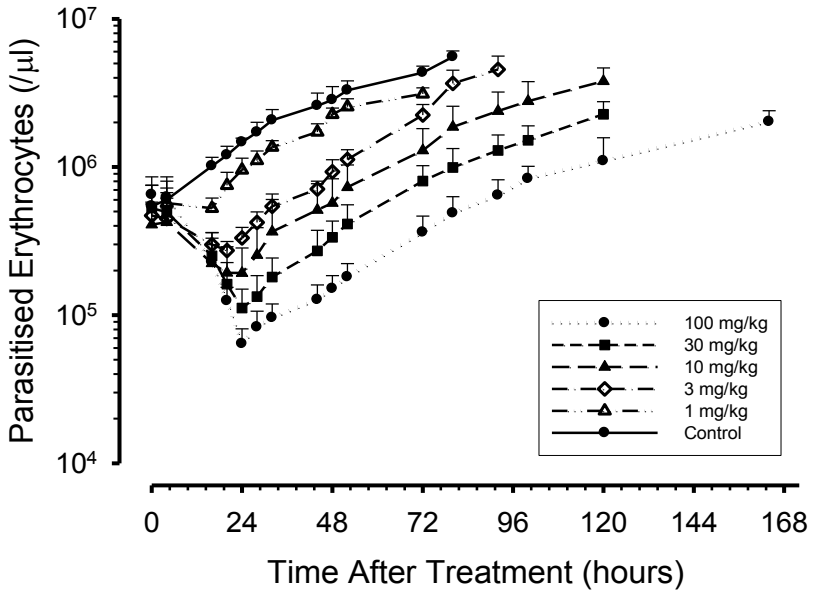

Figure 3.14 – Graded dose response of *P. berghei* infection to 0, 1, 3, 10, 30 and 100mg/kg DHA doses in Swiss mice (mean ± SD; n=8 for each data point).

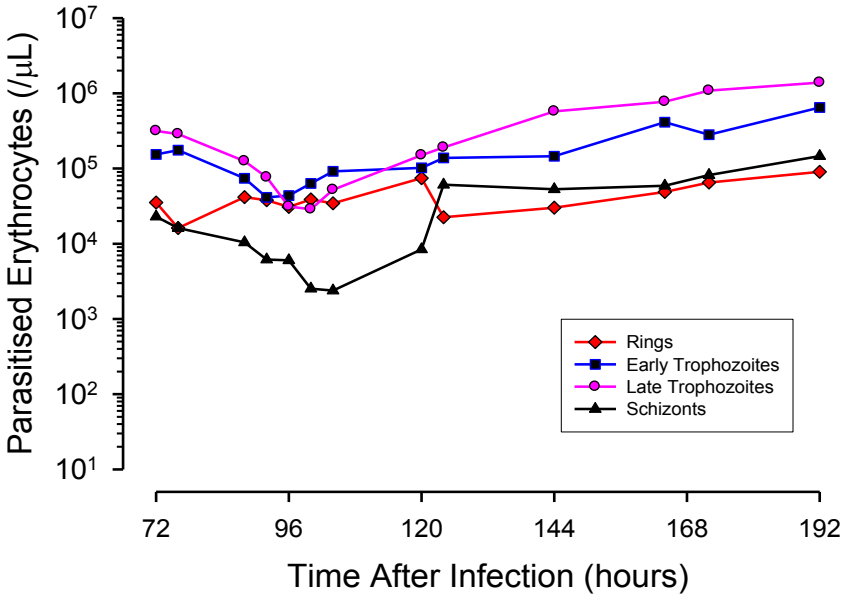

Figure 3.15 – Staging of *P. berghei* infection in a Swiss mouse treated with 100mg/kg DHA at 72 h post inoculation.

3.3.11 Dihydroartemisinin pharmacokinetics

Pharmacokinetic data are shown in Figure 3.16. Analysis of pharmacokinetic data was performed by Professor Kevin Batty (School of Pharmacy, Curtin University). Pharmacokinetic parameters are shown in Table 3.2. The AUC in malaria-infected mice (1.63±0.11mg.h/L) was significantly lower than in healthy mice (1.96±0.10mg.h/L; $P<0.05$). The terminal elimination $t_{½}$ values for DHA for healthy and malaria-infected mice were similar (Table 3.2, Figure 3.16). Data from this study were consistent with previous investigations in rats.

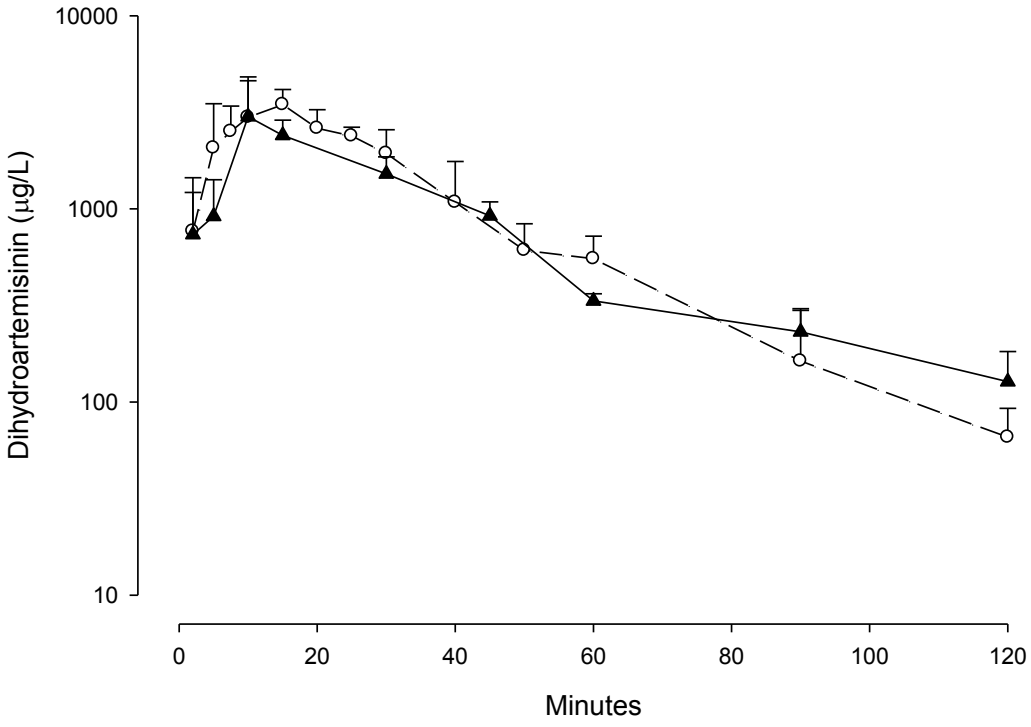

Figure 3.16 – Plasma concentration-time profile for DHA in P. berghei malaria-infected (▲) and uninfected (O) Swiss mice. Data are mean ± SD for 3-6 mice.

Table 3.2 – Pharmacokinetic parameters for IV DHA in mice

	$t_{½}$ (min)	CL/F(L/h/kg)	V/F (L/kg)
Healthy Mice	18.8	50.9	23.0
Malaria-infected Mice	24.6	61.3	36.3

3.4 Discussion

A murine model of malaria infection has been established. 10^7 infected erythrocytes administered i.p. were used to infect 5 week old male Swiss mice. Treatment commenced 72 h after infection when parasitaemia reached approximately 5% to allow treatment to be monitored in an established infection. Thin blood films were prepared regularly after drug administration and the mice can be carefully monitored as the infection progresses.

An important consideration in establishing a model of antimalarial treatment was to characterise the level of parasitaemia at which treatment should begin. Starting treatment at a parasitaemia of 5% did not cause any visible distress to the mice, nor was it related to any significant changes in body weight, erythrocyte count or liver and spleen weights. Furthermore, the infection-time profile after DHA treatment could be followed until pre-determined experimental endpoints were reached (parasitaemia >40% and/or body weight decline by >10% in 24 h period), which was usually at least 3–5 days longer than controls, depending on the DHA dose. At starting parasitaemias of 0.5–1%, DHA was also effective, but due to low post-treatment parasitaemias it was only possible to characterise a partial infection-time profile across the full range of DHA doses. Hence it was concluded that the optimum starting parasitaemia for pharmacodynamic studies was 5%.

Ishih *et al* [182] reported that a complex relationship exists between parasite load and efficacy, and parasite levels influenced the outcome of CQ treatment in a *P. berghei* NK-65 model. It is therefore important that any *in vivo* malaria model should have a well defined treatment parasitaemia and be able to produce consistent and reproducible starting parasitaemia. For this reason 5% parasitaemia, rather than 72 h post inoculation, should be the trigger for commencement of treatment in the model.

Characterising the time-dependent change in parasitaemia in the model described here depends on being able to accurately and efficiently determine parasite counts by light microscopy. In this regard, valid parasite densities at a parasitaemia of 0.5% can be determined by counting up to 30 fields of view (normally >6000 erythrocytes). By comparison, if 100 fields of view are counted, the limit of detection is a parasitaemia of about 0.004%. Hence, regular thin blood film monitoring of the malaria infection in this model can provide graded dose–response data over at least three orders of magnitude below the starting parasitaemia of 5%. In addition, if the decline and recrudescence phases of the infection are well characterised, it is possible to estimate a nadir at a parasitaemia of <0.0001% (<10 parasites/μL) by logarithmic extrapolation. The level of PD evaluation that is possible with the model presented here is a substantial advance on conventional animal methods of measuring antimalarial efficacy. The 'Peters 4-day test' in which parasite inoculation is followed by four, once-daily doses of drug, commencing at the time of inoculation [293],

demonstrates suppression of parasite growth/multiplication and is a well established rodent test for screening antimalarial drugs. By contrast, the Rane test [293] evaluates the effect of a drug on parasite elimination in an established infection, as has been demonstrated in efficacy studies of trioxolane antimalarial drugs [402]. Recent studies in rat models also show some features of the Rane test, but detailed dose–response relationships were not reported [226, 285, 443].

The model development work described here is based on the principles of the Rane test, but there has been allowance made for both variation in parasite multiplication rate and changes in the erythrocyte count in describing progression of the infection. Characterisation of changes to the erythrocyte population during infection, allow for a more accurate and decoupled estimation of parasite population changes, which is particularly relevant as parasite densities exceed 10%.

Hence the model presented in these studies provides a more flexible and pathophysiologically appropriate experimental framework for investigation of drug action and study of dosing regimens. The basic protocol for the experimental *in vivo* PD *P. berghei* murine model is summarised in Figure 3.17.

The method was validated using graded single doses of DHA which provided detailed PD data of the *P. berghei* infection during drug treatment. Parasitaemia decreased quickly after DHA administration to nadir at between 18 and 24 h.

Interestingly the peak in parasite decline is approximately 24 h post administration while DHA has a very short plasma half-life of ~25 minutes in Swiss mice [39]. This would suggest that there is either a delay in the DHA induced killing of parasites and/or a delay in erythrocyte removal. Determination of the PK parameters for DHA in mice has not been previously reported, and while DHA pharmacokinetics were not the focus of these studies, it was demonstrated that detailed PK-PD data and relationships can be studied in this model.

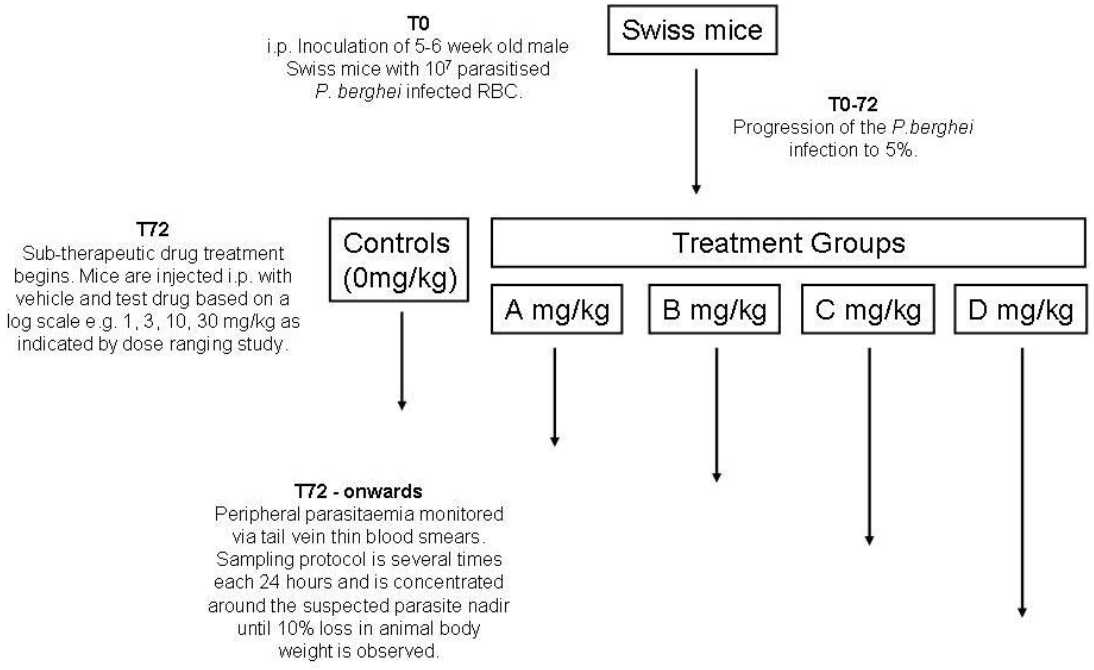

Figure 3.17 – Schematic representation of the study protocol used for antimalarial pharma-codynamic efficacy studies. A 5% parasitaemia rather than a specific time should be used as the start of sub-therapeutic drug treatment.

DHA studies show that a murine model of malaria treatment can provide an array of sub-therapeutic dose-response data that is not possible in clinical

studies. The model appears to be reproducible and stable and has provided robust dose-response data.

CHAPTER FOUR

4. Establishing a mathematical model of murine *P. berghei* infection and single dose monotherapy with dihydroartemisinin

4.1 Introduction

Animal models of human disease can provide valuable information leading to insights into the human disease state. Investigations using animals to examine detailed pharmacodynamic (and PK) relationships between a drug, host and the disease (or parasites) require a large number of animals and a significant time investment. Pharmacokinetic and pharmacodynamic studies in the previous chapter utilised 40 mice to provide PD and 101 mice to provide PK data. While 40 mice per graded single dose PD study may not seem large, when collecting detailed PD data as reported, the 81 data points represented in Figure 3.14 comprise some 648 thin films. Considering future work in multiple and combination dosing studies in the *in vivo P. berghei* model, and the aim of regimen optimisation, use of the model becomes questionable due to the time required without guarantee that optimisation will be truly demonstrable, or the results clinically relevant.

Subsequent to the development of a robust *in vivo* murine model of malaria infection reported in Chapter 3, and embarking upon further PD studies, the question arose as to whether a mathematical model of murine malaria infection and specific drug treatment, could be developed to allow a large portion of experimental work to be carried out *in-silico*, with the results verified by animal

studies. In this way much of the drug treatment regimen design and optimisation could be mathematically simulated and then experimentally verified, saving both time and animals.

4.1.1 Mathematical models – limitations and pitfalls

The use of models is central to the scientific method. However, acceptance and application in the field of physiology and medicine often lags behind that of other disciplines. This is often due to the mismatch between the complexity of the processes in question and the limited data available from *in vivo* studies. The limitations in data collection are basically problems of measurement and are summed up by Cobelli *et al* [91] to include

- restrictions on the number of variables and parameters – some physiological parameters cannot be measured and the frequency of sampling is often restricted;
- many measurements are corrupted by noise due to experimental error or unwanted physiological disturbances; and
- clinically there are some variables (e.g. patient discomfort) for which scales of measurement are not clearly defined and only qualitative concepts exist.

Technological progress in medical imaging including PET (positron emission tomography) and MR (magnetic resonance) imaging are allowing collection of more detailed functional information less intrusively, and is beginning to overcome some of the traditional measurement problems associated with

physiology and medicine. This will likely enhance the scope to construct more accurate models of physiological processes and lead to a greater use of mathematical modelling techniques in the field.

Mathematical modelling or “simulation” is a way of creating an artificial biological system *in vitro* for which properties can be changed. By externally controlling the model, new datasets can be created to explore aspects of the simulated model. In modelling, sets of differential equations and logic clauses are used to create a dynamic systems environment that can be tested. A model is an optimal mix of hypotheses, evidence, and abstraction to explain a phenomenon. Barh and colleagues made the following comment on *in silico* modelling [29]

“in silico modelling in the life sciences is far from straightforward, and suffers from a number of potential pitfalls. Thus, mathematically sophisticated but biologically useless models often arise because of a lack of biological input, leading to models that are biologically unrealistic, or that address a question of little biological importance. On the other hand, models may be biologically realistic but mathematically intractable. This problem usually arises because biologists unfamiliar with the limitations of mathematical analysis want to include every known biological effect in the model. Even if it were possible to produce such models, they would be of little use since their behavior would be as complex to investigate as the experimental situation. These problems can be avoided by formulating clear explicit biological goals before attempting to construct a model. This will ensure that the resulting model is biologically sound,

can be experimentally verified, and will generate biological insight or new biological hypotheses. The aim of a model should not simply be to reproduce biological data. Indeed, often the most useful models are those that exhibit discrepancies from experiment. Such deviations will typically stimulate new experiments or hypotheses. An iterative approach has been proposed, starting with a biological problem, developing a mathematical model, and then feeding back into the biology. Once established, this collaborative loop can be traversed many times, leading to ever increasing understanding."

There are two basic approaches to developing mathematical models. These are the data-driven approach or "modelling the data", which is based upon experimental data, or the "modelling the system" approach, which is based upon a fundamental understanding of the physical and chemical process. These could be considered top down, or bottom up modelling approaches. The modelling discussed in this Chapter is based on data from Chapter 3 and may be regarded as a "modelling the data" approach. There are however inputs from assumptions about malaria in order to ensure the model is physiologically based, which fall under a "system modelling" approach. It can be argued that these assumptions are based on observation of malaria, rather than fundamentally understanding the system, so the model presented in the studies here was largely based on modelling the data.

4.1.2 Data modelling methodology

Data driven or “black box” models seek quantitative descriptions of physiological systems based on input and output descriptions derived from experimental data collected on the system. The methodological framework is shown in Figure 4.1 [90]. These types of models are appropriate where there are gaps in the understanding of the underlying physiology or when an overall representation of the systems dynamic inputs and outputs is required without specifying how the physiological mechanisms give rise to this behaviour [90].

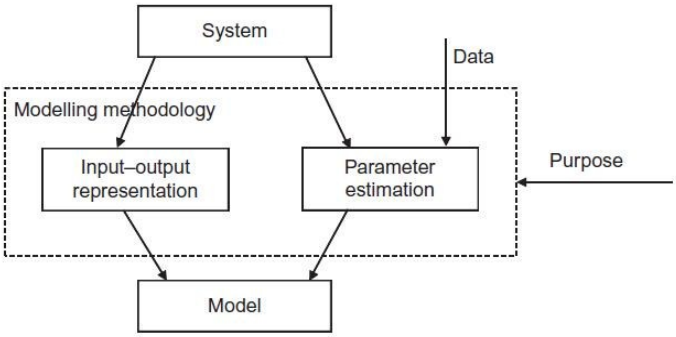

Figure 4.1 – data driven modelling methodological framework, reproduced from Cobelli and Carson 2001 [90]

Once data have been collected a data driven model can be constructed based on representations of input and outputs and initial parameters which are estimated from the data. The model then requires validation, which is an examination of whether the model is sufficient relative to its intended purpose. Is the model credible? Is the model output plausible? The basic methodological process of model construction and model validation is represented in Figure 4.2 [90] and similarly to Barh and colleagues comments [29] highlights that modelling is an iterative approach; from biology, to model development and back

again. There are a number of salient points made by Cobelli and Carson [90] with respect to models

- All models are approximations and should be flexible to include new data and observations.
- A good model is clearly falsifiable.
- Successful modelling is dependent upon quality data, and quality modelling.

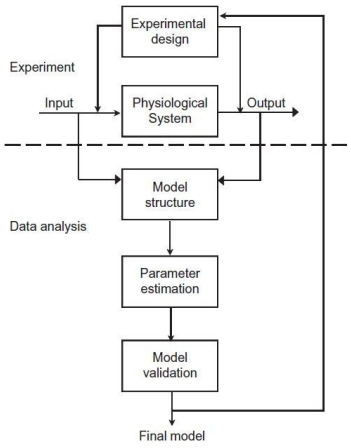

Figure 4.2 – overview of modelling methodological framework, reproduced from Cobelli and Carson 2001 [90]

4.1.3 Mathematical models of infection

There exists a multitude of mathematical models of human infection, from epidemiological models through to individual host-parasite models [15, 69, 76, 92, 181, 202, 283, 310, 385, 392, 396]. The discipline of mathematical modelling of disease grew from the success of this approach in understanding the epidemiology of directly transmitted viral and bacterial infections (e.g. measles,

mumps and rubella), and the impact of mass vaccinations on transmission rates [92]. Anderson in 1994 commented [16]

"distrust of mathematics is easy to understand as it often centres not so much on an unfamiliarity with the language but more on the simplicity of the assumptions embedded in models in the face of known biological complexity."

Similarly to animal models of disease, results from mathematical models should be considered in the context of the assumptions upon which a model is based and a thorough validation of the results against data. The mathematical modelling approach is consistent with the philosophy of experimental science. It is reductionist and should ultimately lead to greater understanding of biological processes which can feedback into more accurate modelling.

4.1.4 Mathematical models of malaria infection

The study of dynamic processes in malaria with the use of mathematical models has its origins in the work of Ross and Macdonald [236, 324], as discussed previously. Malaria models have tended to focus on epidemiological models with little input into the dynamics within individual people, which play a large role in the transmission and spread of malaria. In 1997 McKenzie and Bossert [246] commented that

"Among the hundreds of mathematical models of malaria published since Ross' pioneering work, remarkably few address any aspect of dynamics within an individual host. We have located ten such models ..."

In these models limited clinical PD data [50, 203, 325] has been used to mathematically model aspects of *P. falciparum* infection in humans to examine hypotheses about connections between fluctuations in asexual parasitaemia, gametocytemia and host immune response [17, 103, 148, 209, 246, 400, 424]. Since malaria pathogenesis is related to asexual blood stages of malaria, and prognosis is largely dependent on the level of asexual parasitaemia [41, 150, 163, 269, 356], it is interesting that more epidemiological models do not address individual host dynamics. This is likely due to the difficulty of modelling human *P. falciparum*.

Human mathematical models of malaria infection are, of necessity, complex. Such models, according to Molineaux *et al* [256] require 5 factors to produce the level of realism in simulated versus observed parasitaemia. They are

1. Intra-clonal antigenic variation
2. Large variation of the variants baseline growth rate
3. Innate autoregulation of the asexual parasite density
4. Acquired variant specific immunity
5. Acquired variant-transcending immunity

This form of modelling in humans relies on use of limited historical data, as discussed in 1.2.11. In the clinical setting there are the added complications of

- Reinfection
- Multiple strain and poly-clonal infections
- Drug Resistance
- Co-infections or dietary disorders
- Non-compliance to drug regimens
- Host immune responses
- Sequestration of parasites

In 2002 Gravenor *et al* [147] presented an age-structured compartmental model for estimating total parasite load in falciparum malaria patients. This model employed clinical observations of peripheral parasitaemia to estimate population dynamics of sequestered parasites, which cannot be observed by the clinical investigator. They concluded that the model could not be used to make robust estimates of sequestered parasite dynamics due to insufficient data to construct the model and refine variable parameters [147].

Relative to clinically observed *P. falciparum* parasite population dynamics, *P. berghei* parasite dynamics in laboratory mice, are significantly less complex.

4.1.5 Compartmental modelling

Compartmental models, which form the basis underlying the research presented in this Chapter, are mathematical models used to describe the behaviour of materials or energies in a defined system. A compartment is a defined partition in which the study “material” is assumed to be homogeneously distributed. As

such a compartment is a mathematical concept that does not necessarily correspond to a physiological space or easily defined physical volume. A compartmental system is a finite number of compartments that interact by exchanging the "material" under study. A compartmental model is a mathematical model with equations to describe the transfer or flux of material between compartments. System variables define the amounts of material in each compartment and the changes in these compartments are represented by differential equations. Fractional transfer coefficients are represented by arrows indicating inputs and outputs from compartments. Compartmental analysis is a geometric representation of a system of differential equations. Some key concepts in compartmental modelling are [36]:

- Compartmental models should provide a plausible description of the system being studied in order to justify use of a given model.
- Aspects of a model that are observable or known experimentally can be fitted using a forcing function, which forces contents of a specific compartment to equal a known function and can be used to decouple complex systems.
- Selection of the sampling protocol can have a significant effect on the precision with which parameters are estimated. Data points are especially important in regions where changes in the slope of curves are important so data sampling should be increased in these regions if possible.
- Data weighting is used to fit models to data using a weighted least-squares approach so both the value and the weight of the data are taken

into account in the calculations. When at least two data sets are used, relative data weighting (as opposed to absolute data weighting) allows automated optimisation of each data set weight. When an error structure is not known exactly relative error weighting should be employed.

4.1.6 Aims

The aim of the series of studies presented here was to investigate the feasibility of using *P. berghei* infection and single dose PD treatment data, to design and develop a suitably simplistic and experimentally functional mathematical model of *P. berghei* malaria in Swiss mice. The initial aims were to:

i. Determine a mathematical relationship to describe time and parasite bioburden in Swiss mice infected with *P. berghei* parasites.
ii. Develop a simple and biologically plausible mathematical model of *P. berghei* growth in a Swiss model.
iii. Determine a mathematical relationship to describe time and parasite death and removal after administration of DHA.
iv. Determine if it is possible to introduce a drug-dependent parasite removal term to simultaneously model death, removal and baseline population growth of the parasite.

The hypotheses to be tested were:

i. A mathematical model of *P. berghei* infection progression in Swiss mice can be developed that reflects experimental observations.

ii. A mathematical model of *P. berghei* death and removal in Swiss mice treated with DHA can be developed that reflects experimental observations.

4.2 Methods

4.2.1 Relationship between time and parasite burden

Data presented in Chapter 3 (Figure 3.2 and Figure 3.7) were analysed using the regression function in SigmaPlot to the fit of various functions and approximate the relationship between infection time and parasite bioburden. This was to serve as a starting point for construction of an untreated infection model. In determining the most appropriate fitting function the physiological relevance of the function as well as the r^2 values were considered, particularly as time approached zero (i.e. very early in infection). At t = 0 (time of infection) the parasitaemia should be greater than zero.

The parasitaemia at this time is not a real value but a theoretic value or effective starting parasitaemia. If 1×10^7 infected erythrocytes are injected into the host intra peritoneal cavity, a certain proportion will migrate to the blood stream, while older, fragile and more rigid erythrocytes are more likely to be removed by host mechanisms prior to reaching the peripheral circulation. The actual observed parasitaemia at t = 0 will be zero, but is effectively some number less than 1×10^7 for the purposes of modelling. The Leiden Malaria Research Group have reported that approximately 10% of *P. berghei* parasites survive i.p. injection [185]. Late in the infection, the parasitaemia will approach a maximum which cannot exceed $8.6\text{x}10^6$ infected RBC/μl. Healthy Swiss mice have approximately $8.6\pm0.7\text{x}10^6$ RBC/μl (3.3.3). An infection of $8.6\text{x}10^6$ RBC/μl would represent a theoretically maximum parasitaemia of 100%. This is significantly higher than

the actual maximum achievable level of infection since animals will not survive with such a high level of infection. Additionally RBC destruction associated with infection progression above 10%, results in the total number of RBC being significantly less than 8.6×10^6 RBC/μl.

Based on the need to meet these criteria, the equations tested to approximate infection progression were required to have two horizontal asymptotes and a bell shaped derivative. The bell shaped derivative represents an initial increase in the rate of infection dependent only upon the parasite multiplication, which reaches a maximum, and then the rate of infection begins to fall. This occurs as the available number of uninfected RBC falls and the infection reduces the total number of RBC.

P. berghei parasite growth in a Swiss mouse model which is free of immune interference should approximate a logistic function with a carrying capacity that is no greater than the maximum number of RBC in a Swiss mouse. Logistics functions, which are a type of sigmoid, are commonly used for approximating resource limited population growth. They combine an exponential growth equation with a bounded exponential equation (or exponential growth to a maximum) to produce a curve that meets the requirements for *P. berghei* growth outlined below (Figure 4.3).

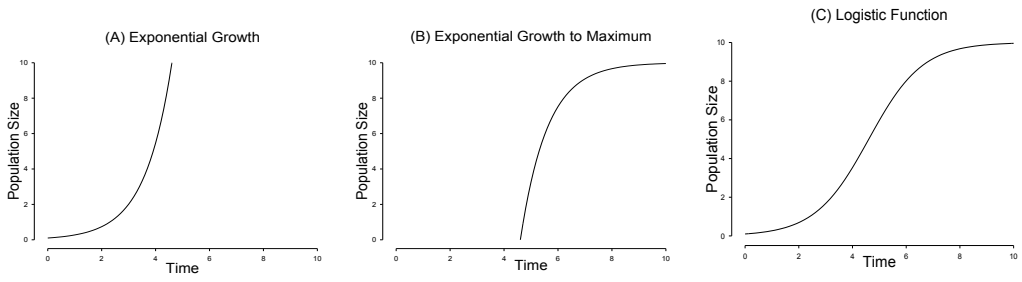

Figure 4.3 – Plots of (A) exponential growth and (B) exponential growth to a maximum which should approximate early and late population growth in a Swiss mouse model. (C) A logistic function should theoretically model both growth phases.

4.2.2 Conceptual model of *P. berghei* infection

The aim of these studies was to develop a model with biologically plausible assumptions and parameter ranges which produced a simulated parasite population that is statistically similar to the *P. berghei* parasite populations observed in Swiss mice. The raw data therefore needed to be reduced to as short a list of variables as possible, without compromising the biological relevance of the model, whose distributions can be used as quantified simulation targets. The following features are apparent on inspection of the data in Chapter 3 so were considered as initial simulation targets for a conceptual model.

- An initial period of possibly exponential increase in parasite population growth (Figure 3.7).
- This is followed by a peak and gradual decline in the rate of parasite population growth to a plateau (Figure 3.7).
- A model should include terms for parasite growth rate (equivalent to number merozoites per schizont, at least in early infection stages) and parasite removal. It is assumed however that in unchallenged infections

parasite removal is minimal due to minimal immunological interference in parasite population development [338-340].

Based on these features a basic conceptual compartmental model of parasite population growth was constructed (Figure 4.4). Initially compartments represented the four main life cycle stages of *P. berghei* being rings, early and late trophozoites and schizonts as categorised previously and shown in Figure 3.1 (Figure 4.4A).

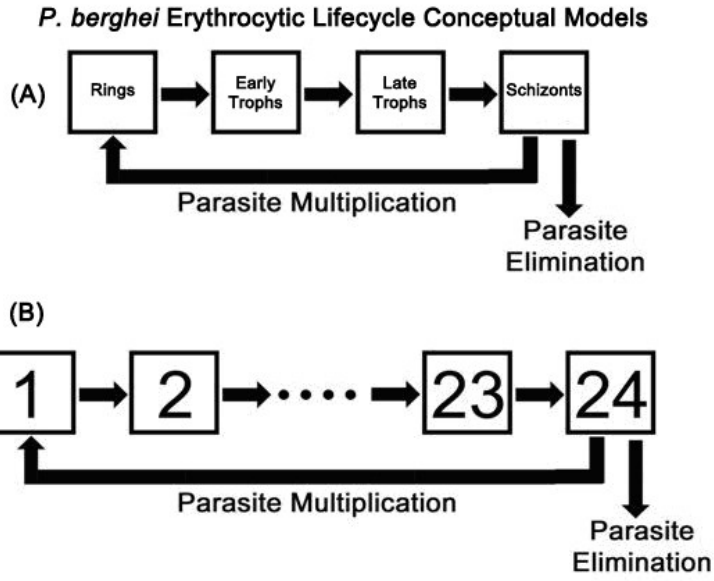

Figure 4.4 – Conceptual compartmental models of *P. berghei* infection. Model (A) differentiates parasite stages of the life cycle based on morphological classification. Model (B) was a modification to characterise the lifecycle into 24 compartments of equal time. This model still allows examination of stages based on a grouping of compartments but removes the dependency of the model on specific stage definitions.

These four lifecycle-stage-compartments were replaced with twenty four compartments representing parasites of hourly ages (Figure 4.4B). This removed the dependence of the model on definitions of parasite stages.

Additionally rather than having four rates, representing progression of parasites from rings to early trophozoites, early trophozoites to late trophozoites and etcetera, there were two rates representing one twenty fourth of the parasites life cycle and parasite multiplication.

4.2.3 Mathematical model of *P. berghei* infection in SAAM II

Once a conceptual model was established it was constructed in SAAM II Simulation, Analysis and Modelling Software for Kinetic Analysis (University of Washington, Seattle, USA). SAAM II is a compartmental and numerical modelling program that was readily available and is commonly used in the pharmaceutical industry for kinetic modelling. The program can create systems of ordinary differential equations from a compartmental model structure and provided a convenient and powerful platform for constructing a mathematical model of malaria that was understood.

Aspects of compartmental modelling to be considered in constructing the model included:

- Model structure and compartmentalisation
- Initial estimates of the parameters
- Use of forcing functions to decouple the model and represent schizont rupture and RBC invasion
- Data weighting

The basis of the SAAM II compartmental model (Figure 4.4) was that the 24 h life cycle of *P. berghei* was divided into compartments, each representing approximately one hour of parasite growth. Twenty four one hour compartments were selected to construct a model independent of life cycle stages while still allowing stages to be examined if required by grouping compartments into domains representing life cycle stages. This also allows the time of life cycle stages to be altered without changes to the operation of the model.

Parameters required in the model of parasite growth and development included parasite progression through compartments, parasite multiplication and parasite elimination rates. The parasite multiplication rate is the only one of these parameters that can be approximated based upon observed experimental results for inclusion into the SAAM II model. Parasite progression through compartments is a number of parasitised erythrocytes per μL of blood moving or aging at one twenty fourth of the parasite life cycle, which is close to 24 h, while parasite elimination should be close to zero assuming minimal immune interference due to immune suppression by *P. berghei* [338].

4.2.4 Validation of mathematical model of *P. berghei* infection

Once a mathematical model of infection was constructed the model needed to be validated to determine whether or not it was adequate for modelling infection. While this validation step may be presented as a seemingly distinct and separate entity, validation was continually carried out as the modelling process was undertaken. Carson *et al* presented the basic outline of the modelling

process (Figure 4.5) in which the processes, including validation, are highly interrelated and essentially iterative [73].

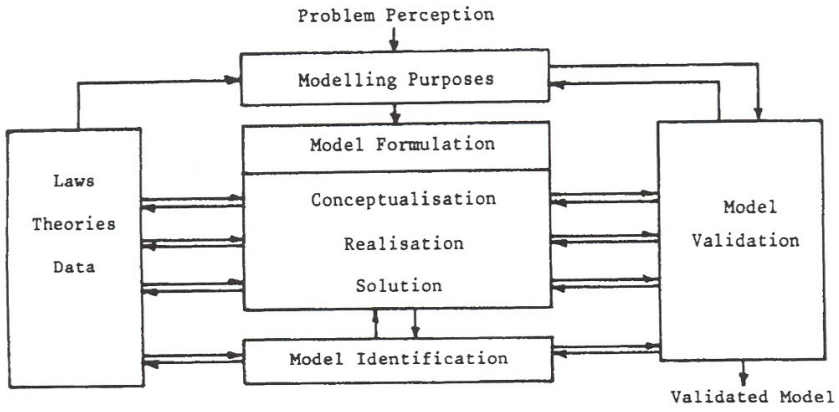

Figure 4.5 – Representation of the basic iterative modelling process reproduced from Carson *et al* 1983 [73]

The validation process followed in these studies was based on methodology presented by Cobelli *et al* [91]. Validity criteria can be separated into internal and external criteria. Internal criteria (e.g. consistency and algorithmic validity) enable the model to be assessed without reference to external criteria (empirical, theoretical, heuristic and practical validity) which refers to aspects external to the model including purpose, theory and data. Each of the validity criteria as discussed by Cobelli *et al* (1984) are defined below

- **Consistency** requires that the model contains no logical, mathematical, or conceptual contradiction.
- **Algorithmic validity** requires the simulation algorithm produces accurate solutions.

- **Empirical validity** requires that the model solutions should correspond to available experimental data with adequate accuracy.
- **Theoretical validity** requires that the model should be consistent with accepted theories.
- **Heuristic validity** refers to the potential of the model to be used for scientific explanation. For example the model may provide information on an unmeasured variable that may indicate that additional experiments should be carried out.
- **Practical validity** refers to the practical usefulness of the information provided by the model, and is over and above the theoretical and empirical validity.

Model validation was considered at all stages in the modelling process from concept to completion. Both internal and external criteria were applied during model formation as it was a requirement that the postulated compartmental system must be in agreement with known physiology. The final stages of validation are primarily concerned with satisfying conditions of empirical validity, which are of necessity, more stringent for a predictive model than for a descriptive model. In the case of the predictive model presented in this Chapter, the model must not only match available experimental data but also interpolated and extrapolated data. Parameter values need to reflect the underlying physical phenomena occurring in the system under study.

4.3 Results

4.3.1 Relationship between time and parasite bioburden

In the *in vivo* model presented in Chapter 3, infection progression was controlled by the size of the inoculation (i.e. $1x10^7$ infected erythrocytes). Visual inspection of the infection curves (Figure 3.7) suggests that in Swiss mice, *P. berghei* population dynamics are limited only by the available pool of uninfected red cells. All infected RBC can be assumed to be visible in peripheral smears, as opposed to *P. falciparum* infections where sequestration reduces the visible parasite population. The parasite bioburden time relationship visually appeared similar to a sigmoid function. The list of potential functions available to meet the required criteria was narrowed to sigmoidal functions which are summarised in Table 4.1. Three and Four parameter sigmoid functions provided the best fit while providing consistency with *in vivo* observations. A 5 parameter sigmoid function provided the best r^2 (Table 4.1), however proved physiologically implausible as time approached 0, or inoculation.

4.3.2 Constructing a compartmental model of *P. berghei* infection

A compartmental model was constructed in SAAM II based upon 24 compartments representing the life of infected erythrocytes from infection (compartment 1) to rupture (compartment 24). A screen shot of the compartment model is shown in Figure 4.6.

Table 4.1 – Equations used to fit untreated *P. berghei* infection data. A 5 parameter sigmoid had the highest r^2 but was an unrealistic fit as t approached 0*. This was similar to the 5 parameter Weibull and 3 parameter Hill, logistic, Chapman and Gompertz functions which have not been included in the table. Three and four parameter sigmoids were the best and most realistic fits.

Function	Equation	r^2
Sigmoid (3 parameter)	$y = \frac{a}{1+e^{-\left(\frac{x-x_0}{b}\right)}}$	0.988
Sigmoid (4 parameter)	$y = y_0 + \frac{a}{1+e^{-\left(\frac{x-x_0}{b}\right)}}$	0.988
Sigmoid (5 parameter)	$y = y_0 + \frac{a}{\left[1+e^{-\left(\frac{x-x_0}{b}\right)}\right]^c}$	0.994*
Logistic (4 parameter)	$y = y_0 + \frac{a}{1+\left(\frac{x}{x_0}\right)^b}$	0.984
Gompertz (4 parameter)	$y = y_0 + ae^{-e^{-\left(\frac{x-x_0}{b}\right)}}$	0.981
Hill (4 parameter)	$y = y_0 + \frac{ax^b}{c^b + x^b}$	0.984
Chapman (4 parameter)	$y = y_0 + a(1-e^{-bx})^c$	0.981

The model was created as a non-cyclic catenery compartmental model, meaning each compartment flows into the next (catenery) and the last compartment does not feedback into the first (non-cyclic). Rather than being cyclic, the model terminates with the red cell death and a forcing function is used to then "inject" newly infected erythrocytes into the model, representing merozoite release and invasion. The first step in characterising the model was determining the infection function, hence forth referred to as the effective parasite multiplication factor (EPMF). The function was referred to using

“effective” and “factor” as it is a simplified function based on physiological data that incorporates several biological functions such as the number of merozoites per schizont, the reduction in uninfected erythrocytes and possibly innate immune removal of parasites, rather than a clearly delineated process.

As well as the EPMF the effective parasite inoculation (EPI) was defined as the theoretic infection at inoculation (t=0). This was assumed from literature and observations to consist predominantly of rings and early to mid trophozoites, since older parasitised erythrocytes are unlikely to survive i.p. injection. The compartments in the model were divided roughly into rings (q1-q2 = approximately 2 h), early trophozoites (q3-q9 = approximately 7 h), late trophozoites (q10-q23 = approximately 14 h) and schizonts (q24 = approximately 1 h). Each of these was entered as a sample region in SAAM II so that it is possible in later experiments to examine parasite stages. Changing parasite stage designations simply requires adjusting of compartments in each sample. For example Sample 1 was designated as ring stages which were defined as q1 and q2. If it was deemed that the *P. berghei* rings stages lasted for 3 h instead of 2, sample 1 could be modified to include q1, q2 and q3.

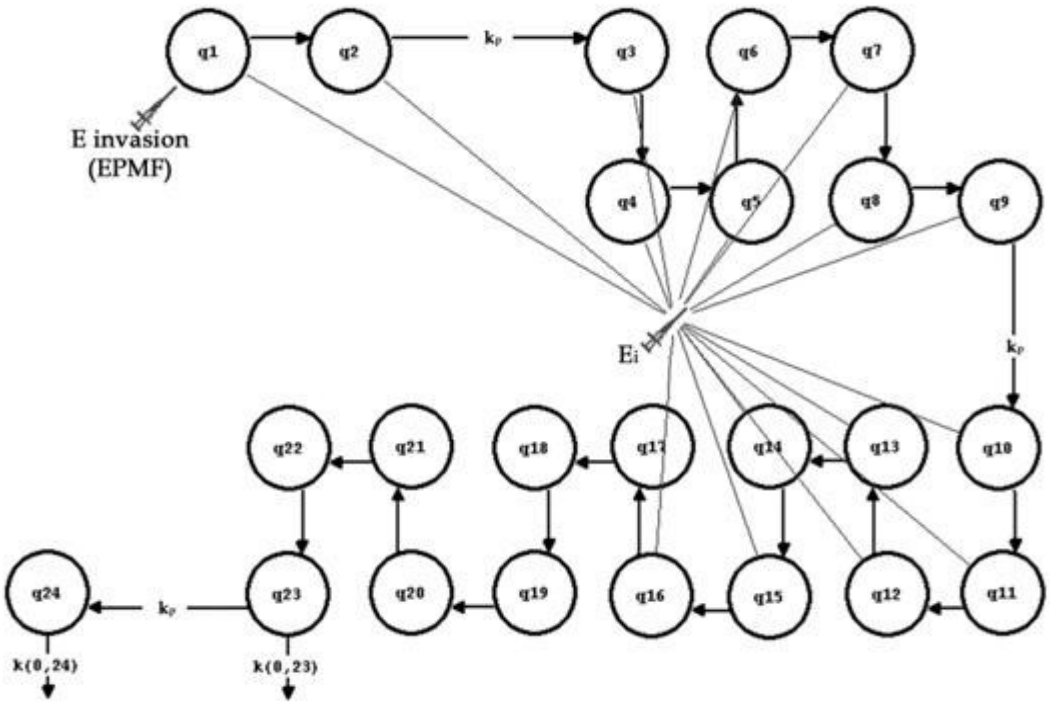

Figure 4.6 – SAAM II compartmental model of *P. berghei* infection in mice based upon conceptual model. E_i represents distribution of infected erythrocytes at inoculation (EPI). k(0,23) and k(0,24) represent drug dependent parasite elimination and schizont rupture. E invasion represents rate of merozoite infection of erythrocytes or the effective parasite multiplication factor (EPMF).

4.3.3 Effective parasite multiplication factor (EPMF)

The parasite multiplication rate largely comprises the rate of schizont rupture and subsequent successful merozoite invasion of erythrocytes. An important consideration in describing the EPMF as infection progresses is the number of available erythrocytes decreases (refer to Figure 3.5 and Figure 3.6). This reduces the carrying capacity of the system, and limits the total resources available for parasites and so reduces parasite multiplication. The EPMF should be described relative to the level of infection, rather than time. The intention is to

eventually model drug treatment, so time will not be a good indication of infection depending on the time of drug administration.

Accordingly in the pharmacodynamic model, an effective parasite multiplication factor (EPMF) was determined experimentally as a function of the proportion of parasitised erythrocytes in whole blood. The effective parasite multiplication factor is a function of the parasite population dynamics (i.e. change in parasite population) relative to the parasite population or ratio of infected to uninfected erythrocytes. This decouples the parasite multiplication from the time after infection, enabling modelling of infection with different initial parasitaemia and infections that are treated, thus altering the parasite population dynamics over time.

To determine the effective parasite multiplication rate (EPMR or change in parasitaemia over time as distinct to EPMF) the change in parasite density every 24 h was determined over the course of infection for individual mouse data (Figure 3.2 – *P. berghei* untreated infection with 10^5, 10^6 and 10^7 infected erythrocytes). The EPMR over the time course of an infection with 10^7 PRBC given i.p. is presented in (Figure 4.7A). The effective parasite multiplication rate was then plotted against parasitaemia (/μl) in order to determine how the infection progresses as the parasite density increases (Figure 4.7B).

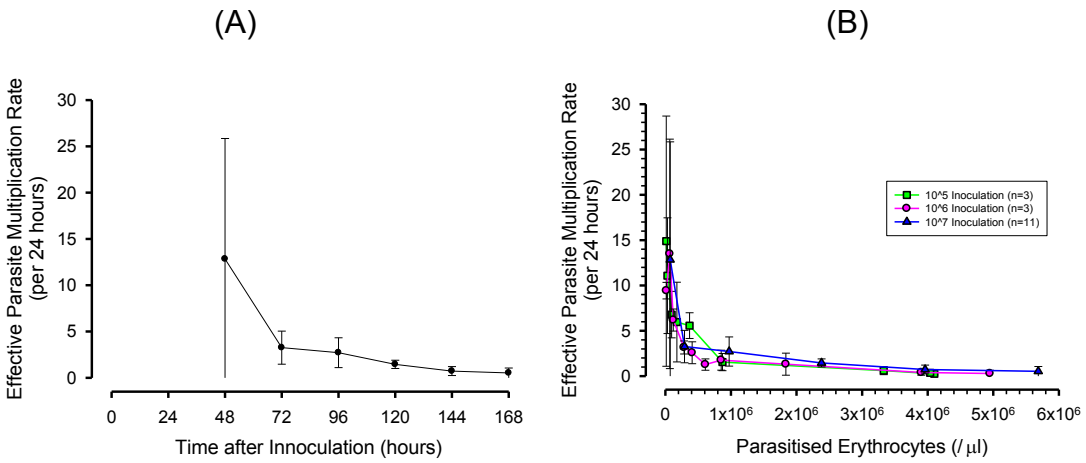

Figure 4.7 (A) – Effective parasite multiplication rate per 24 h life cycle for infection with 10^7 parasitised erythrocytes as a function of time. Data is mean ± SD (n=8)

(B) – Effective parasite multiplication rate per 24 h life cycle as a function of the parasite density in untreated inoculations with 10^5(■), 10^6(●) and 10^7 (▲) parasitised erythrocytes i.p. Data is mean ± SD.

An approximation function for the EPMF was determined by fitting functions to the EPMR versus parasitaemia data as plotted in Figure 4.7B. Requirements of the fitting function were that at low parasitaemia the EPMF should approach a biologically plausible maximal multiplication rate close to the number of merozoites produced per infected erythrocyte. From the literature and observations this should be approximately 6-18 merozoites [135, 185, 212]. Additionally as infection progresses the EPMF should approach zero.

The EPMF was approximated by fitting a 3-parameter power function to experimental data for the difference in parasite density over one life cycle (24 h), in mice inoculated with 10^5, 10^6 or 10^7 parasitised erythrocytes, versus the number of parasitised erythrocytes (Equation 4.1; Figure 4.8A). Initial parameter estimates of y_0, a and b were obtained by fitting Equation 4.1 in SigmaPlot®.

Other functions were tested using the SigmaPlot® regression wizard. However, none provided biologically plausible results at both low and high levels of infection. An example of such biological implausibility is that physiologically the parasitaemia cannot exceed the total number of available erythrocytes. Since erythrocyte numbers per μL decline as infection progresses, the number of infected erythrocytes should never exceed the average healthy number of erythrocytes per μL. Any function used to determine the EPMF should cross the x axis prior to reaching a level of 1×10^7 infected erythrocytes per μL in order to be considered biologically valid. Similarly, the EPMF can never exceed the maximum number of merozoites per schizont. This implies that at x = 0 the EPMF function should not exceed a value of 20.

The parasite EPMF was added to the SAAM II compartmental model which was used to fit the power function to experimental data. Computational settings used relative error specification, with a Rosenbrock integrator function, and data-based optimization with a convergence criterion of 0.001. Fitting was weighted to higher parasitised erythrocyte values as these data points have smaller inherent error.

$$EPMF = y_0 - (a \times E_i^b)$$

Equation 4.1

where: E_i is the number of infected erythrocytes; y_0 is the theoretical maximum EPMF (the practical maximum of y_0 occurs when E_i = 1); a is the coefficient and b is the exponent for the equation.

Model estimates for y_0, a and b were 9.7, 0.73 and 0.16 respectively.

At low levels of infection (e.g. 10^3-10^4 parasitised erythrocytes), EPMF was shown to be of the order of 6.5-7.5, thus representing a biologically plausible 7-fold increase in parasitaemia every 24 h [135, 185, 402]. At higher levels of parasitaemia (e.g. 10^6 parasitised erythrocytes or 10-12% parasitaemia), the EPMF was of the order of 3, reflecting a lower rate of parasite growth, mainly due to the diminishing pool of uninfected erythrocytes.

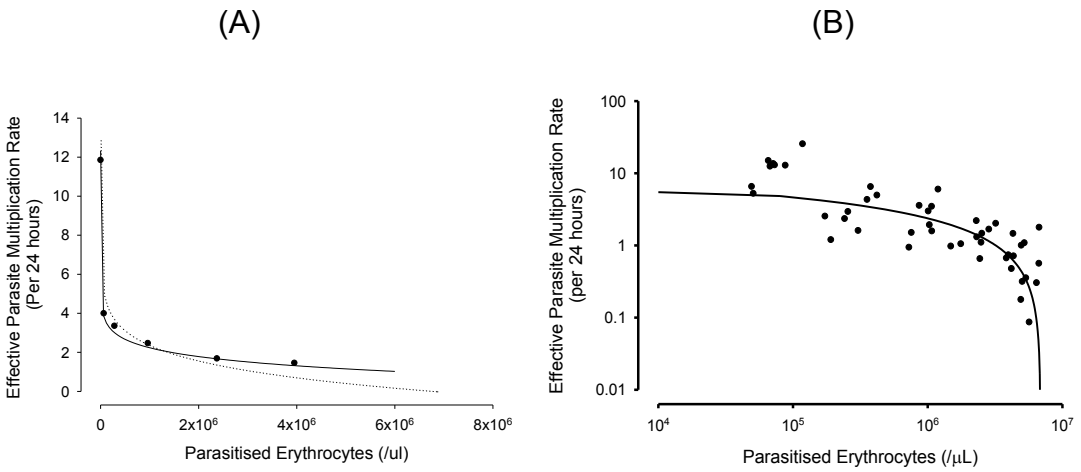

Figure 4.8 – (A) Fitting and optimisation of EMPF for 10^7 inoculation mean data (•) using SAAM II with Equation 4.1 (—). Values from experimental data fit in SigmaPlot were used as initial modelling parameters in SAMM II (·····).

(B) The EPMF as determined by SAAM II (—) with data from untreated individual mouse data (●) following inoculations with 10^5, 10^6 or 10^7 parasitised erythrocytes. The log/log scale allows better visualisation of the function properties as it approaches low infection and high infection. These end points are significant to model validity and biological consistency.

4.3.4 *P. berghei* pharmacodynamic model

As the factors that were most likely to be influential in the pharmacodynamics of *P. berghei* infection had been characterised, the next step was to establish and parameterize the model. The *P. berghei* model of infection contained 24 compartments (Figure 4.6) each representing 1 h of the parasite life cycle. Variable parameters for the model included the parasitaemia at inoculation (EPI, an estimate of viable parasites) and the flux (a rate constant), representing parasite population progression through compartments (k_p). Since the compartments represent a common residence time, the progression through all compartments is equal to k_p and should be in the order of 1 (which represents compartments of approximately 1 h duration or a 24 h life cycle). Immediately following inoculation, the parasite population can be considered as being distributed between all 24 compartments, thus approximating a mixed infection. The results of preliminary modelling indicated however that the immediate post-inoculation parasite population was comprised predominantly of early to mid stage parasites distributed across compartments 1 to 16. This was consistent with observations that erythrocytes with early stage parasites predominate in the thin film examinations, indicating that rings and trophozoites comprise most of the viable parasites in the inoculum and are more resilient to the passage process. The effect of this adjustment of the initial parasite age distribution was that some synchronicity is observed in modelling results at low parasite densities (Figure 4.9). This is what would theoretically be expected. Synchronicity was quickly lost which is also consistent with observations.

The forcing function input of parasites into compartment 1 approximates infection of erythrocytes by released merozoites and multiplication of the infection. The equation for the parasite multiplication was determined to be:

$$\text{Parasite Multiplication} = (q_{24} \times k_p) \times \text{EPMF}$$

Equation 4.2

where: q_{24} is the number of parasites in the 24th compartment (model starts with $q_{24} = 0$ because all parasites were initially distributed across compartments 1 to 16); k_p is the rate of schizont rupture and merozoite release (model commenced with $k_p = 1$). Initial values for EPMF (from Equation 4.1) and parasite progression ($k_p = 1$; represents a parasite life cycle length of 24 h) were determined by modelling untreated infection data.

The *P. berghei* model of infection in mice inoculated with 10^5, 10^6 or 10^7 parasitised erythrocytes is shown in Figure 4.9. From the model, the EPI (the viable parasite biomass) was estimated to be 47 $\pm$ 25% of the inoculum.

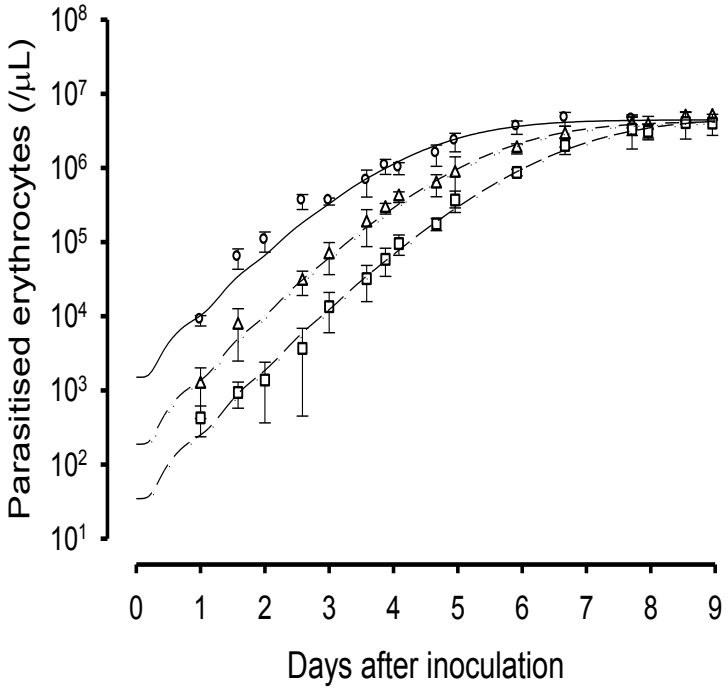

Figure 4.9 – Parasite density-time profile (mean ± SD) of *P. berghei* infection and model fitting results for inoculations of 10^5 (□ ---), 10^6 (△ — · —) and 10^7 (○ ——) parasitised erythrocytes (n = 3 per inoculation). In the first 2 days after inoculation the model shows a partially synchronous infection. Synchronicity is lost by day 3.

4.3.5 Dihydroartemisinin administration and the *P. berghei* model

The final stage in the development of the overall model was to incorporate the effects of drug treatment using DHA. Parasite clearance after drug administration was incorporated into the model, using an elimination function applied to compartment 23. A Gaussian function was used to approximate the parasite clearance in a Swiss mouse model due to DHA treatment. A Gaussian function was selected, as a bell shaped curve was logically appropriate to model parasite elimination, which would increase after drug administration from zero to

a maximal parasite elimination, and then decline back to zero as drug is cleared. Hence, the simplest equation that represented the data was:

$$D_{DHA} = Ae^{k(t-(t_{inj}+T)} + B$$

Equation 4.3

where: D_{DHA} is the drug-dependent parasite elimination as a function of time (t) after inoculation; coefficient A is a function of the drug dose and defines the magnitude of maximum parasite elimination; k is the drug-dependent rate of parasite elimination; t_{inj} is the time of drug administration, T is the time from administration to the peak parasite elimination (according to model estimates) and B represents a time independent increase in parasite elimination.

No improvement in fit was achieved by placing the elimination function in other compartments or in multiple compartments. Elimination from each of the compartmental stage domains (e.g. rings, early trophozoites, late trophozoites and schizont domains) significantly increased the complexity of the model without improvement.

Initial parameter estimates were obtained from graphical data fitting and were inputted into SAAM II. Parameters were assigned upper and lower limits where these were biologically relevant to ensure the model did not produce biologically implausible results. For other parameters, limits were assigned based on observed biological standard deviation.

The final model describes the rise in parasitaemia following infection, its nadir following DHA administration, and the subsequent resurgence of parasitaemia (analogous to 'recrudescence'). The modelling process involved solving Equation 4.2 (parasite multiplication) and Equation 4.3 (drug-dependent parasite elimination) sequentially in SAAM II. In this sequential fitting, Equation 4.2 starts at the time of inoculation (t = 0), while Equation 4.3 becomes active at the time of drug administration (t = 72 h). A switch term (z) was applied to the front of the drug dependent elimination equation which was switched from zero to 1 at 72 h post inoculation.

Assumptions made in the modelling process were that drug treatment did not alter the EPMF (that is, the number of uninfected erythrocytes invaded by viable merozoites) and that the rate of parasite removal was independent of drug dose (parasite removal is host dependent and dead parasites can continue to circulate until removed). Figure 4.10 (n = 8 per group) shows that there was a graded dose-response relationship with increasing single doses of DHA. The time of nadir in parasite density was independent of dose and occurred approximately 24 h after treatment, with a maximum 12-fold reduction in parasite density following 100mg/kg DHA. Estimates of the parameters for the model are summarised in Table 4.2 and Table 4.3.

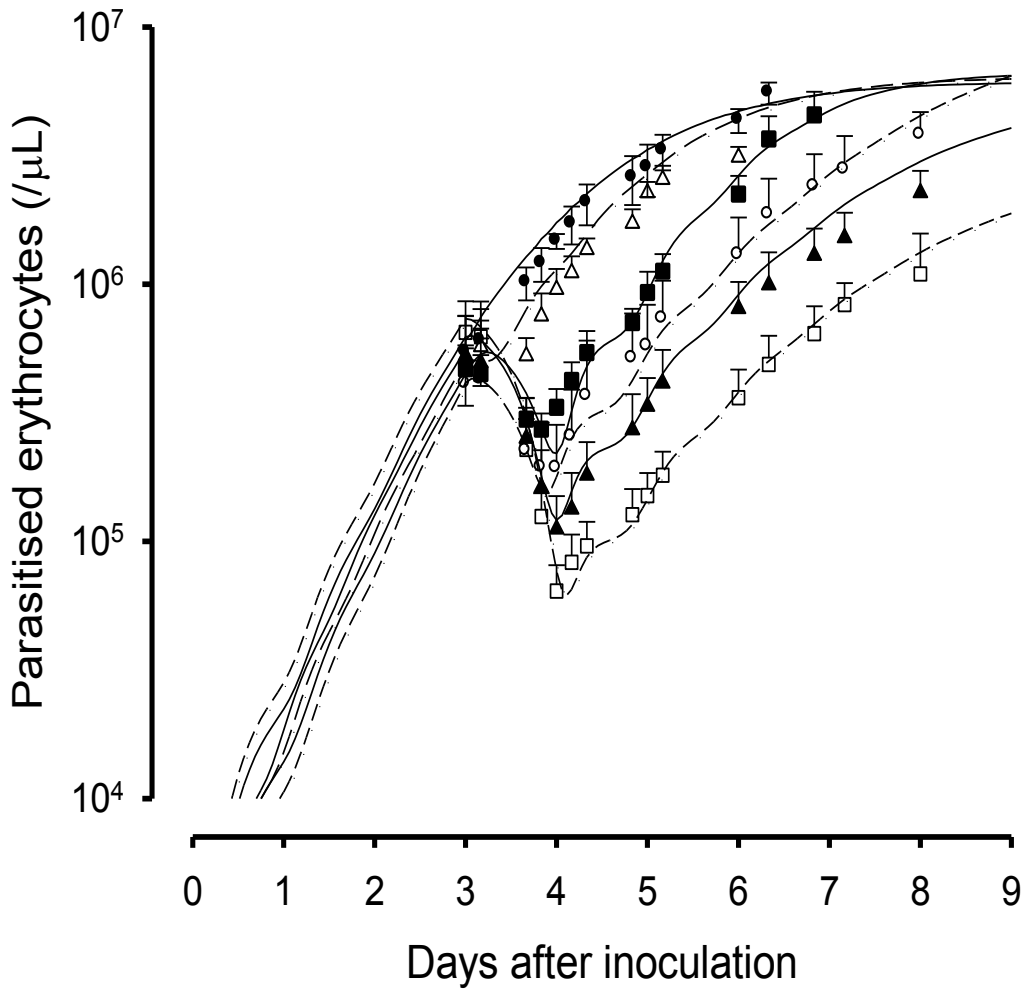

Figure 4.10 – Parasite density-time profiles (mean ± SD; n = 8 per group) and model fits of data in mice treated with DHA, three days after inoculation with 10^7 parasitised erythrocytes. Single doses of DHA were given by intraperitoneal injection at Day 3: Control (DMSO:Polysorbate 80; ● ——), 1mg/kg (△ – –), 3mg/kg (■ ——), 10mg/kg (○ – –), 30mg/kg (▲ ——) and 100mg/kg (□ – –).

Table 4.2 – Pharmacodynamic drug treatment model Bayesian parameters derived from untreated *P. berghei* infection modelling results. y_0 is the maximum EPMF, k_p is one 24^{th} of the parasites life cycle, k_{DHA} is the rate of drug dependent parasite removal and T (T_{inj}+T_{DHA}) is the time after administration to maximal drug dependent parasite removal. Other model parameters (E_i – initial parasitaemia, A – function of drug dose and B – drug independent increase in parasite removal) were entered into the model as adjustable variables (see Table 4.3).

Drug Treatment Model Parameters	Population Mean	Standard Deviation	Lower/Upper Limits	
y_0	9.7	0.5	9	14
a	0.7	0.5	0.1	2
b	0.15	0.1	0.01	0.8
k_p	1	0.05	0.9	1.1
k_{DHA}	0.6	0.1	0.5	1
t_{inj} + T_{DHA}	85	6	72	100

Table 4.3 – Pharmacodynamic model parameters (mean ± SD) determined from Equation 4.3: $D_{DHA} = Ae^{-k(t-T)} + B$, where D_{DHA} is the drug-dependent parasite elimination as a function of time (t) after inoculation; coefficient A is a function of the drug dose; k_{DHA} is the rate of parasite elimination (/hr); T is the time from inoculation to the peak parasite elimination and B_{DHA} represents a time independent increase in parasite elimination.

Parameter	Dihydroartemisinin dose (mg/kg)				
(Data from pharmacodynamic model)	100	30	10	3	1
A_{DHA}	12535 ± 2592	3377 ± 1969	932 ± 695	487 ± 180	14 ± 11
B_{DHA}	0.9 ± 0.4	0.6 ± 0.3	0.9 ± 0.5	0.3 ± 0.2	0.1 ± 0.3
T ($t_{inj} + T_{DHA}$) (h)	84 ± 1.5	84 ± 1.4	83 ± 1.4	85 ± 1.2	84 ± 1.6
k_{DHA} (/h)	0.57 ± 0.04	0.57 ± 0.13	0.57 ± 0.01	0.58 ± 0.02	0.58 ± 0.01
Fold-decrease in parasite density (from time of drug administration to nadir)	12 ± 4	5 ± 1	2.5 ± 1	2 ± 0.2	N/A
Time of maximum parasite elimination, after drug administration (h)	12 ± 1.5	12 ± 1.4	11 ± 1.4	13 ± 1.2	12 ± 1.6
Time of nadir parasite density, after drug administration (h)	26.6 ± 1.8	24.6 ± 1.0	20.9 ± 2.3	21.7 ± 2.0	N/A

4.3.6 Dihydroartemisinin treatment on parasite stages

Staged thin films from a mouse treated with 100mg/kg (Figure 3.15) were used to investigate the ablity of the *in silico* model to simulate parasite life cycle stages. Results are shown in Figure 4.11. *In silico* modelling indicated that the time for rings, early trophozoites, late trophozoites and schizonts (Figure 2.1) were approximately 1, 7, 14 and 2 h respectively. For this reason the elimination compartment for DHA was moved from compartment 23 to 22, so that elimination was occurring during the late trophozoite phase. Modifying the parasite stage definitions and drug dependent parasite elimination compartment did not alter *in silico* modelling results.

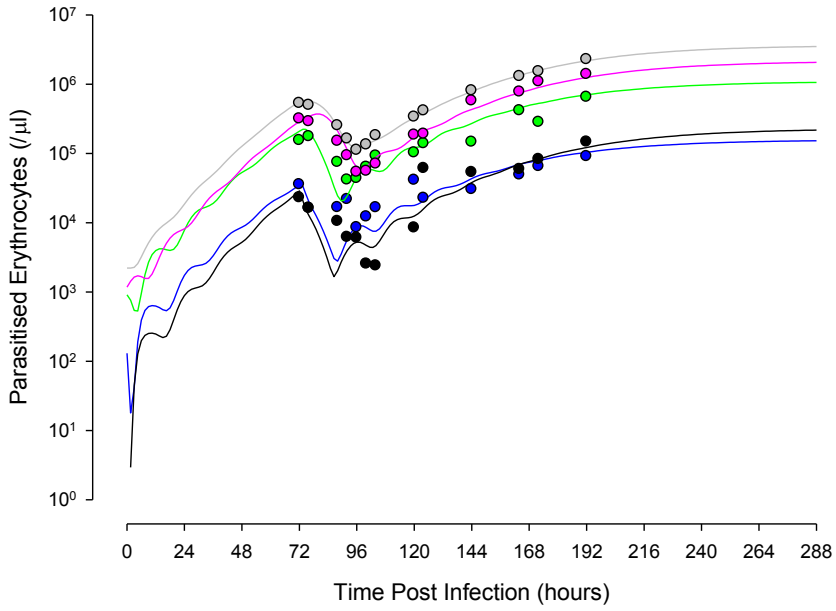

Figure 4.11– Mathematical model simulated pharmacodynamics and staged microscopy counting for total parasitaemia (— ●), and populations of rings (— ●), early trophozoites (— ●), late trophozoites (— ●), and schizonts (— ●) for a 30mg/kg DHA treatment at 72 h post inoculation.

4.4 Discussion

The studies reported here describe the development of a robust *in silico* pharmacodynamic model of murine malaria that incorporates parasite multiplication and changes in the erythrocyte population as a function of parasitaemia. Models of this type can be valuable tools for understanding how drugs, alone or in combination, and their dosing schedules alter the time course and level of infection and the practical application of this model to those ends will be investigated in subsequent chapters.

The studies have shown that an *in vivo* murine model of antimalarial treatment as described in Chapter 3, can provide an array of sub-therapeutic dose-response data that would not be possible in clinical studies. Hence, application of a murine model in the pre-clinical drug development process could assist in selection of candidate antimalarial agents and dosage regimens for drug combination studies during subsequent clinical trials.

Development of an *in silico* model incorporating a simple drug-dependent parasite elimination function as described in this Chapter enables the generation of data characterising the time and level of nadir, as well as peak effect of the drug. The test antimalarial drug, DHA (1 - 100mg/kg), produced a nadir in parasitaemia approximately 24 h after dosing, and the *in silico* PD model revealed a time to peak parasite elimination of only 12 h. This finding suggests that for maximal therapeutic effect in the murine model, DHA should be given at

12-hourly intervals (half of the parasite lifecycle). Delaying drug administration to correspond with the nadir may allow a significant proportion of parasites to recover between each dose. Notably, the data from doses of 10, 30 and 100mg/kg (0.5 log increases) showed a progressive two-fold lower nadir (Table 4.3). Based on this observation, it could be predicted that three appropriately timed 30mg/kg doses of DHA should produce a nadir at least 15-fold lower than the starting parasitaemia (compared to the 12-fold lower nadir with 100mg/kg as a single dose; Figure 4.10).

One of the limitations of murine studies as a conceptual model of therapeutic strategies for clinical trials is the 24 h lifecycle of *P. berghei* compared to the 48 h lifecycle of *P. falciparum*. Hypotheses related to duration of drug administration [420] or comparisons of single-dose and multi-dose regimens of antimalarial drugs could be tested in a murine model, with due regard to the differences in lifecycle duration and the need for allometric scaling of doses, prior to clinical trials. A further potential limitation relates to the pathophysiology of *P. berghei* infection, specifically the starting parasitaemia of ~5% in this model. However, Swiss mice are tolerant of *P. berghei* infection at a low-moderate level of parasite density (<5%), with organ failure and death occurring only at high parasitaemia [97, 213, 293]. Hence, the features of the *P. berghei* model infection are beneficial for PD studies because tolerance to the infection allows the mice to reach a parasite density of up to 5% before drug treatment strategies are commenced and the parasitaemia can be monitored down to a level of approximately 0.005%. In addition, *in vivo* evaluation of stage-specificity

is feasible if parasites are differentially counted as rings, trophozoites and schizonts. Furthermore, sequestration is not a factor in *P. berghei* infection of Swiss and Balb/c mice, hence the total parasitaemia should equate to the total parasite burden.

In addition to recognising differences between murine and human malaria, the studies have been designed to develop an *in silico* PD model that is biologically plausible and adaptable to a variety of general modelling software packages. Preliminary studies showed that the rate of increase in parasitaemia was similar in the first 3-4 days after inoculation with 10^5 to 10^7 parasitised erythrocytes (Figure 4.9), as was recrudescence for approximately two days after the post-treatment nadir (Figure 4.10). At a high parasitaemia, the rate of increase in parasitaemia was substantially reduced but the parasites harvested from these mice show a typical growth pattern when passaged to naïve recipients (data not published). Hence, by quantifying the rise in parasitaemia and incorporating the change in erythrocyte population into the model, a realistic multiplication factor (EPMF) was established as a continuous variable. The simple equations for parasite multiplication (Equation 4.2) and elimination (Equation 4.3) provided a close fit to the experimental data and generated parameters (e.g. time to peak parasite elimination) that should be useful in developing dosage regimens for antimalarial drugs in the murine model.

The model constructed to this point has been demonstrated to be consistent with experimental observations, as well as being algorithmically, empirically and

theoretically valid. These validations will be continued in subsequent studies, which will also examine heuristic and practical validity. It is intended that the model be used to predict the outcomes of multiple-dose treatments and to examine the effects of combination treatment regimens. Such studies should demonstrate the potential value of the murine model for conceptual development of dosage regimens in pre-clinical and clinical studies.

A summary of the SAAM II based mathematical model of *P. berghei* infection in Swiss mice is provided below in Figure 4.12. While individual aspects of the model such as the compartmentalisation, parasite multiplication and drug elimination are in isolation rather simple and straight forward, the final model provides an ability to simulate infection and treatment with DHA based upon the level of infection or parasite density that is complex and novel. A working protocol for development of the model based on Chapters 3 and 4 has also been included.

4.4.1 Protocol for the development of a murine model of infection and drug treatment

- Dose Ranging Studies
    - Preliminary study to determine doses to be used in graded dose response treatment studies. Doses need to be selected to avoid immune responses.
        - ~6 week old male Swiss mice infected with 10^7 infected erythrocytes i.p. at time 0.
        - Use cohorts of ~3 mice.

        - 24 h sampling from 4 h post treatment.
        - Monitor mice until 10% drop in body weight over 24 h period or end of experiment.

- Graded Dose Response Studies
    - Select at least 4 sub therapeutic doses to test based on dose ranging study on a log scale (e.g. 1, 3, 10, 30mg/kg).
    - Select a sampling schedule for adequate data samples (e.g. 8 to 12 h from 24 h post inoculation)
    - A control cohort should be included of ~4-8 mice on which to base *in silico* modelling.

- *In silico* Model Construction
    - Fit mean ± SD control untreated infection data and determine EPMF equation in SAAM II.
    - Fit mean ± SD for graded dose response data with untreated EPMF variables fixed.
    - Examine graded dose response data to determine the drug dependent parasite elimination function.

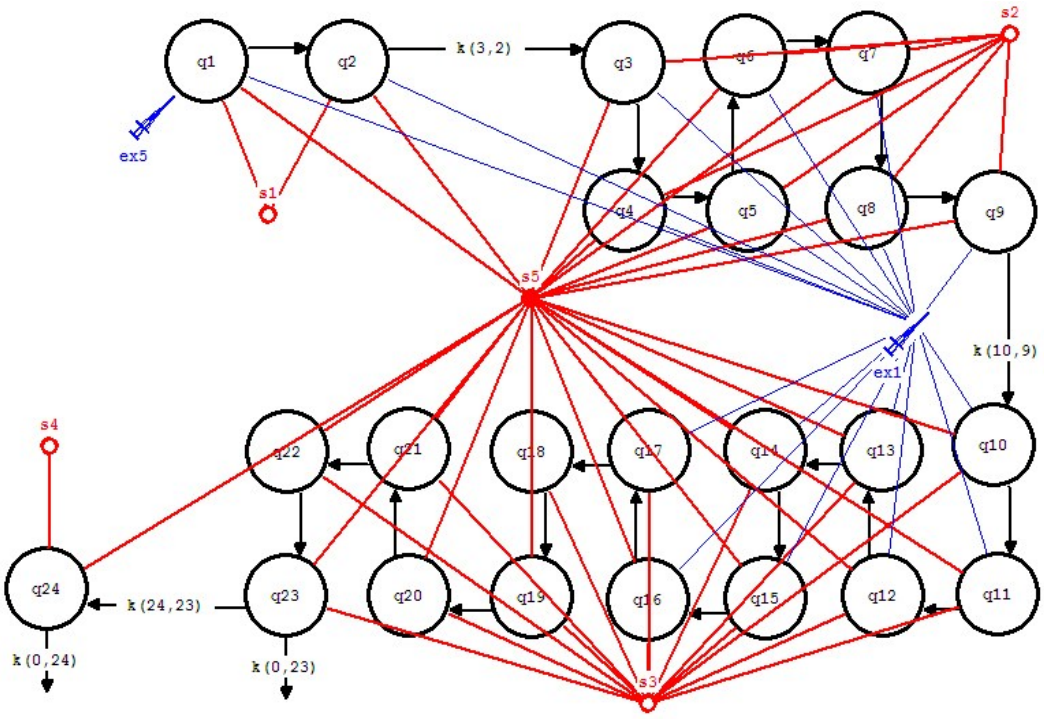

s1 = Rings Stage Simulation Sample*

s2 = Early Trophozoite Simulation Sample

s3 = Late Trophozoite Simulation Sample

s4 = Schizonts Simulation Sample

s5 = Total Parasite Simulation Sample

$k(0,24) = k(2,1) = \ldots\ldots = k(24,23) = k_p$

ex1 = initial inoculation at t=0 or EPI

$ex5 = (q_{24} \times k_p) \times EPMF$

$= (q_{24} \times k_p) \times (y_0 - (a \times E_i^{\,b}))$

$k(0,23) = D_{DHA} = Ae^{-k(t-T)} + B$*

Figure 4.12 – Screenshot of SAAM II compartmental model in experiment mode with definitions of variables and equations. Black circles and lines represent compartments and compartmental fluxes. Blue represents inputs red represents model **sample points or data outputs. *The model was subsequently modified so that S1 was represented by q1, early trophozoites by q2-q8, late trophozoites by q9-q22 and schizonts by q23 and 24. The k(0,23) drug elimination was move to compartment 22. These changes affected only the model definitions of parasite life cycle stages, and did not alter modelling and modelling results otherwise.**

CHAPTER FIVE

5. Using a mathematical model of murine *P. berghei* and single dose monotherapy to predict multiple dose outcomes.

5.1 Introduction

Studies in Chapter 4 demonstrated that it was possible to mathematically model a *P. berghei* infection model in Swiss mice after single dose treatment with DHA. This *in silico* model requires further validation. It is capable of modelling and simulating single dose DHA data. However, its validity depends on it being able to simulate or predict multiple dose therapy based on single dose modelling alone. This is in essence a practical and empirical validity test. Can the model predict and facilitate optimisation of multiple dose monotherapy based on single dose data? What criteria are suitable for judging the success or accuracy of itspredictions? The validity of the model must be demonstrated if the model is to be used to optimise drug treatment and potentially, combination treatment.

While the aim of the series of studies presented here may be considered an intermediate step in moving towards combination treatment optimisation, the importance of monotherapeutic treatment should not be overlooked. Even though current clinical guidelines logically aim for combination treatments, understanding optimum drug monotherapy is critical to successful deployment in combination. Potentially, the model under construction has the ability to examine aspects of monotherapy, dosages and dose intervals and to aid in

understanding and explaining aspects of infection and treatment that are difficult to examine *in vivo*. This will form part of the heuristic validation of the model.

5.1.1 Removing monotherapies from the clinical setting

In 2007 the World Health Assembly passed a mandate calling on the removal of all artemisinin based monotherapies from pharmacies and health clinics around the world [24]. Antimalarial monotherapies are not recommended except in the treatment of severe complicated malaria, and only until patients are able to move to locally effective oral artemisinin-based combination medicines. There are however a significant number of companies still marketing artemisinin monotherapies and regulatory action is required to stop the supply of artemisinin based monotherapies [337]. Despite this active move to stop the supply and use of monotherapies, rational design of combination treatment regimens requires understanding of monotherapy of the individual components.

5.1.2 The importance of antimalarial monotherapies

The Medicines for Malaria Venture (MMV) in its 2010 report on the "Development of combination therapies for treatment of uncomplicated *Plasmodium falciparum* malaria" outlined recommendations to clarify changes in antimalarial therapy development strategies towards combination treatment for 2020 [403]. According to MMV, dose selection "has often been rather empirical". It was also commented that PK evaluation in patients is problematic due to drug sequestration in erythrocytes and tissues, and that the lack of a good basis for PK/PD evaluation for antimalarials makes dose-finding studies difficult. These issues make it hard to provide regulatory authorities with robust rationale for the

dose regimen evaluated in confirmatory studies. MMV concluded that new approaches for dose finding need to be developed for antimalarial combination therapy [403].

With a clinical shift from monotherapy there is also a greater problem for the rational design of future regimens. Demonstrating the contribution of each agent to the combination requires monotherapy studies [403]. In the 2009 approval of Coartem® as a fixed dose combination of artemether-lumefantrine, the FDA emphasised the importance of studies comparing the combination with each component of the combination [6, 403].

5.1.3 New approaches for optimum dose selection

Determining PK-PD relationships for the individual drugs in a combination *in vivo* is critical to enable selection of optimum doses [423]. This should then form the basis for evidence-based dose regimen in phase 3 trials. White [423] argued that failure to achieve this led to deployment of suboptimal antimalarial drugs as monotherapies and combination partners, eventually leading to poor treatment outcomes and the emergence and spread of resistance [423].

An alternative PK-PD approach is suggested by White [423] for dose finding, which could improve and accelerate dose finding and potentially avoid systematic under prescribing and under dosing. The objective is determination of the *in vivo* mean inhibitory concentration (MIC), or dose at which the parasite multiplication factor per asexual cycle is one [423]. This is a concept that has

been successful in the field of antimicrobials. Improved PK-PD approaches to different human populations are required when developing rational antimalarial treatment strategies, particularly for new antimalarials [423]. There are several examples such as pyrimethamine and sulfadoxine and piperaquine doses for children, which were determined from experience with adult populations without sufficient PK-PD analysis in children. PK drug differences between children and adults now suggest that doses in children were (and are in the case of piperaquine) suboptimal [30, 377].

There are implications for the future development of antimalarial combination therapies. How should the individual components be evaluated when they will never be deployed as monotherapies? White [423] suggests the MIC as a potential approach to improve dose regimen design. *In vitro* susceptibility tests and estimation of the MIC in human volunteers receiving subtherapeutic doses, could enable improvement of optimal dose finding and development of treatment regimens. They could enable greater understanding of the relationship between *in vitro* susceptibility data and *in vivo* human data [423]. Some potential problems with this method are discussed by White [423] and include:

- Variation of the MIC between compounds is unknown and so may not provide a useful measure to inform dose finding and optimisation;
- MIC determination in certain compounds (e.g. those with short biological half-lives or pharmacodynamic effects) may be very difficult or not possible;

- Monitoring of parasite bioburden for volunteer human *in vivo* studies would require the use of quantitative real-time polymerase chain reaction (qPCR) since parasitaemia will fall below the microscopy limit of detection. It is possible the MIC may fall below the qPCR limit of detection, or that qPCR results will not be sufficient to accurately determine the MIC.

Improved strategies for developing rational treatments against malaria are necessary to prevent resistance and optimise use of current and future antimalarial treatment. It will however take a significant amount of time and clinical research, which may not in isolation be able to provide the necessary information to rationally develop treatments. There is potential for the use of intermediate animal *in vivo* models to provide useful PK-PD data to improve understanding and plug the gaps between *in vitro* susceptibility data and human PK-PD data. *In vivo* treatment optimisation in an animal model, such as that present here, could provide information to direct clinical trials and develop new approaches for selection of optimum doses, saving time and money. It may also provide an indication of the uses and problems of measures such as MIC in rational design of antimalarial regimens.

5.1.4 Aims

The aim of the present series of studies was to investigate the feasibility of using the established mathematical *in silico* model of *P. berghei* infection

and single dose treatment to predict multiple dose DHA monotherapeutic outcomes in Swiss mice. The initial aims were to:

i. Develop the existing model of *P. berghei* infection and treatment with DHA to incorporate multiple treatment doses.
ii. Investigate multiple dosing regimens using the model to determine the optimum dose interval for DHA.
iii. Use the model to determine the best regimen and develop criteria for evaluating regimens.
iv. Experimentally test selected regimens to assess the value of the mathematical model in predicting multiple dose monotherapeutic outcomes.

The hypothesis to be tested was:

> A mathematical model of *P. berghei* infection and drug treatment in Swiss mice can be developed from single dose, graded pharmacodynamic data and used to predict multiple dose outcomes, thus enabling optimisation of the treatment strategy.

5.2 Methods

5.2.1 Incorporating multiple dose treatment into the compartmental model

To modify the compartmental model developed in Chapter 4 to incorporate multiple drug doses, multiple drug dependent parasite elimination equations were added based on Equation 4.3 and could take one of two forms shown below.

$$D_{DHA} = \left(A_{d1} e^{-k(t-(t_{inj}+T)} + B_{d1}\right) + \left(A_{d2} e^{-k(t-(t_{inj}+T)} + B_{d2}\right) + ...$$

Equation 5.1

$$D_{DHA} = \left(A_{d1} e^{-k(t-(t_{inj}+T)}\right) + \left(A_{d2} e^{-k(t-(t_{inj}+T)}\right) + ... + B$$

Equation 5.2

where: D_{DHA} is the DHA dependent parasite elimination as a function of time (t) after inoculation; coefficient A is a function of each DHA dose and defines the magnitude of maximum parasite elimination for dose 1, 2, etc (d1, d2….); k_{DHA} is the DHA-dependent rate of parasite elimination; t_{inj} is the time of injection or administration of each dose and T_{DHA} is the time from inoculation to the peak parasite elimination (according to model estimates) and B represents a time independent increase in parasite elimination.

To model monotherapy, the terms k_{DHA} and T_{DHA} were entered as fixed variables since their values depend on the drug administered and are independent of dose (Table 4.3). k_{DHA} was estimated as 0.57 and T_{DHA} as 12 h after DHA

administration (Table 4.3). The variability in A depends on the dosing regimen being investigated and was entered as an adjustable parameter. The term B, which represents change in the parasite growth rate after drug administration, was included as either individual dose related variables (Equation 5.1) or as a single variable (Equation 5.2). The term is intended to allow for immunological interference by the host, which was considered negligible for an untreated short duration infection, but may be influential if drug treatment sufficiently prolongs host survival. It was anticipated that in the case of DHA multiple dose modelling, immune interference will be negligible relative to each dose due to short dosage intervals and so Equation 5.2 should be a suitable approximation. However, for future modelling of drugs with longer half-lives (e.g. chloroquine) it is possible that Equation 5.1 may be a more appropriate approximation.

To ensure effective modelling of multiple doses each drug term had a “switch” term (z) added to the front to allow it to be switched on or off. For example, a dose administered at 72 h would have a switch term of 0 prior to 72 h, which was changed to a 1 at 72 h using the change condition function in SAAM II. The switching term was left as 1 from the administration time till the end of the experiment, so drug elimination terms were not artificially switched off by SAAM II once initiated. This meant that a drug elimination term could not inadvertently influence modelling before it had actually been administered or simulated to have been administered. Thus Equation 5.2 becomes Equation 5.3 below.

$$D_{DHA} = z_1\left(A_{d1}e^{-k(t-(t_{inj}+T)}\right)+ z_2\left(A_{d2}e^{-k(t-(t_{inj}+T)}\right)+ .... + B$$

Equation 5.3

Due to the construction of the model, all drug related parasite removal occurs through compartment 22. The biological accuracy of this is arguable, since parasitised RBC are unlikely to be removed at approximately 22 h in their life cycle. The model was not improved by spreading the parasite removal over multiple compartments and single compartment elimination provided a simplified model. The actual time during the life cycle that individual parasites are removed is less important than the influence this has on parasite multiplication. Irrespective of when parasites are removed, the effect of reducing the size of the next generation of parasitised RBC is unchanged. The model parasite elimination function is a model of drug dependent infected RBC removal and models this satisfactorily with single compartment elimination. The individual drug dependent elimination functions are in effect combined in the model into an overall drug dependent parasite elimination term as Equation 5.3.

5.2.2 Predicting outcomes of multiple dose dihydroartemisinin monotherapy

For prediction of DHA multiple dose monotherapy the values in Table 4.2 and Table 4.3 were used with the modified multiple dose model. A value of 1500 was used for EPI (number of infecting erythrocytes) as this provided a simulated parasitaemia of approximately 5% at 72 h. The drug elimination equation used for constructing predicted dynamic curves was Equation 5.3 and B values were taken from Table 4.3. A_{DHA} values were calculated using Equation 5.4 which was determined by a linear fit of model derived A_{DHA} values against the dose administered ($Dose_{DHA}$) in mg/kg as shown in Table 4.3. The relationship had an

r^2 value of 0.9979 and was used to estimate the A_{DHA} values for different doses during modelling.

$$A_{DHA} = 124.03 \times Dose_{DHA}$$

Equation 5.4

Two sub-therapeutic DHA dosing regimens were selected to test the ability of the model to optimise and predict treatment regimen outcomes. Both regimens were designed to deliver the same total dose in a different number of doses using the most optimal dose interval as determined by the *in silico* model. For example, the first regimen delivered a total of 50mg/kg DHA in five equal 10mg/kg doses while the second delivered 50mg/kg as an initial 30mg/kg dose followed by two 10mg/kg doses. These dose regimens were selected as they reflect clinical *P. falciparum* artemisinin based monotherapy studies from which it has been observed that longer courses of daily treatment are more effective than short courses and an initial loading dose is often administered [60-62, 196, 223, 297].

5.2.3 Determining the optimum dose interval for dihydroartemisinin

The optimum DHA dose interval was assumed to be approximately 12 h based on single dose modelling results showing maximum parasite drug dependent elimination at approximately 12 h post administration (Table 4.3). For each of the two test regimens described above, dose intervals of 0, 6, 10, 12, 14, 16, 18, 20 and 24 h were modelled to determine the optimum interval to reduce the parasitaemia as quickly and for as long as possible (i.e. to determine the best sub-therapeutic regimen). For each treatment regimen a dose interval of 0 h

should be equivalent to a single dose of 50mg/kg unless the model is internally invalid.

5.2.4 Criteria for comparing treatment regimens

Predetermined criteria were developed to compare the efficacy of treatment regimen. These were based upon measuring the parasitaemia at the start of regimen administration (P_{INJ}), the minimum parasitaemia reached after drug administration (P_{nadir}) and the time after the commencement of drug administration for parasite population recrudescence (T_{recrud}) to return to the level at drug administration. From these values the parasite reduction ratio can be determined.

5.2.5 Internal validation of the multiple dose model of dihydroartemisinin treatment

Internal model validation was assessed (i.e. consistency, algorithmic and theoretical validity) using the following criteria :

- Multiple doses with a dose interval of zero should provide equivalent results as a single dose of equal concentration. This can be tested using existing single dose data (i.e. 3×10mg/kg doses with zero dose interval should be equivalent to a single dose of 30mg/kg) and extrapolating to modelled data (i.e. 5×10mg/kg doses with zero dose interval should be equivalent to a single dose of 50mg/kg).
- To be theoretically valid the model should demonstrate that (at the optimum dose interval) split dosing is more effective than single dosing (with the same amount of drug delivered) and that a longer dosing

regimen is more effective than a shorter one using the same dose interval.

5.2.6 External validation of the multiple dose model of dihydroartemisinin treatment

The empirical validity of the multiple dosing model was assessed by studying the two dosage regimen experimentally in the *in vivo* model. Infected Swiss mice were randomly divided into controls (n=5) and two treatment regimen groups (n=8) receiving either 5×10mg/kg doses of DHA every 12 h starting from 72 h post inoculation or receiving 30mg/kg DHA at 72 h post inoculation followed by 2×10mg/kg doses every 12 h. Parasitaemia was monitored as previously described and experimental multiple dose *in vivo* PD results were compared with *in silico* model predictions to judge practical validity of the model in predicting the most effective treatment regimen. Subsequently the model was used to fit data to determine the accuracy of the model construction and empirical results.

Model validation and “accuracy” in the context of the series of studies presented here requires definition. Model “accuracy” in predicting the optimal treatment regimen was the aim of the studies, which was to enable regimen optimisation, not perfectly simulate a *P. berghei* infection. The measure of model validation and accuracy that was important was relative. Which regimen is most effective? Is regimen A better than regimen B and do the model and experimental results agree? The model presented here was in development, and based upon a limited number of experimental results. It was expected that there could be

significant discrepancies between the absolute parasite dose response simulations and experimental studies. The following studies did however provide additional experimental data which was used to improve the precision of the model in simulating *P. berghei* infection and treatment.

5.3 Results

5.3.1 Determining the optimum dose interval for dihydroartemisinin

Model simulations for 5×10mg/kg doses at 0, 6, 10, 12, 14, 16, 18, 20, 24 h dose intervals are shown in Figure 5.1. Values used to compare each regimen such as time until nadir and recrudescence and fold decrease in parasitaemia are shown in Table 5.1. Additional dose intervals of 15 and 17 h were also examined. From a comparison of these values (Figure 5.2) it was concluded that a dose interval between 12-18 h was most effective. Results demonstrate that

- Split dosing of DHA is much more effective than a single bolus as demonstrated by 5×10mg/kg doses with a 0 h dose interval (single 50mg/kg dose) compared with 5×10mg/kg doses at any dose interval between 6-24 h.
- Dose intervals greater than 20 h are less effective as parasite removal is slower and the nadir parasitaemia is higher. This is despite similar recrudescence times.
- Dose intervals shorter than 10 h are less effective since the parasite nadir is higher and recrudescence times are shorter. The rate of parasite removal is however slightly faster.
- Nadir parasitaemias for the most effective regimens drop below the limit of detection. With a 12 h dose interval the parasitaemia drops to 0.002%.

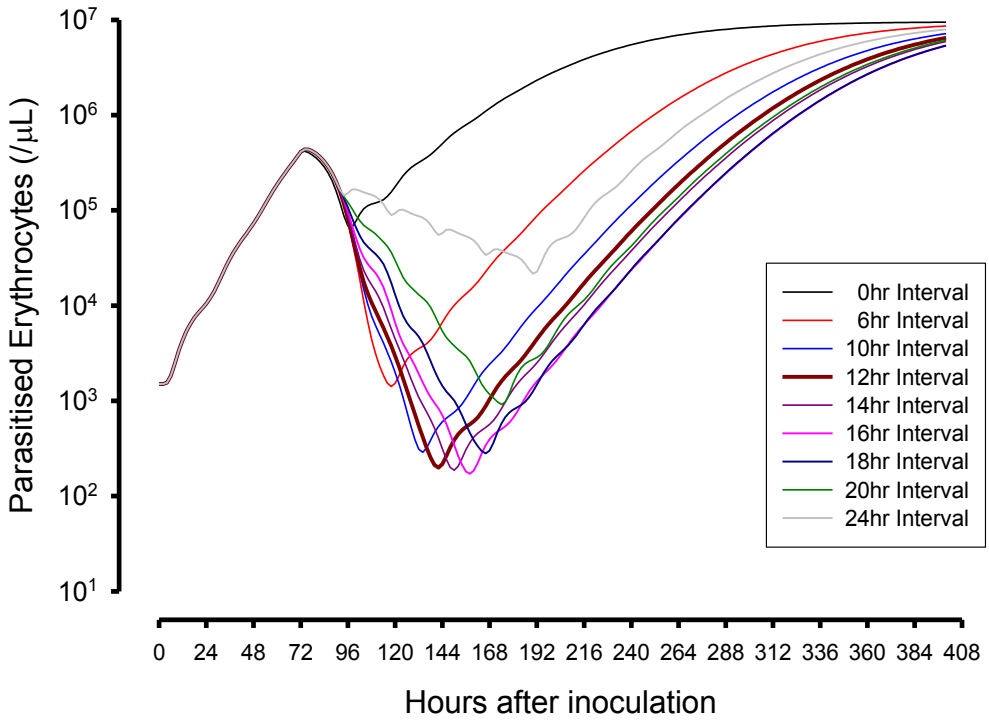

Figure 5.1 – Mathematical model simulated DHA multidose treatment of *P. berghei* infection in Swiss mice. The model simulates 5×10mg/kg multiple dose DHA regimens at varying dosage intervals between 0 and 24 h. An interval of 0 approximates single dose DHA treatment of 50mg/kg.

Table 5.1 – Mathematical model simulated parameter values for 5×10mg/kg multiple dose DHA treated *P. berghei* infection in Swiss mice at varying dosage intervals. An interval of 0 approximates single dose treatment with 50mg/kg.

	DHA Dose Interval (h)										
Model Simulated Parameter Values	**0**	**6**	**10**	**12**	**14**	**15**	**16**	**17**	**18**	**20**	**24**
Nadir Parasitaemia (parasitised erythrocytes/μL)	66011	1412	288	198	186	176	171	205	280	917	21642
Fold Decrease in Parasitaemia	6	291	1427	2069	2204	2335	2404	2006	1465	448	19
Time of Nadir (hrs after start of treatment)	26	46	62	70	78	82	86	90	94	102	118
Time of Recrudescence (hrs after start of treatment)	68	156	198	212	220	220	230	230	230	218	180

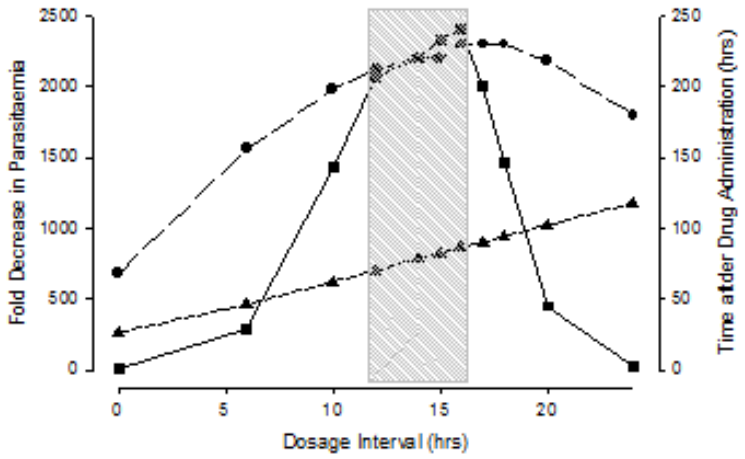

Figure 5.2 – Graphical representation of model simulated parameters from Table 5.1. ■ (—) represents the change in the fold changes in parasitaemia over time while ● (—) and ▲ (--) represent time of recrudescence and time of nadir respectively. The shaded area shows the dose intervals resulting in the most efficient regimen.

5.3.2 Predicting multiple dose dihydroartemisinin treatment outcomes

Similar to the analysis of a simulated 5×10mg/kg DHA treatment regimen a 30mg/kg followed by two 10mg/kg DHA dose regimen was simulated (Figure 5.3). Results on selection of an optimum dose interval were similar to that observed with the 5×10mg/kg regimen in that an interval of between 12-18 h was optimal (Table 5.2 and Figure 5.4). Results support those found examining the 5×10mg/kg regimen. Split dosing is more effective than a single bolus of DHA. Dose intervals below 10 h and above 20 h were less effective. Doses between 12-18 h were most effective with fast parasite elimination, lowest nadirs and longest time to recrudescence.

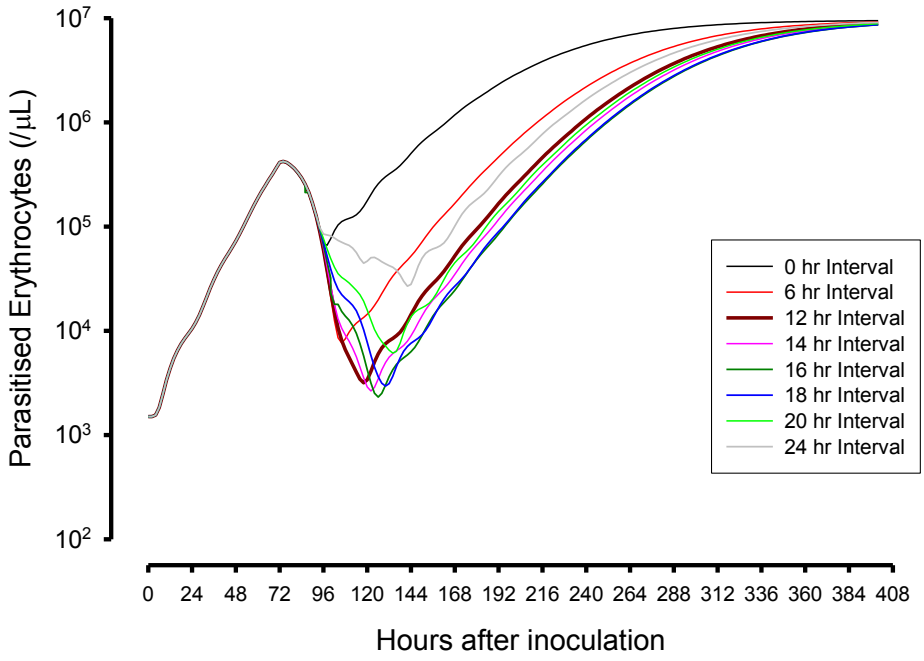

Figure 5.3 – Mathematical model simulated DHA multidose treatment of *P. berghei* infection in Swiss mice. The model simulates a 30+2×10mg/kg dose DHA regimens at varying dosage intervals between 0 and 24 h. An interval of 0 approximates single dose DHA treatment of 50mg/kg.

Table 5.2 – Mathematical model simulated parameter values for 30+2×10mg/kg multiple dose DHA treated *P. berghei* infection in Swiss mice at varying dosage intervals. An interval of 0 is equivalent to a single dose treatment with 50mg/kg.

	DHA Dose Interval (h)							
Model Simulated Parameter Values	**0**	**6**	**12**	**14**	**16**	**18**	**20**	**24**
Nadir Parasitaemia (parasitised erythrocytes/μL)	66011	7615	3171	2644	2312	2942	6102	26749
Fold Decrease in Parasitaemia	6	54	129	155	178	139	67	15
Time of Nadir (hrs after start of treatment)	26	34	46	50	54	58	62	70
Time of Recrudescence (hrs after start of treatment)	68	118	142	150	156	156	146	128

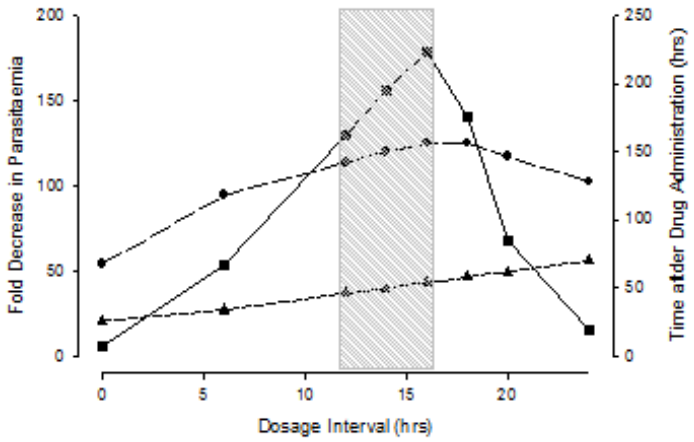

Figure 5.4 – Graphical representation of model simulated parameters from Table 5.2. ■ (—) represents the change in the fold changes in parasitaemia over time while ● (—) and ▲ (--) represent time of recrudescence and time of nadir respectively. The shaded area shows the dose intervals resulting in the most efficient regimen for 5×10mg/kg doses, which overlaps that of the 30+2×10mg/kg regimen.

Comparison of Table 5.1 and Table 5.2 indicate that for 50mg/kg total dose of DHA a 5×10mg/kg dose regimen is much more effective than a 30+2×10mg/kg regimen with equal dose intervals. The two regimens with 12 h dosage intervals were selected to be validated experimentally, based on 12 h being considered within the optimal dose interval range. This schedule is also more comparable to clinical treatment of *P. falciparum* where treatment occurs twice per parasite life cycle (i.e. daily). Comparison of the simulation of these two dose regimens (Figure 5.5) show that the 5-dose regimen is predicted to be significantly more effective than the 3-dose regimen with the same total dose (50mg/kg) and dose intervals. The 5-dose regimen reduces parasitaemia by approximately 16 times that of the 3-dose regimen, extends the time to nadir by 24 h and extends the recrudescence time by 70 h. The benefits of the 5-dose regimen are provided

without sacrificing the speed at which the initial parasite reduction occurs after DHA administration (Figure 5.5).

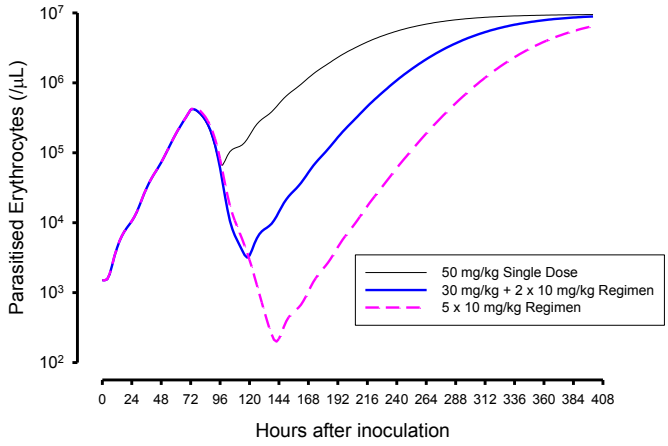

Figure 5.5 – Mathematical model simulated DHA multidose treatment of a 30+2×10mg/kg DHA regimen (—) and a 5×10mg/kg DHA regimen (---) both at 12 h dose intervals. A 50mg/kg single dose of DHA is modelled for comparison (—). The graph represents model simulations of two selected dosage regimens to be tested and validated experimentally.

5.3.3 Dihydroartemisinin *in vivo* multiple dose treatment

Parasite density time profiles with standard errors are shown in Figure 5.6 with respective model predictions. Model predictions for both regimens satisfy relative accuracy with experimental data as shown in Table 5.3. Model precision generally falls within standard errors for experimental data. There was a significant difference between the level (precision) of parasitaemia at nadir between the 5×10mg/kg model and data. This was likely due to the nadir approaching the limit of microscopic detection. This was supported by the data presented in Table 5.3 with close agreement between model and experimental data estimates of fold decrease in parasitaemia and time to recrudescence in

the 30+2×10mg/kg regimen and time to recrudescence in the 5×10mg/kg regimen.

It should be noted that the model predictions were not altered to fit experimental data. The modelling was conducted with a starting parasitaemia at 72 h of 5%. The model curves were not normalised to match the experimental data mean parasitaemia at the time of treatment (Figure 5.6). The mean parasitaemia of the 5×10mg/kg and 30+2×10mg/kg cohorts were 6.8 ± 2.0% and 6.1 ± 1.0% respectively.

The experimental parasitaemia for both regimens appears to show a region of slow growth immediately after nadir followed by a faster rate of increase in the parasite population. This is lacking or much less pronounced in modelling predictions.

Table 5.3 – Comparison of mathematical model simulated parameter values for 5×10mg/kg and 30+2×10mg/kg multiple dose DHA treated *P. berghei* infection in Swiss mice compared to experimental results obtained using the same two regimens.

	Model and Data Regimens			
Model/Data Estimated Values	5×10mg/kg Model	5×10mg/kg Data	30+2×10mg/kg Model	30+2×10mg/kg Data
Nadir Parasitaemia (parasitised erythrocytes/μL)	198	850	3171	3917
Fold Decrease in Parasitaemia	2069	689	129	136
Time of Nadir (hrs after start of treatment)	70	75	46	52
Time of Recrudescence (hrs after start of treatment)	212	212	142	153

(A)

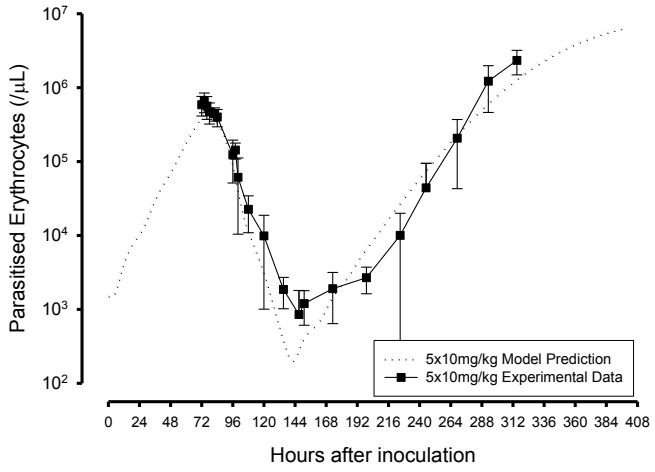

(B)

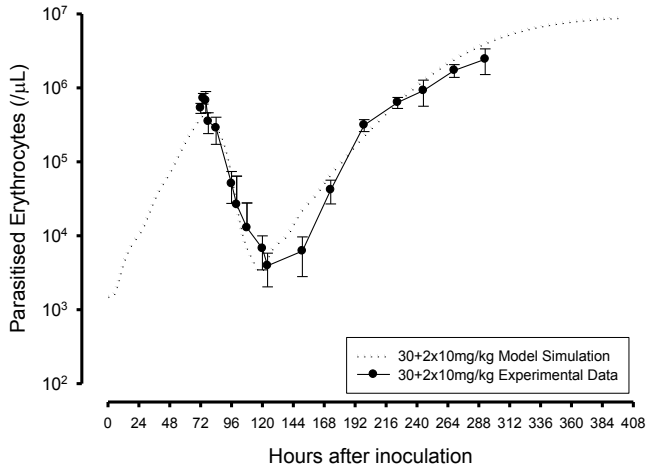

Figure 5.6 (A) – Experimental data (mean and SD; n=8) for mice infected with *P. berghei* and treated with five 10mg/kg doses of DHA every 12 h commencing 72 h after inoculation (■ —). The dotted line shows the mathematical model prediction of the parasite dynamics during DHA treatment which was not normalised for starting parasitmemia.

(B) – Experimental data (mean and SD; n=8) for mice infected with *P. berghei* and treated with three doses of DHA every 12 h of 30, 10 and 10mg/kg commencing 72 h after inoculation (■ —). The dotted line shows the mathematical model prediction of the parasite dynamics during DHA treatment which was not normalised for starting parasitmemia.

5.4 Discussion

The research presented in this Chapter demonstrates that data collected from single dose graded dose response data of DHA treatment of *P. berghei* infection in Swiss mice can be used to accurately predict DHA multiple dose treatment outcomes. The significance is that prediction of multiple dose treatment allows the optimum dose regimen to be determined taking into account different dose intervals and different dose sizes. Importantly it also enables this optimisation to be accomplished more accurately and with significantly fewer *in vivo* studies than could be achieved experimentally (refer to Figure 5.1 and Figure 5.3).

The regimens used to demonstrate this were of equal total dose (50mg/kg) split over 5 and 3 doses. The results show that five doses is much more effective than 3 using the same dosage interval. This is expected from clinical studies which have shown that for artemisinins treatment efficacy is highly related to the duration of treatment and split dosing is much more effective than single dosing [32, 268].

A dose interval of 12-18 h was determined to be optimal for DHA treatment. This is consistent with clinical theory that administration of short half-life antimalarials is optimised at two doses per parasite life cycle (~12 h in *P. berghei* and 24 h in *P. falciparum*). Clinical studies have reported little benefit from administration of artesunate at 12 h intervals compared with 24 h intervals [61]. This supports the model prediction that 12 h intervals are optimal. Additionally modelling

comparing 5×10mg/kg doses at 12 h intervals and 9×5mg/kg dose at 6 h intervals can be simulated and compared as in Figure 5.7.

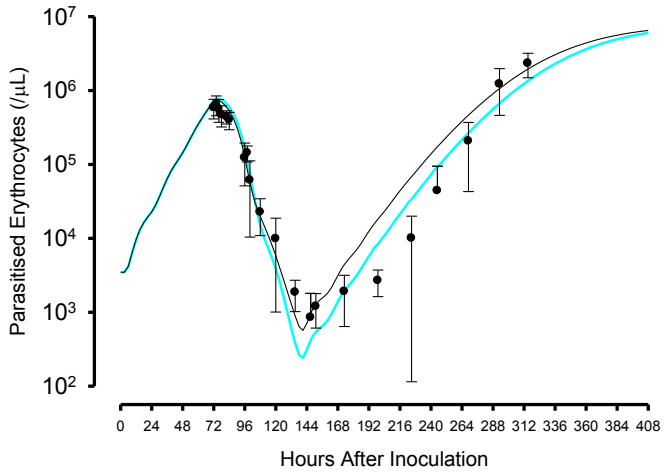

Figure 5.7 - Experimental data (● mean and SD; n=8) and model simulation (—) for mice infected with *P. berghei* and treated with 5x10mg/kg DHA at 12 h dose intervals from 72 h post inoculation and model simulation (—) of treatment with 9x5mg/kg DHA at 6 h dose intervals from 72 h post inoculation. Models have been normalised so that the parasitaemia at 72 h is the mean of the experimental data at 72 h.

The simulations in Figure 5.7 have been normalised to the mean parasitaemia at time of treatment of the 5×10mg/kg experimental data. The model predicts that the split 9×5mg/kg model is slightly more effective (with slightly lower total dose of 45mg/kg. In this way simulated treatment duration is comparable). However, it would be unlikely that there would be significant difference between the two regimens in an *in vivo* model. This result is consistent with clinical observations [61].

Another aspect of the *in silico* model that can be examined using SAAMII is the rate of parasite elimination. The rates of parasite elimination for the two regimens examined in this chapter are plotted in Figure 5.8. The significance or usefulness of this information is unclear. There does not appear to be a relationship between the area under the parasite elimination curves that can be used to determine optimal dosing or intervals. This however may be different for long half-life antimalarials. It is clear however that the regimen duration is longer in Figure 5.8A than B. The usefulness of the drug dependent parasite elimination rate may become clearer with comparison between several antimalarials.

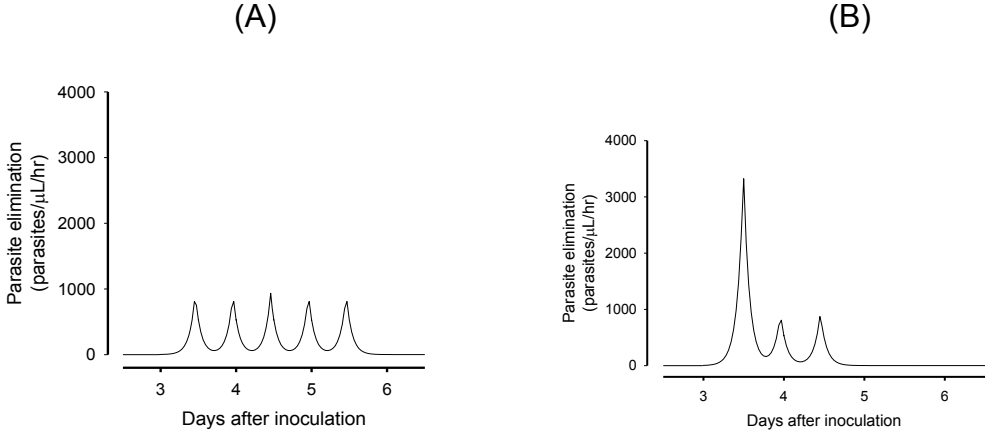

Figure 5.8 – Model derived parasite elimination rate plots for (A) 5x10mg/kg doses of DHA at 12 h intervals from day 3 post inoculation and (B) 30+2x10mg/kg doses of DHA at 12 h intervals from day 3 post inoculation.

It is theoretically possible that the mathematical *in silico* model could be used to determine the MIC. This has not been investigated in the present study as MIC is primarily useful in comparison, and DHA would be an inappropriate antimalarial to explore MIC due to a lack of robust MIC data and its short biological half-life. However, it is possible that the model could be used to

determine a drug concentration and dose interval over which parasite multiplication is maintained at one. If examined across a wide range of antimalarials this could provide evidence for the usefulness of the MIC parameter in comparing antimalarials.

The *in silico* model has been shown to be both internally valid and externally valid. It is consistent within itself as demonstrated since five multiple doses (5×10mg/kg) all applied at the same time is equivalent to one single dose of equivalent concentration (e.g. 50mg/kg). The model is externally valid in that it is able to accurately predict multiple dose outcomes based only upon graded pharmacodynamic data and is physiologically plausible.

An aim of the current experiments was to determine a set of criteria for determining the optimum of two or more sub therapeutic treatment regimens. Regimens were compared on the time to nadir, level of parasite reduction, and the recrudescence time, which was defined as the time for the infection to return to levels when treatment was initiated. These parameters seem adequate in the case of DHA for determining the most effective regimen. The nadir parasitaemia, parasite reduction ratio or time to recrudescence all appear to be consistent with in the frame work of a modelled infection commencing at the same parasitaemia.

An animal model such as that described in this thesis is not going to remove the need to conduct human PK-PD trials. These studies can provide useful insights into PK-PD relationships using a simplified *in vivo* model that may be possible to scale to the clinical setting to provide insights and starting points that may well never be possible from clinical data. It also may be possible to help answer questions such as whether MIC is a useful measure in assisting dose finding and optimisation. As White comments [423] *"The MIC is a useful theoretical concept, but its utility in dose finding and other aspects of therapeutic assessment remains to be defined. It is not known how variable it is."* The ability to experimentally and mathematically model the *P. berghei* infection and treatment also allows in depth examination of theoretical concepts such as MIC, and confirmation of these concepts experimentally *in vivo*.

The significance of these findings are that through use of detailed single dose graded PD data to produce a mathematical model of *P. berghei* infection and treatment with DHA, it is possible to accurately and precisely simulate and predict single and multiple dose monotherapeutic outcomes. This process facilitates optimisation of monotherapy with significantly less time and cost than if optimisation was determined solely through experiments in the *in vivo* system. The mathematical model also allows heuristic *in silico* investigation of aspects of infection and treatment that would be difficult with only *in vivo* data. This has the potential to allow development and assessment of methods to aid monotherapeutic and combination treatment optimisation through examination of concepts such as MIC and parasite elimination functions.

Using the methods described here it is possible to optimise and understand monotherapy treatment, which is a critical component of optimising combination treatment regimens.

CHAPTER SIX

6. Using a mathematical model of murine *P. berghei* single dose monotherapy to predict multiple dose combination outcomes.

6.1 Introduction

In Chapters four and five, it was demonstrated that it was possible to mathematically model a *P. berghei* infection and single dose treatment with DHA. This model was partially validated in that it was capable of accurately modelling the pharmacodynamic response to single dose DHA data and predicting parasite density-time profiles following multiple dose DHA monotherapy. The next stage of the validation for the model was testing the ability to predict multiple dose combination therapy based on single dose modelling. This was a prerequisite if the model is to be used to optimise combination treatment.

Prior to assessing the ability to predict combination outcomes, the ability to model single dose monotherapy of antimalarials other than DHA required attention. Other antimalarials have longer biological half-lives and may require a different parasite elimination equation than previously used to model DHA.

In this Chapter, data collected and analysed by another researcher in our laboratories, using the techniques developed in this thesis, were used to address model validity with chloroquine treatment. The availability of these data provided a valuable, independent practical validation of the mathematical model.

Model development in Chapters 3, 4 and 5 was an iterative process based upon data collected and analysed by one person, the author. It is possible that during this process, idiosyncratic anomalies could have been introduced into the model, based for example upon microscopy techniques or other experimental bias. Modelling data collected and counted by another researcher may indicate if such idiosyncrasy exists, and provide useful practical validation for the model.

6.1.1 History of chloroquine use

Chloroquine, a 4-aminoquinoline was first used as an antimalarial in 1947 [355]. It was synthesised in 1934 at Bayer but was not used as an antimalarial due to toxicity concerns [355]. Its action and toxicity was re-evaluated by the U.S. military in 1946 and Loeb *et al* recommended that CQ be made available for the prophylaxis and treatment of all blood stage malaria infections [229]. CQ quickly became the most widely used antimalarial for several decades due to its effectiveness, tolerability, safety and low cost [164].

CQ treatment was a central pillar of the World Health Organization's global malaria eradication program after World War II with approximately 300 million tablets distributed by the U.S. International Cooperation Administration (the predecessor to U.S.A.I.D.) between 1960 and 1962 [89]. Parasite populations worldwide were subject to an intense selection pressure for CQ resistance. Resistance was first detected in South America in 1959 and independently in South East Asia in 1960 [290]. By the 1970s CQ was no longer effective in the majority of South-East Asia and by 1978 the first cases of resistance in east

Africa were reported. By the early 1980s, 75% and 82% of infections in Kenya and Malawi respectively were found to be CQ resistant [47]. As resistance spread, morbidity and mortality due to malaria increased [391, 452].

Nevertheless, CQ is still widely used, particularly in the treatment of *P. vivax* and in special patient groups such as children and pregnant women [197, 221, 264, 274, 432]. Studies have indicated that clinical efficacy of CQ may return a decade after it has been withdrawn from first line treatment, highlighting its potential re-emergence as an important therapeutic option for malaria, most likely in combination with artemisinin or chemosensitizing agents [141, 162, 218, 241, 262, 263, 383, 414].

The antimalarial mechanism of action of CQ has not been fully elucidated, although the most accepted theory is that CQ interferes with haemoglobin digestion by the parasite [54, 355]. There is also increasing evidence indicating that CQ exerts several modulatory effects on the immune system [241, 383]. Chloroquine resistance is reported to be dependent on direct transport via mutated CQ resistance transporters (PfCRT) [241].

6.1.2 Artemisinin based combinations

The WHO recommends artemisinin-based combination therapy (ACT) for all *P. falciparum* confirmed cases [433]. ACTs are recommended for enhancement of efficacy [305, 418, 426], lowering malaria transmission and the potential to lower the rate at which resistance emerges and spreads [272, 421]. Convincing

evidence for the effectiveness of artemisinin based combination therapy in improving cure rates and decreasing malaria transmission were first systematically collected on the western border of Thailand [272]. This investigation also demonstrated a reversal in mefloquine resistance. Despite the success of the artemisinin-mefloquine combination it is difficult to generalise these results to other ACTs. While combination with an artemisinin does provide advantages such as improved parasite clearance and reduced gametocyte carriage [306, 376, 406], the International Artemisinin Study Group meta-analysis of almost 6000 patients found that for ACTs to lead to high cure rates, reduce transmission and provide protection against resistance, the partner drug needs to be highly effective [9]. This seems to counter the experience with mefloquine. Mefloquine monotherapy had a declining treatment success rate, due to parasite resistance, of approximately 70% prior to the introduction of the combination with artesunate in 1994, which increased treatment success rates to almost 100% [272].

6.1.3 Chloroquine and artemisinin based combinations

Clinical trials have indicated that ACT with artesunate and CQ are superior to CQ monotherapy [139, 354, 374]. The ACT improved 14 and 28 day cure rates as well as faster parasite clearance; however the reported treatment success rates for the ACTs were significantly below the 95% that is desirable. In Sao Tome and Principe, the 14 day failure rate for CQ versus the ACT were 80.1% and 16.6%; however, the 28 day failure rates were 81.1% and 32.4% [139]. Similarly in Burkina Faso for CQ versus artesunate-CQ the 14 day failure rates

were 64% and 20% while the 28 day failure rates were 81% and 51% respectively [354]. In Ivory Coast the 14 day failure rate for CQ versus the ACT were 85% and 77%, and the 28 day failure rates were 96% and 92% respectively [9]. While it is clear that ACTs are a significant improvement on CQ monotherapy, it has not been demonstrated that a CQ-based ACT will be effective clinically.

6.1.4 Chloroquine studies in murine models

As well as its clinical importance, CQ is important as a comparator for *in vitro* and *in vivo* preclinical testing of antimalarial agents [276, 293, 402, 446]. *In vitro* and *in vivo* efficacy studies have produced paradoxical results for CQ and artemisinin based combinations. CQ and artesunate are reported to be antagonistic [83, 367] and additive [127, 160] *in vitro* and additive in *in vivo* preclinical studies with artemisinin and DHA [82, 261]. Recent chemical studies by Haynes *et al* [166] comparing the action of methylene blue and artemisinins, explain the antagonism between CQ and artemisinins *in vitro* and are also reconcilable with the antimalarial mode of action of CQ perturbing intraparasitic redox homeostasis.

The pharmacokinetics [12, 70, 261, 384, 407] and pharmacodynamics [261, 286, 291, 294, 295] of CQ have been studied in murine malaria models. Detailed pharmacodynamic data of CQ treatment collected by Moore *et al* (using the *in vivo* model described in Chapter 3) have indicated that CQ shows a dose related reduction in parasitaemia with a 5-to >500-fold reduction in parasitaemia for

doses between 10 to 50mg/kg and a parasite nadir 2 days after treatment [261]. These studies also found that CQ has a weak additive efficacy combined with DHA. Pharmacokinetic investigation of CQ in mice showed a biphasic profile similar to that for CQ pharmacokinetics in other mammalian species (humans, rats, rabbits, monkeys and dogs) including long elimination half-life, moderate clearance and large volume of distribution, indicating scaling of specific parameters may be plausible for preclinical investigations [261]. Chloroquine efficacy studies by Ishih *et al* in ICR mice using *P. berghei* NK65 based on a Peters 4-day test indicated that a complex relationship exists between the parasite load and the efficacy of the drug [182]. Ishih *et al* also highlighted the requirement to identify the ideal time to initiate treatment in mice models [182].

6.1.5 Aims

The aim of the present series of studies was to investigate the feasibility of using the established mathematical model of *P. berghei* infection and DHA treatment to predict multiple dose combination therapeutic outcomes in Swiss mice. The initial aims were to:

i. Validate that the existing model of *P. berghei* infection and treatment with DHA can be used to model drugs with longer biological half-lives.
ii. Investigate combination therapy dosing regimens using the model to determine the ability to predict parasite dynamics with combination therapy.
iii. Use the model to determine an optimised combination treatment regimen.
iv. Demonstrate practical validity of the *in silico* model.

The hypothesis to be tested was:

- A mathematical model of *P. berghei* infection and treatment in Swiss mice can be developed from single dose graded pharmacodynamic data and can be used to predict combination therapy outcomes.

6.2 Methods

6.2.1 Selection of a dihydroartemisinin combination partner

In order to examine the ability to predict combination therapy outcomes using the mathematical model of malaria it was first necessary to develop a single dose model of another antimalarial as a combination partner with DHA. CQ was chosen for study due to the availability of preclinical pharmacodynamic data in our laboratory and because there is growing interest in the reintroduction of CQ clinically as parasites regain sensitivity to CQ in many endemic areas. There are also questions over the efficacy of artemisinin-CQ combinations with ambiguous or paradoxical results from *in vitro* and *in vivo* preclinical and clinical studies [83, 367] [127, 160] [82, 261].

6.2.2 Chloroquine pharmacodynamic data

Chloroquine pharmacodynamic data were kindly provided by Jillian Stoney from studies conducted in our laboratory (Jillian Stoney, BPharm (Hons) thesis [370]) and subsequently reported as part of a larger study [261]. Experimental animals, parasites and experimental protocols were based upon those described in Chapter 2 and 3. CQ diphosphate in water at 30mg/ml was diluted to the required concentrations in a standard 100µL injection volume. The solution was filtered (Millex-HV 0.45µm filter unit, Millipore, Molsheim, France) prior to i.p. injection [261].

Pharmacodynamic data for single dose CQ treatment of *P. berghei* infection in Swiss mice at 0 (n=4), 10 (n=9), 20 (n=7), 30 (n=9) and 50mg/kg (n=7)

administered 65 h after inoculation at an approximate starting parasitaemia of 5%, are presented in Figure 6.1A. Pharmacodynamic data for multiple dose CQ treatment and combination treatment with CQ plus DHA are presented in Figure 6.1B. Data were collected for two multiple dose treatment regimens of 5×10mg/kg and 2×20+10mg/kg of CQ administered at 12 h dose intervals beginning 65 h post inoculation. Pharmacodynamic data for combination treatment of 30mg/kg CQ plus 30mg/kg DHA administered separately at 65 h post inoculation are also presented (Figure 6.1B). The raw mean percentage parasitaemia data were converted to parasitaemia per μL for each time point as described in Equation 3.1.

The CQ pharmacodynamic experiments were performed as pilot studies and were conducted by a relatively inexperienced researcher, trained in our laboratory in murine handling and malaria microscopy techniques. The data collected were less comprehensive than earlier validation studies and show greater variation than those for DHA presented in Chapter 3. Data were not collected to be modelled, nor to provide detailed and robust pharmacodynamic data for CQ, but to provide baseline data to direct future experimental work. The data provided a valuable test for exploring the use of the mathematical model of malaria in a smaller and sparser data set.

(A)

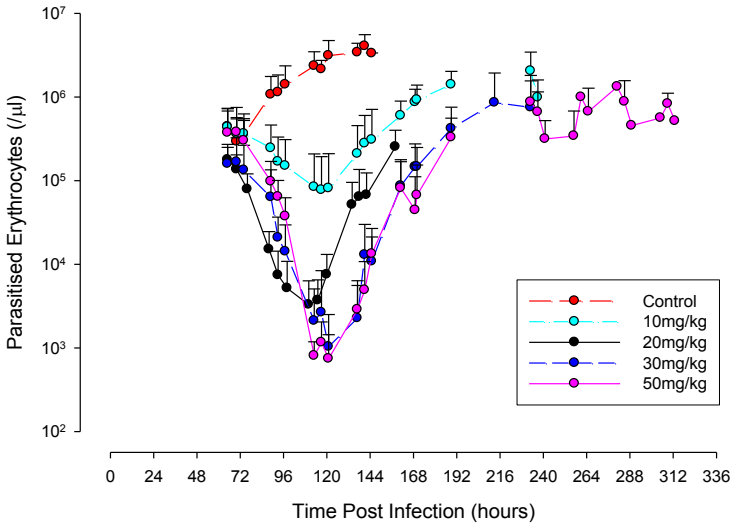

(B)

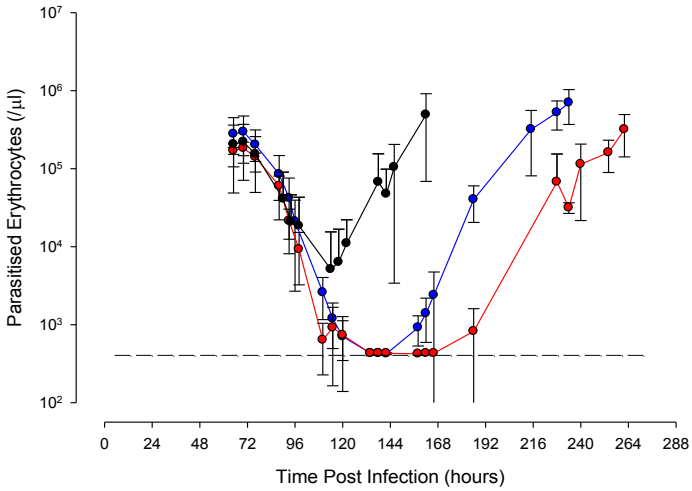

Figure 6.1 – (A) Single dose pharmacodynamic data for untreated (● n=4) Swiss mice infected with *P. berghei* and CQ treatment at 65 h post inoculation with 10mg/kg (●), 20mg/kg (●), 30mg/kg (●) and 50mg/kg (●) chloroquine. Data are mean ± SD and were collected and provided by Jillian Stoney.

(B) Pharmacodynamic data from *P. berghei* infected Swiss mice treated with either 5x10mg/kg CQ at 12h intervals (● n=4), 2x20+10mg/kg CQ at 12h intervals (● n=4) or a combination of 30mg/kg CQ and 30mg/kg DHA **(● n=4)** at 65 h post inoculation. The limit of microscopic detection was approximately 0.005% (---). Data are mean ± SD and were collected and provided by Jillian Stoney [370].

6.2.3 Chloroquine pharmacodynamic model construction

The pharmacodynamic model of CQ was constructed to be conceptually identical to that developed for DHA. An uncoupled 24-compartment model with drug dependent parasite removal occurring from compartment 22 was used. The average parasitised erythrocytes per μL data was used to construct a model of CQ treatment. The first step involved using the model of *P. berghei* infection in Swiss mice developed in Chapter 4 to model untreated data and confirm that parameters were within expected and acceptable biological variation. Figure 6.2 shows the *in silico* model of *P. berghei* infection and the untreated control infection data from four mice. The unfitted model has been shown (solid line), and confirms that untreated *P. berghei* infections in our laboratory using 6 week old male Swiss mice and ANKA *P. berghei* parasites produced a reproducible infection that can be accurately modelled. Model parameters determined in Chapter 4 (Equation 4.1) were used as initial model estimates and were entered as Bayesian terms into SAAM II with standard deviations and lower and upper limits as determined in Chapter 4 and shown in Table 6.1. A starting parasitaemia of 1500 parasites per μL was used which represents approximately 30% of the 10^7 i.p. inoculation being viable. This was used as a starting point based on results from Chapter 4. While the model fell within the standard deviation of the data, SAAM II was used to fit the untreated data and the results are shown in Figure 6.2 and Table 6.1.

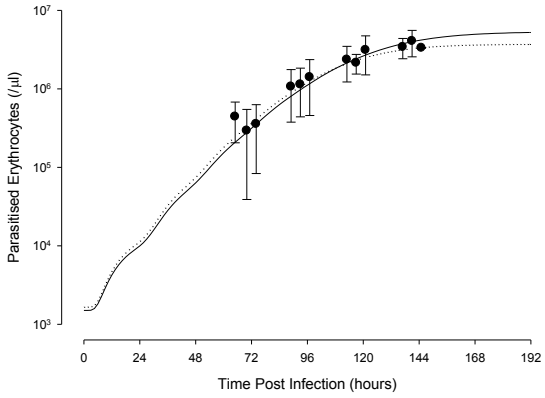

Figure 6.2 - Untreated *P. berghei* pharmacodynamic data (● n=4) in Swiss mice. The untreated model of *P. berghei* infection (—) developed in Chapter 4 falls within data standard deviations without adjustment or fitting. The fitted model is also shown (····). Data are mean ± SD and were collected and provided by Jillian Stoney [370].

Table 6.1 – Untreated model initial estimates based on model development experiments in Chapter 4. The terms were fitted in SAAM II to provide the fitting estimates.

	Data from Chapter 4				
Untreated Model Parameters	Initial Estimate	Standard Deviation	Lower/Upper Limits		Fitting Estimate
y_0	9.7	0.5	9	0.5	9.75
a	0.7	0.5	0.1	0.5	0.55
b	0.16	0.1	0.01	0.8	0.182
k_p	1	0.05	0.9	0.05	1.01
EPI (PRBC/μL)	1500	-	-	-	1678

With confirmation that the underlying infection model adequately represented the infection in this data set the next step was to add drug dependent parasite removal functions as described in Chapter 4, with Equation 4.3 becoming Equation 6.1 below.

$$D_{CQ} = A_{CQ} e^{-k_{CQ}(t-(t_{inj}+T_{CQ}))} + B_{CQ}$$

Equation 6.1

where: D_{CQ} is the CQ dependent parasite elimination as a function of

time (t) after inoculation; coefficient A_{CQ} is a function of the drug dose; k_{CQ} is the rate of parasite elimination; t_{inj} is the time of injection post inoculation; T_{CQ} is the time from injection to the peak parasite elimination and B_{CQ} represents a time independent increase in parasite elimination.

The only modification to Equation 6.1 from Equation 4.3 was that initial modelling was conducted with a B value fixed at zero to determine if this term was necessary for fitting CQ data. Model fitting was only significantly improved by adding a B value in the 10mg/kg treatment group.

Mean data with standard deviation were modelled for CQ rather than modelling of individual mouse data as in Chapter 4 for DHA. This was due to the large variation in the parasitaemia at the time of treatment within and between groups. Single dose data points greater than 240 h post inoculation (Figure 6.1A**)** were excluded from modelling as they were from a small group of surviving mice after euthanasia of the majority of the group. Data points in Figure 6.1B which were near the limit of microscopic detection were also excluded as they do not represent the actual parasitaemia. The LOD for these experiments was 0.005% or ~430 PRBC/μL.

6.2.4 Dihydroartemisinin and chloroquine treatment model

A pharmacodynamic model of DHA and CQ combination treatment was constructed as previously described for multiple dose models so that the drug

dependent parasite elimination function from compartment 22 represented elimination by both DHA and CQ. The elimination equations are additive implying that modelling results represent perfectly additive parasite effects between DHA and CQ. Model parameters for DHA determined in Chapter 4 were used due to the absence of single dose DHA data.

6.3 Results

6.3.1 Chloroquine single dose treatment modelling

Modelling results for CQ single doses and the CQ data (mean ± SD) are presented in Figure 6.3A and Table 6.2. There was a large variation in the parasitaemia at the time of treatment, which was intended to correspond to a 5% parasitaemia or 4.3×10^5 parasitised erythrocytes per μL (represented by the dashed line in Figure 6.3A). Several of the groups fell significantly below this 5% target, with the 20 and 30mg/kg groups having a starting treatment parasitaemia of 2%. Due to this large variation in parasitaemia at the time of treatment, normalised models are presented in Figure 6.3B.

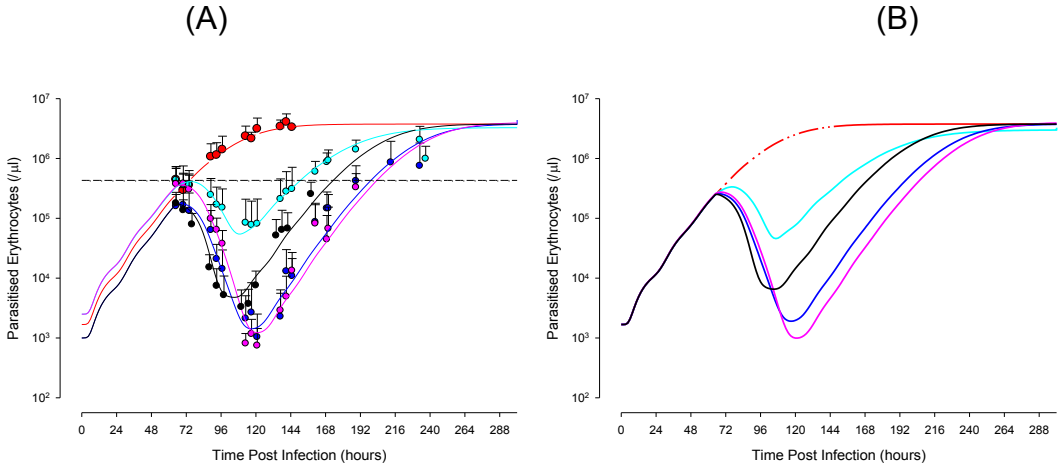

Figure 6.3 – (A) Single dose pharmacodynamic data (mean ± SD) and model fitting results for untreated (— ● n=4) Swiss mice infected with P. berghei and CQ treatment at 65 h post inoculation with 10mg/kg (— ●), 20mg/kg (— ●), 30mg/kg (— ●) and 50mg/kg (— ●) CQ. 5% parasitaemia is indicated by the horizontal dashed line (----).Data were provided by Jillian Stoney [370].

(B) Pharmacodynamic modelling results for untreated (—) and CQ treated groups with 10mg/kg (—), 20mg/kg (—), 30mg/kg (—) and 50mg/kg (—) normalised at a starting inoculation of 1678 parasitised erythrocytes per μL.

Models were normalised by modifying the EPI (number of parasitised erythrocytes at inoculation) to equal to 1678 PRBC/μL without modification of any other model parameters. This value was chosen as it was the estimated number of parasitised erythrocytes at inoculation in the untreated control group from the CQ data set.

Table 6.2 - Pharmacodynamic model parameters for CQ graded single dose pharmacodynamics data determined from model fitting of Equation 6.1

PD Model Parameters	Chloroquine dose (mg/kg)			
	50	**30**	**20**	**10**
A_{CQ}	1568	802	643	211
B_{CQ}	0	0	0	0.35
$t_{inj} + T_{CQ}$ (h)	95.9	92.5	78.0	92.0
k_{CQ} (/h)	0.22	0.20	0.18	0.27
Fold-decrease in parasite density (from time of drug administration to nadir)	278	120	36	6
Time of maximum parasite elimination, after drug administration (h)	30.7	27.5	13	27
Time of nadir parasite density, after drug administration (h)	56.5	52	40.5	44.5

6.3.2 Chloroquine single dose model

To produce a model of CQ single dose treatment, the modelling results in Table 6.2 were used to produce averaged A_{CQ}, T_{CQ} and k_{CQ} values. As B values were not required for fitting except for the 10mg/kg doses, for predictive modelling it was assumed that B was zero in all cases. Values for ($t_{inj} + T_{CQ}$) and k_{CQ} were 89.6 h and 0.22 h^{-1} respectively determined by averaging values in Table 6.2.

Values for A were estimated as 29.19 multiplied by the CQ dose in mg/kg by use of an origin intercepting linear fit of A_{CQ} values from Models were normalised by modifying the EPI (number of parasitised erythrocytes at inoculation) to equal to 1678 PRBC/μL without modification of any other model parameters. This value was chosen as it was the estimated number of parasitised erythrocytes at inoculation in the untreated control group from the CQ data set.

Table 6.2. Model results for 10, 20, 30 and 50mg/kg simulated treatment are presented in Figure 6.4 and can be compared to modelled data in Figure 6.3B. Figure 6.4 includes a simulated dose of 90mg/kg to demonstrate extrapolation outside the experimental data provided to create the model. Interpretation of extrapolated results without experimental validation should be undertaken with caution, but could direct further experimental studies.

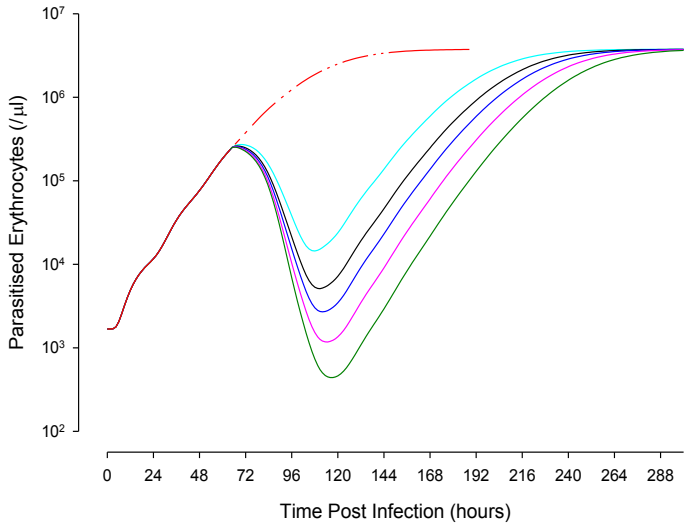

Figure 6.4 – Single dose pharmacodynamic model simulations for untreated (—) Swiss mice infected with *P. berghei* and CQ treatment at 65 h post inoculation with 10mg/kg (—), 20mg/kg (—), 30mg/kg (—), 50mg/kg (—) and 90mg/kg (—) CQ.

6.3.3 Chloroquine multiple dose modelling

Single dose CQ results used to construct the CQ mathematical model were used to predict the multiple dose pharmacodynamics for the two CQ multiple dose regimens presented in Figure 6.1B. Drug dependent parasite elimination equations from compartment 22 for each regimen are shown below as Equation 6.2 and Equation 6.3, which were based upon those developed in Chapter 5 for DHA.

Equation 6.2 for 20+20+10mg/kg CQ Regimen

$$k(0,23) = z\left(A_{20}e^{-k_{CQ}\times\left(t-(t_{inj}-T_{CQ})\right)}\right) + z_1\left(A_{20}e^{-k_{CQ}\times\left(t-(t_{inj}-T_{CQ}+12)\right)}\right) + z_2\left(A_{10}e^{-k_{CQ}\times\left(t-(t_{inj}-T_{CQ}+24)\right)}\right)$$

Equation 6.2

Equation 6.3 for 5×10mg/kg CQ Regimen

$$k(0,23) = z\left(A_{10}e^{-k_{CQ}\times\left(t-(t_{inj}-T_{CQ})\right)}\right) + z_1\left(A_{10}e^{-k_{CQ}\times\left(t-(t_{inj}-T_{CQ}+12)\right)}\right) + \ldots + z_4\left(A_{10}e^{-k_{CQ}\times\left(t-(t_{inj}-T_{CQ}+48)\right)}\right)$$

Equation 6.3

where: k(0,23) is the SAAM II parameter representing D_{CQ} which is the CQ dependent parasite elimination as a function of time (t) after inoculation; z is a switching function to allow activation of each drug function at the time of its administration; coefficient $A_{10/20}$ is a function of the drug dose representing 10 and 20mg/kg CQ; k_{CQ} is the rate of parasite elimination; t_{inj} is the time of injection post inoculation and T_{CQ} is the time from injection to the peak parasite elimination of CQ.

Model predictions are shown with experimental data (mean ± SD) in Figure 6.5A and B.

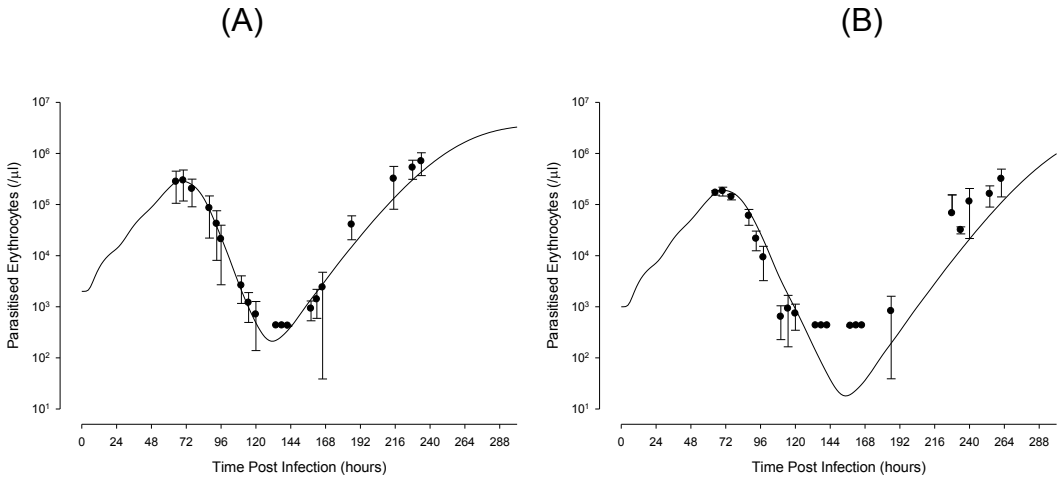

Figure 6.5 – (A) Multiple dose pharmacodynamic data (mean ± SD) and model prediction based on single dose modelling results for a 2x20+10mg/kg CQ regimen commencing at 65 h and with 12 h dose intervals. Data were provided by Jillian Stoney [370].

(B) Multiple dose pharmacodynamic data (mean ± SD) and model prediction based on single dose modelling results for a 5x10mg/kg CQ regimen commencing at 65 h and with 12 h dose intervals. Data were provided by Jillian Stoney [370].

SAAM II was used to adjust or fit model predictions to determine where there could be an improvement to the model predictions and if there were potential errors in model parameters for CQ treatment. Figure 6.6 shows the 5×10mg/kg CQ regimen data (●) and model prediction (----) as well as the model fitting (—). SAAM II achieved a more accurate fit for the data by modifying the peak parasite removal (T_{CQ}) from 24.6 to 15 h. The other CQ model parameters such as A_{CQ} or k_{CQ} were not modified by SAAM II to improve the fit.

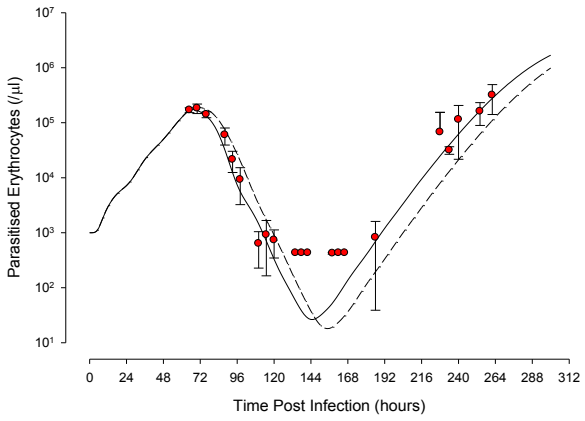

Figure 6.6 – Multiple dose pharmacodynamic data (mean ± SD ●) with model prediction (----) and model fitting (—) by SAAM II for a 5x10mg/kg CQ regimen commencing at 65 h and with 12 h dose intervals. Data were provided by Jillian Stoney [370].

6.3.4 Determination of the optimum dose interval for chloroquine

The multiple dose models of CQ treatment were used to examine the impact of changing the dose interval of CQ treatment. Similar to DHA modelling presented in Chapter 5, this was expected to provide an optimised dose interval for CQ treatment. Model predictions for various dose intervals of the three doses of the 2×20+10mg/kg regimen are presented in Figure 6.7 and Table 6.3. The 12 h dose interval used in experimental work was, as expected, much more effective than a single equivalent dose of 50mg/kg (or zero h interval). Dose intervals of 24 and 48 h were more effective, although the optimum dose interval according to the *in silico* model was approximately 42 h. Only a small increase in recrudescence time was achieved by increasing the dose interval above 42 h, and this occurred with a higher parasite nadir (Figure 6.7). Recrudescence time was defined as the time from drug treatment for the parasitaemia to return to the level at which treatment began.

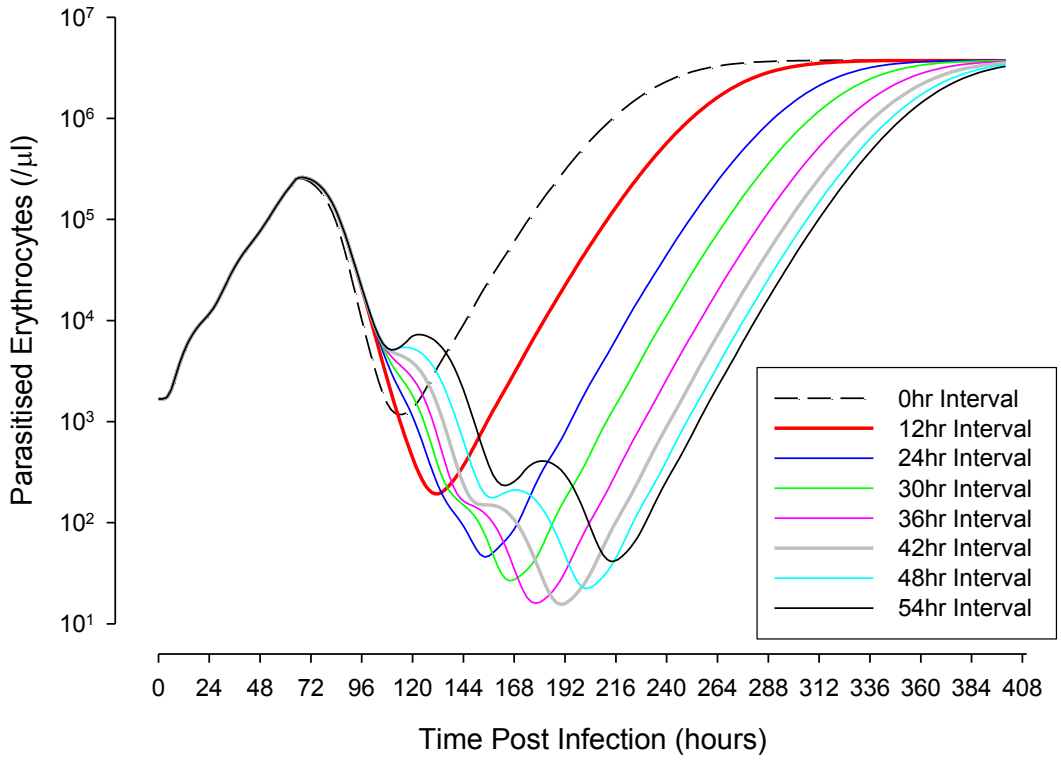

Figure 6.7 – Mathematical model simulated CQ multidose treatment of *P. berghei* infection in Swiss mice. The model simulates 2×20+10mg/kg multiple dose CQ regimens at varying dosage intervals between 0 and 54 h. An interval of 0 approximates single dose CQ treatment of 50mg/kg.

Table 6.3 **– Mathematical model simulated parameter values for 2×20+10mg/kg multiple dose CQ treated *P. berghei* infection in Swiss mice at varying dosage intervals.**

	CQ Dose Interval (h)							
Model Simulated Parameter Values	**0**	**12**	**24**	**30**	**36**	**42**	**48**	**54**
Nadir Parasitaemia (parasitised erythrocytes/μL)	1173	193.0	45.8	26.6	15.9	15.5	22.3	41.5
Fold Decrease in Parasitaemia	214	1299	5481	9420	15735	16155	11263	6045
Time of Nadir (hrs after start of treatment)	48.5	67	89	101	113	125	137	150
Time of Recrudescence (hrs after start of treatment)	125	217	255	273	291	303	311	317

Model predictions for various dose intervals of the five doses of the 5×10mg/kg regimen are presented in Figure 6.8 and Table 6.4. Similar to the 3-dose regimen, the 5-dose regimen with 12 h dose interval (used in experimental work) was much more effective than a single equivalent dose of 50mg/kg (or zero hour interval). The 36 h dose interval regimen was the most effective modelled result and the parasite nadir occurred at a parasitaemia below one parasite per μL (Figure 6.8).

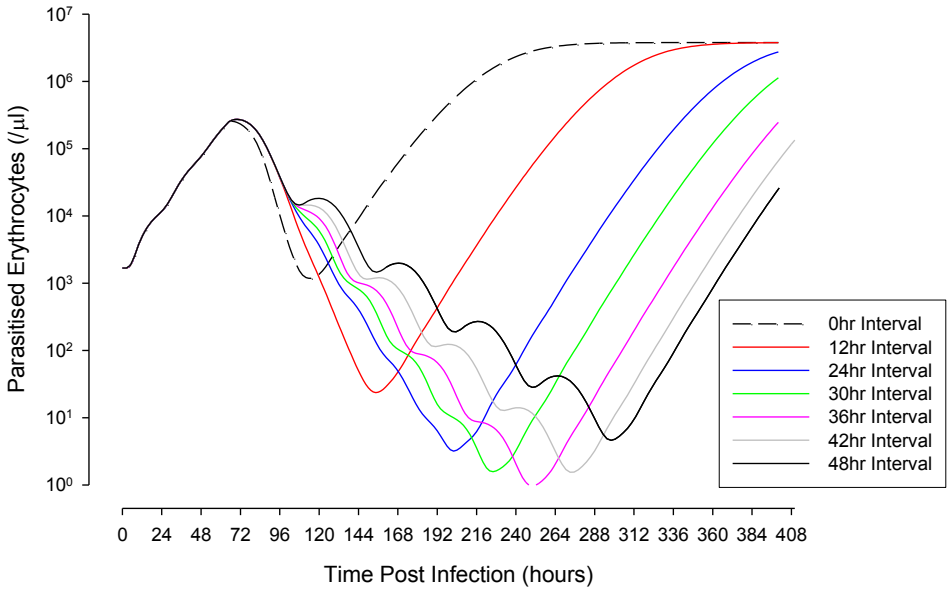

Figure 6.8 – Mathematical model simulated CQ multidose treatment of *P. berghei* infection in Swiss mice. The model simulates 5×10mg/kg multiple dose CQ regimens at varying dosage intervals between 0 and 54 h. An interval of 0 approximates single dose CQ treatment of 50mg/kg.

Comparing the two multiple dose regimens delivering a total 50mg/kg of CQ over either 3 or 5 doses, as anticipated 5 split doses of 10mg/kg was more effective than 3 doses of 20+20+10mg/kg over any dose interval (greater than

zero). However, the rate of reduction in parasite density was greater with the higher doses of CQ (Figure 6.7 and Figure 6.8).

Table 6.4 – Mathematical model simulated parameter values for 5×10mg/kg multiple dose CQ treated *P. berghei* infection in Swiss mice at varying dosage intervals.

	CQ Dose Interval (h)						
Model Simulated Parameter Values	**0**	**12**	**24**	**30**	**36**	**42**	**48**
Nadir Parasitaemia (parasitised erythrocytes/μL)	1178	23.6	3.2	1.6	0.97	1.5	4.6
Fold Decrease in Parasitaemia	213	10651	78928	159711	260669	162812	54600
Time of Nadir (hrs after start of treatment)	48.5	89.5	137	161	185	208	233
Time of Recrudes-cence (hrs after start of treatment)	125	207	276	308	335	355	367

6.3.5 Dihydroartemisinin and chloroquine combination modelling

The equation for the combination parasite elimination for DHA and CQ was constructed similarly to that used in multiple dose treatments and took the form shown in Equation 6.4 for elimination in a DHA and CQ combination regimen.

$$k(0,23) = z_{DHA}\left(A_{DHA}e^{-k_{DHA}\times\left(t-(t_{inj}+T_{DHA})\right)}\right)+ z_{CQ}\left(A_{CQ}e^{-k_{CQ}\times\left(t-(t_{inj}+T_{CQ})\right)}\right)$$

Equation 6.4

The equation parameters to model a 30mg/kg combination dose of both DHA and CQ are shown in Table 6.5. T_{DHA} and k_{DHA} parameters were determined from Table 4.3 and the A_{DHA} for 30mg/kg by using Equation 5.3. T_{CQ}, k_{CQ}, and A_{CQ} for 30mg/kg CQ were determined as described in 6.3.3. Model prediction for a combination treatment of 30mg/kg DHA and 30mg/kg CQ administration at 65

h is presented in Figure 6.9A. Model single doses of 30mg/kg DHA and 30mg/kg CQ are added in Figure 6.9B for comparison with the combination prediction.

Table 6.5 - Mathematical model parameter values for *P. berghei* infection and combination treatment with 30mg/kg CQ and 30mg/kg DHA.

Drug Treatment Model Parameters	Value
y_0	9.75
a	0.55
b	0.182
k_p	1.01
A_{DHA} / A_{CQ}	3720.9 / 875.7
k_{DHA} / k_{CQ} (h^{-1})	0.57 / 0.22
T_{DHA} / T_{CQ} (h)	12 / 24.6

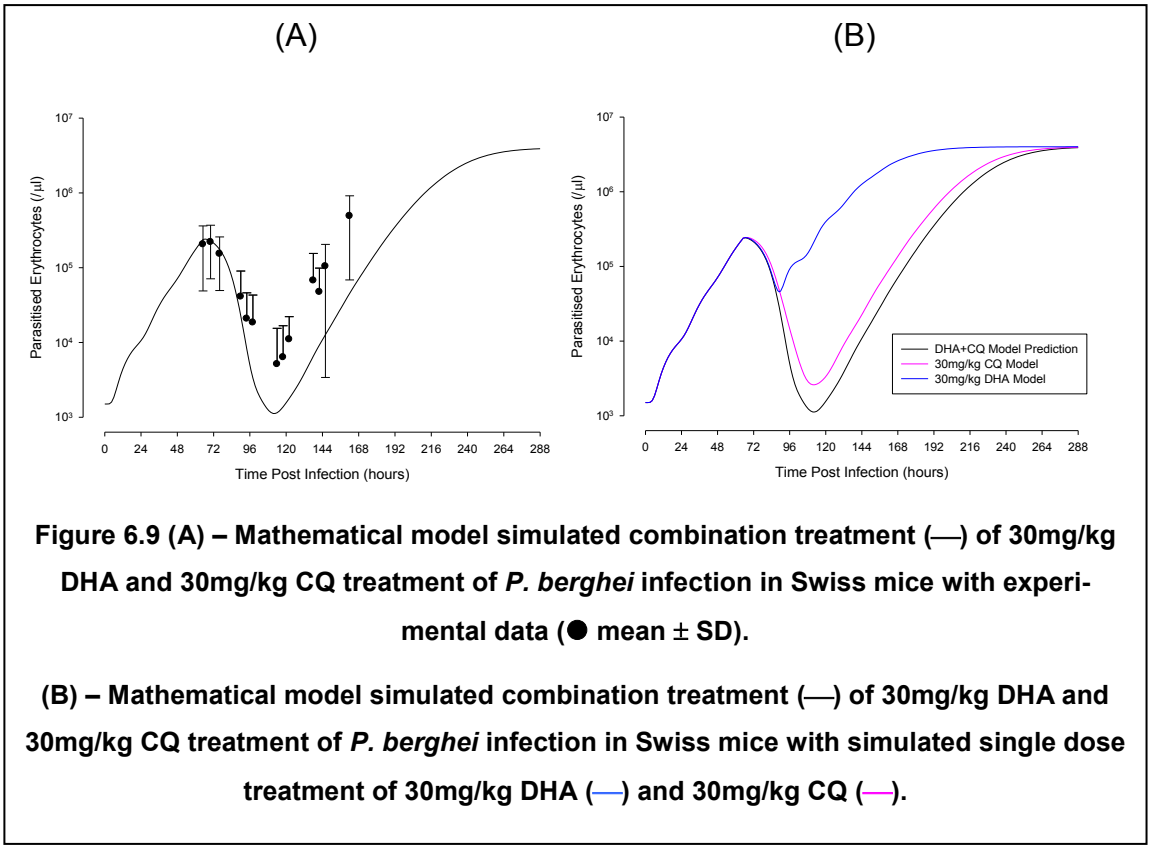

Figure 6.9 (A) – Mathematical model simulated combination treatment (—) of 30mg/kg DHA and 30mg/kg CQ treatment of *P. berghei* infection in Swiss mice with experimental data (● mean ± SD).

(B) – Mathematical model simulated combination treatment (—) of 30mg/kg DHA and 30mg/kg CQ treatment of *P. berghei* infection in Swiss mice with simulated single dose treatment of 30mg/kg DHA (—) and 30mg/kg CQ (—).

6.3.6 Optimum dose interval for a dihydroartemisinin and chloroquine combination

The model of DHA and CQ combination treatment was used to determine the optimum dose interval for a single 30mg/kg dose of DHA and CQ. The t_{inj} term in Equation 6.3 was modified to simulate differing injection times. Results of modification of the dose interval are presented in Figure 6.10 and Table 6.6. For a combination of 30mg/kg single doses of DHA and CQ the optimum treatment outcome in the Swiss murine model was obtained by administering DHA 42 to 48 h after CQ (Figure 6.10B —). The rationale for choosing this dose interval rather than administering CQ 24 h after DHA was the much more rapid parasite reduction which was delayed in the 24 h interval (Figure 6.10A —).

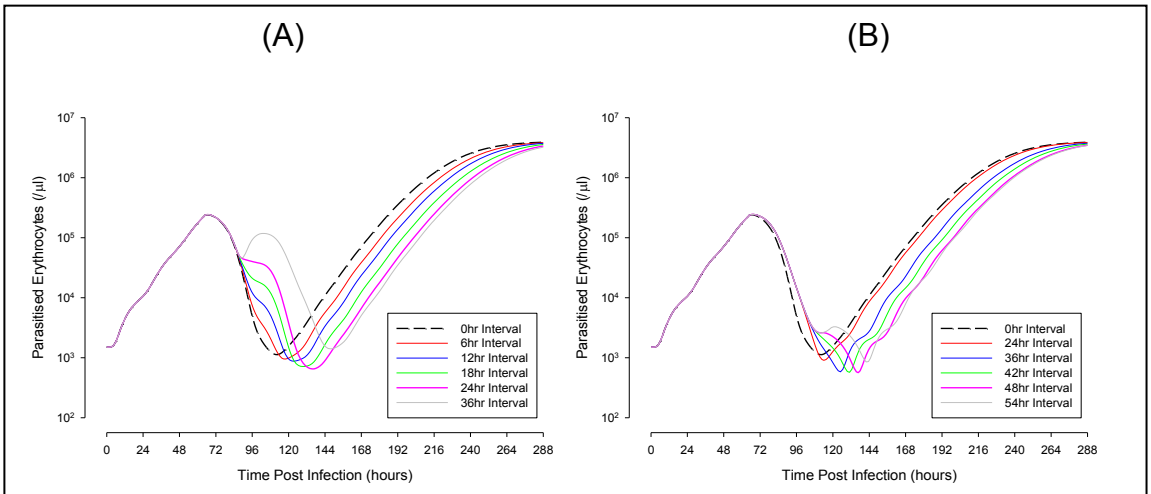

Figure 6.10 – (A) Mathematical model simulated combination treatment of 30mg/kg DHA at 65 h and 30mg/kg CQ at 0 (----), 6 (—), 12 (—), 18 (—), 24 (—) and 36 (—) h after the DHA dose.

(B) Mathematical model simulated combination treatment of 30mg/kg CQ at 65 h and 30mg/kg DHA at 0 (----),24(—), 36 (—), 42 (—), 48 (—) and 54 (—) h after the CQ dose.

Table 6.6 - Mathematical model simulated parameter values for 30mg/kg DHA and CQ combination regimens in a *P. berghei* infection in Swiss mice at varying dosage intervals.

	Combo Dose	CQ Dose Interval after DHA (h)			DHA Dose Interval after CQ (h)		
Model Simulated Parameter Values	**0**	**18**	**24**	**36**	**42**	**48**	**54**
Nadir Parasitaemia (parasitised erythrocytes/μL)	1123	713	649	1403	571	563	2598
Fold Decrease in Parasitaemia	212	334	367	170	417	423	92
Time of Nadir (hrs after start of treatment)	46.5	64.5	70.5	82.5	66	72	78
Time of Recrudes-cence (hrs after start of treatment)	121	143.5	151	155	140	148	149

6.3.7 Parasite elimination functions for single, multiple and combination regimens

Using the models of DHA and CQ single, multiple and combination treatments it was possible to simulate PD data as shown in Chapters 4, 5 and 6. Using the models it was also possible to examine other functions such as the number of parasitised erythrocytes eliminated over time due to drug administration or the parasite elimination rate function. This was discussed in 5.4. These parameters may provide an explanation of the observed PD effects by simulation of data that is difficult or impossible to measure *in vivo*. The parameters may also identify a parameter whose measure can be used to indicate which of multiple regimens is optimal similar to measures such as the parasite reduction ratio or mean inhibitory concentration often used in *in vitro* studies to compare efficacy.

Such parameters may provide a more simple method for determining the most optimal regimen than using nadir, time of nadir and time to recrudescence.

The parasite elimination rates for single 30mg/kg doses of DHA and CQ are presented in Figure 6.11A. As expected CQ has a much broader elimination profile than DHA. Figure 6.11B shows combination treatment PRBC elimination for 30mg/kg of DHA and CQ at 65 h. This demonstrates that the combination model predicts an additive outcome, combining the elimination functions for the individual components. Figure 6.11C shows combination treatment with 30mg/kg CQ followed by administration of 30mg/kg DHA 48 h later. Similarly Figure 6.12A and B show parasite elimination during the course of treatment with a single dose of 50mg/kg CQ or 20+20+10mg/kg regimen of CQ at a dose interval of 12 h (Figure 6.11A) or 42 h (Figure 6.11B). Both of the split dose regimens provide significantly better treatment than the single dose, and the 42 h multiple dose interval is significantly better than the 24 h interval.

(A)

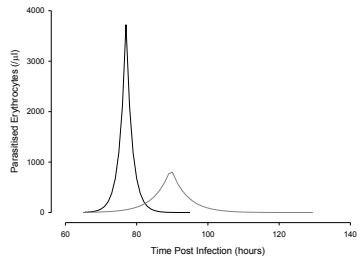

Figure 6.11 - (A) – Mathematical model simulated parasite elimination for a single 30mg/kg dose of DHA (—) and 30mg/kg dose of CQ (—) at 65 h post inoculation.

(B)

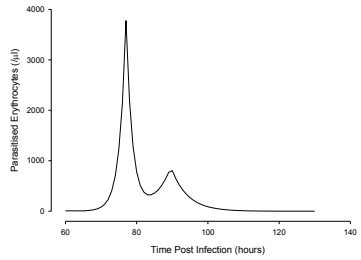

(B) – Mathematical model simulated parasite elimination for a combination regimen of 30mg/kg DHA and 30mg/kg CQ at 65 h post inoculation.

(C)

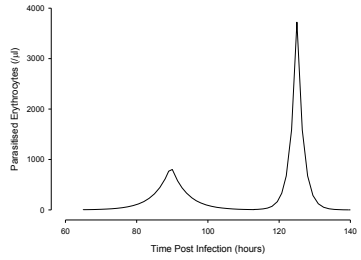

(C) – Mathematical model simulated parasite elimination for a combination regimen of 30mg/kg CQ administered at 65 h post inoculation followed by a 30mg/kg dose of DHA administered 48 h after the CQ.

(A) (B)

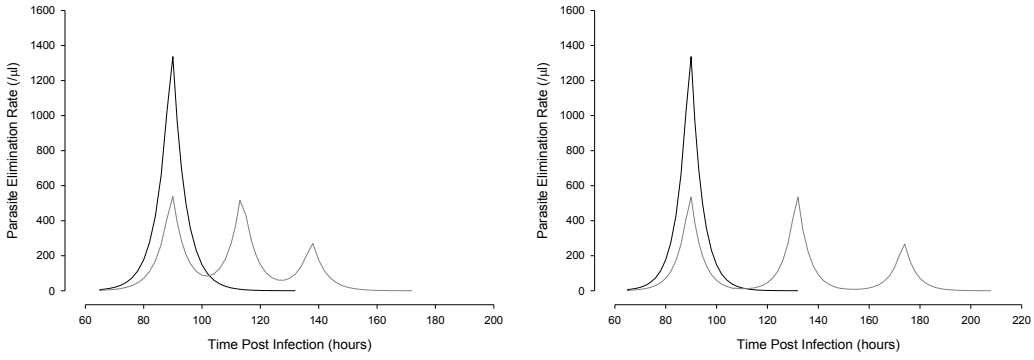

Figure 6.12 – (A) Mathematical model simulated parasite elimination for two multiple dose regimens of 20+20+10mg/kg at dose intervals of 0 h (or a single 50mg/kg dose —) and 12 h (—) commencing at 65 h post inoculation.

(B) Mathematical model simulated parasite elimination for two multiple dose regimens of 20+20+10mg/kg at dose intervals of 0 h (or a single 50mg/kg dose —) and 42 h (—) commencing at 65 h post inoculation.

6.3.8 Staging of parasites following treatment with chloroquine

It was demonstrated previously (4.3.6) that it is possible to examine changes in parasite population stages using the *in silico P. berghei* model and DHA treatment. The model was used to produce a simulated staged model of 30mg/kg CQ treatment (Figure 6.12A) with total CQ parasitaemia data. No staged data were available for CQ. DHA staged data is provided in Figure 6.12B for comparison (copy of Figure 4.11). An equivalent dose of CQ had a greater effect on the parasite density than DHA, but there did not appear to be a significant difference in the distribution of the parasite population stages after treatment.

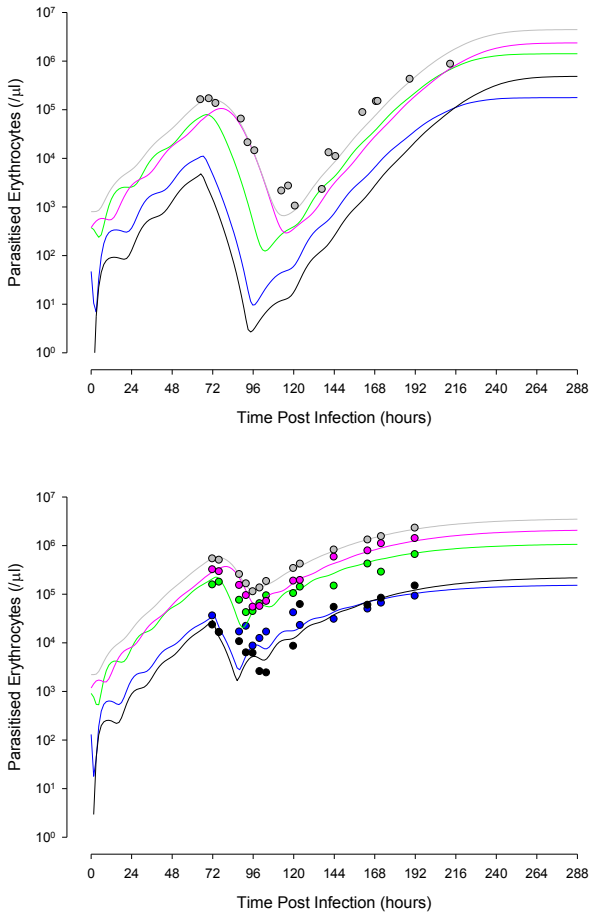

Figure 6.13 - (A) – Mathematical model simulated pharmacodynamics for total parasitaemia (—), and populations of rings (—), early trophozoites (—), late trophozoites (—), and schizonts (—) for a 30mg/kg CQ treatment at 65 h post inoculation.

(B) – Mathematical model simulated pharmacodynamics and staged microscopy counting for total parasitaemia (— ●), and populations of rings (— ●), early trophozoites (— ●), late trophozoites (— ●), and schizonts (— ●) for a 30mg/kg DHA treatment at 72 h post inoculation. Scaling is the same as Figure 6.13B to compare DHA and CQ staging.

6.3.9 Effects of parasitaemia at the time of drug treatment

Ishih *et al* [182] have reported that a complex relationship exists between the parasite load and the efficacy of the drug for CQ treatment of *P. berghei* NK65 infections. Due to the large variation in the level of parasitaemia at treatment of some of the data in the present study, the *in silico* model was used to simulate modifying the parasitaemia at which treatment starts, to examine the effect on drug efficacy. Results for a single dose of 100mg/kg DHA and 50mg/kg CQ at treatment parasitaemia varying between approximately 1-12% are summarised in Table 6.7.

Table 6.7– Mathematical model simulated parameter values for single dose treatment with 100mg/kg DHA and 50mg/kg CQ in a *P. berghei* infection in Swiss mice with treatment beginning at different parasite bioburdens.

	100mg/kg DHA			50mg/kg CQ		
Parasi-taemia at Inj. %	Parasi-taemia at Injection /μL	Parasi-taemia at Nadir /μL	Fold Decrease in Parasi-taemia	Parasi-taemia at Injection /μL	Parasi-taemia at Nadir /μL	Fold Decrease in Parasi-taemia
1%	85018	9287	9.2	85467	286	221.4
2%	168642	17250	9.8	168142	666	252.5
3%	250318	24508	10.2	250592	910	275.4
5%	406267	37401	10.9	408551	1314	310.9
8%	624029	53936	11.6	633875	1801	352.0
10%	775102	64645	12.0	775752	2070	374.8
12%	909657	73751	12.3	909969	2305	394.8

6.4 Discussion

In this chapter it has been demonstrated that the model of *P. berghei* infection and DHA treatment developed in Chapters 4 and 5 was capable of modelling the pharmacodynamics of CQ treatment. By combining an infection model with two models of drug treatment it was possible to predict combination therapy outcomes (Figure 6.9) in Swiss mice from graded single dose pharmacodynamic data (Figure 3.14 and Figure 6.1). This is a novel form of modelling that has several potential benefits. The model is capable of reducing *in vivo* experimental work therefore saving time, money and large numbers of animals through simulation of infection and treatment. The model allows examination and exploration of *P. berghei* treatment pharmacodynamics in ways that would be impractical experimentally, such as exploring the effect of starting parasitaemia at the time of treatment. It also allows *in vivo* results to be explained through examination of parasite multiplication and elimination functions and examination of parasite staging and parasite densities below the limit of detection of experimental techniques. In this way the model can add value to *in vivo* results through greater certainty of results, or in explaining results such as determining if a combination is more effective, or if the *in vivo* results are additive, antagonistic or synergistic. These demonstrate both the practical and heuristic validity and potential of the *in silico* model of *P. berghei* malaria.

6.4.1 Treatment parasite density and efficacy studies

Chloroquine data were collected by an inexperienced researcher and microscopist which contributed to large variation in parasitaemia at time of

treatment resulting in two distinct infection cohorts. In Figure 6.1A the control, 10mg/kg and 50mg/kg groups have a treatment parasitaemia of approximately 417180 parasites per μL, or 5.1%, while the 20mg/kg and 30mg/kg groups have a treatment parasitaemia of 168052 parasites per μL, or 2.0%. This could be a significant difference for a drug treatment study as literature [182] and results in Table 6.7 indicate that parasite density at the time of treatment does have a significant influence on the apparent efficacy of the drug treatment.

Modelling results in Table 6.7 also provide a plausible explanation for the influence of parasite density on treatment outcomes. As the parasite density increases the parasite effective multiplication rate declines. This explains the model prediction that there is a greater fold decrease in parasitaemia for the same dose of either DHA or CQ as the level of infection increases. This provides a warning for *in vivo* malaria experiments. Care should be taken in making conclusions where there is a discrepancy in the level of infection at treatment. Normalising data should also be avoided as this will artificially increase or reduce the apparent efficacy of treatments relative to each other and potentially produce conclusions that are incorrect. Results in Table 6.7 indicate that a discrepancy in treatment parasitaemia of 3%, as is the case in CQ single dose data in Figure 6.1A, could lead to an 11% discrepancy in treatment outcome or fold decrease in parasitaemia for 100mg/kg DHA or a 23% discrepancy for CQ. Comparing treatments with a significant difference in treatment parasitaemia should be avoided or undertaken with caution.

6.4.2 Modelling chloroquine treatment

Chloroquine treatment was successfully modelled and internally and externally validated. A single dose model of 50mg/kg was shown to be equivalent to 5 10mg/kg doses administered simultaneously. It was also shown that the model could accurately and precisely simulate multiple dose treatments of CQ on parasite dynamics. Results in Figure 6.5 show that model simulations are accurate as they fall within biological variation of the *in vivo* data. The model accurately indicated that split dosing of CQ is more effective than single dosing and that split dosing over 5 days is significantly more effective than a 3 day regimen (Figure 6.7 and Figure 6.8). Results indicate that a CQ dose interval of 36 to 48 h in the *P. berghei* malaria model provides theoretical optimal treatment outcome in the two regimens examined. This equates to a dose interval of 1.5-2.0 erythrocytic life cycles, which has practical limitations and may not provide overall benefits compared to a dose interval of about 0.5 erythrocytic life cycles.

Figure 6.5 demonstrates that the CQ model can simulate multiple dose treatment accurately to determine which of two treatment regimens will be most effective. The model indicates that a 5×10mg/kg regimen with 12 h dose intervals is significantly more effective when considering the three factors of parasite reduction rate, the parasite density at nadir and the time to recrudescence. This regimen was more effective than a 20+20+10mg/kg regimen with 12 h dose intervals and more practical than other dose intervals. Nevertheless, a dose interval of 1.0 erythrocytic life cycles provides an impressive parasite reduction rate (Figure 6.8) and a nadir almost one order of

magnitude lower (Figure 6.8, Table 6.4) and might be considered implausible only because of the contemporary dogma of two doses per erythrocytic lifecycle. Both of these split regimens are significantly more effective than a single 50mg/kg dose of CQ.

6.4.3 Modelling dihydroartemisinin and chloroquine combination treatment

A further outcome was to demonstrate the use of the models of CQ and DHA treatment to simulate combination treatment. The mathematical model provides an additive simulation. This is shown in Figure 6.11 which demonstrates that the parasite elimination functions for DHA and CQ single dose treatment are combined in the combination model. The significance of this is that the combination model provides a tool to determine whether a combination in the *in vivo* malaria model is antagonistic, additive or synergistic by comparing it to *in vivo* data as described below.

Figure 6.9A shows the predicted combination model with *in vivo* data for a combination of 30mg/kg DHA and CQ. The (additive) model predicts a larger PD effect of the combination than observed *in vivo,* which suggests that the DHA-CQ combination is antagonistic in the Swiss *P. berghei* model. This result is supported by *in vitro* findings [83, 166, 367]; however some *in vivo* findings have indicated an additive effect [82, 261]. Clinical results of a study comparing CQ combined with artesunate versus CQ monotherapy in uncomplicated falciparum infections in children in Gambia concluded that CQ plus artesunate is not sufficiently efficacious to justify its introduction as a replacement for chloroquine

monotherapy [374]. The 28 day treatment failure was not improved in the combination regimen of 25mg base/kg of CQ given over three days with 4mg/kg artesunate given each of the three days. These results however may have been influenced by CQ resistance in Gambia. Another similar study in Malawi also comparing CQ monotherapy and in combination with artesunate failed to show significant benefit of the combination over CQ alone, in an area of CQ sensitivity [217]. Caution should be taken in comparing preclinical findings to clinical findings, however available clinical data does seem to suggest that combinations of artemisinins and CQ are not synergistic and there is little evidence to support introduction of CQ ACT.

The combination model was further used to examine optimal dose intervals for CQ and DHA. Treatment improvement can be marginally achieved by splitting doses of CQ and DHA so that CQ treatment occurs approximately 24 h after DHA treatment or DHA treatment occurs approximately 48 h after CQ treatment (Figure 6.10 and Table 6.6). It should be noted that splitting DHA and CQ doses reduces the rate of fall in parasite density, but extends the recrudescence time and lowers the parasite nadir. Chloroquine followed by a DHA dose at 48 h is a more effective regimen than the DHA followed by CQ regimen but is contrary to ACT dogma. Both regimens have similar nadirs and recrudescence times, however CQ followed by DHA at 48 h provides a much faster parasite clearance (Figure 6.10 and Table 6.6). These results were not intended for comparison with clinical CQ ACTs. The combination of a single dose of DHA and CQ is not a clinically relevant regimen and even if it was, model simulations in Figure 6.10

would indicate that splitting a single dose of DHA and CQ would be unlikely to provide a significant or observable *in vivo* result. The exercise was performed to validate the ability to simulate combination treatment and examine optimisation in a *P. berghei* murine model which has been shown to be possible.

7. Conclusion

The series of studies presented in this thesis demonstrate establishment of a novel *in vivo-in silico* model of *P. berghei* malaria for investigation of antimalarial pharmacodynamics and pharmacokinetics based upon the established Rane and Peters 4-day tests. The studies have demonstrated that the *in vivo* murine malaria model was suitable to generate detailed PD data that is impossible to obtain clinically. The subsequent development and validation of this unique mathematical model of a rodent malaria infection, capable of simulating and predicting parasite population changes during multiple dose *in vivo* treatment in Swiss mice, demonstrates the power of an *in vivo* preclinical malaria model.

The applications for the *in vivo* and *in silico* model of malaria developed in this thesis are several fold. They provide a validated, standard platform for collection and comparison of detailed PD-PK data. Coupled with a robust mathematical model, the possibility exists to complement preclinical research with *in silico* investigation of optimum doses, dose intervals and combinations, to direct *in vivo* experimental outcomes, and reduce the number of studies required. The ability to perform three preclinical studies using two antimalarials and elucidate their PK-PD parameters and determine if they display antagonism or synergy and to what extent, is also significant. The *in silico* model enables the *in vivo P. berghei* model to be useful practically (by reducing the time, cost and experimental studies required) for exploring detailed pharmacodynamics and as a tool for dose and combination optimisation.

Another application for the *in silico* malaria model is the ability for it to be used for scientific explanation. Two examples from the work presented here demonstrate this heuristic potential of the model. Firstly, indication that the peak parasite elimination occurs 12 h after DHA administration provided an objective explanation as to why 12 h dose intervals (half erythrocytic life cycle) were most effective for multiple dose DHA treatment in the murine model. Secondly, *in silico* prediction that DHA and CQ efficacy is dependent upon parasite density at the time of treatment is due, at least in part, to changes in the parasite multiplication dynamics, provides an explanation for the experimental observations. The ability to explore infection and treatment to improve conceptual understanding is significant. These explanations can then be accurately and precisely tested using the *in vivo* model. The data can then be used iteratively to improve the *in silico* model of malaria.

The *in silico* model has been developed so that it can be easily used and manipulated by biological scientists, who may make use of the *in vivo* model of murine malaria. Its use is not dependent on difficult or complex mathematical equations that may deter use by scientists unfamiliar with sophisticated PK-PD modelling. More complex models can be designed, as has been demonstrated by Patel *et al* [281] using concepts, methods and data collected as described in this thesis and previously reported [138].

The series of studies presented in this thesis established that the *in vivo–in silico* model of *P. berghei* malaria is suitable for detailed preclinical investigations of

antimalarial compounds. These investigations were the first known to describe detailed characterisation of *P. berghei* infection and PK-PD data for DHA in a murine model. They were the first to mathematically model parasite dynamics of *P. berghei* infection and treatment with DHA and CQ. The *in silico P. berghei* model was a novel, viable and practically achievable solution to the question of how to optimise antimalarial treatment *in vivo*. It is therefore concluded that the work described in this thesis is a valuable contribution to the preclinical investigation of antimalarial drugs.

References

Every reasonable effort has been made to acknowledge the owners of copyright material. I would be pleased to hear from any copyright owner who has been omitted or incorrectly acknowledged.

1. *Antimalarial efficacy and mode of action of qinghaosu and its derivatives in experimental models. China Cooperative Research Group on qinghaosu and its derivatives as antimalarials.* J Tradit Chin Med, 1982. **2**(1): p. 17-24.

2. *Chemical studies on qinghaosu (artemisinine). China Cooperative Research Group on qinghaosu and its derivatives as antimalarials.* J Tradit Chin Med, 1982. **2**(1): p. 3-8.

3. *The chemistry and synthesis of qinghaosu derivatives. China Cooperative Research Group on qinghaosu and its derivatives as antimalarials.* J Tradit Chin Med, 1982. **2**(1): p. 9-16.

4. *Metabolism and pharmacokinetics of qinghaosu and its derivatives. China Cooperative Research Group on qinghaosu and its derivatives as antimalarials.* Journal of Traditional Chinese Medicine = Chung i Tsa Chih Ying Wen Pan / Sponsored By All-China Association of Traditional Chinese Medicine, Academy of Traditional Chinese Medicine, 1982. **2**(1): p. 25-30.

5. *Implementation of the global malaria control strategy. Report of a WHO Study Group on the Implementation of the Global Plan of Action for Malaria Control 1993-2000.* World Health Organ Tech Rep Ser, 1993. **839**: p. 1-57.

6. *Coartem (artemether/lumefantrine)*. CentreWatch - FDA Approved Drugs 2009 [cited 2014; Available from: https://www.centerwatch.com/drug-information/fda-approved-drugs/drug/1019/coartem-artemether-lumefantrine.

7. Adachi, K., H. Tsutsui, S. Kashiwamura, E. Seki, H. Nakano, O. Takeuchi, K. Takeda, K. Okumura, L. Van Kaer, H. Okamura, S. Akira, and K. Nakanishi, *Plasmodium berghei infection in mice induces liver injury by an IL-12- and toll-like receptor/myeloid differentiation factor 88-dependent mechanism.* J Immunol, 2001. **167**(10): p. 5928-34.

8. Adam, E., C. Pierrot, S. Lafitte, C. Godin, A. Saoudi, M. Capron, and J. Khalife, *The age-related resistance of rats to Plasmodium berghei infection is associated with differential cellular and humoral immune responses.* Int J Parasitol, 2003. **33**(10): p. 1067-78.

9. Adjuik, M., A. Babiker, P. Garner, P. Olliaro, W. Taylor, N. White, and G. International Artemisinin Study, *Artesunate combinations for treatment of malaria: meta-analysis.* Lancet, 2004. **363**(9402): p. 9-17.

10. Aguilar Torrentera, F., M.A. Lambot, J.D. Laman, M. Van Meurs, R. Kiss, J.C. Noel, and Y. Carlier, *Parasitic load and histopathology of cutaneous lesions, lymph node, spleen, and liver from BALB/c and C57BL/6 mice infected with Leishmania mexicana.* Am J Trop Med Hyg, 2002. **66**(3): p. 273-9.

11. Aikawa, M., *Parasitological review. Plasmodium: the fine structure of malarial parasites.* Exp Parasitol, 1971. **30**(2): p. 284-320.

12. Ali, B.H., A. Al-Qarawi, and H.M. Mousa, *Effect of grapefruit juice on plasma chloroquine kinetics in mice.* Clin Exp Pharmacol Physiol, 2002. **29**(8): p. 704-6.

13. Amani, V., A.M. Vigario, E. Belnoue, M. Marussig, L. Fonseca, D. Mazier, and L. Renia, *Involvement of IFN-gamma receptor-medicated signaling in pathology and anti-malarial immunity induced by Plasmodium berghei infection.* Eur J Immunol, 2000. **30**(6): p. 1646-55.

14. Amaratunga, C., S. Sreng, S. Suon, E.S. Phelps, K. Stepniewska, P. Lim, C. Zhou, S. Mao, J.M. Anderson, N. Lindegardh, H. Jiang, J. Song, X.Z. Su, N.J. White, A.M. Dondorp, T.J. Anderson, M.P. Fay, J. Mu, S. Duong, and R.M. Fairhurst, *Artemisinin-resistant Plasmodium falciparum in Pursat province, western Cambodia: a parasite clearance rate study.* Lancet Infect Dis, 2012. **12**(11): p. 851-8.

15. Anderson, R.M., *The role of mathematical models in helminth population biology.* Int J Parasitol, 1987. **17**(2): p. 519-29.

16. Anderson, R.M., *Mathematical studies of parasitic infection and immunity.* Science, 1994. **264**(5167): p. 1884-6.

17. Anderson, R.M., R.M. May, and S. Gupta, *Non-linear phenomena in host-parasite interactions.* Parasitology, 1989. **99 Suppl**: p. S59-79.

18. Angulo-Barturen, I. and S. Ferrer, *Humanised models of infection in the evaluation of anti-malarial drugs.* Drug Discov Today Technol, 2013. **10**(3): p. e351-7.

19. Angus, B.J., K. Chotivanich, R. Udomsangpetch, and N.J. White, *In vivo removal of malaria parasites from red blood cells without their destruction in acute falciparum malaria.* Blood, 1997. **90**(5): p. 2037-40.

20. Arnold, L., R.K. Tyagi, P. Meija, C. Swetman, J. Gleeson, J.L. Perignon, and P. Druilhe, *Further improvements of the P. falciparum humanized mouse model.* PLoS One, 2011. **6**(3): p. e18045.

21. Ashley, E., R. McGready, S. Proux, and F. Nosten, *Malaria.* Travel Med Infect Dis, 2006. **4**(3-4): p. 159-73.

22. Ashley, E.A. and N.J. White, *Artemisinin-based combinations.* Curr Opin Infect Dis, 2005. **18**(6): p. 531-6.

23. Ashton, M., T.N. Hai, N.D. Sy, D.X. Huong, N. Van Huong, N.T. Nieu, and L.D. Cong, *Artemisinin pharmacokinetics is time-dependent during repeated oral administration in healthy male adults.* Drug Metab Dispos, 1998. **26**(1): p. 25-7.

24. Sixtieth World Health Assembly, *Agenda Item 12.5 Malaria*. 2007.

25. Avery Jones, S., *Mass treatment with pyrimethamine A study of resistance and cross resistance resulting from a field trial in the hyperendemic malarious area of Makueni, Kenya. September 1952—September 1953.* Transactions of the Royal Society of Tropical Medicine and Hygiene, 1958. **52**(6): p. 547-561.

26. Bailey, N.T.J., *The Biomathematics of Malaria*. 1982: Charles Griffin.

27. Baird, J.K., *Effectiveness of antimalarial drugs.* N Engl J Med, 2005. **352**(15): p. 1565-77.

28. Banchereau, J., F. Briere, C. Caux, J. Davoust, S. Lebecque, Y.J. Liu, B. Pulendran, and K. Palucka, *Immunobiology of dendritic cells.* Annu Rev Immunol, 2000. **18**: p. 767-811.

29. Barh, D., V. Chaitankar, E.C. Yiannakopoulou, E.O. Salawu, S. Chowbina, P. Ghosh, and V. Azevedo, *Chapter 21 - In Silico Models: From Simple Networks to Complex Diseases*, in *Animal Biotechnology*, A.S.V. Singh, Editor. 2014, Academic Press: San Diego. p. 385-404.

30. Barnes, K.I., F. Little, P.J. Smith, A. Evans, W.M. Watkins, and N.J. White, *Sulfadoxine-pyrimethamine pharmacokinetics in malaria: pediatric dosing implications.* Clin Pharmacol Ther, 2006. **80**(6): p. 582-96.

31. Barradell, L. and A. Fitton, *Artesunate.* Drugs, 1995. **50**(4): p. 714-741.

32. Barradell, L.B. and A. Fitton, *Artesunate. A review of its pharmacology and therapeutic efficacy in the treatment of malaria.* Drugs, 1995. **50**(4): p. 714-41.

33. Barry, A.E., L. Schultz, C.O. Buckee, and J.C. Reeder, *Contrasting population structures of the genes encoding ten leading vaccine-candidate antigens of the human malaria parasite, Plasmodium falciparum.* PLoS One, 2009. **4**(12): p. e8497.

34. Basco, L.K., *Molecular epidemiology of malaria in Cameroon. XVI. Longitudinal surveillance of in vitro pyrimethamine resistance in Plasmodium falciparum.* Am J Trop Med Hyg, 2003. **69**(2): p. 174-8.

35. Basco, L.K. and P. Ringwald, *In vitro activities of piperaquine and other 4-aminoquinolines against clinical isolates of Plasmodium falciparum in Cameroon.* Antimicrob Agents Chemother, 2003. **47**(4): p. 1391-4.

36. Bassingthwaighte, J.B., E. Butterworth, B. Jardine, and G.M. Raymond, *Compartmental modeling in the analysis of biological systems.* Methods Mol Biol, 2012. **929**: p. 391-438.

37. Batty, K.T., *Pharmacokinetic studies of artesunate and dihydroartemisinin*, in *Medicine and Pharmacology*. 1999, University of Western Australia: Perth (WA).

38. Batty, K.T., T.M. Davis, L.T. Thu, T.Q. Binh, T.K. Anh, and K.F. Ilett, *Selective high-performance liquid chromatographic determination of artesunate and alpha- and beta-dihydroartemisinin in patients with falciparum malaria.* J Chromatogr B Biomed Appl, 1996. **677**(2): p. 345-50.

39. Batty, K.T., P.L. Gibbons, T.M. Davis, and K.F. Ilett, *Pharmacokinetics of dihydroartemisinin in a murine malaria model.* Am J Trop Med Hyg, 2008. **78**(4): p. 641-2.

40. Batty, K.T., K.E. Ilett, S.M. Powell, J. Martin, and T.M.E. Davis, *Relative bioavailability of artesunate and dihydroartemisinin: investigations in the isolated perfused rat liver and in healthy Caucasian volunteers.* The American Journal of Tropical Medicine and Hygiene, 2002. **66**(2): p. 130-136.

41. Beadle, C., P.D. McElroy, C.N. Oster, J.C. Beier, A.J. Oloo, F.K. Onyango, D.K. Chumo, J.D. Bales, J.A. Sherwood, and S.L. Hoffman, *Impact of transmission intensity and age on Plasmodium falciparum density and associated fever: implications for malaria vaccine trial design.* J Infect Dis, 1995. **172**(4): p. 1047-54.

42. Billker, O., M.K. Shaw, G. Margos, and R.E. Sinden, *The roles of temperature, pH and mosquito factors as triggers of male and female gametogenesis of Plasmodium berghei in vitro.* Parasitology, 1997. **115 (Pt 1)**: p. 1-7.

43. Bjorkman, A. and P.A. Phillips-Howard, *The epidemiology of drug-resistant malaria.* Trans R Soc Trop Med Hyg, 1990. **84**(2): p. 177-80.

44. Black, R.H., *The absorption of inoculated blood containing Plasmodium berghei from the peritoneal cavity of the mouse.* Ann Trop Med Parasitol, 1952. **46**(2): p. 144-9.

45. Bloland, P.B., *Drug resistance in malaria*. 2001, World Health Organisation.

46. Bloland, P.B., M. Ettling, and S. Meek, *Combination therapy for malaria in Africa: hype or hope?* Bulletin of the World Health Organization, 2000. **78**: p. 1378-1388.

47. Bloland, P.B., E.M. Lackritz, P.N. Kazembe, J.B. Were, R. Steketee, and C.C. Campbell, *Beyond chloroquine: implications of drug resistance for evaluating malaria therapy efficacy and treatment policy in Africa.* J Infect Dis, 1993. **167**(4): p. 932-7.

48. Borrmann, S., R.K. Binder, A.A. Adegnika, M.A. Missinou, S. Issifou, M. Ramharter, W.H. Wernsdorfer, and P.G. Kremsner, *Reassessment of the resistance of Plasmodium falciparum to chloroquine in Gabon: implications for the validity of tests in vitro vs. in vivo.* Trans R Soc Trop Med Hyg, 2002. **96**(6): p. 660-3.

49. Bouma, M.J. and H.J. van der Kaay, *The El Nino Southern Oscillation and the historic malaria epidemics on the Indian subcontinent and Sri Lanka: an early warning system for future epidemics?* Trop Med Int Health, 1996. **1**(1): p. 86-96.

50. Boyd, M.F., *Epidemiology of Malaria: Factors related to the intermediate host*, in *Malariology*, M.F. Boyd, Editor. 1949, W. B. Saunders: Philadelphia. p. 551-607.

51. Boyd, M.F., *Historical Review*, in *Malariology*, M.F. Boyd, Editor. 1949, W.B. Saunders: Philadelphia. p. 3-25.

52. Boyd, M.F. and S.F. Kitchen, *Observations on Induced Falciparum Malaria.* The American Journal of Tropical Medicine and Hygiene, 1937. **s1-17**(2): p. 213-235.

53. Boyd, M.F. and S.F. Kitchen, *On the Infectiousness of Patients Infected with Plasmodium Vivax and Plasmodium Falciparum.* The American Journal of Tropical Medicine and Hygiene, 1937. **s1-17**(2): p. 253-262.

54. Bray, P.G., S.R. Hawley, M. Mungthin, and S.A. Ward, *Physicochemical properties correlated with drug resistance and the reversal of drug*

resistance in Plasmodium falciparum. Mol Pharmacol, 1996. **50**(6): p. 1559-66.

55. Breman, J.G. and A.D. Brandling-Bennett, *The challenge of malaria eradication in the twenty-first century: research linked to operations is the key.* Vaccine, 2011. **29 Suppl 4**: p. D97-103.

56. Bruce-Chwatt, L.J., *Alphonse Laveran's discovery 100 years ago and today's global fight against malaria.* J R Soc Med, 1981. **74**(7): p. 531-6.

57. Bruce-Chwatt, L.J., *History of malaria from prehistory to eradication*, in *Malaria: Principles and Practice of Malariology*, W.H. Wernsdorfer and I. McGregor, Editors. 1988, Churchill Livingstone: Edinburgh. p. 1-59.

58. Bull, P.C., B.S. Lowe, N. Kaleli, F. Njuga, M. Kortok, A. Ross, F. Ndungu, R.W. Snow, and K. Marsh, *Plasmodium falciparum infections are associated with agglutinating antibodies to parasite-infected erythrocyte surface antigens among healthy Kenyan children.* J Infect Dis, 2002. **185**(11): p. 1688-91.

59. Bull, P.C. and K. Marsh, *The role of antibodies to Plasmodium falciparum-infected-erythrocyte surface antigens in naturally acquired immunity to malaria.* Trends Microbiol, 2002. **10**(2): p. 55-8.

60. Bunnag, D., C. Viravan, S. Looareesuwan, J. Karbwang, and T. Harinasuta, *Clinical trial of artesunate and artemether on multidrug resistant falciparum malaria in Thailand. A preliminary report.* Southeast Asian J Trop Med Public Health, 1991. **22**(3): p. 380-5.

61. Bunnag, D., C. Viravan, S. Looareesuwan, J. Karbwang, and T. Harinasuta, *Double blind randomised clinical trial of oral artesunate at once or twice daily dose in falciparum malaria.* Southeast Asian J Trop Med Public Health, 1991. **22**(4): p. 539-43.

62. Bunnag, D., C. Viravan, S. Looareesuwan, J. Karbwang, and T. Harinasuta, *Double blind randomised clinical trial of two different regimens of oral artesunate in falciparum malaria.* Southeast Asian J Trop Med Public Health, 1991. **22**(4): p. 534-8.

63. Butcher, G.A., R.E. Sinden, and O. Billker, *Plasmodium berghei: infectivity of mice to Anopheles stephensi mosquitoes.* Exp Parasitol, 1996. **84**(3): p. 371-9.

64. Butler, A.R., S. Khan, and E. Ferguson, *A brief history of malaria chemotherapy.* J R Coll Physicians Edinb, 2010. **40**(2): p. 172-7.

65. Butler, N.S., A.M. Vaughan, J.T. Harty, and S.H.I. Kappe, *Whole parasite vaccination approaches for prevention of malaria infection.* Trends in Immunology. **33**(5): p. 247-254.

66. Bwijo, B., M.H. Alin, N. Abbas, W. Wernsdorfer, and A. Bjorkman, *Efficacy of artemisinin and mefloquine combinations against Plasmodium falciparum. In vitro simulation of in vivo pharmacokinetics.* Trop Med Int Health, 1997. **2**(5): p. 461-7.

67. Cadigan, F.C., Jr. and V. Chaicumpa, *Plasmodium falciparum in the white-handed gibbon: protection afforded by previous infection with homologous and heterologous strains obtained in Thailand.* Mil Med, 1969. **134**(10): p. 1135-9.

68. Cadigan, F.C., Jr., R.O. Spertzel, V. Chaicumpan, and S. Puhomchareon, *Plasmodium falciparum in non-human primates (macaque monkeys).* Mil Med, 1966. **131**(9): p. Suppl:959-60.

69. Cai, L., X. Li, and M. Ghosh, *Global dynamics of a mathematical model for HTLV-I infection of CD4+ T-cells.* Applied Mathematical Modelling, 2011. **35**(7): p. 3587-3595.

70. Cambie, G., F. Verdier, C. Gaudebout, F. Clavier, and H. Ginsburg, *The pharmacokinetics of chloroquine in healthy and Plasmodium chabaudi-infected mice: implications for chronotherapy.* Parasite, 1994. **1**(3): p. 219-26.

71. Canfield C. J., Pudney M., and Gutteridge W. E., *Interactions of Atovaquone with Other Antimalarial Drugs against Plasmodium falciparum in Vitro.* Experimental Parasitology, 1995. **80**(3): p. 373-381.

72. Carlton, J.M., K. Hayton, P.V. Cravo, and D. Walliker, *Of mice and malaria mutants: unravelling the genetics of drug resistance using rodent malaria models.* Trends Parasitol, 2001. **17**(5): p. 236-42.

73. Carson, E.R., C. Cobelli, and L. Finkelstein, *Mathematical Modeling of Metabolic and Endocrine Systems*. 1983, New York: Wiley.

74. Carter, R. and C.L. Diggs, *Plasmodia of rodents*, in *Parasitic Protozoa*. 1977. p. 359-465.

75. Carter, R. and K.N. Mendis, *Evolutionary and historical aspects of the burden of malaria.* Clin Microbiol Rev, 2002. **15**(4): p. 564-94.

76. Castro Sanchez, A.Y., M. Aerts, Z. Shkedy, P. Vickerman, F. Faggiano, G. Salamina, and N. Hens, *A mathematical model for HIV and hepatitis C co-infection and its assessment from a statistical perspective.* Epidemics, 2013. **5**(1): p. 56-66.

77. Cavanagh, D.R., I.M. Elhassan, C. Roper, V.J. Robinson, H. Giha, A.A. Holder, L. Hviid, T.G. Theander, D.E. Arnot, and J.S. McBride, *A longitudinal study of type-specific antibody responses to Plasmodium falciparum merozoite surface protein-1 in an area of unstable malaria in Sudan.* J Immunol, 1998. **161**(1): p. 347-59.

78. CDC. *The History of Malaria, an Ancient Disease*. 2014 November 2012 [cited 2014.

79. Celluzzi, C.M., P.L. Liem, T. van de Wiel, and W.M. Eling, *Attenuated immunogenic parasites are essential in the transfer of immunity to virulent Plasmodium berghei.* Immunology, 1995. **85**(3): p. 509-15.

80. Charles, L., *Field trials with chlorproguanil in the prophylaxis of malaria in Ghana.* Bulletin of the World Health Organization, 1961. **24**(4-5): p. 457.

81. Chawira, A., D. Warhurst, and W. Peters, *Qinghaosu resistance in rodent malaria.* Trans R Soc Trop Med Hyg, 1986. **80**: p. 477-480.

82. Chawira, A., D. Warhurst, B.L. Robinson, and W. Peters, *The effect of combinations of qinghaosu (artemisinin) with standard antimalarial drugs in the suppressive treatment of malaria in mice.* Trans R Soc Trop Med Hyg, 1987. **81**: p. 554-558.

83. Chawira, A.N. and D.C. Warhurst, *The effect of artemisinin combined with standard antimalarials against chloroquine-sensitive and chloroquine-resistant strains of Plasmodium falciparum in vitro.* J Trop Med Hyg, 1987. **90**(1): p. 1-8.

84. Chitnis, N., A. Schapira, D.L. Smith, T. Smith, S.I. Hay, and R. Steketee, *Mathematical modelling to support malaria control and elimination.* 2010.

85. Chotivanich, K., R. Udomsangpetch, A. Dondorp, T. Williams, B. Angus, J.A. Simpson, S. Pukrittayakamee, S. Looareesuwan, C.I. Newbold, and N.J. White, *The mechanisms of parasite clearance after antimalarial treatment of Plasmodium falciparum malaria.* J Infect Dis, 2000. **182**(2): p. 629-33.

86. Chotivanich, K., R. Udomsangpetch, R. McGready, S. Proux, P. Newton, S. Pukrittayakamee, S. Looareesuwan, and N.J. White, *Central role of the spleen in malaria parasite clearance.* J Infect Dis, 2002. **185**(10): p. 1538-41.

87. Chretien, J.P., M. Fukuda, and H. Noedl, *Improving surveillance for antimalarial drug resistance.* JAMA, 2007. **297**(20): p. 2278-81.

88. Cigel, F., J. Batchelder, J.M. Burns, Jr., D. Yanez, H. van der Heyde, D.D. Manning, and W.P. Weidanz, *Immunity to blood-stage murine*

malarial parasites is MHC class II dependent. Immunol Lett, 2003. **89**(2-3): p. 243-9.

89. Coatney, G.R., *Pitfalls in a discovery: the chronicle of chloroquine.* Am J Trop Med Hyg, 1963. **12**: p. 121-8.

90. Cobelli, C. and E. Carson, *Chapter 1 - An Introduction to Modelling Methodology*, in *Modeling Methodology for Physiology and Medicine*, E.C. Cobelli, Editor. 2001, Academic Press: San Diego. p. 1-13.

91. Cobelli, C., E.R. Carson, L. Finkelstein, and M.S. Leaning, *Validation of simple and complex models in physiology and medicine.* Am J Physiol, 1984. **246**(2 Pt 2): p. R259-66.

92. Coen, P.G., *How mathematical models have helped to improve understanding the epidemiology of infection.* Early Human Development, 2007. **83**(3): p. 141-148.

93. Cohen, J.M., D.L. Smith, C. Cotter, A. Ward, G. Yamey, O.J. Sabot, and B. Moonen, *Malaria resurgence: a systematic review and assessment of its causes.* Malar J, 2012. **11**: p. 122.

94. Coleman, R.E., J. Sattabongkot, S. Promstaporm, N. Maneechai, B. Tippayachai, A. Kengluecha, N. Rachapaew, G. Zollner, R.S. Miller, J.A. Vaughan, K. Thimasarn, and B. Khuntirat, *Comparison of PCR and microscopy for the detection of asymptomatic malaria in a Plasmodium falciparum/vivax endemic area in Thailand.* Malar J, 2006. **5**: p. 121.

95. Conway, D.J., D.R. Cavanagh, K. Tanabe, C. Roper, Z.S. Mikes, N. Sakihama, K.A. Bojang, A.M. Oduola, P.G. Kremsner, D.E. Arnot, B.M. Greenwood, and J.S. McBride, *A principal target of human immunity to malaria identified by molecular population genetic and immunological analyses.* Nat Med, 2000. **6**(6): p. 689-92.

96. Cox-Singh, J., T.M. Davis, K.S. Lee, S.S. Shamsul, A. Matusop, S. Ratnam, H.A. Rahman, D.J. Conway, and B. Singh, *Plasmodium knowlesi malaria in humans is widely distributed and potentially life threatening.* Clin Infect Dis, 2008. **46**(2): p. 165-71.

97. Cox, F., *Major animal models in malaria research: Rodent*. Malaria Principles and Practice of Malariology, ed. W. Wernsdorfer and I. McGregor. Vol. 2. 1988, New York: Churchill Livingstone. 1503-1543.

98. Cox, F.E., *History of the discovery of the malaria parasites and their vectors.* Parasit Vectors, 2010. **3**(1): p. 5.

99. Craig, A.G., G.E. Grau, C. Janse, J.W. Kazura, D. Milner, J.W. Barnwell, G. Turner, J. Langhorne, and M. participants of the Hinxton Retreat

meeting on Animal Models for Research on Severe, *The role of animal models for research on severe malaria.* PLoS Pathog, 2012. **8**(2): p. e1002401.

100. Curd, F.H., D.G. Davey, and F.L. Rose, *Studies on synthetic antimalarial drugs; biological methods.* Ann Trop Med Parasitol, 1945. **39**: p. 139-56.

101. Davey, D.G., *Chapter 12*, in *Experimental Chemotherapy*, R.J. Schnitzer and F. Hawking, Editors. 1963, Academic Press: New York.

102. Davis, T.M., H.A. Karunajeewa, and K.F. Ilett, *Artemisinin-based combination therapies for uncomplicated malaria.* Med J Aust, 2005. **182**(4): p. 181-5.

103. Davis, T.M., S. Krishna, S. Looareesuwan, W. Supanaranond, S. Pukrittayakamee, K. Attatamsoonthorn, and N.J. White, *Erythrocyte sequestration and anemia in severe falciparum malaria. Analysis of acute changes in venous hematocrit using a simple mathematical model.* J Clin Invest, 1990. **86**(3): p. 793-800.

104. Davis, T.M. and R.B. Martin, *Clearance of young parasite forms following treatment of falciparum malaria in humans: comparison of three simple mathematical models.* Epidemiol Infect, 1997. **119**(1): p. 61-9.

105. Day, N., T. Pham, T. Phan, X. Dinh, P. Pham, V. Ly, T. Tran, T. Nguyen, D. Bethell, H. Nguyan, and N. White, *Clearance kinetics of parasites and pigment-containing leukocytes in severe malaria.* Blood, 1996. **88**(12): p. 4694-4700.

106. de Vries, P.J. and T.K. Dien, *Clinical pharmacology and therapeutic potential of artemisinin and its derivatives in the treatment of malaria.* Drugs, 1996. **52**(6): p. 818-36.

107. De Vries, P.J., K.D. Tran, X.K. Nguyen, B. Le Nguyen, T.Y. Pham, D.D. Dao, C.J. Van Boxtel, and P.A. Kager, *The pharmacokinetics of a single dose of artemisinin in patients with uncomplicated falciparum malaria.* Am J Trop Med Hyg, 1997. **56**(5): p. 503-7.

108. Deharo, E., F. Coquelin, A.G. Chabaud, and I. Landau, *The erythrocytic schizogony of two synchronized strains of plasmodium berghei, NK65 and ANKA, in normocytes and reticulocytes.* Parasitol Res, 1996. **82**(2): p. 178-82.

109. Delves, M., D. Plouffe, C. Scheurer, S. Meister, S. Wittlin, E.A. Winzeler, R.E. Sinden, and D. Leroy, *The activities of current antimalarial drugs on the life cycle stages of Plasmodium: a comparative study with human and rodent parasites.* PLoS Med, 2012. **9**(2): p. e1001169.

110. Desjardins, R.E., E.B. Doberstein, and W.H. Wernsdorfer, *The treatment and prophylaxis of malaria*, in *Malaria: Principles and Practice of Malariology*, W.H. Wernsdorfer and I. McGregor, Editors. 1988, Churchill Livingstone: London. p. 827-823.

111. Dhangadamajhi, G., S.K. Kar, and M.R. Ranjit, *High prevalence and gender bias in distribution of Plasmodium malariae infection in central east-coast India.* Trop Biomed, 2009. **26**(3): p. 326-33.

112. Diebner, H.H., M. Eichner, L. Molineaux, W.E. Collins, G.M. Jeffery, and K. Dietz, *Modelling the transition of asexual blood stages of Plasmodium falciparum to gametocytes.* J Theor Biol, 2000. **202**(2): p. 113-27.

113. Dietz, K., *Mathematical models for transmission and control of malaria*, in *Malaria*, W.H. Wernsdorfer and I. McGregor, Editors. 1988, Churchill Livingstone. p. 1091-1133.

114. Dondorp, A.M., F. Nosten, P. Yi, D. Das, A.P. Phyo, J. Tarning, K.M. Lwin, F. Ariey, W. Hanpithakpong, S.J. Lee, P. Ringwald, K. Silamut, M. Imwong, K. Chotivanich, P. Lim, T. Herdman, S.S. An, S. Yeung, P. Singhasivanon, N.P. Day, N. Lindegardh, D. Socheat, and N.J. White, *Artemisinin resistance in Plasmodium falciparum malaria.* N Engl J Med, 2009. **361**(5): p. 455-67.

115. Dondorp, A.M., S. Yeung, L. White, C. Nguon, N.P. Day, D. Socheat, and L. von Seidlein, *Artemisinin resistance: current status and scenarios for containment.* Nat Rev Microbiol, 2010. **8**(4): p. 272-80.

116. Dreyer, A.M., H. Matile, P. Papastogiannidis, J. Kamber, P. Favuzza, T.S. Voss, S. Wittlin, and G. Pluschke, *Passive immunoprotection of Plasmodium falciparum-infected mice designates the CyRPA as candidate malaria vaccine antigen.* J Immunol, 2012. **188**(12): p. 6225-37.

117. Dye, C. and G. Hasibeder, *Population dynamics of mosquito-borne disease: effects of flies which bite some people more frequently than others.* Trans R Soc Trop Med Hyg, 1986. **80**(1): p. 69-77.

118. Earle, W.C. and M. Perez, *Enumeration of Parasites in the Blood of Malarial Patients.* The Journal of Laboratory and Clinical Medicine, 1931: p. 1124-1130.

119. Engwerda, C.R., G. Minigo, F.H. Amante, and J.S. McCarthy, *Experimentally induced blood stage malaria infection as a tool for clinical research.* Trends Parasitol, 2012. **28**(11): p. 515-21.

120. Etlinger, H.M., E.P. Heimer, A. Trzeciak, A.M. Felix, and D. Gillessen, *Assessment in mice of a synthetic peptide-based vaccine against the*

sporozoite stage of the human malaria parasite, P. falciparum. Immunology, 1988. **64**(3): p. 551-8.

121. Eyles, D.E. and M.D. Young, *The duration of untreated or inadequately treated Plasmodium falciparum infections in the human host.* J Natl Malar Soc, 1951. **10**(4): p. 327-36.

122. Fairhurst, R.M., *Transgenic parasites: improving our understanding of innate immunity to malaria.* Cell Host Microbe, 2007. **2**(2): p. 75-6.

123. Fairhurst, R.M., G.M. Nayyar, J.G. Breman, R. Hallett, J.L. Vennerstrom, S. Duong, P. Ringwald, T.E. Wellems, C.V. Plowe, and A.M. Dondorp, *Artemisinin-resistant malaria: research challenges, opportunities, and public health implications.* Am J Trop Med Hyg, 2012. **87**(2): p. 231-41.

124. Favre, N., C. Da Laperousaz, B. Ryffel, N.A. Weiss, B.A. Imhof, W. Rudin, R. Lucas, and P.F. Piguet, *Role of ICAM-1 (CD54) in the development of murine cerebral malaria.* Microbes Infect, 1999. **1**(12): p. 961-8.

125. Feachem, R. and O. Sabot, *A new global malaria eradication strategy.* The Lancet. **371**(9624): p. 1633-1635.

126. Field, J.W., *Blood examination and prognosis in acute falciparum malaria.* Trans R Soc Trop Med Hyg, 1949. **43**(1): p. 33-48.

127. Fivelman, Q.L., J.C. Walden, P.J. Smith, P.I. Folb, and K.I. Barnes, *The effect of artesunate combined with standard antimalarials against chloroquine-sensitive and chloroquine-resistant strains of Plasmodium falciparum in vitro.* Trans R Soc Trop Med Hyg, 1999. **93**(4): p. 429-32.

128. Flegg, J.A., P.J. Guerin, N.J. White, and K. Stepniewska, *Standardizing the measurement of parasite clearance in falciparum malaria: the parasite clearance estimator.* Malar J, 2011. **10**: p. 339.

129. Fletcher, K.A. and H.M. Gilles, *The Chemical Pathology of Malaria*, in *Malaria:principles and practice of malariology*, W.H. Wernsdorfer and I. McGregor, Editors. 1988, Churchill Livingstone: Edinburgh. p. 647-671.

130. Francis, N. and D.A. Warrell, *Pathology and pathophysiology of human malaria*, in *Bruce-Chwatt's Essential Malariology*, H.M. Gilles and D.A. Warrell, Editors. 1993, Edward Arnold: London. p. 50-59.

131. Franke-Fayard, B., A.P. Waters, and C.J. Janse, *Real-time in vivo imaging of transgenic bioluminescent blood stages of rodent malaria parasites in mice.* Nat Protoc, 2006. **1**(1): p. 476-85.

132. Fried, M., F. Nosten, A. Brockman, B.J. Brabin, and P.E. Duffy, *Maternal antibodies block malaria.* Nature, 1998. **395**(6705): p. 851-2.

133. Galinski, M.R. and J.W. Barnwell, *Chapter 5 - Nonhuman Primate Models for Human Malaria Research*, in *Nonhuman Primates in Biomedical Research (Second Edition)*, C.R.A.M.T. Morris, Editor. 2012, Academic Press: Boston. p. 299-323.

134. Gallup, J.L. and J.D. Sachs, *The economic burden of malaria.* Am J Trop Med Hyg, 2001. **64**(1-2 Suppl): p. 85-96.

135. Garnham, P., *Rodent species of malaria parasites*, in *Malaria parasites and other haemosporidia*, P. Garnham, Editor. 1966, Blackwell: Oxford. p. 431-475.

136. Genton, B., V. D'Acremont, L. Rare, K. Baea, J.C. Reeder, M.P. Alpers, and I. Muller, *Plasmodium vivax and mixed infections are associated with severe malaria in children: a prospective cohort study from Papua New Guinea.* PLoS Med, 2008. **5**(6): p. e127.

137. Gething, P.W., A.P. Patil, D.L. Smith, C.A. Guerra, I.R. Elyazar, G.L. Johnston, A.J. Tatem, and S.I. Hay, *A new world malaria map: Plasmodium falciparum endemicity in 2010.* Malar J, 2011. **10**: p. 378.

138. Gibbons, P.L., K.T. Batty, P.H.R. Barrett, T.M.E. Davis, and K.F. Ilett, *Development of a pharmacodynamic model of murine malaria and antimalarial treatment with dihydroartemisinin.* International Journal for Parasitology, 2007. **37**(14): p. 1569-1576.

139. Gil, V.S., M.C. Ferreira, F.S. d'Alva, J.A. d'Abreu, I.M. Will, M.L. Gomes, F. Castelli, W.R. Taylor, P. Olliaro, and U. D'Alessandro, *Efficacy of artesunate plus chloroquine for uncomplicated malaria in children in Sao Tome and Principe: a double-blind, randomized, controlled trial.* Trans R Soc Trop Med Hyg, 2003. **97**(6): p. 703-6.

140. Gilles, H.M., *Diagnostic Methods in Malaria*, in *Bruce-Chwatt's Essential Malariology*, H.M. Gilles and D.A. Warrell, Editors. 1993, Edward Arnold: London. p. 78-95.

141. Ginsburg, H., *Should chloroquine be laid to rest?* Acta Trop, 2005. **96**(1): p. 16-23.

142. Giusti, P., B.C. Urban, G. Frascaroli, L. Albrecht, A. Tinti, M. Troye-Blomberg, and S. Varani, *Plasmodium falciparum-Infected erythrocytes and β-hematin induce partial maturation of human dendritic cells and increase their migratory ability in response to lymphoid chemokines.* Infection and immunity, 2011. **79**(7): p. 2727-2736.

143. Gobburu, J.V.S. and W.J. Jusko, *Role of dosage regimen in controlling indirect pharmacodynamic responses.* Advanced Drug Delivery Reviews, 2001. **46**(1–3): p. 45-57.

144. Gomes-Santos, C.S., M.A. Itoe, C. Afonso, R. Henriques, R. Gardner, N. Sepulveda, P.D. Simoes, H. Raquel, A.P. Almeida, L.F. Moita, F. Frischknecht, and M.M. Mota, *Highly dynamic host actin reorganization around developing Plasmodium inside hepatocytes.* PLoS One, 2012. **7**(1): p. e29408.

145. Gordi, T., R. Xie, N.V. Huong, D.X. Huong, M.O. Karlsson, and M. Ashton, *A semiphysiological pharmacokinetic model for artemisinin in healthy subjects incorporating autoinduction of metabolism and saturable first-pass hepatic extraction.* Br J Clin Pharmacol, 2005. **59**(2): p. 189-98.

146. Gould, D.J., F.C. Cadigan, and R.A. Ward, *Falciparum malaria: transmission to the gibbon by Anopheles balabacensis.* Science, 1966. **153**(3742): p. 1384.

147. Gravenor, M.B., A.L. Lloyd, P.G. Kremsner, M.A. Missinou, M. English, K. Marsh, and D. Kwiatkowski, *A model for estimating total parasite load in falciparum malaria patients.* J Theor Biol, 2002. **217**(2): p. 137-48.

148. Gravenor, M.B., A.R. Mclean, and D. Kwiatkowski, *The regulation of malaria parasitaemia: parameter estimates for a population model.* Parasitology, 1995. **110**(02): p. 115-122.

149. Greenwood, B., *Can malaria be eliminated?* Transactions of the Royal Society of Tropical Medicine and Hygiene, 2009. **103**(1, Supplement): p. S2-S5.

150. Greenwood, B., K. Marsh, and R. Snow, *Why do some African children develop severe malaria?* Parasitol Today, 1991. **7**(10): p. 277-81.

151. Greenwood, B.M. and J.R. Armstrong, *Comparison of two simple methods for determining malaria parasite density.* Trans R Soc Trop Med Hyg, 1991. **85**(2): p. 186-8.

152. Group, Q.A.C.R., *Antimalaria studies on Qinghaosu.* Chin Med J (Engl), 1979. **92**(12): p. 811-6.

153. Guerin, P.J., S.J. Bates, and C.H. Sibley, *Global resistance surveillance: ensuring antimalarial efficacy in the future.* Curr Opin Infect Dis, 2009. **22**(6): p. 593-600.

154. Guerin, P.J., P. Olliaro, F. Nosten, P. Druilhe, R. Laxminarayan, F. Binka, W.L. Kilama, N. Ford, and N.J. White, *Malaria: current status of control,*

diagnosis, treatment, and a proposed agenda for research and development. The Lancet Infectious Diseases, 2002. **2**(9): p. 564-573.

155. Guerra, C.A., R.W. Snow, and S.I. Hay, *Defining the global spatial limits of malaria transmission in 2005.* Adv Parasitol, 2006. **62**: p. 157-79.

156. Guerra, C.A., R.W. Snow, and S.I. Hay, *A global assessment of closed forests, deforestation and malaria risk.* Ann Trop Med Parasitol, 2006. **100**(3): p. 189-204.

157. Guerra, C.A., R.W. Snow, and S.I. Hay, *Mapping the global extent of malaria in 2005.* Trends Parasitol, 2006. **22**(8): p. 353-8.

158. Gupta, S., N. Ferguson, and R. Anderson, *Chaos, persistence, and evolution of strain structure in antigenically diverse infectious agents.* Science, 1998. **280**(5365): p. 912-5.

159. Gupta, S., R.W. Snow, C.A. Donnelly, K. Marsh, and C. Newbold, *Immunity to non-cerebral severe malaria is acquired after one or two infections.* Nat Med, 1999. **5**(3): p. 340-3.

160. Gupta, S., M.M. Thapar, S.T. Mariga, W.H. Wernsdorfer, and A. Bjorkman, *Plasmodium falciparum: in vitro interactions of artemisinin with amodiaquine, pyronaridine, and chloroquine.* Exp Parasitol, 2002. **100**(1): p. 28-35.

161. Hamon, J., J. Mouchet, G. Chauvet, and R. Lumaret, *[Review of 14 Years of Malaria Control in the French-Speaking Countries of Tropical Africa and in Madagascar. Considerations on the Persistence of Transmission and Future Prospects].* Bull Soc Pathol Exot Filiales, 1963. **56**: p. 933-71.

162. Hand, C.C. and S.R. Meshnick, *Is chloroquine making a comeback?* J Infect Dis, 2011. **203**(1): p. 11-2.

163. Harinasuta, T. and D. Bunnag, *The clinical features of malaria*, in *Malaria*, W.H. Wernsdorfer and I. McGregor, Editors. 1988, Churchill Livingstone: Edinburgh. p. 709-734.

164. Harinasuta, T., P. Suntharasamai, and C. Viravan, *Chloroquine-resistant falciparum malaria in Thailand.* Lancet, 1965. **2**(7414): p. 657-60.

165. Hastings, I.M. and U. D'Alessandro, *Modelling a predictable disaster: the rise and spread of drug-resistantmalaria.* Parasitol Today, 2000. **16**(8): p. 340-7.

166. Haynes, R.K., K.W. Cheu, K.Y. Li, M.M. Tang, H.N. Wong, M.J. Chen, Z.F. Guo, Z.H. Guo, P. Coghi, and D. Monti, *A partial convergence in action of methylene blue and artemisinins: antagonism with chloroquine,*

a reversal with verapamil, and an insight into the antimalarial activity of chloroquine. ChemMedChem, 2011. **6**(9): p. 1603-15.

167. Haynes, R.K. and S. Krishna, *Artemisinins: activities and actions.* Microbes Infect, 2004. **6**(14): p. 1339-46.

168. Hearn, J., N. Rayment, D.N. Landon, D.R. Katz, and J.B. de Souza, *Immunopathology of cerebral malaria: morphological evidence of parasite sequestration in murine brain microvasculature.* Infect Immun, 2000. **68**(9): p. 5364-76.

169. Hermsen, C., T. van de Wiel, E. Mommers, R. Sauerwein, and W. Eling, *Depletion of CD4+ or CD8+ T-cells prevents Plasmodium berghei induced cerebral malaria in end-stage disease.* Parasitology, 1997. **114 (Pt 1)**: p. 7-12.

170. Hien, T.T., *An overview of the clinical use of artemisinin and its derivatives in the treatment of falciparum malaria in Viet Nam.* Transactions of the Royal Society of Tropical Medicine and Hygiene, 1994. **88**(1): p. S7-S8.

171. Hien, T.T. and N.J. White, *Qinghaosu.* Lancet, 1993. **341**(8845): p. 603-8.

172. Hoffman, S.L., D.L. Doolan, M. Sedegah, R. Wang, L.F. Scheller, A. Kumar, W.R. Weiss, T.P. Le, D.M. Klinman, P. Hobart, J.A. Norman, and R.C. Hedstrom, *Toward clinical trials of DNA vaccines against malaria.* Immunol Cell Biol, 1997. **75**(4): p. 376-81.

173. Hollingdale, M.R., J.L. Leef, M. McCullough, and R.L. Beaudoin, *In vitro cultivation of the exoerythrocytic stage of Plasmodium berghei from sporozoites.* Science, 1981. **213**(4511): p. 1021-2.

174. Hommel, M., *Diagnostic methods in malaria*, in *Essential Malarialology*, D.A. Warrell and H.M. Gilles, Editors. 2002, Arnold: London.

175. Hoshen, M.B., R. Heinrich, W.D. Stein, and H. Ginsburg, *Mathematical modelling of the within-host dynamics of Plasmodium falciparum.* Parasitology, 2000. **121 (Pt 3)**: p. 227-35.

176. Hoshen, M.B., K. Na-Bangchang, W.D. Stein, and H. Ginsburg, *Mathematical modelling of the chemotherapy of Plasmodium falciparum malaria with artesunate: postulation of 'dormancy', a partial cytostatic effect of the drug, and its implication for treatment regimens.* Parasitology, 2000. **121 (Pt 3)**: p. 237-46.

177. Hoshen, M.B., W.D. Stein, and H. Ginsburg, *Mathematical modelling of malaria chemotherapy: combining artesunate and mefloquine.* Parasitology, 2002. **124**(Pt 1): p. 9-15.

178. Hoshen, M.B., W.D. Stein, and H.D. Ginsburg, *Pharmacokinetic-pharmacodynamic modelling of the antimalarial activity of mefloquine.* Parasitology, 2001. **123**(4): p. 337-346.

179. Hsu, D.Y. and Q.M. Geiman, *Synergistic effect of Haemobartonella muris on Plasmodium berghei in white rats.* Am J Trop Med Hyg, 1952. **1**(5): p. 747-60.

180. Ibezim, E.C. and U. Odo, *Current trends in malarial chemotherapy.* African Journal of Biotechnology, 2008. **7**(4).

181. Inaba, H. and H. Sekine, *A mathematical model for Chagas disease with infection-age-dependent infectivity.* Mathematical Biosciences, 2004. **190**(1): p. 39-69.

182. Ishih, A., T. Suzuki, F.W. Muregi, K. Matsui, and M. Terada, *Chloroquine efficacy in Plasmodium berghei NK65-infected ICR mice, with reference to the influence of initial parasite load and starting day of drug administration on the outcome of treatment.* Southeast Asian J Trop Med Public Health, 2006. **37**(1): p. 13-7.

183. Jacob, S.W. and E.E. Rosenbaum, *The Toxicology of Dimethyl Sulfoxide (DMSO).* Headache: The Journal of Head and Face Pain, 1966. **6**(3): p. 127-136.

184. Janse, C.J., J. Ramesar, F.M. van den Berg, and B. Mons, *Plasmodium berghei: in vivo generation and selection of karyotype mutants and non-gametocyte producer mutants.* Exp Parasitol, 1992. **74**(1): p. 1-10.

185. Janse, C.J. and A.P. Waters. *The Plasmodium berghei research model of malaria*. [homepage on the internet] 2006 2006 March 5 [cited 2006 December 11]; Available from: http://www.lumc.nl/1040/research/malaria/model.html.

186. Janse, C.J., A.P. Waters, J. Kos, and C.B. Lugt, *Comparison of in vivo and in vitro antimalarial activity of artemisinin, dihydroartemisinin and sodium artesunate in the Plasmodium berghei-rodent model.* Int J Parasitol, 1994. **24**(4): p. 589-594.

187. Jeffery, G.M. and D.E. Eyles, *The duration in the human host of infections with a Panama strain of Plasmodium falciparum.* Am J Trop Med Hyg, 1954. **3**(2): p. 219-24.

188. Jeffery, G.M., M.D. Young, R.W. Burgess, and D.E. Eyles, *Early activity in sporozoite-induced Plasmodium falciparum infections.* Ann Trop Med Parasitol, 1959. **53**(1): p. 51-8.

189. Jian-ping, S., D. Socheat, and S. Seila, *A comparative study of dihydroartemisinin compounds in treatment of uncomplicated falciparum malaria in Kampong of Cambodia.* Chinese Journal of Integrative Medicine, 2003. **9**(1): p. 31-34.

190. Jiang, J.B., *Plasmodium: experimental animals for human malaria and research needs. A review.* Exp Parasitol, 1978. **46**(2): p. 339-52.

191. Johnston, G.L., D.L. Smith, and D.A. Fidock, *Malaria's missing number: calculating the human component of R0 by a within-host mechanistic model of Plasmodium falciparum infection and transmission.* PLoS Comput Biol, 2013. **9**(4): p. e1003025.

192. Jongwutiwes, S., C. Putaporntip, T. Iwasaki, T. Sata, and H. Kanbara, *Naturally acquired Plasmodium knowlesi malaria in human, Thailand.* Emerg Infect Dis, 2004. **10**(12): p. 2211-3.

193. Kakkilaya, B.S. *Malaria Website*. 2011. http://www.malariasite.com/malaria-parasites/

194. Kaliste, E., M. Linnainmaa, T. Meklin, E. Torvinen, and A. Nevalainen, *The bedding of laboratory animals as a source of airborne contaminants.* Laboratory Animals, 2004. **38**(1): p. 25-37.

195. Kamiyama, T., M. Tatsumi, J. Matsubara, K. Yamamoto, Z. Rubio, G. Cortes, and H. Fujii, *Manifestation of cerebral malaria-like symptoms in the WM/Ms rat infected with Plasmodium berghei strain NK65.* J Parasitol, 1987. **73**(6): p. 1138-45.

196. Karbwang, J., K. Na-Bangchang, A. Thanavibul, D. Bunnag, T. Chongsuphajaisiddhi, and T. Harinasuta, *Comparison of oral artesunate and quinine plus tetracycline in acute uncomplicated falciparum malaria.* Bull World Health Organ, 1994. **72**(2): p. 233-8.

197. Karunajeewa, H.A., S. Salman, I. Mueller, F. Baiwog, S. Gomorrai, I. Law, M. Page-Sharp, S. Rogerson, P. Siba, K.F. Ilett, and T.M. Davis, *Pharmacokinetics of chloroquine and monodesethylchloroquine in pregnancy.* Antimicrob Agents Chemother, 2010. **54**(3): p. 1186-92.

198. Kawamoto, F., *Rapid diagnosis of malaria by fluorescence microscopy with light microscope and interference filter.* Lancet, 1991. **337**(8735): p. 200-2.

199. Khan, Z.M. and J.P. Vanderberg, *Role of host cellular response in differential susceptibility of nonimmunized BALB/c mice to Plasmodium berghei and Plasmodium yoelii sporozoites.* Infect Immun, 1991. **59**(8): p. 2529-34.

200. Killick-Kendrick, R., *Malaria parasites of Thamnomys rutilans (Rodentia, Muridae) in Nigeria.* Bull World Health Organ, 1968. **38**(5): p. 822-4.

201. Killick-Kendrick, R., *Taxonomy, Zoography and Evolution*, in *Rodent Malaria*, R. Killick-Kendrick and W. Peters, Editors. 1978, Academic Press: London. p. 1-52.

202. Kim, S., S. Choe, J. Kim, S. Nam, Y. Shin, and S. Lee, *What Does a Mathematical Model Tell About the Impact of Reinfection in Korean Tuberculosis Infection?* Osong Public Health and Research Perspectives, 2014. **5**(1): p. 40-45.

203. Kitchen, S.F. and P. Putnam, *Observations on the Mechanism of the Parasite Cycle in Falciparum Malaria.* The American Journal of Tropical Medicine and Hygiene, 1942. **s1-22**(4): p. 361-386.

204. Knight, D.J. and P. Williamson, *The antimalarial activity of N-benzyl-oxydihydrotriazines. IV. The development of resistance to BRL 6231 (4,6-diamino-1,2-dihyydro-2-,2-dimethyl-1-(2,4,5-trichloropropyloxy)-1,3,5 triazine hydrochloride) by Plasmodium berghei.* Ann Trop Med Parasitol, 1982. **76**(1): p. 9-14.

205. Knudsen, A.B. and R. Sloof, *Vector-borne disease problems in rapid urbanization: new approaches to vector control.* Bulletin of World Health Organization, 1992. **70**: p. 1-6.

206. Koella, J.C., *On the use of mathematical models of malaria transmission.* Acta Trop, 1991. **49**(1): p. 1-25.

207. Kremsner, P.G. and S. Krishna, *Antimalarial combinations.* Lancet, 2004. **364**(9430): p. 285-94.

208. Kumar, A., S.B. Katiyar, A. Agarwal, and P.M. Chauhan, *Perspective in antimalarial chemotherapy.* Curr Med Chem, 2003. **10**(13): p. 1137-50.

209. Kwiatkowski, D. and M. Nowak, *Periodic and chaotic host-parasite interactions in human malaria.* Proc Natl Acad Sci U S A, 1991. **88**(12): p. 5111-3.

210. Kyes, S., P. Horrocks, and C. Newbold, *Antigenic variation at the infected red cell surface in malaria.* Annu Rev Microbiol, 2001. **55**: p. 673-707.

211. Landau, I., *[Description of Plasmodium Chabaudi N. Sp., Parasite of African Rodents].* C R Hebd Seances Acad Sci, 1965. **260**: p. 3758-61.

212. Landau, I. and Y. Boulard, *Life Cycles and Morphology*, in *Rodent Malaria*, R. Killick-Kendrick and W. Peters, Editors. 1978, Academic Press: London. p. 53-84.

213. Landau, I. and P. Gautret, *Animal models: rodents*, in *Malaria: Parasite Biology, Pathogenesis and Protection.*, I.W. Sherman, Editor. 1998, American Society for Microbiology: Washington, DC. p. 401-417.

214. Landau, I. and R. Killick-Kendrick, *Rodent plasmodia of the Republique Centrafricaine: the sporogony and tissue stages of Plasmodium chabaudi and P. berghei yoelii.* Trans R Soc Trop Med Hyg, 1966. **60**(5): p. 633-49.

215. Langhorne, J., P. Buffet, M. Galinski, M. Good, J. Harty, D. Leroy, M.M. Mota, E. Pasini, L. Renia, E. Riley, M. Stins, and P. Duffy, *The relevance of non-human primate and rodent malaria models for humans.* Malar J, 2011. **10**(1): p. 23.

216. Langhorne, J., S.J. Quin, and L.A. Sanni, *Mouse models of blood-stage malaria infections: immune responses and cytokines involved in protection and pathology.* Chem Immunol, 2002. **80**: p. 204-28.

217. Laufer, M.K., P.C. Thesing, F.K. Dzinjalamala, O.M. Nyirenda, R. Masonga, M.B. Laurens, A. Stokes-Riner, T.E. Taylor, and C.V. Plowe, *A longitudinal trial comparing chloroquine as monotherapy or in combination with artesunate, azithromycin or atovaquone-proguanil to treat malaria.* PLoS One, 2012. **7**(8): p. e42284.

218. Laufer, M.K., P.C. Thesing, N.D. Eddington, R. Masonga, F.K. Dzinjalamala, S.L. Takala, T.E. Taylor, and C.V. Plowe, *Return of chloroquine antimalarial efficacy in Malawi.* N Engl J Med, 2006. **355**(19): p. 1959-66.

219. Le, T.A., T.M. Davis, Q.B. Tran, V.P. Nguyen, and K.A. Trinh, *Delayed parasite clearance in a splenectomized patient with falciparum malaria who was treated with artemisinin derivatives.* Clin Infect Dis, 1997. **25**(4): p. 923-5.

220. Lee, K.S., J. Cox-Singh, and B. Singh, *Morphological features and differential counts of Plasmodium knowlesi parasites in naturally acquired human infections.* Malar J, 2009. **8**: p. 73.

221. Lee, S.J., R. McGready, C. Fernandez, K. Stepniewska, M.K. Paw, S.J. Viladpai-nguen, K.L. Thwai, L. Villegas, P. Singhasivanon, B.M. Greenwood, N.J. White, and F. Nosten, *Chloroquine pharmacokinetics in pregnant and nonpregnant women with vivax malaria.* Eur J Clin Pharmacol, 2008. **64**(10): p. 987-92.

222. Li, G., X. Guo, K. Arnold, H. Jian, and L. Fu, *Randomised comparative study of mefloquine, qinghaosu, and pyrimethamine-sulfadoxine in patients with falciparum malaria.* The Lancet, 1984. **324**(8416): p. 1360-1361.

223. Li, G.Q., X.B. Guo, R. Jin, Z.C. Wang, H.X. Jian, and Z.Y. Li, *Clinical studies on treatment of cerebral malaria with qinghaosu and its derivatives.* J Tradit Chin Med, 1982. **2**(2): p. 125-30.

224. Li, Q., L.H. Xie, Y. Si, E. Wong, R. Upadhyay, D. Yanez, and P.J. Weina, *Toxicokinetics and hydrolysis of artelinate and artesunate in malaria-infected rats.* Int J Toxicol, 2005. **24**(4): p. 241-50.

225. Li, Q.G., J.O. Peggins, L.L. Fleckenstein, K. Masonic, M.H. Heiffer, and T.G. Brewer, *The pharmacokinetics and bioavailability of dihydroartemisinin, arteether, artemether, artesunic acid and artelinic acid in rats.* The Journal of Pharmacy and Pharmacology, 1998. **50**(2): p. 173-182.

226. Li, Y., J.M. Wu, F. Shan, G.S. Wu, J. Ding, D. Xiao, J.X. Han, G. Atassi, S. Leonce, D.H. Caignard, and P. Renard, *Synthesis and cytotoxicity of dihydroartemisinin ethers containing cyanoarylmethyl group.* Bioorg Med Chem, 2003. **11**(6): p. 977-84.

227. Lin, A.J., L.Q. Li, D.L. Klayman, C.F. George, and J.L. Flippen-Anderson, *Antimalarial activity of new water-soluble dihydroartemisinin derivatives. 3. Aromatic amine analogues.* J Med Chem, 1990. **33**(9): p. 2610-4.

228. Liu, J., S. Modrek, R.D. Gosling, and R.G. Feachem, *Malaria eradication: is it possible? Is it worth it? Should we do it?* Lancet Glob Health, 2013. **1**(1): p. e2-3.

229. Loeb, F.F., W.M. Clark, G.R. Coatney, and et al., *Activity of a new antimalarial agent, chloroquine (sn 7618): Statement approved by the board for coordination of malarial studies.* Journal of the American Medical Association, 1946. **130**(16): p. 1069-1070.

230. Looareesuwan, S., T.M. Davis, S. Pukrittayakamee, W. Supanaranond, V. Desakorn, K. Silamut, S. Krishna, S. Boonamrung, and N.J. White, *Erythrocyte survival in severe falciparum malaria.* Acta Trop, 1991. **48**(4): p. 263-70.

231. Looareesuwan, S., M. Ho, Y. Wattanagoon, N.J. White, D.A. Warrell, D. Bunnag, T. Harinasuta, and D.J. Wyler, *Dynamic alteration in splenic function during acute falciparum malaria.* N Engl J Med, 1987. **317**(11): p. 675-679.

232. Looareesuwan, S., S. Vanijanonta, C. Viravan, P. Wilairatana, P. Charoenlarp, and M. Andrial, *Randomized trial of mefloquine alone and artesunate followed by mefloquine for the treatment of acute uncomplicated falciparum malaria.* Ann Trop Med Parasitol, 1994. **88**(2): p. 131-6.

233. Looareesuwan, S., C. Viravan, S. Vanijanonta, P. Wilairatana, P. Charoenlarp, C.J. Canfield, and D.E. Kyle, *Randomized trial of mefloquine-doxycycline, and artesunate-doxycycline for treatment of acute uncomplicated falciparum malaria.* Am J Trop Med Hyg, 1994. **50**(6): p. 784-9.

234. Looareesuwan, S., C. Viravan, H.K. Webster, D.E. Kyle, D.B. Hutchinson, and C.J. Canfield, *Clinical studies of atovaquone, alone or in combination with other antimalarial drugs, for treatment of acute uncomplicated malaria in Thailand.* Am J Trop Med Hyg, 1996. **54**(1): p. 62-6.

235. Looareesuwan, S., P. Wilairatana, S. Vanijanonta, P. Pitisuttithum, Y. Ratanapong, and M. Andrial, *Monotherapy with sodium artesunate for uncomplicated falciparum malaria in Thailand: a comparison of 5- and 7-day regimens.* Acta Trop, 1997. **67**(3): p. 197-205.

236. Macdonald, G., *The Epidemiology and Control of Malaria*. 1957, Oxford: University Press.

237. Mackenstedt, U., C.R. Brockelman, H. Mehlhorn, and W. Raether, *Comparative morphology of human and animal malaria parasites. I. Host-parasite interface.* Parasitol Res, 1989. **75**(7): p. 528-35.

238. Malaria, R.B., *The Global Malaria Action Plan*. 2008, Roll Back Malaria Partnership: Geneva.

239. Mandal, S., R.R. Sarkar, and S. Sinha, *Mathematical models of malaria--a review.* Malar J, 2011. **10**: p. 202.

240. Marsh, K., *Clinical Features of Malaria*, in *Malaria - Molecualr and Clinical Aspects*, M. Wahlgren and P. Perlmann, Editors. 1999, Harwood Academic. p. 87-118.

241. Martin, R.E., R.V. Marchetti, A.I. Cowan, S.M. Howitt, S. Broer, and K. Kirk, *Chloroquine transport via the malaria parasite's chloroquine resistance transporter.* Science, 2009. **325**(5948): p. 1680-2.

242. Martinelli, A., R. Moreira, and P.V. Ravo, *Malaria combination therapies: advantages and shortcomings.* Mini Rev Med Chem, 2008. **8**(3): p. 201-12.

243. Matteelli, A., F. Castelli, and S. Caligaris, *Life cycle of malaria parasites*, in *Handbook of Malaria Infection in the Tropics*, G. Carosi and F. Castelli, Editors. 1997, Associazione Italiana 'Amici di R Follereau' Organizzazione per la Cooperazione Sanitaria Internazionale: Bologna. p. 17-23.

244. McCarthy, J.S., S. Sekuloski, P.M. Griffin, S. Elliott, N. Douglas, C. Peatey, R. Rockett, P. O'Rourke, L. Marquart, C. Hermsen, S. Duparc, J. Mohrle, K.R. Trenholme, and A.J. Humberstone, *A pilot randomised trial of induced blood-stage Plasmodium falciparum infections in healthy volunteers for testing efficacy of new antimalarial drugs.* PLoS One, 2011. **6**(8): p. e21914.

245. McKenzie, F.E., *Why model malaria?* Parasitol Today, 2000. **16**(12): p. 511-6.

246. McKenzie, F.E. and W.H. Bossert, *The dynamics of Plasmodium falciparum blood-stage infection.* J Theor Biol, 1997. **188**(1): p. 127-40.

247. McKenzie, S.B., *Textbook of Hematology*. 2nd ed. Vol. 16. 1996, Baltimore: Williams & Wilkins.

248. McPhee, S.J., M. Papadakis, and M.W. Rabow, *CURRENT Medical Diagnosis and Treatment 2011*. 2010: McGraw-Hill Education.

249. Menard, R., A.A. Sultan, C. Cortes, R. Altszuler, M.R. van Dijk, C.J. Janse, A.P. Waters, R.S. Nussenzweig, and V. Nussenzweig, *Circumsporozoite protein is required for development of malaria sporozoites in mosquitoes.* Nature, 1997. **385**(6614): p. 336-40.

250. Mercado, T.I. and G.R. Coatney, *The course of the blood-induced Plasmodium berghei infection in white mice.* J Parasitol, 1951. **37**(5 1): p. 479-82.

251. Mideo, N., D.A. Kennedy, J.M. Carlton, J.A. Bailey, J.J. Juliano, and A.F. Read, *Ahead of the curve: next generation estimators of drug resistance in malaria infections.* Trends Parasitol, 2013. **29**(7): p. 321-8.

252. Millington, O.R., C. Di Lorenzo, R.S. Phillips, P. Garside, and J.M. Brewer, *Suppression of adaptive immunity to heterologous antigens during Plasmodium infection through hemozoin-induced failure of dendritic cell function.* Journal of biology, 2006. **5**(2): p. 5.

253. Millington, O.R., V.B. Gibson, C.M. Rush, B.H. Zinselmeyer, R.S. Phillips, P. Garside, and J.M. Brewer, *Malaria impairs T cell clustering and immune priming despite normal signal 1 from dendritic cells.* PLoS Pathog, 2007. **3**(10): p. 1380-7.

254. Milne, L.M., M.S. Kyi, P.L. Chiodini, and D.C. Warhurst, *Accuracy of routine laboratory diagnosis of malaria in the United Kingdom.* J Clin Pathol, 1994. **47**(8): p. 740-2.

255. Miyagami, T., I. Igarshi, and M. Suzuki, *Plasmodium berghei: long lasting immunity induced by a permanent attenuated mutant.* Zentralbl Bakteriol Mikrobiol Hyg A, 1987. **264**(3-4): p. 502-12.

256. Molineaux, L., H.H. Diebner, M. Eichner, W.E. Collins, G.M. Jeffery, and K. Dietz, *Plasmodium falciparum parasitaemia described by a new mathematical model.* Parasitology, 2001. **122**(Pt 4): p. 379-91.

257. Molyneux, D.H., K. Floyd, G. Barnish, and E.M. Fevre, *Transmission control and drug resistance in malaria: a crucial interaction.* Parasitol Today, 1999. **15**(6): p. 238-40.

258. Mons, B., *Intra erythrocytic differentiation of Plasmodium berghei.* Acta Leiden, 1986. **54**: p. 1-124.

259. Moody, A., *Rapid diagnostic tests for malaria parasites.* Clin Microbiol Rev, 2002. **15**(1): p. 66-78.

260. Moon, D.K., V. Singhal, N. Kumar, T.A. Shapiro, and G.H. Posner, *Antimalarial Preclinical Drug Development: A Single Oral Dose of A 5-Carbon-linked Trioxane Dimer Plus Mefloquine Cures Malaria-Infected Mice.* Drug Dev Res, 2009. **71**(1): p. 76-81.

261. Moore, B.R., M. Page-Sharp, J.R. Stoney, K.F. Ilett, J.D. Jago, and K.T. Batty, *Pharmacokinetics, pharmacodynamics, and allometric scaling of chloroquine in a murine malaria model.* Antimicrob Agents Chemother, 2011. **55**(8): p. 3899-907.

262. Mushtaque, M. and Shahjahan, *Reemergence of chloroquine (CQ) analogs as multi-targeting antimalarial agents: A review.* European Journal of Medicinal Chemistry, 2015. **90**(0): p. 280-295.

263. Mwai, L., E. Ochong, A. Abdirahman, S.M. Kiara, S. Ward, G. Kokwaro, P. Sasi, K. Marsh, S. Borrmann, M. Mackinnon, and A. Nzila, *Chloroquine resistance before and after its withdrawal in Kenya.* Malar J, 2009. **8**: p. 106.

264. Naing, C., K. Aung, D.K. Win, and M.J. Wah, *Efficacy and safety of chloroquine for treatment in patients with uncomplicated Plasmodium vivax infections in endemic countries.* Trans R Soc Trop Med Hyg, 2010. **104**(11): p. 695-705.

265. Najera, J.A., M. Gonzalez-Silva, and P.L. Alonso, *Some lessons for the future from the Global Malaria Eradication Programme (1955-1969).* PLoS Med, 2011. **8**(1): p. e1000412.

266. Ndungu, F.M., B.C. Urban, K. Marsh, and J. Langhorne, *Regulation of immune response by Plasmodium-infected red blood cells.* Parasite Immunol, 2005. **27**(10-11): p. 373-84.

267. Neill, A.L. and N.H. Hunt, *Pathology of fatal and resolving Plasmodium berghei cerebral malaria in mice.* Parasitology, 1992. **105 (Pt 2)**: p. 165-75.

268. Newton, P. and N. White, *Malaria: New developments in treatment and prevention.* Annual Review of Medicine, 1999. **50**: p. 179-92.

269. Nguyen, P.H., N. Day, T.D. Pram, D.J. Ferguson, and N.J. White, *Intraleucocytic malaria pigment and prognosis in severe malaria.* Trans R Soc Trop Med Hyg, 1995. **89**(2): p. 200-4.

270. Noedl, H., *Artemisinin resistance: how can we find it?* Trends Parasitol, 2005. **21**(9): p. 404-5.

271. Noedl, H., Y. Se, K. Schaecher, B.L. Smith, D. Socheat, M.M. Fukuda, and C. Artemisinin Resistance in Cambodia 1 Study, *Evidence of artemisinin-resistant malaria in western Cambodia.* N Engl J Med, 2008. **359**(24): p. 2619-20.

272. Nosten, F., M. van Vugt, R. Price, C. Luxemburger, K.L. Thway, A. Brockman, R. McGready, F. ter Kuile, S. Looareesuwan, and N.J. White, *Effects of artesunate-mefloquine combination on incidence of Plasmodium falciparum malaria and mefloquine resistance in western Thailand: a prospective study.* Lancet, 2000. **356**(9226): p. 297-302.

273. Nussenzweig, V. and R.S. Nussenzweig, *Rationale for the development of an engineered sporozoite malaria vaccine.* Adv Immunol, 1989. **45**: p. 283-334.

274. Obua, C., U. Hellgren, M. Ntale, L.L. Gustafsson, J.W. Ogwal-Okeng, T. Gordi, and M. Jerling, *Population pharmacokinetics of chloroquine and sulfadoxine and treatment response in children with malaria: suggestions for an improved dose regimen.* Br J Clin Pharmacol, 2008. **65**(4): p. 493-501.

275. Ochola, L.B., P. Vounatsou, T. Smith, M.L.H. Mabaso, and C. Newton, *The reliability of diagnostic techniques in the diagnosis and management of malaria in the absence of a gold standard.* The Lancet Infectious Diseases, 2006. **6**(9): p. 582-588.

276. Opsenica, I., N. Terzic, D. Opsenica, G. Angelovski, M. Lehnig, P. Eilbracht, B. Tinant, Z. Juranic, K.S. Smith, Y.S. Yang, D.S. Diaz, P.L. Smith, W.K. Milhous, D. Dokovic, and B.A. Solaja, *Tetraoxane*

antimalarials and their reaction with Fe(II). J Med Chem, 2006. **49**(13): p. 3790-9.

277. Organization, W.H., *Roll Back Malaria Partnership - A Decade of Partnership and Results*. 2011, World Health Organization: Geneva.

278. Osdene, T.S., P.B. Russell, and L. Rane, *2,4,7-Triamino-6-ortho-substituted Arylpteridines. A New Series of Potent Antimalarial Agents.* J Med Chem, 1967. **10**(3): p. 431-4.

279. Packard, R.M., *'No other logical choice': global malaria eradication and the politics of international health in the post-war era.* Parassitologia, 1998. **40**(1-2): p. 217-29.

280. Packard, R.M., *The Making of a Tropical Disease: A Short History of Malaria*. 2007: Johns Hopkins University Press.

281. Patel, K., K.T. Batty, B.R. Moore, P.L. Gibbons, J.B. Bulitta, and C.M. Kirkpatrick, *Mechanism-based model of parasite growth and dihydroartemisinin pharmacodynamics in murine malaria.* Antimicrob Agents Chemother, 2013. **57**(1): p. 508-16.

282. Patz, J.A., T.K. Graczyk, N. Geller, and A.Y. Vittor, *Effects of environmental change on emerging parasitic diseases.* Int J Parasitol, 2000. **30**(12-13): p. 1395-405.

283. Pawelek, K.A., S. Liu, F. Pahlevani, and L. Rong, *A model of HIV-1 infection with two time delays: Mathematical analysis and comparison with patient data.* Mathematical Biosciences, 2012. **235**(1): p. 98-109.

284. Payne, D., *Did medicated salt hasten the spread of chloroquine resistance in< i> Plasmodium falciparum</i>?* Parasitology today, 1988. **4**(4): p. 112-115.

285. Pedroni, H.C., C.C. Bettoni, S.M. Spalding, and T. Dalla Costa, *Plasmodium berghei: development of an irreversible experimental malaria model in Wistar rats.* Exp Parasitol, 2006. **113**(3): p. 193-6.

286. Peters, W., *Drug resistance in Plasmodium berghei Vincke and Lips, 1948. I. Chloroquine resistance.* Experimental Parasitology, 1965. **17**(1): p. 80-89.

287. Peters, W., *Drug resistance in malaria--a perspective.* Trans R Soc Trop Med Hyg, 1969. **63**(1): p. 25-45.

288. Peters, W., *Malaria. Chemoprophylaxis and chemotherapy.* Br Med J, 1971. **2**(5753): p. 95-8.

289. Peters, W., *The chemotherapy of rodent malaria, XXII. The value of drug-resistant strains of P. berghei in screening for blood schizontocidal activity.* Ann Trop Med Parasitol, 1975. **69**(2): p. 155-71.

290. Peters, W., *Resistance of Human Malaria I, III and IV*, in *Chemotherapy and drug resistance in malaria*. 1987, Academic Press: London. p. 543-68, 593-658, 659-786.

291. Peters, W., S.L. Fleck, B.L. Robinson, L.B. Stewart, and C.W. Jefford, *The chemotherapy of rodent malaria. LX. The importance of formulation in evaluating the blood schizontocidal activity of some endoperoxide antimalarials.* Ann Trop Med Parasitol, 2002. **96**(6): p. 559-73.

292. Peters, W., Z.L. Li, B.L. Robinson, and D.C. Warhurst, *The chemotherapy of rodent malaria, XL. The action of artemisinin and related sesquiterpenes.* Ann Trop Med Parasitol, 1986. **80**(5): p. 483-9.

293. Peters, W. and B.L. Robinson, *Malaria*, in *Handbook of animal models of infection*, O. Zak and M. Sande, Editors. 1999, Academic Press: San Diego, CA. p. 757-773.

294. Peters, W. and B.L. Robinson, *The chemotherapy of rodent malaria. LVIII. Drug combinations to impede the selection of drug resistance, Part. 2: The new generation--artemisinin or artesunate with long-acting blood schizontocides.* Ann Trop Med Parasitol, 2000. **94**(1): p. 23-35.

295. Peters, W., B.L. Robinson, L.B. Stewart, and G.A. Butcher, *The chemotherapy of rodent malaria. LIX. Drug combinations to impede the selection of drug resistance, Part 3: Observations on cyproheptadine, an antihistaminic agent, with chloroquine.* Ann Trop Med Parasitol, 2000. **94**(7): p. 689-97.

296. Phillips, R.S., *Current status of malaria and potential for control.* Clin Microbiol Rev, 2001. **14**(1): p. 208-26.

297. Phu, N.H., P.Q. Tuan, N. Day, N.T. Mai, T.T. Chau, L.V. Chuong, D.X. Sinh, N.J. White, J. Farrar, and T.T. Hien, *Randomized controlled trial of artesunate or artemether in Vietnamese adults with severe falciparum malaria.* Malar J, 2010. **9**: p. 97.

298. Phyo, A.P., S. Nkhoma, K. Stepniewska, E.A. Ashley, S. Nair, R. McGready, C. ler Moo, S. Al-Saai, A.M. Dondorp, K.M. Lwin, P. Singhasivanon, N.P. Day, N.J. White, T.J. Anderson, and F. Nosten, *Emergence of artemisinin-resistant malaria on the western border of Thailand: a longitudinal study.* Lancet, 2012. **379**(9830): p. 1960-6.

299. Piguet, P.F., C. Da Laperrousaz, C. Vesin, F. Tacchini-Cottier, G. Senaldi, and G.E. Grau, *Delayed mortality and attenuated*

thrombocytopenia associated with severe malaria in urokinase- and urokinase receptor-deficient mice. Infect Immun, 2000. **68**(7): p. 3822-9.

300. Playfair, J.H., J.B. De Souza, and B.J. Cottrell, *Protection of mice against malaria by a killed vaccine: differences in effectiveness against P. yoelii and P. berghei.* Immunology, 1977. **33**(4): p. 507-15.

301. Plebanski, M. and A.V. Hill, *The immunology of malaria infection.* Curr Opin Immunol, 2000. **12**(4): p. 437-41.

302. Ploemen, I.H., M. Prudencio, B.G. Douradinha, J. Ramesar, J. Fonager, G.J. van Gemert, A.J. Luty, C.C. Hermsen, R.W. Sauerwein, F.G. Baptista, M.M. Mota, A.P. Waters, I. Que, C.W. Lowik, S.M. Khan, C.J. Janse, and B.M. Franke-Fayard, *Visualisation and quantitative analysis of the rodent malaria liver stage by real time imaging.* PLoS One, 2009. **4**(11): p. e7881.

303. Plowe, C.V., *The evolution of drug-resistant malaria.* Trans R Soc Trop Med Hyg, 2009. **103 Suppl 1**: p. S11-4.

304. Porter, R.S. and J.L. Kaplan. *Malaria*. The Merck Manual Online 2014.

305. Price, R.N., *Artemisinin drugs: novel antimalarial agents.* Expert Opin Investig Drugs, 2000. **9**(8): p. 1815-27.

306. Price, R.N., F. Nosten, C. Luxemburger, F.O. ter Kuile, L. Paiphun, T. Chongsuphajaisiddhi, and N.J. White, *Effects of artemisinin derivatives on malaria transmissibility.* Lancet, 1996. **347**(9016): p. 1654-8.

307. Prokopev, D.I., *Resistance of Malaria Parasites to Drugs. Report of a Who Scientific Group.* World Health Organ Tech Rep Ser, 1965. **296**: p. 1-65.

308. Quintana, M., R. Piper, H.L. Boling, M. Makler, C. Sherman, E. Gill, E. Fernandez, and S. Martin, *Malaria diagnosis by dipstick assay in a Honduran population with coendemic Plasmodium falciparum and Plasmodium vivax.* Am J Trop Med Hyg, 1998. **59**(6): p. 868-71.

309. Rabinovich, S.A., *[Morphology of the strains of Plasmodium berghei berghei with "acquired" resistance to antimalarial drugs of different chemical groups. I. Morphologic features of strains resistant to derivatives of 4-aminoquinoline and diaminopyrimidine].* Med Parazitol (Mosk), 1969. **38**(3): p. 287-94.

310. Rahman, S.M.A., N.K. Vaidya, and X. Zou, *Impact of Tenofovir gel as a PrEP on HIV infection: A mathematical model.* Journal of Theoretical Biology, 2014. **347**(0): p. 151-159.

311. Rajanikanth, M., K.P. Madhusudanan, and R.C. Gupta, *Liquid chromatographic-mass spectrometric method for the determination of alpha-,beta-arteether in rat serum.* J Chromatogr B Analyt Technol Biomed Life Sci, 2003. **783**(2): p. 391-9.

312. Ramaiya, M.L., V.R. Kamath, and D.M. Renapurkar, *Long-term in vitro cultivation of Plasmodium berghei.* Int J Parasitol, 1987. **17**(7): p. 1329-31.

313. Ramakrishnan, S.P. and P. Satya, *Studies on Plasmodium berghei n. sp. Vincke and Lips, 1948. I. Variations in susceptibility in albino mice.* Indian J Malariol, 1950. **4**(3): p. 361-7.

314. Ramjanee, S., J.S. Robertson, B. Franke-Fayard, R. Sinha, A.P. Waters, C.J. Janse, Y. Wu, A.M. Blagborough, A. Saul, and R.E. Sinden, *The use of transgenic Plasmodium berghei expressing the Plasmodium vivax antigen P25 to determine the transmission-blocking activity of sera from malaria vaccine trials.* Vaccine, 2007. **25**(5): p. 886-94.

315. Randall, L.M., F.H. Amante, Y. Zhou, A.C. Stanley, A. Haque, F. Rivera, K. Pfeffer, S. Scheu, G.R. Hill, K. Tamada, and C.R. Engwerda, *Cutting edge: selective blockade of LIGHT-lymphotoxin beta receptor signaling protects mice from experimental cerebral malaria caused by Plasmodium berghei ANKA.* J Immunol, 2008. **181**(11): p. 7458-62.

316. Rodhain, J., *[Plasmodium vinckei n. sp.; second plasmodium parasite of wild rodents at Katange].* Ann Soc Belg Med Trop (1920), 1952. **32**(3): p. 275-9.

317. Rodhain, J. and I. Vincke, *[Experiment in development of Plasmodium berghei, Vincke and Lips in Anopheles maculipennis (var. atroparvus)].* Ann Soc Belg Med Trop (1920), 1951. **31**(2): p. 297-301.

318. Roestenberg, M., G.A. O'Hara, C.J.A. Duncan, J.E. Epstein, N.J. Edwards, A. Scholzen, A.J.A.M. van der Ven, C.C. Hermsen, A.V.S. Hill, and R.W. Sauerwein, *Comparison of Clinical and Parasitological Data from Controlled Human Malaria Infection Trials.* PLoS ONE, 2012. **7**(6): p. e38434.

319. Rogerson, S.J. and R. Carter, *Severe vivax malaria: newly recognised or rediscovered.* PLoS Med, 2008. **5**(6): p. e136.

320. Rollo, I.M., *Daraprim-experimental chemotherapy.* Trans R Soc Trop Med Hyg, 1952. **46**(5): p. 474-84; discussion, 498-508.

321. Rosenthal, P.J., *Antimalarial Chemotherapy: Mechanisms of Action, Resistance, and New Directions in Drug Discovery*. 2001: Humana Press.

322. Rosenthal, P.J., *Antimalarial drug discovery: old and new approaches.* J Exp Biol, 2003. **206**(Pt 21): p. 3735-44.

323. Ross, R., *On some Peculiar Pigmented Cells Found in Two Mosquitos Fed on Malarial Blood.* Br Med J, 1897. **2**(1929): p. 1786-8.

324. Ross, R., *SOME A PRIORI PATHOMETRIC EQUATIONS.* Br Med J, 1915. **1**(2830): p. 546-7.

325. Ross, R. and D. Thomson, *Some Enumerative Studies on Malarial Fever.* Proceedings of the Royal Society of London. Series B, Containing Papers of a Biological Character, 1910. **83**(562): p. 159-173.

326. Ross, R. and D. Thomson, *Some Enumerative Studies on Malarial Fever.* Roy. Soc. Proc., 1910. **82**: p. 159-173.

327. Rowe, R.C., P.J. Sheskey, and S.C. Owen, *Handbook of Pharmaceutical Excipients*. 5th ed. 2005, London: Pharmaceutical Press.

328. Rudin, W., H.P. Eugster, G. Bordmann, J. Bonato, M. Muller, M. Yamage, and B. Ryffel, *Resistance to cerebral malaria in tumor necrosis factor-alpha/beta-deficient mice is associated with a reduction of intercellular adhesion molecule-1 up-regulation and T helper type 1 response.* Am J Pathol, 1997. **150**(1): p. 257-66.

329. Rudin, W., V. Quesniaux, N. Favre, and G. Bordmann, *Malaria toxins from P. chabaudi chabaudi AS and P. berghei ANKA cause dyserythropoiesis in C57BL/6 mice.* Parasitology, 1997. **115 (Pt 5)**: p. 467-74.

330. Sabarinath, S., K.P. Madhusudanan, and R.C. Gupta, *Pharmacokinetics of the diastereomers of arteether, a potent antimalarial drug, in rats.* Biopharm Drug Dispos, 2005. **26**(6): p. 211-23.

331. Sachs, J. and P. Malaney, *The economic and social burden of malaria.* Nature, 2002. **415**(6872): p. 680-5.

332. Sadun, E.H., J.S. Williams, F.C. Meroney, and G. Hutt, *Pathophysiology of Plasmodium berghei Infection in Mice.* Exp Parasitol, 1965. **17**: p. 277-286.

333. Santana-Morales, M.A., R.N. Afonso-Lehmann, M.A. Quispe, F. Reyes, P. Berzosa, A. Benito, B. Valladares, and E. Martinez-Carretero, *Microscopy and molecular biology for the diagnosis and evaluation of malaria in a hospital in a rural area of Ethiopia.* Malar J, 2012. **11**: p. 199.

334. Sauerwein, R.W., M. Roestenberg, and V.S. Moorthy, *Experimental human challenge infections can accelerate clinical malaria vaccine development.* Nat Rev Immunol, 2011. **11**(1): p. 57-64.

335. Sautet, J., J. Aldighieri, and R. Aldighieri, *[Studies on the experimental production of resistance to various antimalarial products in a strain of Plasmodium berghei].* Bull Soc Pathol Exot Filiales, 1959. **52**: p. 331-45.

336. Schaer, J., S.L. Perkins, J. Decher, F.H. Leendertz, J. Fahr, N. Weber, and K. Matuschewski, *High diversity of West African bat malaria parasites and a tight link with rodent Plasmodium taxa.* Proc Natl Acad Sci U S A, 2013. **110**(43): p. 17415-9.

337. Schwarte, S., P. Ringwald, K. Mendis, and A. Bosman, *Regulatory action needed to stop the sale of oral artemisinin-based monotherapy*, in *WHO Drug Information Essential Medicines*. 2010, WHO: Geneva.

338. Sengers, R.C., C.R. Jerusalem, and W.H. Doesburg, *Murine malaria. IV. Disturbed immunological responsiveness during Plasmodium berghei infection.* Exp Parasitol, 1971. **30**(1): p. 41-53.

339. Sengers, R.C., P.L. Liem, and W.H. Doesburg, *Murine malaria. II. Relationship between number of inoculated parasites (Plasmodium berghei) and survival time.* Exp Parasitol, 1971. **29**(1): p. 98-102.

340. Sengers, R.C., P.L. Liem, and P. van Elteren, *Murine malaria. I. Measurement of the mean rate of increase in vivo of Plasmodium berghei.* Exp Parasitol, 1971. **29**(1): p. 94-7.

341. Sharma, A. and W.J. Jusko, *Characteristics of indirect pharmacodynamic models and applications to clinical drug responses.* Br J Clin Pharmacol, 1998. **45**(3): p. 229-39.

342. Sherman, I.W., *A brief history of malaria and discovery of the parasite's life cycle*, in *Malaria: parasite biology, pathogenesis and protection*, I.W. Sherman, Editor. 1998, ASM Press: Washington DC.

343. Shretta, R. and P. Yadav, *Stabilizing supply of artemisinin and artemisinin-based combination therapy in an era of wide-spread scale-up.* Malar J, 2012. **11**: p. 399.

344. Shultz, L.D., F. Ishikawa, and D.L. Greiner, *Humanized mice in translational biomedical research.* Nat Rev Immunol, 2007. **7**(2): p. 118-30.

345. Shute, G.T., *The microscopic diagnosis of malaria.*, in *Malaria: principles and practices of malariology*, W.H. Wernsdorfer and I. McGregor, Editors. 1988, Churchill Livingstone: Edinburgh.

346. Sibley, C.H. and R.N. Price, *Monitoring antimalarial drug resistance: Applying lessons learned from the past in a fast-moving present.* Int J Parasitol Drugs Drug Resist, 2012. **2**: p. 126-33.

347. Simpson, J.A., E.R. Watkins, R.N. Price, L. Aarons, D.E. Kyle, and N.J. White, *Mefloquine pharmacokinetic-pharmacodynamic models: implications for dosing and resistance.* Antimicrob Agents Chemother, 2000. **44**(12): p. 3414-3424.

348. Sinden, R. and H.M. Gilles, *The Malaria Parasites*, in *Essential Malariology*, D.A. Warrell and H.M. Gilles, Editors. 2002, Arnold: London. p. 8-34.

349. Sinden, R.E. and P.C. Garnham, *A comparative study on the ultrastructure of Plasmodium sporozoites within the oocyst and salivary glands, with particular reference to the incidence of the micropore.* Trans R Soc Trop Med Hyg, 1973. **67**(5): p. 631-7.

350. Singer, I., *The Course of Infection with Plasmodium Berghei in Inbred CF 1 Mice.* Journal of Infectious Diseases, 1954. **94**: p. 237-240.

351. Singh, B., L. Kim Sung, A. Matusop, A. Radhakrishnan, S.S. Shamsul, J. Cox-Singh, A. Thomas, and D.J. Conway, *A large focus of naturally acquired Plasmodium knowlesi infections in human beings.* Lancet, 2004. **363**(9414): p. 1017-24.

352. Singh, B., B.P. Nayak, K.V. Rao, and P. Sharma, *Immune responses mediating survival of naive BALB/c mice experimentally infected with lethal rodent malaria parasite, Plasmodium yoelii nigeriensis.* Microbes Infect, 2000. **2**(5): p. 473-80.

353. Singh, N., A. Saxena, and N. Valecha, *Field evaluation of the ICT malaria P.f/P.v immunochromatographic test for diagnosis of Plasmodium falciparum and P.vivax infection in forest villages of Chhindwara, central India.* Trop Med Int Health, 2000. **5**(11): p. 765-70.

354. Sirima, S.B., A.B. Tiono, A. Konate, A. Diarra, F. Castelli, L. Pinoges, K. Mugittu, W.R. Taylor, and P.L. Olliaros, *Efficacy of artesunate plus chloroquine for the treatment of uncomplicated malaria in children in Burkina Faso: a double-blind, randomized, controlled trial.* Trans R Soc Trop Med Hyg, 2003. **97**(3): p. 345-9.

355. Slater, A.F., *Chloroquine: mechanism of drug action and resistance in Plasmodium falciparum.* Pharmacol Ther, 1993. **57**(2-3): p. 203-35.

356. Smith, T., B. Genton, K. Baea, N. Gibson, J. Taime, A. Narara, F. Al-Yaman, H.P. Beck, J. Hii, and M. Alpers, *Relationships between*

Plasmodium falciparum infection and morbidity in a highly endemic area. Parasitology, 1994. **109 (Pt 5)**: p. 539-49.

357. Sneader, W., *Drug Prototypes and Their Exploitation*. 1996: Wiley.

358. Snowden, F., *The Conquest of Malaria: Italy, 1900-1962*. 2006, Yale University Press.

359. Song, J., D. Socheat, B. Tan, S. Seila, Y. Xu, F. Ou, S. Sokunthea, L. Sophorn, C. Zhou, C. Deng, Q. Wang, and G. Li, *Randomized trials of artemisinin-piperaquine, dihydroartemisinin-piperaquine phosphate and artemether-lumefantrine for the treatment of multi-drug resistant falciparum malaria in Cambodia-Thailand border area.* Malar J, 2011. **10**: p. 231.

360. Sousa, M., A. Pozniak, and M. Boffito, *Pharmacokinetics and pharmacodynamics of drug interactions involving rifampicin, rifabutin and antimalarial drugs.* J Antimicrob Chemother, 2008. **62**(5): p. 872-8.

361. Sowunmi, A., E.O. Adewoye, G.O. Gbotsho, C.T. Happi, A. Sijuade, O.A. Folarin, T.M. Okuboyejo, and O.S. Michael, *Factors contributing to delay in parasite clearance in uncomplicated falciparum malaria in children.* Malar J, 2010. **9**: p. 53.

362. Srichaikul, T., *Hematologic changes in human malaria.* J Med Assoc Thai, 1973. **56**(11): p. 658-63.

363. Srichaikul, T., C. Pulket, T. Sirisatepisarn, and W. Prayoonwiwat, *Platelet dysfunction in malaria.* Southeast Asian J Trop Med Public Health, 1988. **19**(2): p. 225-33.

364. Srichaikul, T., P. Puwasatien, J. Karnjanajetanee, V.A. Bokisch, and P. Pawasatien, *Complement changes and disseminated intravascular coagulation in Plasmodium falciparum malaria.* Lancet, 1975. **1**(7910): p. 770-2.

365. Srinivasan, S., A.H. Moody, and P.L. Chiodini, *Comparison of blood-film microscopy, the OptiMAL dipstick, Rhodamine-123 fluorescence staining and PCR, for monitoring antimalarial treatment.* Ann Trop Med Parasitol, 2000. **94**(3): p. 227-32.

366. Srivastava, P., S.K. Puri, and V.C. Pandey, *Effect of Plasmodium berghei infection and antimalarial treatment on heme synthesis in mice.* Int J Parasitol, 1994. **24**(5): p. 677-9.

367. Stahel, E., P. Druilhe, and M. Gentilini, *Antagonism of chloroquine with other antimalarials.* Transactions of the Royal Society of Tropical Medicine and Hygiene, 1988. **82**(2): p. 221.

368. Stevenson, M.M. and E.M. Riley, *Innate immunity to malaria.* Nat Rev Immunol, 2004. **4**(3): p. 169-80.

369. Stoltzfus, R.J., F. Jalal, P.W. Harvey, and M.C. Nesheim, *Interactions between vitamin A deficiency and Plasmodium berghei infection in the rat.* The Journal of Nutrition, 1989. **119**(12): p. 2030-2037.

370. Stoney, J., *Chloroquine pharmacodynamics in a murine malaria model*, in *School of Pharmacy*. 2005, Curtin University: Perth, Western Australia.

371. Sultan, A.A., V. Thathy, T.F. de Koning-Ward, and V. Nussenzweig, *Complementation of Plasmodium berghei TRAP knockout parasites using human dihydrofolate reductase gene as a selectable marker.* Mol Biochem Parasitol, 2001. **113**(1): p. 151-6.

372. Sultan, A.A., V. Thathy, U. Frevert, K.J. Robson, A. Crisanti, V. Nussenzweig, R.S. Nussenzweig, and R. Menard, *TRAP is necessary for gliding motility and infectivity of plasmodium sporozoites.* Cell, 1997. **90**(3): p. 511-22.

373. Surrey, A.R. and H.F. Hammer, *Some 7-substituted 4-aminoquinoline derivatives.* J Am Chem Soc, 1946. **68**: p. 113-6.

374. Sutherland, C.J., C.J. Drakeley, U. Obisike, R. Coleman, M. Jawara, G.A.T. Targett, P. Milligan, M. Pinder, and G. Walraven, *The addition of artesunate to chloroquine for treatment of plasmodium falciparum malaria in gambian children delays, but does not prevent treatment failure.* The American Journal of Tropical Medicine and Hygiene, 2003. **69**(1): p. 19-25.

375. Talisuna, A.O., P. Bloland, and U. D'Alessandro, *History, dynamics, and public health importance of malaria parasite resistance.* Clin Microbiol Rev, 2004. **17**(1): p. 235-54.

376. Targett, G., C. Drakeley, M. Jawara, L. von Seidlein, R. Coleman, J. Deen, M. Pinder, T. Doherty, C. Sutherland, G. Walraven, and P. Milligan, *Artesunate reduces but does not prevent posttreatment transmission of Plasmodium falciparum to Anopheles gambiae.* J Infect Dis, 2001. **183**(8): p. 1254-9.

377. Tarning, J., I. Zongo, F.A. Some, N. Rouamba, S. Parikh, P.J. Rosenthal, W. Hanpithakpong, N. Jongrak, N.P. Day, N.J. White, F. Nosten, J.B. Ouedraogo, and N. Lindegardh, *Population pharmacokinetics and pharmacodynamics of piperaquine in children with uncomplicated falciparum malaria.* Clin Pharmacol Ther, 2012. **91**(3): p. 497-505.

378. Tarun, A.S., X. Peng, R.F. Dumpit, Y. Ogata, H. Silva-Rivera, N. Camargo, T.M. Daly, L.W. Bergman, and S.H. Kappe, *A combined*

transcriptome and proteome survey of malaria parasite liver stages. Proc Natl Acad Sci U S A, 2008. **105**(1): p. 305-10.

379. Taylor-Robinson, A.W., *Murine models of cerebral malaria: a qualified defence.* Parasitol Today, 1995. **11**(11): p. 407-9.

380. Taylor-Robinson, A.W., *Regulation of immunity to malaria: valuable lessons learned from murine models.* Parasitology Today, 1995. **11**(9): p. 334-342.

381. Taylor, J., E.S. Josephson, J. Greenberg, and G.R. Coatney, *The in vitro activity of certain antimalarials against erythrocytic forms of Plasmodium gallinaceum.* Am J Trop Med Hyg, 1952. **1**(1): p. 132-9.

382. ter Kuile, F., N.J. White, P. Holloway, G. Pasvol, and S. Krishna, *Plasmodium falciparum: in vitro studies of the pharmacodynamic properties of drugs used for the treatment of severe malaria.* Exp Parasitol, 1993. **76**(1): p. 85-95.

383. Thomé, R., S.C.P. Lopes, F.T.M. Costa, and L. Verinaud, *Chloroquine: Modes of action of an undervalued drug.* Immunology Letters, 2013. **153**(1–2): p. 50-57.

384. Thompson, P.E., B. Olszewski, A. Bayles, and J.A. Waitz, *Relations among antimalarial drugs: results of studies with cycloguanil-, sulfone-, or chloroquine-resistant Plasmodium berghei in mice.* Am J Trop Med Hyg, 1967. **16**(2): p. 133-45.

385. Thornley, S., C. Bullen, and M. Roberts, *Hepatitis B in a high prevalence New Zealand population: A mathematical model applied to infection control policy.* Journal of Theoretical Biology, 2008. **254**(3): p. 599-603.

386. Thurston, J.P., *The action of antimalarial drugs in mice infected with Plasmodium berghei.* Br J Pharmacol Chemother, 1950. **5**(3): p. 409-16.

387. Thurston, J.P., *Plasmodium berghei.* Experimental Parasitology, 1953. **2**(3): p. 311-332.

388. Tjitra, E., N.M. Anstey, P. Sugiarto, N. Warikar, E. Kenangalem, M. Karyana, D.A. Lampah, and R.N. Price, *Multidrug-resistant Plasmodium vivax associated with severe and fatal malaria: a prospective study in Papua, Indonesia.* PLoS Med, 2008. **5**(6): p. e128.

389. Tonkin, I.M. and F. Hawking, *The technique of testing chemotherapeutic action on plasmodium gallinaceum.* Br J Pharmacol Chemother, 1947. **2**(4): p. 221-33.

390. Trape, J.F., *The public health impact of chloroquine resistance in Africa.* Am J Trop Med Hyg, 2001. **64**(1-2 Suppl): p. 12-7.

391. Trape, J.F., G. Pison, M.P. Preziosi, C. Enel, A. Desgrees du Lou, V. Delaunay, B. Samb, E. Lagarde, J.F. Molez, and F. Simondon, *Impact of chloroquine resistance on malaria mortality.* C R Acad Sci III, 1998. **321**(8): p. 689-97.

392. Trauer, J.M., J.T. Denholm, and E.S. McBryde, *Construction of a mathematical model for tuberculosis transmission in highly endemic regions of the Asia-pacific.* Journal of Theoretical Biology, 2014. **358**(0): p. 74-84.

393. Treeratanapiboon, L., K. Psathaki, J. Wegener, S. Looareesuwan, H.J. Galla, and R. Udomsangpetch, *In vitro study of malaria parasite induced disruption of blood-brain barrier.* Biochem Biophys Res Commun, 2005. **335**(3): p. 810-8.

394. Tsibulsky, V.L. and Z. Amit, *Tolerance to effects of high doses of ethanol: 1. Lethal effects in mice.* Pharmacol Biochem Behav., 1993. **45**(2): p. 465-72.

395. Tumwiine, J., S. Luckhaus, J. Mugisha, and L. Luboobi, *An age-structured mathematical model for the within host dynamics of malaria and the immune system.* Journal of Mathematical Modelling and Algorithms, 2008. **7**(1): p. 79-97.

396. Tuon, F.F., J.L. Rocha, T.M. Leite, and C. Dias, *A simple mathematical model to determine the ideal empirical antibiotic therapy for bacteremic patients.* The Brazilian Journal of Infectious Diseases, 2014. **18**(4): p. 360-363.

397. Umotong, A.B., E.N. Ezedinachi, A.A. Okerengwo, E.A. Usanga, J.J. Udo, and A.I. Williams, *Correlation between in vivo and in vitro response of chloroquine-resistant Plasmodium falciparum in Calabar, south-eastern Nigeria.* Acta Trop, 1991. **49**(2): p. 119-25.

398. Urban, B.C., R. Ing, and M.M. Stevenson, *Early interactions between blood-stage plasmodium parasites and the immune system.* Curr Top Microbiol Immunol, 2005. **297**: p. 25-70.

399. van Agtmael, M.A., S. Cheng-Qi, J.X. Qing, R. Mull, and C.J. van Boxtel, *Multiple dose pharmacokinetics of artemether in Chinese patients with uncomplicated falciparum malaria.* Int J Antimicrob Agents, 1999. **12**(2): p. 151-8.

400. Van den Ende, J., G. Moorkens, A. Van Gompel, H. Demey, R. Lins, P. Maldague, E. Pelfrene, E. Van den Enden, H. Taelman, P. Van der

Stuyft, and et al., *Twelve patients with severe malaria treated with partial exchange transfusion. Comparison between mathematically predicted and observed effect on parasitaemia.* Trop Geogr Med, 1994. **46**(6): p. 340-5.

401. Varma, R., R. Kaushal, A. Junnarkar, G. Thomas, M. Naidu, P. Singh, R. Tripathi, and D. Shridhar, *Polysorbate 80: a pharmacological study.* Arzneimittel-Forschung, 1985. **35**(5): p. 804-8.

402. Vennerstrom, J.L., S. Arbe-Barnes, R. Brun, S.A. Charman, F.C. Chiu, J. Chollet, Y. Dong, A. Dorn, D. Hunziker, H. Matile, K. McIntosh, M. Padmanilayam, J. Santo Tomas, C. Scheurer, B. Scorneaux, Y. Tang, H. Urwyler, S. Wittlin, and W.N. Charman, *Identification of an antimalarial synthetic trioxolane drug development candidate.* Nature, 2004. **430**(7002): p. 900-4.

403. Venture, M.f.M., *Development of combination therapies for the treatment of uncomplicated Plasmodium falciparum malaria*. 2010, MEDICINES FOR MALARIA VENTURE (MMV): Geneva, Switzerland.

404. Vestergaard, L.S. and P. Ringwald, *Responding to the challenge of antimalarial drug resistance by routine monitoring to update national malaria treatment policies.* Am J Trop Med Hyg, 2007. **77**(6 Suppl): p. 153-9.

405. Vincke, I.H. and M. Lips, *Un nouveau plasmodium d'un ondeur sauvage du Congo (Plasmodium berghei n. sp.).* Ann Soc Belg Med Trop (1920), 1948. **28**(1): p. 97-104.

406. von Seidlein, L., M. Jawara, R. Coleman, T. Doherty, G. Walraven, and G. Targett, *Parasitaemia and gametocytaemia after treatment with chloroquine, pyrimethamine/sulfadoxine, and pyrimethamine/sulfadoxine combined with artesunate in young Gambians with uncomplicated malaria.* Trop Med Int Health, 2001. **6**(2): p. 92-8.

407. Waitz, J.A., A. Smith, A. Bayles, and P.E. Thompson, *Activity of chloroquine against Plasmodium berghei in mice both with and without previous exposure to chloroquine.* Am J Trop Med Hyg, 1967. **16**(1): p. 11-2.

408. Walliker, D., *The genetic basis of diversity in malaria parasites.* Adv Parasitol, 1983. **22**: p. 217-59.

409. Walliker, D., R. Carter, and S. Morgan, *Genetic recombination in malaria parasites.* Nature, 1971. **232**(5312): p. 561-2.

410. Ward, R.A. and F.C. Cadigan, Jr., *The development of erythrocytic stages of Plasmodium falciparum in the gibbon, Hylobates lar.* Mil Med, 1966. **131**(9): p. Suppl:944-51.

411. Warhurst, D.C. and J.E. Williams, *Laboratory diagnosis of malaria.* J Clin Pathol, 1996. **49**(7): p. 533-8.

412. Warrell, D.A., W.M. Watkins, and P.A. Winstanley, *Treatment and prevention of malaria*, in *Essential Malariology*, D.A. Warrell and H.M. Gilles, Editors. 2002, Arnold: London. p. 268-312.

413. Weiss, M.L., *Plasmodium berghei: Ectopic antibody synthesis in splenectomized rodents.* Experimental Parasitology, 1985. **59**(1): p. 108-117.

414. Wellems, T.E. and C.V. Plowe, *Chloroquine-resistant malaria.* J Infect Dis, 2001. **184**(6): p. 770-6.

415. Wernsdorfer, W.H., *Epidemiology of drug resistance in malaria.* Acta Trop, 1994. **56**(2-3): p. 143-56.

416. Wernsdorfer, W.H. and H. Noedl, *Molecular markers for drug resistance in malaria: use in treatment, diagnosis and epidemiology.* Curr Opin Infect Dis, 2003. **16**(6): p. 553-8.

417. Wernsdorfer, W.H. and D. Payne, *The dynamics of drug resistance in Plasmodium falciparum.* Pharmacol Ther, 1991. **50**(1): p. 95-121.

418. White, N., *Antimalarial drug resistance and combination chemotherapy.* Philos Trans R Soc Lond B Biol Sci, 1999. **354**(1384): p. 739-49.

419. White, N.J., *Antimalarial drug resistance: the pace quickens.* J Antimicrob Chemother, 1992. **30**(5): p. 571-85.

420. White, N.J., *Assessment of the pharmacodynamic properties of antimalarial drugs in vivo.* Antimicrob Agents Chemother, 1997. **41**(7): p. 1413-22.

421. White, N.J., *Delaying antimalarial drug resistance with combination chemotherapy.* Parassitologia, 1999. **41**(1-3): p. 301-8.

422. White, N.J., *The assessment of antimalarial drug efficacy.* Trends in Parasitology, 2002. **18**(10): p. 458-464.

423. White, N.J., *Pharmacokinetic and pharmacodynamic considerations in antimalarial dose optimization.* Antimicrob Agents Chemother, 2013. **57**(12): p. 5792-807.

424. White, N.J., D. Chapman, and G. Watt, *The effects of multiplication and synchronicity on the vascular distribution of parasites in falciparum malaria.* Trans R Soc Trop Med Hyg, 1992. **86**(6): p. 590-7.

425. White, N.J. and S. Krishna, *Treatment of malaria: some considerations and limitations of the current methods of assessment.* Trans R Soc Trop Med Hyg, 1989. **83**(6): p. 767-77.

426. White, N.J. and P. Olliaro, *Artemisinin and derivatives in the treatment of uncomplicated malaria.* Med Trop (Mars), 1998. **58**(3 Suppl): p. 54-6.

427. White, N.J., G.D. Turner, I.M. Medana, A.M. Dondorp, and N.P. Day, *The murine cerebral malaria phenomenon.* Trends Parasitol, 2010. **26**(1): p. 11-5.

428. White, N.J., D. Waller, J. Crawley, F. Nosten, D. Chapman, D. Brewster, and B.M. Greenwood, *Comparison of artemether and chloroquine for severe malaria in Gambian children.* Lancet, 1992. **339**(8789): p. 317-21.

429. Whittingham, D.G. and M.J. Wood, *Reproductive Physiology*, in *In The Mouse in Biomedical Research*, H.L. Foster, J.D. Small, and J.G. Fox, Editors. 1983 Academic Press: New York. p. 137-164.

430. WHO/UNICEF, *World Malaria Report 2009*. 2009, World Health Organization: Geneva.

431. WHO/UNICEF, *Basic Malaria Microscopy*. Edition 2 ed. 2010, Geneva Switzerland: World Health Organisation.

432. WHO/UNICEF, *Guidelines for the treatment of malaria.* 2010, World Health Organisation: Geneva, Switzerland.

433. WHO/UNICEF, *World Malaria Report 2011*. 2011, WHO: Geneva.

434. WHO/UNICEF, *World Malaria Report 2013*. 2013, WHO: Geneva.

435. WHO/UNICEF, *World Malaria Report 2014*. 2014, World Health Organization: Geneva.

436. Wiser, M.F. *Malaria*. 2013.

437. Wongsrichanalai, C., M.J. Barcus, S. Muth, A. Sutamihardja, and W.H. Wernsdorfer, *A review of malaria diagnostic tools: microscopy and rapid diagnostic test (RDT).* Am J Trop Med Hyg, 2007. **77**(6 Suppl): p. 119-27.

438. Wongsrichanalai, C., A.L. Pickard, W.H. Wernsdorfer, and S.R. Meshnick, *Epidemiology of drug-resistant malaria.* The Lancet Infectious Diseases, 2002. **2**(4): p. 209-218.

439. Wongsrichanalai, C., J. Pornsilapatip, V. Namsiripongpun, H.K. Webster, A. Luccini, P. Pansamdang, H. Wilde, and M. Prasittisuk, *Acridine orange fluorescent microscopy and the detection of malaria in populations with low-density parasitemia.* Am J Trop Med Hyg, 1991. **44**(1): p. 17-20.

440. Wongsrichanalai, C., J. Sirichaisinthop, J.J. Karwacki, K. Congpuong, R.S. Miller, L. Pang, and K. Thimasarn, *Drug resistant malaria on the Thai-Myanmar and Thai-Cambodian borders.* Southeast Asian J Trop Med Public Health, 2001. **32**(1): p. 41-9.

441. Wykes, M., C. Keighley, A. Pinzon- Charry, and M.F. Good, *Dendritic cell biology during malaria.* Cellular microbiology, 2007. **9**(2): p. 300-305.

442. Wykes, M.N., J.G. Kay, A. Manderson, X.Q. Liu, D.L. Brown, D.J. Richard, J. Wipasa, S.H. Jiang, M.K. Jones, and C.J. Janse, *Rodent blood-stage Plasmodium survive in dendritic cells that infect naive mice.* Proceedings of the National Academy of Sciences, 2011. **108**(27): p. 11205-11210.

443. Xie, L.H., T.O. Johnson, P.J. Weina, Y. Si, A. Haeberle, R. Upadhyay, E. Wong, and Q. Li, *Risk assessment and therapeutic indices of artesunate and artelinate in Plasmodium berghei-infected and uninfected rats.* Int J Toxicol, 2005. **24**(4): p. 251-64.

444. Xing, J., H. Yan, S. Zhang, G. Ren, and Y. Gao, *A high-performance liquid chromatography/tandem mass spectrometry method for the determination of artemisinin in rat plasma.* Rapid Commun Mass Spectrom, 2006. **20**(9): p. 1463-8.

445. Xing, J., H.X. Yan, R.L. Wang, L.F. Zhang, and S.Q. Zhang, *Liquid chromatography-tandem mass spectrometry assay for the quantitation of beta-dihydroartemisinin in rat plasma.* J Chromatogr B Analyt Technol Biomed Life Sci, 2007. **852**(1-2): p. 202-7.

446. Yeates, C.L., J.F. Batchelor, E.C. Capon, N.J. Cheesman, M. Fry, A.T. Hudson, M. Pudney, H. Trimming, J. Woolven, J.M. Bueno, J. Chicharro, E. Fernandez, J.M. Fiandor, D. Gargallo-Viola, F. Gomez de las Heras, E. Herreros, and M.L. Leon, *Synthesis and structure-activity relationships of 4-pyridones as potential antimalarials.* J Med Chem, 2008. **51**(9): p. 2845-52.

447. Yoeli, M. and H. Most, *Pre-Erythrocytic Development of Plasmodium Berghei.* Nature, 1965. **205**: p. 715-6.

448. Yoshida, S., S.-I. Kashiwamura, Y. Hosoya, E. Luo, H. Matsuoka, A. Ishii, A. Fujimura, and E. Kobayashi, *Direct Immunization of Malaria DNA Vaccine into the Liver by Gene Gun Protects against Lethal Challenge of*

Plasmodium berghei Sporozoite. Biochemical and Biophysical Research Communications, 2000. **271**(1): p. 107-115.

449. Young, M.D., D.C. Baerg, and R.N. Rossan, *Studies with induced malarias in Aotus monkeys.* Lab Anim Sci, 1976. **26**(6 Pt 2): p. 1131-7.

450. Young, M.D., J.A. Porter, and C.M. Johnson, *Plasmodium vivax Transmitted from Man to Monkey to Man.* Science, 1966. **153**(3739): p. 1006-1007.

451. Zaloumis, S., A. Humberstone, S.A. Charman, R.N. Price, J. Moehrle, J. Gamo-Benito, J. McCaw, K.M. Jamsen, K. Smith, and J.A. Simpson, *Assessing the utility of an anti-malarial pharmacokinetic-pharmacodynamic model for aiding drug clinical development.* Malar J, 2012. **11**: p. 303.

452. Zucker, J.R., E.M. Lackritz, T.K. Ruebush, 2nd, A.W. Hightower, J.E. Adungosi, J.B. Were, B. Metchock, E. Patrick, and C.C. Campbell, *Childhood mortality during and after hospitalization in western Kenya: effect of malaria treatment regimens.* Am J Trop Med Hyg, 1996. **55**(6): p. 655-60.

453. Zuckermann, A. and M. Yoeli, *Age and Sex as Factors Influencing Plasmodium Berghei Infections In Intact and Splenectomized Rats.* Journal of Infectious Diseases, 1954. **94**: p. 225-236.

454. Zuzarte-Luis, V., M.M. Mota, and A.M. Vigario, *Malaria infections: what and how can mice teach us.* J Immunol Methods, 2014. **410**: p. 113-22.

455. Zuzarte-Luis, V., J. Sales-Dias, and M.M. Mota, *Simple, sensitive and quantitative bioluminescence assay for determination of malaria pre-patent period.* Malar J, 2014. **13**: p. 15.

APPENDIX 1 – Development of a pharmacodynamic model of murine malaria and treatment with dihydroartemisinin

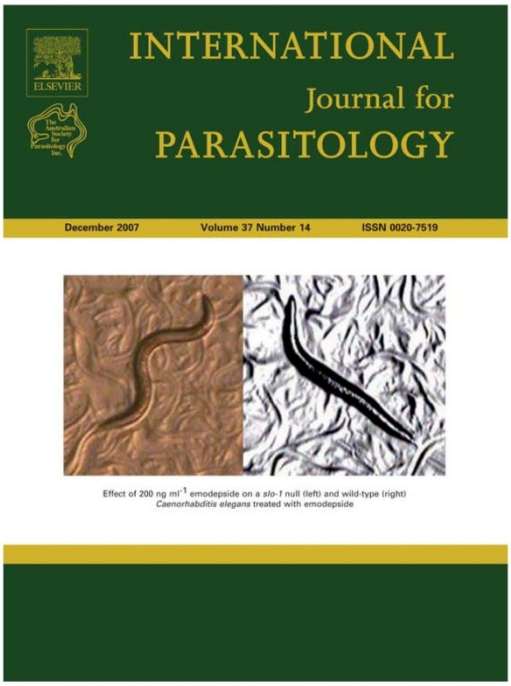

Effect of 200 ng ml^{-1} emodepside on a *slo-1* null (left) and wild-type (right) *Caenorhabditis elegans* treated with emodepside

Available online at www.sciencedirect.com
ScienceDirect
International Journal for Parasitology 37 (2007) 1569–1576
www.elsevier.com/locate/ijpara

Development of a pharmacodynamic model of murine malaria and antimalarial treatment with dihydroartemisinin

Peter L. Gibbons [a], Kevin T. Batty [a,*], P. Hugh R. Barrett [b], Timothy M.E. Davis [b], Kenneth F. Ilett [b,c]

[a] School of Pharmacy, Curtin University of Technology, Bentley, GPO Box U1987, Perth, WA 6845, Australia
[b] School of Medicine and Pharmacology, University of Western Australia, Crawley, WA, Australia
[c] Clinical Pharmacology & Toxicology Laboratory, PathWest Laboratory Medicine, Nedlands, WA, Australia

Received 20 March 2007; received in revised form 4 May 2007; accepted 10 May 2007

Abstract

Antimalarial treatment strategies based on in vitro studies are limited by the paucity of pharmacodynamic information for dosage regimen design. We postulated that a murine model could be used for pre-clinical stages of drug development, especially in dose–response studies and evaluation of combination therapies. Swiss mice infected with *Plasmodium berghei* parasites (2–5% starting parasitaemia) were given dihydroartemisinin (0–100 mg/kg single dose). Parasite density was regularly determined from thin blood films. A parasite population growth model comprising parasite multiplication, decline in erythrocyte count with increasing parasitaemia and parasite clearance after drug administration was developed. This model described the rise in parasitaemia following inoculation, the nadir following dihydroartemisinin administration, and the subsequent resurgence of parasitaemia (analogous to 'recrudescence'). At doses of 10, 30 and 100 mg/kg dihydroartemisinin, there was a graded response with 2.5 ± 1, 5 ± 1 and 12 ± 4-fold decreases in parasitaemia, respectively. The nadir parasitaemia (at 21–27 h) was also dose-dependent. This study demonstrates that a murine malaria pharmacodynamic model is a valuable tool for understanding how single drugs and their dosing schedules alter the time course and level of infection.

Keywords: *Plasmodium berghei*; Malaria; Mouse; Dihydroartemisinin; Pharmacodynamics

1. Introduction

Antimalarial treatment regimens have traditionally been based on in vitro and clinical studies of drugs given alone or in combination, with particular focus on their efficacy against *Plasmodium falciparum*. Although in vitro studies are valuable for screening antimalarial candidates and sensitivity testing (Bwijo et al., 1997; Gupta et al., 2002), they provide limited pharmacodynamic information for dosage regimen design. By comparison, well conducted clinical trials aim to assess parasite clearance and do not generate dose–response relationships that can be used in developing rational dosage strategies, despite detailed pharmacokinetic data being available for most antimalarial drugs. Novel pharmacodynamic models have been developed for a range of drugs (Sharma and Jusko, 1998), but there is a paucity of graded dose–response data from clinical studies of falciparum malaria and various pharmacodynamic models have been proposed (Day et al., 1996; Davis and Martin, 1997; Simpson et al., 2000; Hoshen et al., 2002). Hence, we postulated that animal studies could be used as an appropriate intermediate stage of drug regimen development, between in vitro studies and clinical trials. A murine model was considered to be an established, convenient and cost-effective choice, whilst the use of an artemisinin drug has contemporary clinical relevance in pharmacodynamic model development.

Artemisinin drugs have become an integral component of antimalarial treatment strategies. Early problems with

* Corresponding author. Tel.: +61 8 9266 7369; fax: +61 8 9266 2769.
E-mail address: Kevin.Batty@curtin.edu.au (K.T. Batty).

0020-7519/$30.00
doi:10.1016/j.ijpara.2007.05.001

recrudescence after short-course treatment were resolved by prolonged daily dosing or the use of combination therapy with a longer-acting quinoline partner (Hien and White, 1993; Adjuik et al., 2004). Currently, artemisinin-based combination therapy is regarded as best practice, although the choice of partner drugs varies according to local experience and prescribing guidelines (Davis et al., 2005). There is, however, justifiable concern that the value of combination chemotherapies could be compromised by multi-drug resistance resulting from inappropriate treatment strategies (Ronn et al., 1996). Hence, dosing regimens must be rationally designed to optimise patient outcomes and ensure safe, well-tolerated, inexpensive and convenient treatment (Kremsner and Krishna, 2004).

Murine malaria models are used routinely in preclinical studies of drug activity and toxicology. They have been used to screen activity of candidate antimalarial compounds (Sadun et al., 1965; Peters, 1975; Lin et al., 1987; Janse et al., 1994; Loiseau and Nguyen, 1996; Girault et al., 2001), study mechanisms of drug action (Zhao et al., 1987; Janse et al., 1994) or resistance (Peters, 1975; Fonseca et al., 1995; Walker et al., 2000; Deharo et al., 2003; Afonso et al., 2006), and to investigate host-parasite immunology (Stoltzfus et al., 1997; Murata et al., 1999; Ang et al., 2001; de Souza and Riley, 2002; Adam et al., 2003; Cigel et al., 2003). Murine malaria models are particularly valuable in studies of the erythrocytic stage of malaria infection, because the morphology and parasite development stages are similar to those in human malaria infections. An important advantage with murine malaria models is that all parasite stages can be observed in the peripheral circulation (Mackenstedt et al., 1989).

In the present study, we sought to develop a pharmacodynamic murine malaria model that could be used to investigate both dose–response and regimen characteristics for antimalarial drugs and, ultimately, to develop strategies for combination therapies. Dihydroartemisinin (DHA), an artemisinin derivative that has proven efficacy and an established role in combination therapy, was chosen for model development.

2. Materials and methods

2.1. Chemicals

DHA was obtained from Dafra Pharma NV (Turnhout, Belgium). All general chemicals were of analytical grade and were obtained from Sigma–Aldrich (St. Louis, MO, USA) or BDH Laboratory Supplies (Poole, England).

2.2. Parasites and hosts

This study was approved by the Animal Ethics Committee of Curtin University of Technology. *Plasmodium berghei* ANKA strain parasites, from the Australian Army Malaria Institute (Enoggera, QLD, Australia), were used in all experiments. Erythrocytic stages of *P. berghei* were maintained in 8-week-old male Balb/c mice (Animal Resources Centre, Murdoch, Western Australia) and passaged weekly (Batty et al., 1998). Parasitised erythrocytes were obtained from the donor Balb/c mice via cardiac puncture and diluted with citrate phosphate dextrose solution pH 6.9 (30 g/L trisodium citrate, 0.16 g/L sodium dihydrogen phosphate, 2 g/L anhydrous dextrose) to 10^7 *P. berghei* parasitised erythrocytes per 100 μL. Recipient male Swiss mice aged 5 weeks received an i.p. inoculation containing 10^7 parasites. Animals were housed at 22 °C in a 12 h day/12 h night cycle with free access to sterilised commercial rodent food (Glen Forrest Stockfeeds, Perth, Western Australia) and sterilised acidified water (pH 2.5).

2.3. Parasite enumeration

Parasitaemia was measured by microscopic quantitation from Giemsa-stained thin blood film smears made from tail vein bleeds. Parasitaemias <0.5%, 0.5–5% and >5% were determined by counting 100, 30 and 10 fields of view, respectively. In general, one field of view contained approximately 200 erythrocytes.

2.4. Erythrocyte population studies

Erythrocyte population studies were conducted on 5-week-old Swiss mice infected with 10^7 parasites. Eight mice were euthanased (pentobarbitone sodium 100 mg/kg i.p.) every 24 h for 7 days after inoculation. Heparinised blood was harvested by cardiac puncture and the red cell blood count (mean of triplicate measurements) was determined using a Cell-Dyn® 3500 automated Haematology Analyser (Diamond Diagnostics, Massachusetts, USA). Parasitaemia in the blood was also measured at each time point.

2.5. Dihydroartemisinin treatment

DHA was formulated in 60% v/v dimethyl sulfoxide in Polysorbate 80, with a final injection volume of 100 μL. The vehicle dose was less than 25% of the LD_{50} for both dimethyl sulfoxide and Polysorbate 80 in mice (Rowe et al., 2005). Initial safety studies were conducted using the drug vehicle at doses up to 400 μL (for 30 g mice), with no observed adverse effects.

Five groups ($n = 8$) of 5-week-old male Swiss mice received a single i.p. treatment 72 h after inoculation with 10^7 parasites, with either 0, 1, 3, 10, 30 or 100 mg/kg DHA. Parasitaemia was monitored as described above until mice were euthanased according to pre-determined guidelines (parasitaemia >40% and/or body weight decline by >10% in 24 h, both of which we have found are indicative of terminal deterioration in health of malaria-infected mice).

2.6. Data analysis

The pharmacodynamic model of *P. berghei* infection in Swiss mice was developed using the SAAM II modelling

program (University of Washington, Seattle, WA, USA). All data are summarised as mean ± SD unless otherwise indicated. Analysis and presentation of data was performed with SigmaStat® Version 3.1 and SigmaPlot® Version 9.0 (SPSS Inc., Michigan, Chicago, IL, USA).

3. Results

3.1. Conceptual model of P. berghei infection

A compartmental model of parasite population growth was constructed, with the 24 h asexual erythrocytic cycle of *P. berghei* being divided into 24 compartments, each representing 1 h of parasite growth. Parameters required to model the parasite growth and development included parasite progression through compartments, parasite multiplication and parasite elimination rates.

3.2. Erythrocyte population studies

Quantification of parasitaemia in a murine model is traditionally measured as a proportion or percentage of infected erythrocytes. However, to facilitate the modelling process it was necessary to convert the proportion of infected erythrocytes to the number of parasitised erythrocytes per μL of whole blood (parasite density). This was dependent on the erythrocyte count, which declines as malaria infection progresses, mainly due to clearance of parasitised erythrocytes by the spleen (Looareesuwan et al., 1987, 1991). Since the decline in erythrocyte count with increasing parasitaemia was to be incorporated into the model, the first step in model development was to undertake erythrocyte population studies and define the relationship between the degree of parasitaemia and the erythrocyte count.

These studies showed a significant inverse linear relationship between the parasitaemia and the number of erythrocytes (Fig. 1; $r^2 = 0.99$; $n = 64$; $P = 0.05$). The mean erythrocyte count in healthy mice ($n = 8$) was $8.6 \pm 0.7 \times 10^6$/μL. The relationship between erythrocyte count and parasitaemia was used to convert the percentage of parasitised erythrocytes determined by microscopy to parasitised erythrocytes/μL using the equation:

$$E_i(/\mu L) = [E_i(\%) \times 0.01] \times \{[-0.085 \times E_i(\%)] + 8.6) \times 10^6 \quad (1)$$

where E_i is the number of infected erythrocytes and $E_i(\%)$ is the proportion of infected erythrocytes (parasitaemia; expressed as a percentage) determined from the thin blood film examination. The slope (−0.085) and intercept (8.6×10^6) values were derived from the erythrocyte count versus parasitaemia data shown in Fig. 1.

3.3. Effective parasite multiplication factor (EPMF)

The parasite multiplication rate largely comprises the rate of schizont rupture and subsequent successful merozoite invasion of erythrocytes. In the pharmacodynamic model, an effective parasite multiplication factor (EPMF) was experimentally determined as a function of the proportion of parasitised erythrocytes in whole blood (E_i).

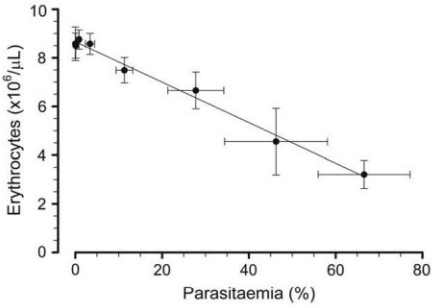

Fig. 1. Erythrocyte count (mean ± SD; $n = 8$; triplicate analysis of each sample) versus parasitaemia in Swiss mice inoculated with *Plasmodium berghei*. There was a significant linear correlation between erythrocyte count and parasitaemia ($P = 0.05$; $r^2 = 0.99$; $n = 64$).

EPMF was determined by fitting a three-parameter power function to experimental data for the difference in parasite density over one asexual erythrocytic cycle (24 h), in mice inoculated with 10^5, 10^6 or 10^7 parasitised erythrocytes, versus the number of parasitised erythrocytes per μL (Eq. (2); Fig. 2). Initial parameter estimates of y_0, a and b were obtained by fitting Eq. (2) in SigmaPlot and SAAM II was used to fit the power function to these data. Computational settings used relative error specification, with a Rosenbrock integrator function, and data-based optimisation with a convergence criterion of 0.001.

$$\text{EPMF} = y_0 - \left(a \times E_i^b\right) \quad (2)$$

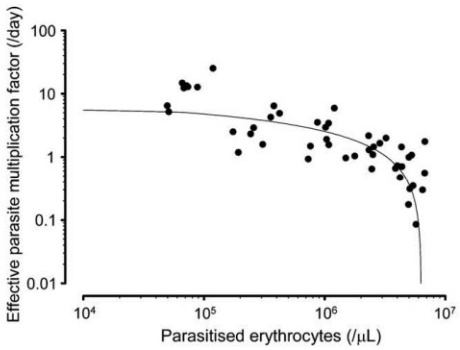

Fig. 2. The effective parasite multiplication factor as a function of the number of infected erythrocytes. The solid line is the line of best fit using SAAM II to fit the function [Eq. (2)] to the data from untreated mice (●) following inoculations with 10^5, 10^6 or 10^7 parasitised erythrocytes.

where E_i is the number of infected erythrocytes/μL; y_0 is the theoretical maximum EPMF (the practical maximum of y_0 occurs when $E_i = 1$); a is the coefficient and b is the exponent for the equation. Model estimates for y_0, a and b were 9.7, 0.73 and 0.15, respectively (Table 1).

At low levels of infection (e.g. 10^3–10^4 parasitised erythrocytes/μL), EPMF was shown to be of the order of 6.5–7.5, thus representing a biologically plausible 7-fold increase in parasite density every 24 h (Garnham, 1966; Janse, C.J., Waters, A.P. 2006. The *Plasmodium berghei* research model of malaria. Leiden Malaria Research Group. <http://www.lumc.nl/1040/research/malaria/model.html> (accessed 11.12.06.)). At higher parasite densities (e.g. 10^6 parasitised erythrocytes/μL or 10–12% parasitaemia), the EPMF was of the order of 3, reflecting a lower rate of parasite growth, mainly due to the diminishing pool of uninfected erythrocytes. More complex functions were investigated but did not improve the fit (data not shown).

3.4. Plasmodium berghei pharmacodynamic model

As the factors that were most likely to be influential in the pharmacodynamics of *P. berghei* infection had been characterised, the next step was to establish and parameterize the model. As before, the *P. berghei* model of infection contained 24 compartments each representing 1 h of the asexual erythrocytic life cycle of the parasite. Variable parameters for the model included the parasite density at inoculation (q, an estimate of viable parasites) and a fractional transfer coefficient (k_p), representing parasite population progression through compartments. Since the compartments represent a common residence time, the rate of progression through all compartments is equal. Immediately following inoculation, the parasite population could be considered as being distributed between all 24 compartments, thus approximating asynchronous infection. However, the results of preliminary modelling indicated that the immediate post-inoculation parasite population was comprised predominantly of early to mid-stage parasites distributed across compartments 1–16. This was consistent with our observations that erythrocytes with early stage parasites predominated in the thin film examinations up to 48 h after inoculation (data not shown), indicating that rings and trophozoites comprise most of the viable parasites in the inoculum and are more resilient to the passaging process. Within 3–4 days post-inoculation, a typical uniformly asynchronous infection was established.

The input of parasites into the first compartment of the model (compartment 1) approximates infection of erythrocytes by released merozoites and multiplication of the infection. The equation for the parasite multiplication is

$$\text{Parasite multiplication} = q_{24} \times k_p \times \text{EPMF} \quad (3)$$

where q_{24} is the number of parasites in the 24th compartment (at $t = 0, q_{24} = 0$ because all parasites were initially distributed across compartments 1–16); k_p is the parasite transfer coefficient (model commenced with $k_p = 1\ h^{-1}$). Initial values for EPMF [from Eq. (2)] and parasite progression in the model ($k_p = 1\ h^{-1}$; represents the asexual erythrocytic cycle length of 24 h) were determined by modelling untreated infection data.

The *P. berghei* model of infection in mice inoculated with 10^5, 10^6 or 10^7 parasitised erythrocytes is shown in Fig. 3. From the model, the initial parasite density at the time of inoculation (the viable parasite biomass) was estimated to represent 47 ± 25% of the inoculum.

3.5. DHA administration and P. berghei model

The final stage in the development of the overall model was to incorporate the effects of treatment with DHA. Parasite clearance after drug administration was incorporated into the model, using an elimination function applied to compartment 23. No improvement in fit was achieved by placing the elimination function in other compartments or in multiple compartments. Hence, the simplest equation that represented the data was

$$D_{\text{Elim}} = Ae^{-k(t-T)} + B \quad (4)$$

where D_{Elim} is the drug-dependent parasite elimination as a function of time (t) after inoculation; coefficient A is a function of the drug dose and defines the magnitude of maximum parasite elimination; k is the drug-dependent rate of parasite elimination; T is the time from inoculation to the peak parasite elimination (according to model estimates) and B represents a time-independent increase in parasite elimination.

The final model describes the rise in parasite density following infection, its nadir following DHA administration, and the subsequent resurgence of parasite density (analogous to 'recrudescence'). The modelling process involved solving Eq. (3) (parasite multiplication) and Eq. (4) (drug-dependent parasite elimination) sequentially in SAAM II. In this sequential fitting, Eq. (3) starts at the

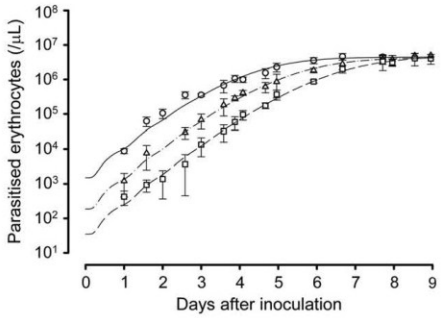

Fig. 3. Parasite density-time profile (mean ± SD) of *Plasmodium berghei* infection and model fitting results for inoculations of 10^5 (□---), 10^6 (△-·-) and 10^7 (○—) parasitised erythrocytes ($n = 3$ per inoculation).

time of inoculation ($t = 0$), while Eq. (4) starts at the time of drug administration ($t = 72$ h).

Assumptions made in the modelling process were that drug treatment did not alter the EPMF (that is, the number of uninfected erythrocytes invaded by viable merozoites) and that the rate of parasite removal was independent of drug dose. Fig. 4 ($n = 8$ per group) shows that there was a graded dose–response relationship with increasing single doses of DHA. The time of nadir in parasite density was independent of dose and occurred approximately 24 h after treatment, with a maximum 12-fold reduction in parasite density following 100 mg/kg DHA. Estimates of the parameters for the model are summarised in Tables 1 and 2.

4. Discussion

This report describes the development of a novel pharmacodynamic model of murine malaria that incorporates parasite multiplication and changes in erythrocyte count as a function of parasite density. We propose that models of this type are a valuable tool for understanding how drugs, alone or in combination, and their dosing schedules alter the time course and level of infection.

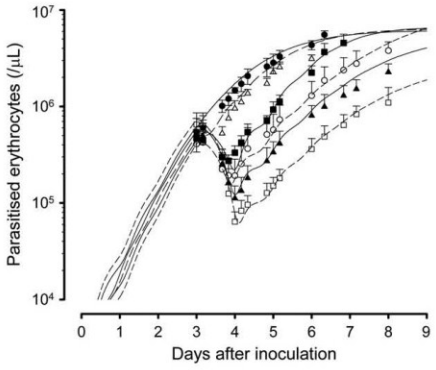

Fig. 4. Parasite density-time profiles (mean ± SD; $n = 8$ per group) and model fits of data in mice treated with DHA, 3 days after inoculation with 10^7 parasitised erythrocytes. Single doses of DHA were given by i.p. injection at day 3: Control (DMSO: Polysorbate 80; ●), 1 mg/kg (△), 3 mg/kg (■), 10 mg/kg (○), 30 mg/kg (▲) and 100 mg/kg (□).

Table 1
Bayesian parameters derived from untreated *Plasmodium berghei* infection modelling for the pharmacodynamic drug treatment model

Drug treatment model parameters	Population mean	SD	Lower limits	Upper limits
y_0	9.7	0.5	9	14
a	0.7	0.5	0.1	2
b	0.15	0.1	0.01	0.8
k_p	1	0.05	0.9	1.1
k	0.6	0.1	0.5	1
T	85	6	72	100

Other model parameters (E_1, A and B) were entered into the model as adjustable variables (Table 2).

Our study has shown that a murine model of antimalarial treatment can provide an array of sub-therapeutic dose–response data that would not be possible in clinical studies. Hence, application of a murine model in the pre-clinical drug development process could assist in selection of candidate antimalarial agents and dosage regimens for drug combination studies during subsequent clinical trials.

An important consideration in establishing a model of antimalarial treatment was to characterise the level of parasitaemia that was achieved following *P. berghei* inoculation. In our laboratory, mice are inoculated with 10^7 parasitised erythrocytes, which consistently results in a 2–5% parasitaemia some 65–70 h later. Thin blood films are prepared regularly after drug administration and the mice can be carefully monitored as the infection progresses. A slightly smaller starting parasitaemia is achieved with a 10^6 inoculum (typically 1–2%), but with 10^4–10^5 inoculations the parasitaemia usually does not exceed 0.5% within 72 h (Fig. 3). Preliminary studies demonstrated that DHA treatment decreased the parasitaemia in mice with starting parasite densities in the order of 10%, but survival of the mice was not substantially prolonged and it was, therefore, only possible to characterise a partial infection-time profile. By comparison, a 2–5% starting parasitaemia did not cause any visible distress to the mice, nor any significant changes in body weight (data not shown) or erythrocyte count (Fig. 1). Furthermore, the infection-time profile after DHA treatment could be followed until pre-determined experimental endpoints were reached (parasitaemia >40% and/or body weight decline by >10% in 24 h), which was usually at least 3–5 days longer than controls, depending on DHA dose. At starting parasitaemias of 0.5–1%, DHA was also effective, but due to low post-treatment parasitaemias it was only possible to characterise a partial infection-time profile across the full range of DHA doses. Hence we concluded that the optimum starting parasitaemia was 2–5%.

Characterising the time-dependent change in parasitaemia in our model depends on being able to accurately and efficiently determine parasite counts by light microscopy. In this regard, valid parasite densities at a parasitaemia of $\geqslant 0.5\%$ can be determined by counting up to 30 fields of view (normally >6000 erythrocytes). By comparison, if 100 fields of view are counted, the limit of detection is a parasitaemia of about 0.004%. Hence, regular thin blood film monitoring of the malaria infection in our model can provide graded dose–response data over at least three orders of magnitude below the starting parasitaemia of 2–5%. In addition, if the decline and recrudescence phases of the infection are well characterised, it is possible to estimate a nadir at a parasitaemia of <0.0001% (<10 parasites/μL) by logarithmic extrapolation.

The level of pharmacodynamic evaluation that is possible with our model is a substantial advance on conventional animal methods of measuring antimalarial efficacy.

Table 2
Pharmacodynamic model parameters (mean ± SD) determined from Eq. (4): $D_{Elim} = Ae^{-k(t-T)} + B$, where D_{Elim} is the drug-dependent parasite elimination as a function of time (t) after inoculation; coefficient A is a function of the drug dose; k is the rate of parasite elimination; T is the time from inoculation to the peak parasite elimination and B represents a time-independent increase in parasite elimination

Parameter (Data from pharmacodynamic model)	Dihydroartemisinin dose (mg/kg)				
	100	30	10	3	1
A	12535 ± 2592	3377 ± 1969	932 ± 695	487 ± 180	14 ± 11
B	0.9 ± 0.4	0.6 ± 0.3	0.9 ± 0.5	0.3 ± 0.2	0.1 ± 0.3
T (h)	84 ± 1.5	84 ± 1.4	83 ± 1.4	85 ± 1.2	84 ± 1.6
k (h^{-1})	0.57 ± 0.04	0.57 ± 0.13	0.57 ± 0.01	0.58 ± 0.02	0.58 ± 0.01
Fold-decrease in parasite density (from time of drug administration to nadir)	12 ± 4	5 ± 1	2.5 ± 1	2 ± 0.2	N/A
Time of maximum parasite elimination, after drug administration (h)	12 ± 1.5	12 ± 1.4	11 ± 1.4	13 ± 1.2	12 ± 1.6
Time of nadir parasite density, after drug administration (h)	26.6 ± 1.8	24.6 ± 1.0	20.9 ± 2.3	21.7 ± 2.0	N/A

The 'Peters 4 day test' in which parasite inoculation is followed by four, once-daily doses of drug, commencing at the time of inoculation (Peters and Robinson, 1999), demonstrates suppression of parasite growth/multiplication and is a well established rodent test for screening antimalarial drugs. By contrast, the Rane test (Peters and Robinson, 1999) evaluates the effect of a drug on parasite elimination in an established infection, as has been demonstrated in efficacy studies of trioxolane antimalarial drugs (Vennerstrom et al., 2004). Recent studies in rat models also show some features of the Rane test, but detailed dose–response relationships were not reported (Li et al., 2003; Xie et al., 2005; Pedroni et al., 2006). Our model is based on the principles of the Rane test, but we have allowed for both variation in parasite multiplication rate and changes in the erythrocyte count in describing progression of the infection. Hence our model provides a more flexible and pathophysiologically appropriate experimental framework for investigation of drug action.

Incorporation of a simple drug-dependent parasite elimination function enables the generation of data characterising the time and level of nadir, as well as the peak effect of the drug. The test antimalarial drug, DHA (10–100 mg/kg), produced a nadir in parasite density approximately 24 h after dosing, but the pharmacodynamic model revealed a time to peak parasite elimination of only 12 h. This finding suggests that for maximal therapeutic effect in the murine model, DHA should be given at 12-h intervals (half of the asexual erythrocytic life cycle). Delaying drug administration to correspond with the nadir may allow a significant proportion of parasites to recover between each dose. Notably, the data from doses of 10, 30 and 100 mg/kg (0.5 log increases) showed a progressive 2-fold lower nadir (Table 2). Based on this observation, three appropriately timed 30 mg/kg doses of DHA should produce a nadir at least 15-fold lower than the starting parasitaemia (compared with the 12-fold lower nadir with 100 mg/kg as a single dose; Fig. 4). Relating principles of dose regimen design from murine models to the clinical setting would require cautious extrapolation, but the strategy of once-daily antimalarial treatment for a period of several days, especially with combination therapy in uncomplicated malaria, is well established and effectively represents two doses per asexual erythrocytic cycle for *P. falciparum*, consistent with our murine model (White, 1997).

One limitation of murine studies as a conceptual model of therapeutic strategies for clinical trials is the 24-h erythrocytic cycle and asynchronous schizogony of *P. berghei*, compared with the 48-h erythrocytic cycle and generally synchronous schizogony of *P. falciparum*. Nevertheless, hypotheses related to duration of drug administration (White, 1997) or comparisons of single-dose and multi-dose regimens of antimalarial drugs could be tested in a murine model, with due regard to the differences in asexual erythrocytic cycle duration and the need for allometric scaling of doses, prior to clinical trials. A further potential limitation relates to the pathophysiology of *P. berghei* infection, specifically the starting parasitaemia of 2–5% in our model and the normally lethal course of infection in untreated mice. However, Swiss mice are tolerant of *P. berghei* infection at a low-moderate level of parasitaemia (<5%), with organ failure and death occurring only at high parasitaemia (Cox, 1988; Landau and Gautret, 1998; Peters and Robinson, 1999). Hence, the features of our *P. berghei* infection model are beneficial for pharmacodynamic studies because tolerance of the infection allows the mice to reach a parasitaemia of up to 5% before drug treatment strategies are commenced and the parasitaemia can be monitored down to a level of approximately 0.005%. In addition, in vivo evaluation of stage specificity is feasible if parasites are differentially counted as rings, trophozoites and schizonts. Furthermore, sequestration is not a factor in *P. berghei* infection of Swiss and Balb/c mice, hence the total peripheral parasitaemia should represent the total parasite burden.

In addition to recognising differences between murine and human malaria, we sought to develop a pharmacodynamic model that was biologically plausible and adaptable to a variety of general modelling software packages. Preliminary studies showed that the rate of increase in

parasitaemia was similar in the first 3–4 days after inoculation with 10^5–10^7 parasitised erythrocytes (Fig. 3), as was recrudescence for approximately 2 days after the post-treatment nadir (Fig. 4). At a high parasitaemia, the rate of increase in parasitaemia was substantially reduced but the parasites harvested from these mice show a typical growth pattern when passaged to naïve recipients. Hence, by quantifying the rise in parasitaemia and incorporating the change in erythrocyte count into the model, a realistic multiplication factor (EPMF) was established as a continuous variable. The simple equations for parasite multiplication [Eq. (3)] and elimination [Eq. (4)] provided a close fit to the experimental data and generated parameters (e.g. time to peak parasite elimination) that should be useful in developing dosage regimens for antimalarial drugs.

In future studies, we intend to use the model to predict the outcomes of multiple-dose treatments and to examine the effects of combination treatment regimens. Such studies should demonstrate the potential value of the murine model for conceptual development of dosage regimens in pre-clinical and clinical studies.

Acknowledgements

Financial support was received from the National Health and Medical Research Council of Australia (NHMRC New Investigator Grant 141103 – KTB). PHRB is a Research Fellow of the NHMRC and is supported in part by NIH NIBIB P41 EB-001975. Laboratory assistance from Ms. Brioni Moore and Ms. Claire MacDonald is gratefully acknowledged. This work was presented in part at the XVI International Congress for Tropical Medicine and Malaria; Marseilles, France; September 2005 (Abstract No. P446).

References

Adam, E., Pierrot, C., Lafitte, S., Godin, C., Saoudi, A., Capron, M., Khalife, J., 2003. The age-related resistance of rats to *Plasmodium berghei* infection is associated with differential cellular and humoral immune responses. Int. J. Parasitol. 33, 1067 1078.

Adjuik, M., Babiker, A., Garner, P., Olliaro, P., Taylor, W., White, N., 2004. Artesunate combinations for treatment of malaria: meta-analysis. Lancet 363, 9 17.

Afonso, A., Hunt, P., Cheesman, S., Alves, A.C., Cunha, C.V., do Rosario, V., Cravo, P., 2006. Malaria parasites can develop stable resistance to artemisinin but lack mutations in candidate genes atp6 (encoding the sarcoplasmic and endoplasmic reticulum Ca^{2+} ATPase), tctp, mdr1, and cg10. Antimicrob. Agents Chemother. 50, 480 489.

Ang, K.K., Holmes, M.J., Kara, U.A., 2001. Immune-mediated parasite clearance in mice infected with *Plasmodium berghei* following treatment with manzamine A. Parasitol. Res. 87, 715 721.

Batty, K.T., Ilett, K.F., Edwards, G., Powell, S.M., Maggs, J.L., Park, B.K., Davis, T.M., 1998. Assessment of the effect of malaria infection on hepatic clearance of dihydroartemisinin using rat liver perfusions and microsomes. Br. J. Pharmacol. 125, 159 167.

Bwijo, B., Alin, M.H., Abbas, N., Wernsdorfer, W., Bjorkman, A., 1997. Efficacy of artemisinin and mefloquine combinations against *Plasmodium falciparum*. In vitro simulation of in vivo pharmacokinetics. Trop. Med. Int. Health 2, 461 467.

Cigel, F., Batchelder, J., Burns Jr., J.M., Yanez, D., van der Heyde, H., Manning, D.D., Weidanz, W.P., 2003. Immunity to blood-stage murine malarial parasites is MHC class II dependent. Immunol. Lett. 89, 243 249.

Cox, F., 1988. Major animal models in malaria research: rodent. In: Wernsdorfer, W.H., McGregor, I. (Eds.), Malaria Principles and Practice of Malariology, vol. 2. Churchill Livingstone, New York, pp. 1503 1543.

Davis, T.M., Karunajeewa, H.A., Ilett, K.F., 2005. Artemisinin-based combination therapies for uncomplicated malaria. Med. J. Aust. 182, 181 185.

Davis, T.M., Martin, R.B., 1997. Clearance of young parasite forms following treatment of falciparum malaria in humans: comparison of three simple mathematical models. Epidemiol. Infect. 119, 61 69.

Day, N., Pham, T., Phan, T., Dinh, X., Pham, P., Ly, V., Tran, T., Nguyen, T., Bethell, D., Nguyan, H., White, N., 1996. Clearance kinetics of parasites and pigment-containing leukocytes in severe malaria. Blood 88, 4694 4700.

de Souza, J.B., Riley, E.M., 2002. Cerebral malaria: the contribution of studies in animal models to our understanding of immunopathogenesis. Microbes Infect. 4, 291 300.

Deharo, E., Barkan, D., Krugliak, M., Golenser, J., Ginsburg, H., 2003. Potentiation of the antimalarial action of chloroquine in rodent malaria by drugs known to reduce cellular glutathione levels. Biochem. Pharmacol. 66, 809 817.

Fonseca, L., Vigario, A.M., Seixas, E., do Rosario, V.E., 1995. *Plasmodium berghei*: selection of mefloquine-resistant parasites through drug pressure in mosquitoes. Exp. Parasitol. 81, 55 62.

Garnham, P., 1966. Rodent species of malaria parasites. In: Garnham, P. (Ed.), Malaria Parasites and Other Haemosporidia. Blackwell, Oxford, pp. 431 475.

Girault, S., Delarue, S., Grellier, P., Berecibar, A., Maes, L., Quirijnen, L., Lemiere, P., Debreu-Fontaine, M.A., Sergheraert, C., 2001. Antimalarial in-vivo activity of bis(9-amino-6-chloro-2-methoxyacridines). J. Pharm. Pharmacol. 53, 935 938.

Gupta, S., Thapar, M.M., Mariga, S.T., Wernsdorfer, W.H., Bjorkman, A., 2002. *Plasmodium falciparum*: in vitro interactions of artemisinin with amodiaquine, pyronaridine, and chloroquine. Exp. Parasitol. 100, 28 35.

Hien, T.T., White, N.J., 1993. Qinghaosu. Lancet 341, 603 608.

Hoshen, M.B., Stein, W.D., Ginsburg, H., 2002. Mathematical modelling of malaria chemotherapy: combining artesunate and mefloquine. Parasitology 124, 9 15.

Janse, C.J., Waters, A.P., Kos, J., Lugt, C.B., 1994. Comparison of in vivo and in vitro antimalarial activity of artemisinin, dihydroartemisinin and sodium artesunate in the *Plasmodium berghei*-rodent model. Int. J. Parasitol. 24, 589 594.

Kremsner, P.G., Krishna, S., 2004. Antimalarial combinations. Lancet 364, 285 294.

Landau, I., Gautret, P., 1998. Animal models: rodents. In: Sherman, I.W. (Ed.), Malaria: Parasite Biology, Pathogenesis and Protection. American Society for Microbiology, Washington, DC, pp. 401 417.

Li, Q.G., Si, Y.Z., Lee, P., Wong, E., Xie, L.H., Kyle, D.E., Dow, G.S., 2003. Efficacy comparison of intravenous artelinate and artesunate in *Plasmodium berghei*-infected Sprague Dawley rats. Parasitology 126, 283 291.

Lin, A.J., Klayman, D.L., Milhous, W.K., 1987. Antimalarial activity of new water-soluble dihydroartemisinin derivatives. J. Med. Chem. 30, 2147 2150.

Loiseau, P.M., Nguyen, D.X., 1996. *Plasmodium berghei* mouse model: antimalarial activity of new alkaloid salts and of thiosemicarbazone and acridine derivatives. Trop. Med. Int. Health 1, 379 384.

Looareesuwan, S., Davis, T.M., Pukrittayakamee, S., Supanaranond, W., Desakorn, V., Silamut, K., Krishna, S., Boonamrung, S., White, N.J., 1991. Erythrocyte survival in severe falciparum malaria. Acta Trop. 48, 263 270.

Looareesuwan, S., Ho, M., Wattanagoon, Y., White, N.J., Warrell, D.A., Bunnag, D., Harinasuta, T., Wyler, D.J., 1987. Dynamic alteration in splenic function during acute falciparum malaria. N. Engl. J. Med. 317, 675 679.

Mackenstedt, U., Brockelman, C.R., Mehlhorn, H., Raether, W., 1989. Comparative morphology of human and animal malaria parasites. I. Host-parasite interface. Parasitol. Res. 75, 528 535.

Murata, K., Takano, F., Fushiya, S., Oshima, Y., 1999. Potentiation by febrifugine of host defense in mice against *Plasmodium berghei* NK65. Biochem. Pharmacol. 58, 1593 1601.

Pedroni, H.C., Bettoni, C.C., Spalding, S.M., Dalla Costa, T., 2006. *Plasmodium berghei*: development of an irreversible experimental malaria model in Wistar rats. Exp. Parasitol. 113, 193 196.

Peters, W., 1975. The chemotherapy of rodent malaria, XXII. The value of drug-resistant strains of *Plasmodium berghei* in screening for blood schizontocidal activity. Ann. Trop. Med. Parasitol. 69, 155 171.

Peters, W., Robinson, B.L., 1999. Malaria. In: Zak, O., Sande, M. (Eds.), Handbook of Animal Models of Infection: Experimental Models in Antimicrobial Chemotherapy. Academic Press, London, pp. 757 773.

Ronn, A.M., Msangeni, H.A., Mhina, J., Wernsdorfer, W.H., Bygbjerg, I.C., 1996. High level of resistance of *Plasmodium falciparum* to sulfadoxine-pyrimethamine in children in Tanzania. Trans. R. Soc. Trop. Med. Hyg. 90, 179 181.

Rowe, R.C., Sheskey, P.J., Owen, S.C., 2005. Handbook of Pharmaceutical Excipients. Pharmaceutical Press, London.

Sadun, E.H., Williams, J.S., Meroney, F.C., Hutt, G., 1965. Pathophysiology of *Plasmodium berghei* infection in mice. Exp. Parasitol. 17, 277 286.

Sharma, A., Jusko, W.J., 1998. Characteristics of indirect pharmacodynamic models and applications to clinical drug responses. Br. J. Clin. Pharmacol. 45, 229 239.

Simpson, J.A., Watkins, E.R., Price, R.N., Aarons, L., Kyle, D.E., White, N.J., 2000. Mefloquine pharmacokinetic-pharmacodynamic models: implications for dosing and resistance. Antimicrob. Agents Chemother. 44, 3414 3424.

Stoltzfus, R.J., Chwaya, H.M., Albonico, M., Schulze, K.J., Savioli, L., Tielsch, J.M., 1997. Serum ferritin, erythrocyte protoporphyrin and hemoglobin are valid indicators of iron status of school children in a malaria-holoendemic population. J. Nutr. 127, 293 298.

Vennerstrom, J.L., Arbe-Barnes, S., Brun, R., Charman, S.A., Chiu, F.C., Chollet, J., Dong, Y., Dorn, A., Hunziker, D., Matile, H., McIntosh, K., Padmanilayam, M., Santo Tomas, J., Scheurer, C., Scorneaux, B., Tang, Y., Urwyler, H., Wittlin, S., Charman, W.N., 2004. Identification of an antimalarial synthetic trioxolane drug development candidate. Nature 430, 900 904.

Walker, D.J., Pitsch, J.L., Peng, M.M., Robinson, B.L., Peters, W., Bhisutthibhan, J., Meshnick, S.R., 2000. Mechanisms of artemisinin resistance in the rodent malaria pathogen *Plasmodium yoelii*. Antimicrob. Agents Chemother. 44, 344 347.

White, N.J., 1997. Assessment of the pharmacodynamic properties of antimalarial drugs in vivo. Antimicrob. Agents Chemother. 41, 1413 1422.

Xie, L.H., Johnson, T.O., Weina, P.J., Si, Y., Haeberle, A., Upadhyay, R., Wong, E., Li, Q., 2005. Risk assessment and therapeutic indices of artesunate and artelinate in *Plasmodium berghei*-infected and uninfected rats. Int. J. Toxicol. 24, 251 264.

Zhao, Y., Hall, I.H., Oswald, C.B., Yokoi, T., Lee, K.H., 1987. Antimalarial agents. III. Mechanism of action of artesunate against *Plasmodium berghei* infection. Chem. Pharm. Bull. (Tokyo) 35, 2052 2061.

APPENDIX 2 – Reagents and Buffers

A2.1 1M Acetic Acid

Acetic Acid Glacial……..	57.4mL
Water ……...	to 1 Litre

A2.2 Alsever's Solution

Dextrose (anhydrous)…….....	20.5g
Trisodium Citrate ($Na_3C_6H_5O_7.2H_2O$)……..	8.0g
Sodium Chloride…….....	4.2g
Citric Acid (monohydrate)……..	0.5g
Water…….....	to 1 Litre

A2.3 Citrate Phosphate Dextrose Solution (pH 6.9)

Trisodium Citrate ($Na_3C_6H_5O_7.2H_2O$).....	30.0g
Sodium Dihydrogen Phosphate($NaH_2PO_4.2H_2O$).	0.16g
Dextrose (anhydrous).....	2.0g
Water.....	to 1 Litre

Note: Sterilised by filtration (0.22μm Millex® OR filter unit; Millipore Bedford, MA, USA)

A2.4 Formaldehyde-Citrate Solution

Formaldehyde Solution (40% w/w CH_2O)……..	10mL
Trisodium citrate Solution (109mM)……	to 1 Litre

A2.5 Glycerol in Alsever's Solution

Glycerol……	10mL

Alsever's Solution……... to 1 Litre

Note: Sterilised by filtration (0.45μm Millex® HA filter unit; Millipore Bedford, MA, USA)

A2.6 Phosphate Buffer 0.1M pH 7.4

Potassium dihydrogen phosphate (KH_2PO_4)……. 2.72g

Disodium hydrogen phosphate (Na_2HPO_4)…… 11.36g

Alsever's Solution……... to 1 Litre

A2.7 Potassium Chloride – Phosphate Buffer

Potassium Chloride…… 11.5g

Phosphate Buffer 0.1M pH 7.4……. 100mL

Water…… to 1 Litre

A2.8 Sodium Acetate Solution

Sodium acetate (CH_3COONa)……. 82.04g

Water…… to 1 Litre

A2.9 Sorenson's Phosphate Buffer pH 7.0

Potassium dihydrogen phosphate (KH_2PO_4)……. 3.75g

Disodium hydrogen phosphate (Na_2HPO_4)…… 5.56g

Alsever's Solution……... to 1 Litre

A2.10 Trisodium Citrate Solution 109mM

Trisodium citrate ($Na_3C_6H_5O_7.2H_2O$)..... 32g

Water……... to 1 Litre

A2.11 Walpole's Acetate Buffer 0.1M pH 4.8

Acetic acid 1M…… 40mL

Sodium acetate solution 1M…….	60mL
Water……	to 1 Litre

A2.12 Walpole's Acetate Buffer 0.1M pH 5.0

Acetic acid 1M…….	29.6mL
Sodium acetate solution 1M…….	70.4mL
Water……	to 1 Litre